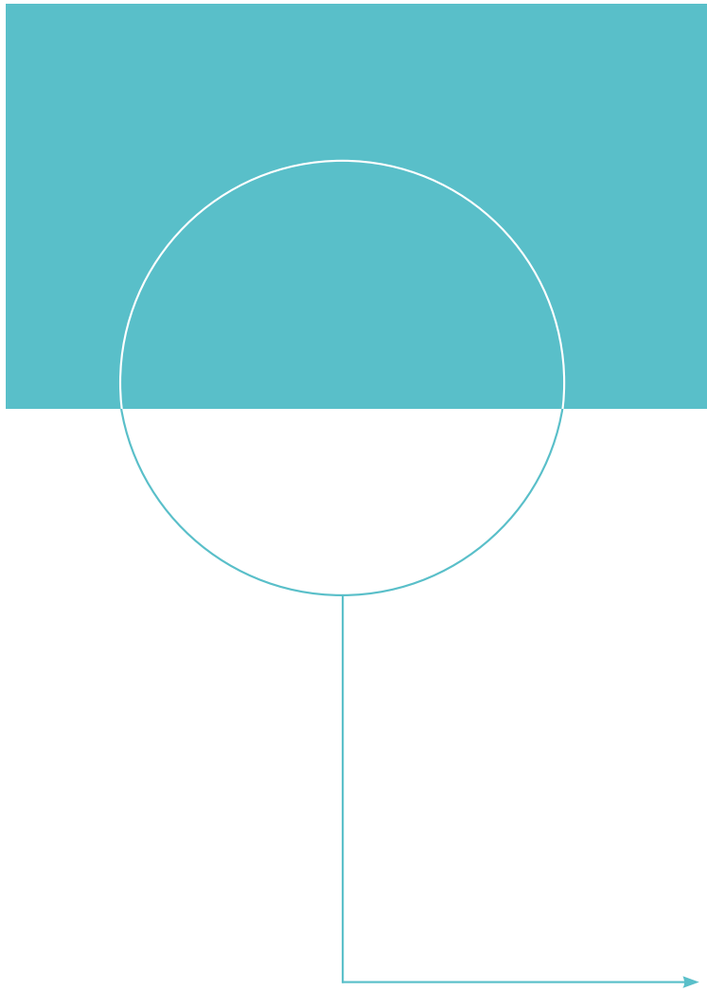

Master's thesis

2020

Luca Contiero

NTNU
Norwegian University of
Science and Technology
Faculty of Engineering
Department of Energy and Process Engineering

Luca Contiero

Experimental analysis of advanced R744 refrigeration system

July 2020

NTNU
Norwegian University of
Science and Technology

NTNU
Norwegian University of
Science and Technology

NTNU

Norwegian University of
Science and Technology

Experimental analysis of advanced R744 refrigeration system

Luca Contiero

Master's thesis in Energetic Engineering

Submission date: July 2020

Supervisor: Armin Hafner & Davide Del Col

Co-supervisor: Dr. Ángel Álvarez Pardiñas
Khuram Baig
Iolanda Manescu & Dr. Yosr Allouche

Norwegian University of Science and Technology
Department of Energy and Process Engineering

NTNU

Norwegian University
of Science and Technology

Department of Energy
and Process Engineering

EPT-M-2019

MASTER THESIS

for

student Luca Contiero
Autumn 2019

Experimental analysis of advanced R744 refrigeration system

Background and objective

There is a large transition in supermarket refrigeration with a strong focus on energy consumption. Highly efficient system configurations with R744 are introduced in various locations throughout Europe; however further improvements are necessary and possible, for example with the use of ejector-based expansion work recovery, pivoting compressor arrangements, implementation of local cold storages, etc.

Multi-ejector expansion modules, intended as a substitute for standard high-pressure electronic expansion valve (HPV), were designed by SINTEF/Danfoss and experimentally investigated at the SuperSmart-Rack test rig (Varmeteknisk laboratory, Trondheim). The implementation of a low-pressure lift multiejector block for air conditioning (AC) production has also been tested in the past at NTNU's laboratory, showing its potential for reducing the power consumption of integrated CO_2 refrigeration systems. The pivoting compressor principle complements these advances and allows to make the aforementioned solutions cost-effective. It is based on switching compressors between the different suction groups, so that less units are needed to meet the requirements in the different seasons. However, the control of this feature has to be investigated and further adapted as an objective of this master thesis.

On the other hand, the implementation of local cold storages connected to the R744 refrigeration system helps reducing the peak load and shifting it to periods with low electricity cost or high electricity production with renewables (e.g. solar panels). The first approach to thermosyphon-driven, local cold storages has been experimentally investigated at NTNU's laboratory, but the concept needs to be refined and deeply investigated within this master thesis.

The following tasks are to be considered:

1. Literature review on R744 ejector and refrigeration technology
2. Preparation of SuperSmart-Rack test rig to allow pivoting compressor automatic control. Update of the HSE documentation.
3. Preparation of an experiment plan to investigate the performance of the refrigeration system with different compressor combinations.
4. Test campaign to analyse the correct control and performance of the refrigeration system with pivoting compressors.
5. Design of cold storage unit that would be integrated in a display cabinet connected to the SuperSmart CO_2 refrigeration system.
6. First test campaign for the cold thermal energy storage integrated in the display cabinet, if time allows it.

7. Data processing and analysis of results implemented in a master thesis including discussion and conclusion
8. Draft version of a scientific paper
9. Conclusions and proposal for further work

-- ” --

Within 14 days of receiving the written text on the master thesis, the candidate shall submit a research plan for his project to the department.

When the thesis is evaluated, emphasis is put on processing of the results, and that they are presented in tabular and/or graphic form in a clear manner, and that they are analyzed carefully.

The thesis should be formulated as a research report with summary both in English and Italian, conclusion, literature references, table of contents etc. During the preparation of the text, the candidate should make an effort to produce a well-structured and easily readable report. In order to ease the evaluation of the thesis, it is important that the cross-references are correct. In the making of the report, strong emphasis should be placed on both a thorough discussion of the results and an orderly presentation.

The candidate is requested to initiate and keep close contact with his/her academic supervisor(s) throughout the working period. The candidate must follow the rules and regulations of NTNU as well as passive directions given by the Department of Energy and Process Engineering.

Risk assessment of the candidate's work shall be carried out according to the department's procedures. The risk assessment must be documented and included as part of the final report. Events related to the candidate's work adversely affecting the health, safety or security, must be documented and included as part of the final report. If the documentation on risk assessment represents a large number of pages, the full version is to be submitted electronically to the supervisor and an excerpt is included in the report.

Pursuant to “Regulations concerning the supplementary provisions to the technology study program/Master of Science” at NTNU §20, the Department reserves the permission to utilize all the results and data for teaching and research purposes as well as in future publications.

The final report is to be submitted digitally in DAIM. An executive summary of the thesis including title, student’s name, supervisor's name, year, department name, and NTNU's logo and name, shall be submitted to the department as a separate pdf file. Based on an agreement with the supervisor, the final report and other material and documents may be given to the supervisor in digital format.

☒ Work to be done in lab (Water power lab, Fluids engineering lab, Thermal engineering lab)
☐ Field work

Department of Energy and Process Engineering, 17. September 2019

Prof. Dr.-Ing. Armin Hafner
Academic Supervisor

Co-Supervisors: Dr. Yosr Allouche, Postdoc EPT
Dr. Ángel Álvarez Pardiñas, Researcher / Forsker
Iolanda Manescu, PhD Candidate

I. Acknowledgments

The past two years have been the beginning of my changing, leading me to improve my knowledge and passion, as well as enthusiasm for many fields in which technology is a solid base. This long period is finished here at NTNU, where I could grow both personally and intellectually.

I would take this moment to thank first of all my parents which have supported me through all this process, and mostly the wonderful people I found here at NTNU. I have learned a lot from all my supervisors and it's difficult now to decide where to start, because all of them left something really important in my life, helping to improve and supporting me every day. I would also to thank my supervisor Davide Del Col for giving me the opportunity to start this experience.

I would start to express my gratitude to the two people I worked very closely over all my studies, which have provided me knowledge, moral support and incitement for doing a good job. Prof. Armin Hafner, for always being available to share his knowledge and precious time, I would like to thank him for his goodness, and his attention has been a great value to me pushing to work harder. Dr. Ángel Álvarez Pardiñas, he was since the beginning inspiration for me, guiding me through all the whole year and helping me a lot. The thesis wouldn't have been completed without his immense support and advice, as well as constructive feedback over all my period in Norway.

I would also take the opportunity to thank my co-supervisor Iolanda Raluca Manescu and Yosr Allosche, who helped me with the precious suggestion for modeling and writing.

In the end, but not least, I am deeply grateful to Khuram Baig, for his incredible help, for the long discussions and for being very friendly, sharing his knowledge and his logical ways of thinking. Furthermore, I would say thanks to my friend Hamza Bajja for being very kind and friendly with me since I arrived in Norway and for helping me with his suggestions over all my period in Norway.

II. Abstract

Carbon dioxide is one of the oldest refrigerants, as it was used widely at the end of the nineteenth century. However, around 1931 it started its decline when synthetic refrigerants came into the market showing a higher efficiency and a cheaper implementation in the refrigeration systems, in terms of equipment. Nonetheless, carbon dioxide as a refrigerant is gaining more and more space over the last years due to its thermodynamic properties, the capability to be an optimal refrigerant for many applications and its usage reduces the emissions of greenhouse gases (GHG). Its wide implementation is confirmed by the fact that the energy demand of supermarkets can be fully satisfied by subcritical or transcritical cycles, depending on whether the climate is cold or hot respectively.

In this thesis, the background of the description of refrigeration cycles using R744, both with ejector and not, are introduced at the beginning of the first chapter. The chapter continues with the description of Cold Thermal Energy Storages, i.e. CTES, which are currently investigated as an optimal solution that grants an enhancement in terms of energy saving. This technology allows energy production and storage when the electricity prices are at their lowest (when charged during the night), in order to provide further cooling capacity when the electricity prices are at their highest (during the day, when people come back from work) and to smooth the usage peak which normally happens over the afternoon.

This Master Thesis project is focused on two different tasks. The first part of the Master Thesis is dealing with the investigation on the pivoting technology which is capable to reduce the number of compressors installed in the rack by using at the suction port of some compressors two valves that switch according to their position and the need. The second part is dealing with the design of a CTES located on the top of a supermarket's display cabinet.

The first task was planned to start from a numerical simulation to simulate the performance of a simplified refrigeration system using the polynomial equations for each compressor, ending with an experimental campaign that has been carried out at the SuperSmart-Rack at NTNU, Trondheim. The investigation of the pivoting technology has been done considering two different high-pressure (HP) control devices, as high-pressure valve and high pressure lift multi–ejector block, and many different temperatures at the outlet of the gas cooler to reproduce different ambient conditions. As it has been seen during the experimental campaign the most critical situation to predict accurately is when the HP multi-

ejector is in operation because of the performance of the block itself. This allowed also to highlight the need to improve the ejector, since it is an expensive technology and can be used only over a certain period of the year, depending on the geographical area.

From the obtained results, the pivoting enhances the flexibility of the rack lowering the number of compressors installed by one, and when the multi-ejector block is used to control the high pressure the number can be reduced further by another compressor. However, the implementation of the ejector without pivoting technology would be unsatisfactory as the number of compressors needed would raise. Because of the ejector, a lot of capacity is shifted to the parallel side. A common practice will be to include a new compressor to cover the load, that it will be used for few operating conditions. Moreover, no degradation has been seen when pivoting are working, leading to the same power consumption and COP.

The second task of this Master Thesis is the modeling of a phase change thermal storage, that uses R744 as refrigerant, and water as the phase change material. The task required the design and the numerical simulation of the phase change process that occurs inside the CTES during the discharging stage. As reported widely in literature, the key factor of a two-phase thermosyphon loop is the investigation of the pressure losses over all the circuits. The cabinet available at the NTNU/SINTEF laboratories in Trondheim was used as a reference for the installation of the CTES on the top of the cabinet itself, considering the evaporator installed with its own geometric and construction features. The CTES has been modeled to match the duty of this evaporator, as well as the liquid and vapor line that linked the inlet-outlet of the evaporator with outlet-inlet of the CTES.

It was concluded that, because of the low heat transfer in the CTES, stable and effective use of the thermosyphon principle can be used for a higher temperature application, for instance, the conservation of vegetables. It has been proven that a very small temperature difference between CTES and the evaporator leads to a huge heat transfer area. The cold storage was designed like a tank with circular finned over smooth tubes and is used to condensate the vapor coming from the evaporator. A liquid head of approximately 1.8 meters is used to overcome all the pressure losses in the system. The design was followed by numerical simulation of the implemented system.

III. Sommario

L’anidride carbonica è uno dei più antichi refrigeranti, essendo stata ampiamente utilizzata dalla fine del diciannovesimo secolo. Tuttavia, attorno al 1931 è iniziato il suo declino quando i refrigeranti sintetici sono stati introdotti nel mercato mostrando migliori efficienze e una più facile introduzione nei sistemi refrigerativi, in termini di componenti necessari al suo utilizzo. Ciò nonostante, l’anidride carbonica sta guadagnando sempre più spazio negli ultimi anni per via delle sue proprietà termodinamiche, per la capacità di essere un ottimo refrigerante in molte applicazioni e per le basse emissioni di gas ad effetto serra che ne derivano dal suo utilizzo (GHG). Il suo ampio utilizzo è confermato dal fatto che la domanda energetica dei supermercati può essere totalmente soddisfatta da cicli subcritici o transcritici, a seconda del clima se freddo o caldo, rispettivamente.

In questa tesi, una panoramica descrittiva dei cicli frigoriferi ad anidride carbonica, con eiettori e non, è stata introdotta nel primo capitolo. Il capitolo continua con la descrizione del Cold Thermal Energy Storages, accumulatore di energia termica fredda, il quale è oggetto di studio essendo un’ottima soluzione che garantisce un efficientamento in termini di energia risparmiata. Questa tecnologia consente una produzione e un’immagazzinamento energetico quando i prezzi dell’energia elettrica sono al loro minimo (quando il CTES viene caricato durante la notte), al fine di fornire ulteriore capacità refrigerativa quando i prezzi dell’energia elettrica sono al loro massimo (durante la giornata, quando le persone finiscono il turno lavorativo) e di appiattire il picco energetico che solitamente avviene durante il pomeriggio.

La tesi magistrale è rivolta verso due differenti aspetti. La prima parte della Tesi tratta la tecnologia Pivoting, la quale è in grado di ridurre il numero di compressori installati nel sistema sfruttando l’intercambiabilità della sezione di aspirazione degli stessi mediante l’uso di valvole. La seconda parte tratta il design del CTES, posizionato sulla sommità del banco refrigerativo di un supermercato.

La prima parte prevede di partire con una simulazione numerica al fine di simulare le prestazioni di un ciclo refrigerativo semplificato utilizzando le equazioni polinomiali di ogni compressore, finendo per svolgere dei test sperimentali presso il sistema SuperSmart-Rack all’NTNU, che si trova a Trondheim. Lo studio della tecnologia Pivoting è stata fatta considerando due dispositivi per il controllo dell’alta pressione, come la valvola di espansione e l’eiettore, e differenti scenari che prevedono differenti temperature all’uscita del gas cooler

al fine di replicare differenti condizioni ambientali. Come risulta dai test sperimentali, lo scenario più difficile da prevedere è quello con l'eiettore per via della difficile determinazione delle sue prestazioni. Questo ha permesso di sottolineare la necessità di migliore l'eiettore stesso, essendo una tecnologia costosa e che può essere utilizzata solo in un certo periodo dell'anno, a seconda dell'area geografica.

Dai risultati ottenuti, la tecnologia Pivoting consente di aumentare la flessibilità del sistema diminuendo il numero di compressori installati di uno, e quando l'eiettore sta regolando l'alta pressione il numero può scendere a due. Tuttavia, l'implementazione dell'eiettore senza il supporto della tecnologia Pivoting sarebbe insoddisfacente in quanto il numero di compressori richiesti salirebbe. Per via dell'eiettore, molta capacità è richiesta nei compressori ausiliari. Una pratica comune è quella di includere un ulteriore compressore per fornire il carico refrigerativo, ma utilizzandolo solo per poche condizioni operative. Inoltre, nessuna degradazione è stata registrata quando la tecnologia Pivoting viene implementata, risultando nello stesso consumo di potenza e COP.

Il secondo obiettivo di Tesi prevede la modelizzazione di un CTES, che utilizza R744 come refrigerante e acqua come PCM. Ciò ha richiesto la progettazione e simulazione numerica del processo di cambiamento di fase che si verifica all'interno del CTES durante la fase di scarico. Come ampiamente riportato in letteratura, un fattore chiave per un ciclo a termosifone a due fasi è lo studio delle perdite di pressione lungo tutto il circuito. Il sistema frigorifero disponibile nel laboratorio NTNU/SINTEF in Trondheim è stato utilizzato come riferimento per l'installazione del CTES sulla sua sommità, considerando l'evaporatore installato con le sue relative grandezze geometriche e caratteristiche. CTES è stato modelizzato per uguagliare il carico termico dell'evaporatore, come anche le tubazioni che collegano l'ingresso-uscita dell'evaporatore con l'uscita-ingresso del CTES.

È stato concluso che, a causa del basso coefficiente di scambio termico all'interno del CTES, uno stabile ed efficiente sistema a termosifone può essere utilizzato solo per applicazioni ad alta temperatura, come per esempio la conservazione di vegetali. È stato dimostrato che una piccola differenza di temperatura tra CTES e l'evaporatore comporta un'enorme area di scambio termico. CTES risulta come un box con all'interno una serie di tubi alettati circolari dove il vapore che arriva dall'evaporatore viene condensato. Una colonna di liquido di 1.8 metri è usata per compensare le perdite di carico. La modelizzazione è seguita da una simulazione numerica.

IV. Nomenclature

Symbols

PL	Pressure lift	[bar]
$\dot{m}$	Mass flow rate	$[\frac{kg}{s}]$
$\dot{V}$	Volumetric flow rate	$[\frac{m^3}{s}]$
COP	Coefficient of Performance	[-]
h	Specific enthalpy	$[\frac{kJ}{kg}]$
P	Power	[kW]
p	Pressure	[bar]
s	Entropy	$[\frac{kJ}{kg*K}]$
T	Temperature	[°C]
x	Vapor quality	[-]
Q	Refrigeration capacity	[kW]
d	Diameter	[m]
r	Radius	[m]
A_c	Cross sectional area	$[m^2]$
ρ	Density	$[\frac{kg}{m^3}]$
μ	Dynamic viscosity	$[\frac{Pa}{s}]$
$\Delta h_{melting}$	Latent heat of phase change	$[\frac{kJ}{kg}]$

k	Thermal conductivity	$[\frac{W}{m*K}]$
g	Gravity acceleration	$[\frac{m}{s^2}]$
H	Liquid head	[m]
α	Heat transfer coefficient	$[\frac{W}{m^2*K}]$
β	Two-phase multiplier	[-]
η	Efficiency	[-]
$\emptyset$	Entrainment ratio	[-]
π	Pressure ratio	[-]
n	Recirculation number	[-]
F	Working frequency compressor	[Hz]
Δp	Pressure drop	[bar]
v	Specific volume	$[\frac{m^3}{kg}]$
z	Number of coils in parallel	[-]
Θ	Pressure drop ratio liquid only/vapor only	[-]
U	Overall heat transfer coefficient	$[\frac{W}{m^2*K}]$
Re	Reynolds number	[-]

Subscripts

AC	Air conditioning
s	Solid

l	Liquid
m	Melting
IT	Intermediate temperature
MT	Medium temperature
LT	Low temperature
sf	Suction flow
mf	Motive flow
amb	Ambient
evap	Evaporator
suc,IT	Suction IT compressors
sat	Saturated
vol	Volumetric
is	Isentropic
in	Inner
out	Outer
m	Mean
o	Outlet evaporator
i	Referred to feed line or evaporator inlet

Abbreviations

AC	Air Conditioning

AKV	Electronic Expansion Valve
CFC	Chlorofluorocarbon
CTES	Cold Thermal Energy Storage
DHW	Domestic Hot Water
DSH	Desuperheater
DX	Direct Expansion
EJ	Ejector
FGV	Flash gas bypass valve
GC	Gas cooler
GWP	Global warming potential
HCFC	Hydrochlorofluorocarbon
HFO	Hydrofluoroolefins
HP	High-pressure
HPV	High pressure valve
HTF	Heat transfer fluid
IESPC	Integrated ejector supported parallel compression
IHX	Internal heat exchanger
IT	Intermediate temperature
LHTS	Latent heat thermal storage
LP	Low-pressure

LT	Low temperature
MT	Medium temperature
PIV	Pivoting
PCM	Phase change material
R744	Refrigeration number of CO_2
SHTS	Sensible heat thermal storage
SS-R	SuperSmart-Rack
VSD	Variable speed drive

V. Table of Contents

1 Introduction

This chapter starts with the motivation for the research in R744 (CO_2) refrigeration systems, focusing on two aspects: the pivoting technology to reduce the number of compressors used in the system, and the implementation of cold thermal energy storage in a supermarket display cabinet. The chapter continues with the objectives and of the Master Thesis project and finishes with an overview of the structure of this project.

1.1 Motivation

The increasing effect of greenhouse gases has encouraged the research to go towards environmentally friendly natural refrigerants such as R744 (CO_2) as an alternative to the traditional refrigerants widely used in the past, such as Chlorofluorocarbon (CFC_s) and hydro-chlorofluorocarbon ($HCFC_s$). The ozone-depleting problem together with the greenhouse gases effects brought to a new transition in the last 10-20 years where natural refrigerants play an important role [1].

R744 was used mostly on the ships at the beginning of the 20^{th} century until it was replaced by the synthetic refrigerant in the middle of the century, as stated in many articles in literature [1-3]. However, when the Montreal Protocol was applied there was the face out of most CFC and HCFC compounds, and natural refrigerants such as R744 have taken place for many applications emerging as one of the best options among the natural refrigerants, although there is no refrigerant which satisfies all the requirements (no flammability, toxicity, cost, availability, etc.)[1].

The reintroduction of R744 took place in parallel with a great research effort that was related to the proliferation of refrigerants for domestic and commercial refrigeration systems [2]. Today is a fact that the supermarket refrigeration is considering CO_2 as one of the best options, claiming it will have a major impact on the environmental footprint of this sector. In particular, CO_2 transcritical refrigeration systems have proved their reliability and good performance in Northern Europe even though the development of cost- and energy-efficient units able to operate under different climatic conditions constitutes a remarkable challenge.

The particular thermodynamic properties of carbon dioxide and the low efficiency of the transcritical cycles at high ambient temperatures have driven the development of new

technologies to improve this efficiency, such as ejectors as high-pressure control device replacing the expansion valve [4]. Nowadays, the trend is to integrate heating, ventilation and air conditioning in the CO_2 refrigeration systems (HVAC&R), with a single unit called “3rd generation system” [5].

The proliferation of this kind of system has been subject to continuous modifications with the aid of the concurrent implementation of several energy-efficient measures [6], such as parallel compression, overfed evaporators [7] and multi-ejector and pivoting concept. Here, the concept of pivoting compressors was first developed by Hafner [8]. The adoption of this technology favors greater flexibility enlarging the operation range of the refrigeration plant as stated by Pardiñas [9]. For this purpose, an experimental campaign at the Super-Smart facility has been performed to test the operation of the refrigeration system having a pivoting compressor, mainly focused on the supply of the cooling load and operating conditions of the system itself, as well as the performance.

Moreover, Cold Thermal Energy Storage might be an interesting approach to reduce further the energy consumption [10], since the supermarkets are currently accounting around 3-4 % of the annual electric consumption in industrialized countries [6]. A deep reading of the concept of thermosyphon loop reveals how this technology needs further studies because it can be applied on a small scale, to a small power unit and with an operation that is difficult to predict. The approach found in the literature is usually to design the heat exchangers and all the equipment, build it and finally test it in order to obtain more detailed information that can improve its future design. Basically no general guidelines exists, but the main approach is to overcome the pressure drop along the tubes with the liquid line thanks of the gravitational force.

1.2 Objectives

The main objectives of the project are:

- Perform a literature review of CO_2 refrigeration systems, ejector technology, pivoting technology and two-phase thermosyphon loop integrated with CTES
- Model theoretically a refrigeration system to analyze which compressors in the rack are in use to supply the design load, under different ambient conditions
- Preparation of the test-rig to allow pivoting compressor automatic control

- Perform an experimental campaign leading to the generation of a kind of guidelines, allowing to highlight the steps necessary to obtain a more economical and compact system
- Comparison of the experimental – theoretical results
- Thermal design of the CTES
- Modeling of the TPTL, integrated with the CTES acting as a condenser

1.3 Project structure

This thesis consists of eight chapters. This section has the goal to summarize the contents of each chapter and serve as a guideline to understand them better.

- The literature review of R744 refrigeration unit including all the technical aspects of the R744 multi-ejector, AC integration and CTES applications is giving in Chapter 2
- In Chapter 3, the theory of R744 refrigeration systems are deeply presented focusing on the thermodynamic properties of the refrigerant, different layouts of such kinds of a system with their relative improvements as ejectors
- In Chapter 4, the set-up in the facility with a description of the main components is introduced at first. The modifications done in the laboratory are also exposed
- In Chapter 5, experimental results regarding the oil management are discussed in detail and the theoretical model used to analyze the pivoting compressors is presented
- In Chapter 6, the numerical and experimental results are provided and discussed making a comparison among them
- Chapter 7 presents the numerical procedure for designing the CTES and the TPTL ideally used to supply the refrigerating load during the discharging process.
- Chapter 8 presents the numerical simulation using Ansys Fluent to quantify the melting rate
- In the last chapter, the conclusion from the research is presented and further suggestions as future work are illustrated
- The thesis ends with the Appendix section were a scientific paper, the different P&IDs of the systems and some graphs related to the theoretical and experimental results.

2 Literature review

This chapter aims to introduce the topic of commercial R744 refrigeration systems. Moreover, great importance has been given to updating the readers about the current situation of such systems, investigating the previous and current research on R744 transcritical parallel compression and ejector system technologies. Furthermore, a brief overview of the evolution of the CTES application and the thermosyphon loop concept has been included.

With the adoption of the EU F-Gas Regulation 517/2014 [11], it has been prompted to use heavily natural refrigerants such as NH_3 and CO_2 instead of synthetic refrigerants, leading the market towards less environment-damaging alternatives. This holds particularly true for high-energy demand applications, such as supermarkets. In this contest, Europe is trying to encourage supermarket stakeholders to implement environmentally friendly and energy-efficient technologies thus reducing the impact of those systems on the environment. Worldwide, the growth in the number of supermarkets can be explained by many factors, such as globalization, urbanization, etc. Because of their highest specific energy consumptions among commercial buildings due to air conditioning and space heating, they necessarily need continuous improvements.

The environmental effects of the global warming impact of refrigeration systems that arise from direct emission (in terms of leakages) [12] can be attributed to 3-22 % as stated by many researchers. All the remaining emissions are coming from indirect emissions, implying electricity production burning fossil fuels. Because of the largest share of the market by commercial refrigeration, and with increasing demand especially for air conditioning during summer days, there is still today a great emphasis on the overall efficiency of the system (Figure 2.1) [13], because the high consumption and emissions of such systems reflect the total carbon footprint of supermarkets.

As the demand increases over the years, more and more emphasis has been given to natural refrigerants and this process started with the banning of CFC_s by the Montreal Protocol [14], Kyoto – Protocol. Graphically, a stepwise reduction plan will lead to the use of low GWP fluids (Figure 2.2)[14]. This transition is favored by lower investment costs than in the past thanks to the innovations introduced over the last decade.

In parallel with these restrictions, a lot of work has been done improving systems using natural refrigerants. In the following subchapter, the R744 state-of-art for commercial refrigeration systems has been examined highlighting the major improvements over the years, ensuring their reliability and projecting them as the future systems used on widespread.

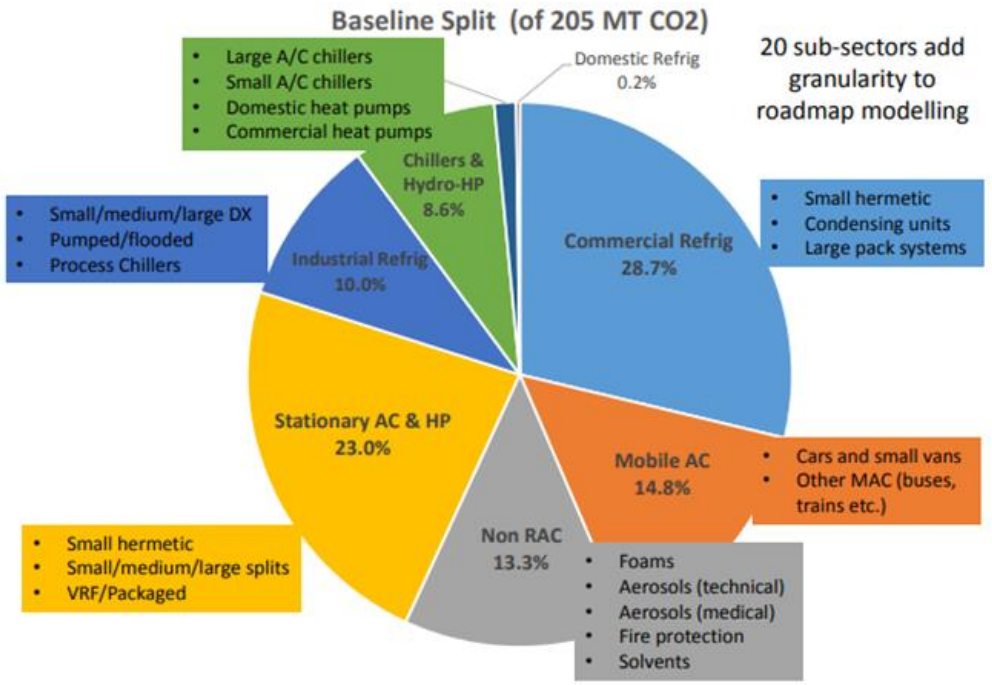

Figure 2.1: Drivers of HFC demand summarized in 8 main market sectors [12].

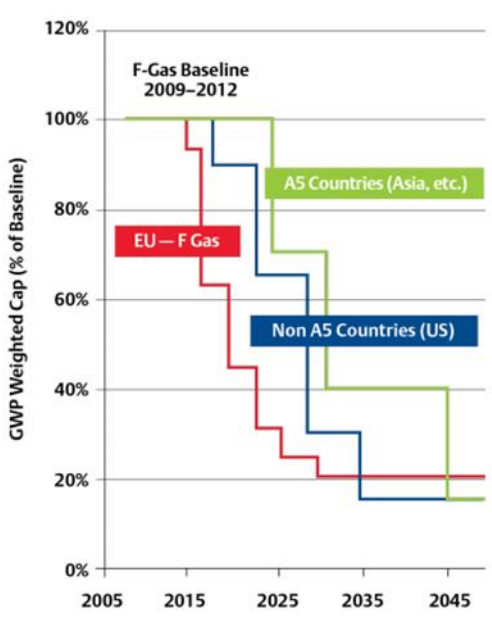

Service and maintenance bans	GWP	Timing
HFC's	2,500	Jan. 2020
'Placing on the market' (new equipment) bans		
Domestic refrigerators and freezers	150	Jan. 2015
Refrigerators and freezers for commercial use (hermetically sealed systems)	2,500	Jan. 2020
Refrigerators and freezers for commercial use (hermetically sealed systems)	150	Jan. 2022
Stationary refrigeration equipment (except equipment for temperatures below -50 °C)	2,500	Jan. 2020
Multipack centralized refrigeration systems for commercial use with a capacity of ≥ 40 kW (140 kBTU/hr) (except in the primary refrigerant circuit of cascade systems, where fluorinated greenhouse gases with a GWP of less than 1,500 may be used)	150	Jan. 2022
Movable room air-conditioning appliances (hermetically sealed equipment which is movable between rooms by the end user)	150	Jan. 2020
Single split air-conditioning systems containing < 3 kg	770	Jan. 2025

Figure 2.2: An overview of the EU F-gas Regulation [14].

2.1 Evolution of R744 Commercial refrigeration systems

In the last decade, the CO_2 refrigeration systems have experienced a remarkable evolution, being pushed by all the climatic regulations. It is worth mentioning that the first usage of CO_2 in supermarkets was as a secondary fluid thanks to its good heat transfer properties and lower viscosity which allows having the required power consumption considerably lower than the traditional secondary fluids [15]. The second generation of supermarket CO_2 refrigeration systems were such plants where R744 was used either in the MT and LT level, while the heat was rejected into an upper cycle where another type of refrigerant is used (usually a refrigerant with insignificant GWP). This further heat exchange lowers the overall efficiency of the system, increasing the overall costs. The next refrigeration system was the traditional transcritical booster system with a flash gas by-pass valve. After that, the supermarket refrigeration systems have experienced a considerable evolution. As typically called in the refrigeration field, the carbon dioxide refrigeration system moved from the 1st (system with FGV) to the 3rd generation (Figure 2.3). These kinds of systems are commonly working as a transcritical cycle because of the low critical temperature of R744.

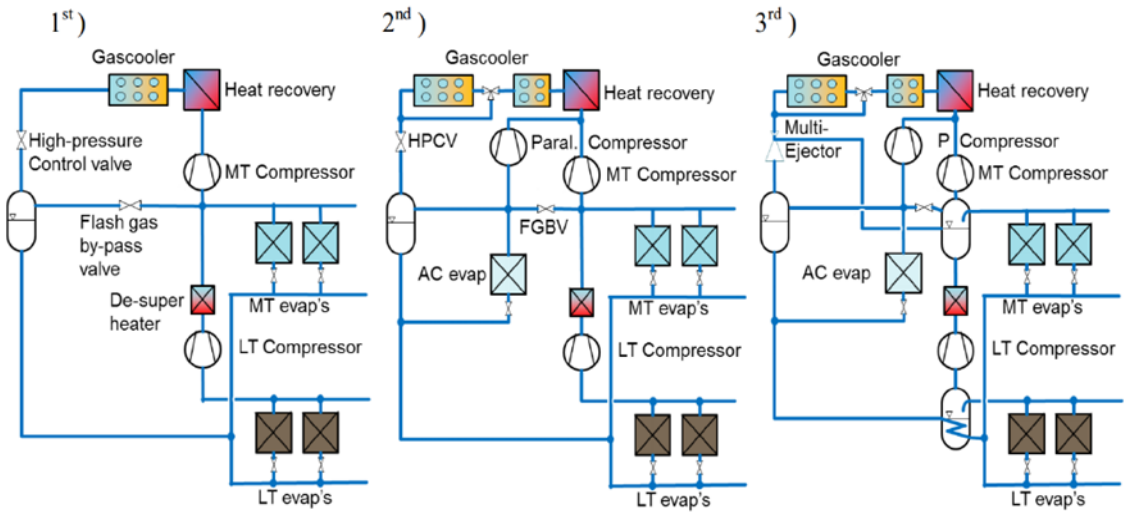

Figure 2.3: Schematic of the 1st, 2nd, and 3rd generation of "CO_2 only"booster supermarket refrigeration system layouts [16].

The first generation of the R744 booster system was developed at the Danish Technological Institute in June 2006, fitting best to cold climates and making this layout as the most widely applied solution in Northern Europe.

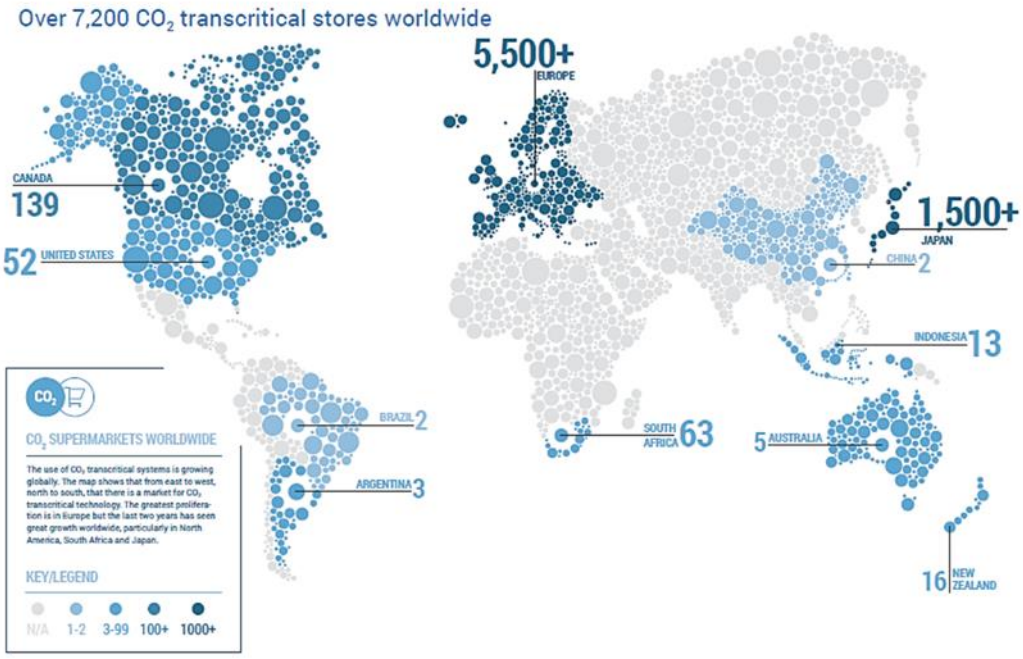

Figure 2.4: Worldwide map of the stores using CO_2 transcritical booster [17].

Since a lot of research has been done providing various collected field data that CO_2 transcritical booster systems have either higher or comparable COPs to conventional HFC systems in mild-cold climates, as stated by Sawalha [18], its diffusion was very rapid until it even became well known in other continents (Figure 2.4) [17]. The successful transfer has also taken place from Japan to Indonesia as stated by [19].

The booster layout has been widely investigated by many authors in literature [20, 21], proving as already explained that the performance is similar or even better than what is achievable with HFC solutions. Dynamic models have been implemented [21, 22] and validated against laboratory data. The COPs measured by Sharma et al. [20] in a laboratory-scale R744 booster system were compared with a direct expansion system with R404A [23], have shown an improvement around 15% in a wide range of ambient temperatures (from 10 to 35 °C). Furthermore, Gullo et al. [24] has theoretically estimated an energy-saving around 7.5 – 17 % in mild-cold climates comparing the 1st generation layout with a similar R404A unit.

An acceptable cost of ownership for end-users is very important for rapid and successful implementation of R744 refrigeration units, but also the efficiency of such systems must be improved, mainly in warmer climates. As discovered with the standard booster system layout, warmer climates make clear the drawback of having high exergy losses in a CO_2 transcritical

refrigeration unit due to the thermophysical properties of the refrigerant itself [25, 26] and because of the large amount of refrigerant throttled trough the FGV, but this aspect can partially turn into benefit recovering the heat released in the gas cooler. Since supermarkets have a rather wide range of heating demands, and tap water heating the most energy-efficient and cost-effective method is to use the waste heat rejected by the refrigeration system through the gas cooler, increasing the overall efficiency of the refrigeration unit and simultaneously lowering the heating purchase demand [27].

As long as the outdoor temperature rises, the amount of flash gas contained in the liquid receiver increases reaching 45% of the total mass flow rate implying very poor performance [28], leading to innovative solutions to improve the performance of the standard booster system even in warm climates. One of them is the implementation of parallel compressors to compress the flash gas vapor directly from the receiver to the high-pressure side enhancing the overall performance of the unit, because of the lower pressure ratio under which those compressors work. In this way is possible to unload the MT compressors and many authors have concluded that the improvement in terms of energy efficiency is significant by 10-15 % [29-31]. Several papers discussed many aspects coming with the installation of the parallel compressors in the rack, i.e. the time where they can be employed [29], a proper and careful design looking the investment costs and life-time of the compressor pack [32], the optimal receiver pressure [33, 34]. Several studies have noticed the optimal receiver pressure is a function of the load ratio and condensing/gas cooler outlet temperatures [35], as well as the displacement ratio of the parallel to the main compressors [34]. Javerscheck et al. [29] estimated an increment of the COP between 8.4 % and 13.6% for an outdoor range temperature of 25-42.5 °C. Nowadays, the so-called 2nd generation layout is the starting point to spread and accelerating the usage of the parallel compression system across Europe and it is illustrated in Figure 2.3.

As mentioned before, high outdoor temperature leads to a much larger amount of vapor contained in the receiver. One suitable technique for R744 refrigeration unit is the sub-cooling to lower the total power consumption of the system, increase the cooling effect, and exergy efficiency [36]. Some southern European supermarkets use the mechanical sub-cooling where NH_3 can be used to have an eco-friendly solution but required in this case an expense of using an extra unit, and a more complicated control system rather with only parallel compressors employed.

Two possible alternatives can be considered as reliable solution for replacing the HPV: an ejector or an expander. A great improvement that came into the market in the last decade was the ejector that immediately showed its potential at the expense of expander. The ejector is a simple component where a primary flow enters into a primary nozzle accelerating and expanding entraining a secondary flow entering from a suction chamber. The flow mix and a diffuser compress the stream because of the geometric shape at the outlet. An expander is a device that decreases the pressure of the refrigerant flow. The reasons are the much simpler manufacturing, operation and controlling setup, as well as the little reliability of the expanders being easily damageable at high liquid levels [37]. Furthermore, ejectors do not have moving parts making them easier to manufacture than expanders, but paying particular attention to the irreversibility due to wall roughness along with the mixed chamber [38] and therefore proving how it is necessary a well-geometric design [39]. Several works have been carried out to investigate the performance of such devices, among them Elbel et al. [40] who achieved an improvement in terms of COP of 7%, while Nakagawa et al. [41] of 26 %. Because the ejectors replace the primary function which was used to be of HPV, the high pressure has to be accurately controlled being the COP strongly depending on that [25]. Being the ejector geometry fixed, optimal control of the high pressure cannot be reached pointing out the poor ability in the high-pressure control function and effectively recover expansion work [42]. Thus, the multi-ejector block concept pointed out by Hafner et al. [4] had a great impact on the layout of R744 systems, creating a new transition from the 2nd to the 3rd generation "all-in-one" system. This concept was for the first time applied to a Swiss supermarket in 2013. The multi-ejector block can be employed for controlling the heat rejection pressure, constantly satisfying the capacity by varying the combination of vapor cartridges and simultaneously pre-compressing some vapor sucked by MT accumulator, unloading the MT compressors. Hafner et al. [4] investigated the enhancement of the COP using "all-in-one" R744 refrigeration unit in many locations (North, Middle and South Europe) highlighting as the highest COP improvement is achieved in a warmer climate (by 17%). As stated by Pardiñas et al. [9], the simulations conducted at 30 °C revealed a power reduction by 17% when parallel compressors are in use, and in addition, another 6% when high-pressure lift multi-ejector is in operation.

Coming with the multi-ejector concept, overfed evaporators were deeply studied by many authors [7, 43], improving further the overall performance of the 3rd generation cycles.

Today, the R744 refrigeration unit in the form of 3rd generation has become the current tendency as regards to transcritical CO_2 supermarket refrigeration systems. Such kind of system is called IESPC (Integrated Ejector Supported Parallel Compression) with the purpose to entirely satisfy the refrigeration load, air conditioning, DHW demands [31, 44, 45]. Hafner et al. [44] stated that the IESPC unit consumes less than a system with parallel compression depending on the external temperature and AC needs. Since AC demand is becoming more and more important, the "all-in-one" layout should include two multi-ejector blocks where one is dedicated to the AC load while the other to the refrigeration load [30]. With this outperforming of R744 systems rather HFC-solutions, the "CO_2 equator" disappeared in Europe, meaning that it is pushed further south employing those systems everywhere in Europe, even in warm climates, and with a great efficiency [46].

In Figure 2.5 [6], a comparison between the three different R744 layouts and an R404A direct expansion cycle has been performed considering different locations, and it is worth to highlight how the third generation layout has the smallest energy consumption.

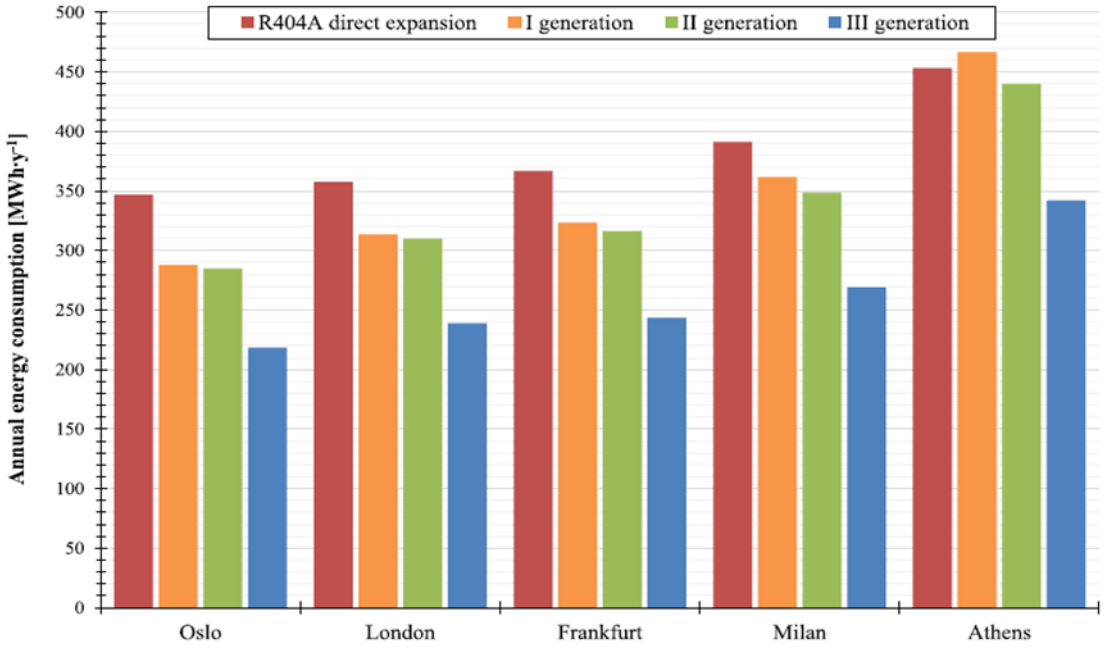

Figure 2.5: Annual consumption of the 1st, 2nd and 3rd generation of "CO_2 only" supermarket refrigeration systems compared to that of an R404A direct expansion unit in the European climate context [25].

Nowadays, many research studies are still working to enhance the overall performance of cycles, introducing new technologies such as CTES (Cold Thermal Energy Storage), internal heat exchangers, flooded evaporators [7], etc. As mentioned before, a great impact

on the total energy demand is coming from the AC and space heating demand and it has been estimated around 20 % of the supermarket consumption [4]. Because the supply and return temperatures of the water as secondary fluid in the AC heat exchanger are typically about 7 and 12 °C, the R744 refrigeration unit by using the sensible cooling process (gas cooling) can more suitably fit the water temperature profile than conventional synthetic refrigerants. This has led R744 as one of the best eco-friendly refrigerants among the entire refrigeration market.

2.2 R744 ejector technologies: current status

As long as R744 refrigeration units are proposed as one of the best eco-friendly and energy-efficient solutions, its spread has been characterized by many types of research on the ejector technology. The drawback of a large amount of heat released in a warm climate is turned into a benefit with the heat recovery and simultaneously with the arrival of ejector technology the high exergy losses due to the throttling process are almost disappeared.

CO_2 is rapidly conquering the commercial refrigeration market thanks all the improvement coming out with the researches in the last 10 years, even though as stated by Hafner et al. [30, 44] and Schönenberger et al. [47] R22 is still the most employed working fluid around the world, featuring a refrigerant leakage rate almost equal to 30 % and impacting a lot the carbon footprint. The outcome of ejectors, heat recovery process implementations, have made CO_2 systems more competitive, compact and cheaper than HFC-solutions [48].

The ejector was invented and patented in 1858 by Henry Giffard, with the aim of pumping water into steam locomotives boilers using vapor as the motive fluid. In 1901, Charles Parson first mentioned the possibility of using an ejector to use vapor to pump vapor. In 1919 Maurice Leblanc developed the first ejector application in refrigeration, but the development of ejector as a device to recover part of the expansion work to circulate liquid refrigerant into flooded evaporators derives from Gay [49]. He basically patented the two-phase ejector describing the potential advantages coming with its implementation, therefore higher efficiency since the throttling losses are reduced. All the remarks were not specified for an R744 cycle, but it substantially contributed to look the expansion work recovery even in CO_2 applications, whenever transcritical conditions arise. In 1983 Lorentzen et al. [50]

proposed the use of the ejector to pre-compress vapor before compressor suction, which is the most popular application nowadays because of the revival of carbon dioxide. The simplified layout and T-s diagram can be seen in Figure 2.6 [51].

In the beginning, the high pressure was controlled by the ejector in parallel with HPV which with its opening/closing is allowed to compensate a too small or too large variation of the high pressure. To overcome this issue, two approaches have been investigated in order to accurately control the high pressure: the first consists in using a variable motive nozzle geometry but it is not yet a reliable solution, with some inconvenient at partial load as mentioned before [52]; the second control strategy introduce by Hafner et al. [4] is the multi-ejector block (Figure 2.7 [53]).

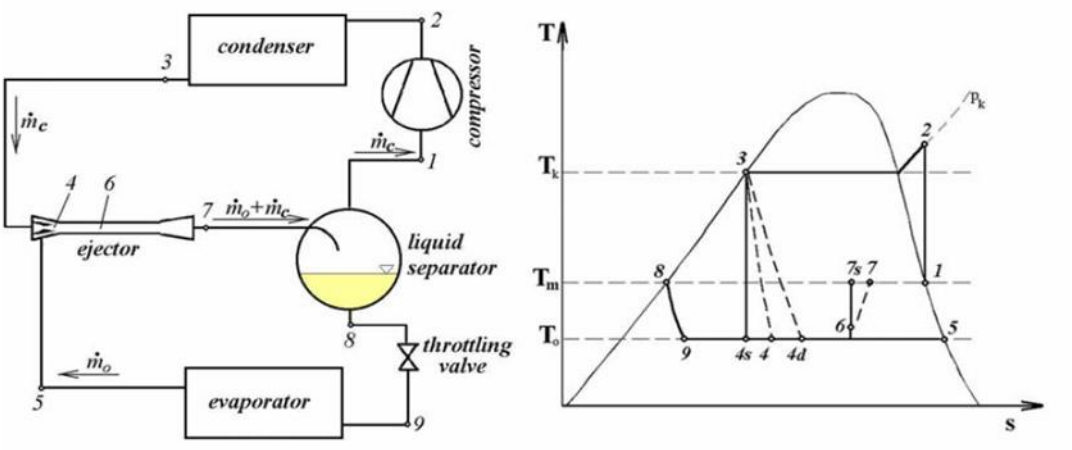

Figure 2.6: Structure of two-phase ejector [51].

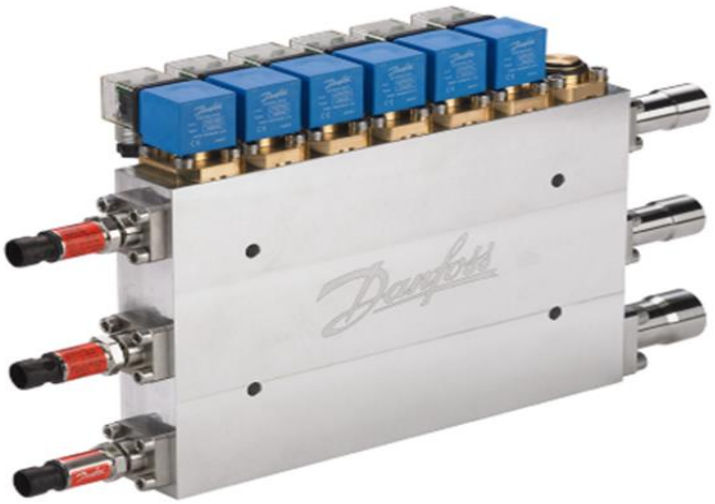

Figure 2.7: Multi-ejector block from Danfoss [53].

The Multi-ejector consists of several fixed geometry cartridges of different sizes, which are combined depending on the load. Usually, 4-6 vapor cartridges and 2 liquid cartridges are implemented in the multi-ejector block. All the vapor cartridges have a different cross-section area therefore the high pressure can be accurately controlled in accordance to the load requirement and ambient conditions. The liquid cartridges allow correct operation of the compressors sucking the excessive amount of liquid at the outlet of the evaporator, enabling the benefit coming from the overfed evaporators concept (better use of the heat transfer area, increasing the evaporating temperature). As asserted by Banasiak et al. [42], the system's response when subjected to a shock increment in the load or ambient conditions was relatively similar when HPV or Multi-ejector block are used. Unlike the HPV, the Multi-ejector suffers the increment in the mass flow rate and therefore the efficiency degraded gradually because of the high and high irreversibility (friction, imperfect mixing, etc.). The computational model of two-phase flow ejector developed by Smolka et al. [54] was later validated by Palacz [55] and employed by many researchers in order to optimize the multi-ejector performance looking, in particular, the geometry features of the block itself [56-59]. Possible approximation functions to simulate the multi-ejector rack have been developed using the experimental data from [55, 58], pointing out a prediction of one of the most important parameters of multi-ejector block: entrainment ratio [60]. This measure of ejector performance was defined as a function of both the gas cooler outlet temperature and optimal pressure lift. The multi-ejector device as stated by Hafner et al. [4, 61] can improve the system efficiency by 20%, and Girotto et al. [43] even more depending on the external conditions. Kriezi et al. [62] suggested the implementation of a liquid ejector designed for winter operation regimes and one for summer conditions, enhancing the overall performance of the system as long as the boundary conditions change over the year. Furthermore, Javerschek et al. [63] claimed that multi-ejector block can successfully reduce the required nominal displacement. This technology has been subjected to many improvements in the recent years, leading some experts in the field to claim the "CO_2 efficiency equator" is removed.

The unloading of the MT compressors due to ejector operation leads to enhance the life-time of the compressors pack and enhancing the overall efficiency of the system [64]. Thus, the partial unloading of MT compressors and the simultaneously increasing of the vapor compressed by IT compressors highlighted the need to take into account the interactions between the multi-ejector block operation and the compressor packs in the design step of the refrigeration plant. As experimentally demonstrated by Pardiñas et al. [65], maintaining high

compression efficiency in the MT compressor pack becomes crucial even at partial load when ejector is in operation in order to maximize the overall efficiency, otherwise, part of the gain of the work recovery coming from the ejector is partially wasted because of the lower efficiency of the compressor pack, remembering that small machines tend to have lower efficiency than bigger machines. Moreover, [9] showed how food retailers should be encouraged to use air conditioning systems designed for the highest temperature possible increasing as much as possible the AC evaporating pressure. The huge amount of vapor that has to be compressed at very high temperature requires a considerable capacity and therefore the pivoting suction solution becomes a way that has to be investigated to adapt the capacity to the load requirements and outdoor temperature.

The wide usage of air conditioning has moved the research towards systems having two multi-ejector blocks, one with high-pressure lift (HP) and one with low-pressure lift (LP). As can be seen downstream in the Theory Chapter, the pressure lift and entrainment ratio are directly linked among them and when one of them increases, the other decreases. The HP multi-ejector is dedicated to the refrigeration loads and the LP multi-ejector block to the AC load. In both cases, as stated by Banasiak et al. [42] applying common boundary conditions to optimize the efficiency of each cartridge simultaneously is not possible therefore the overall performance has to be maximized. This explains why two different multi-ejector blocks are employed. However, even though the power consumption is further reduced with their implementation as demonstrated by Pardiñas et al. [9] and particularly at high ambient temperatures, might be challenge the regulation of the high pressure since the motive flow is shared into two different nozzles. The authors used and suggested a control strategy where adjusting the pressure lift in the LP ejector and AC evaporating pressure can solve the problem.

The AC load can be supplied in two different ways depending on the position of the heat exchanger. If the $EVAP_{(AC,2)}$ is operating upstream of the liquid receiver, it allows the implementation of AC even in a standard booster system, while $EVAP_{(AC,1)}$ is ejector-supported and based on utilizing the LP multi-ejector.

Nowadays, since it had been proven theoretically and by field measurements, as R744 booster systems perform better than HFC-solution, with the recent work if the performance during the whole year accomplished an energy-saving as well as an eco-friendly solution, the

R744 system will be implemented in any kind of climate replacing the synthetic refrigeration unit.

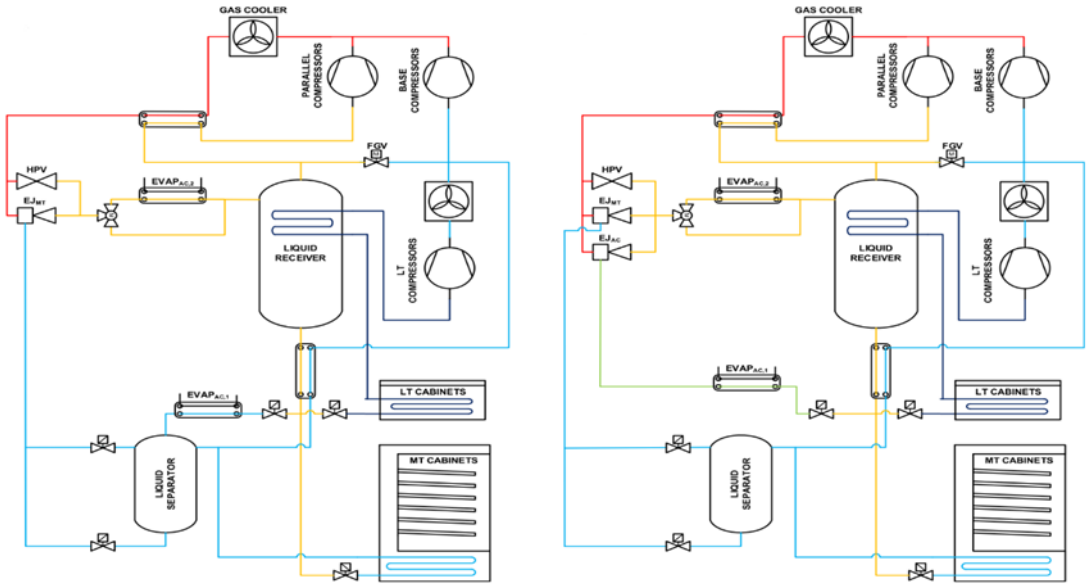

Figure 2.8: a) Parallel compression with HP multi-ejector block. b) Parallel compression with both multi-ejector blocks [9].

2.3 CTES: a technology to reduce further the supermarket energy impact

TES (Thermal Energy Storage) is a system where the energy can be stored and used later on. One suitable material for this purpose is the PCM (Phase Change Material), which usually refers to a material with high latent heat value. This feature allows the PCMs to absorb or release heat when they are in transition from one phase to the other (solid–liquid or liquid-solid) at an almost constant temperature, making them very suitable as energy storage, PCMs can store a certain amount of heat that can be used during a specific time-frame of the day. Since in this Thesis we are interested in investigating a heat exchanger working with ice placed in a closed thermosyphon loop, we need to take into account the complete cycle, the charging and discharging processes [66]. Two different types of CTES exists latent and sensible heat storages. The first one implies that the heat is coming from the phase transition [67], where the charging process is represented by solidification of the storage material while discharging by melting of it.

Since the supermarket applications feature highly fluctuating refrigeration loads over the day because of the opening-closing hours, the CTES is a potential candidate to reduce the

energy consumptions shifting part of the peak load which is cut in the morning/afternoon to the night-time. Unfortunately, the concept of CTES in the supermarket has been introduced only a few years ago and still at the theoretical phase, is still a challenge and with some unknown aspects. Over the years many authors proposed different solutions, such as: integration with a booster transcritical CO_2 cycles [67-70], display cabinets with integrated heat pipes and phase change material, but the major push comes from Manescu et al. [10] with an innovative concept to use the thermosyphon loop in order to maintain constant the air cabinet temperature, suitable for small capacity storages as defined by Fidorra et al. [70]. The CTES as can be seen in Figure 2.9 is located on the top of the display cabinet, and the liquid-vapor movement occurs by gravity difference. As stated by Fidorra et al. [67] there are two ways to integrate the CTES into the supermarket refrigeration systems, which is in a central position or a decentral position near the food stored.

The main issue in such configuration is to ensure correct flow of the refrigerant when the valves that command the flow coming from the compressors are closed since the pressure drops could be too high to stop the system and raising the air temperature in the display cabinet. Furthermore, it is not known the ice heat transfer coefficient during the real operation and thus the thermal performance of the condenser, nevertheless by its design.

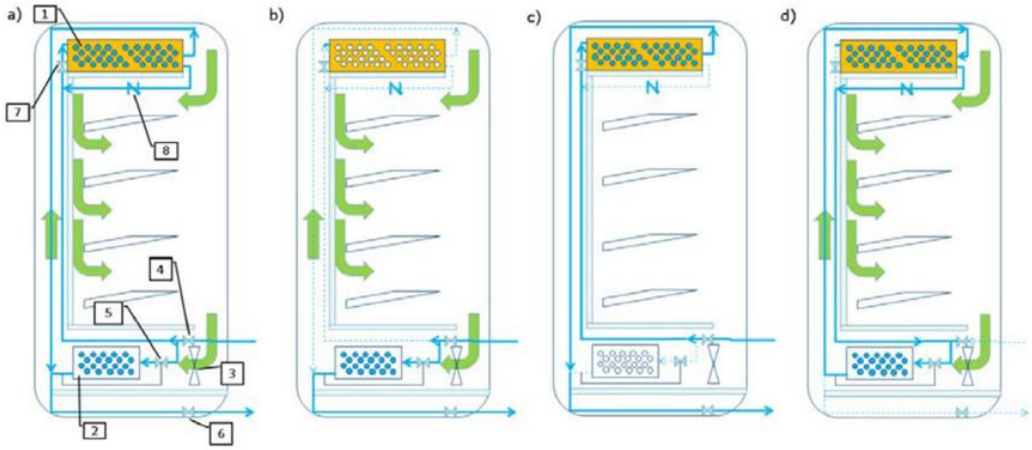

Figure 2.9: a) Charging mode and normal operation of the cabinet; b) normal operation; c) charging mode of the CTES; d) discharging by thermosyphon circulation [10].

Manescu et al. [10] have theoretically investigated a thermosyphon loop with an evaporating temperature of -5 °C by using Modelica language, proving the drawback to use the thermosyphon concept because of its own challenges in regards to the two-phase pressure drops, and flow instabilities.

As reported by Paliwoda et al. [71], -in order to achieve higher efficiencies-, overfeed (flooded) evaporators should be applied., working independently on the condensing pressure and having the advantages over the pump systems. The calculations of the refrigerant two-phase pressure drop over pipes and pipe components [72] are crucial to estimate and verify that the liquid heat can overcome the pressure drop in the evaporator and pipes. Although the thermosyphon concept is very old, those systems are limited to small capacity characterized by great uncertainty about its proper design. In the design of such systems, the dimensions of the connecting tubes and evaporator channels affect the packaging and the thermal performance of the system [73], and including the presence of a heat exchanger working with ice, the working principle is even more difficult to predict since all the different interactions are occurring during melting/freezing of the PCM [74, 75].

Only one paper, to the best of our knowledge, [76] claimed that the two-phase thermosyphon loop is currently used and manufactured by the industry, pointing out once again the difficulty of realizing on an industrial scale due to design issues. More phenomena occur during the discharging process of TPTL (two-phase thermosyphon loop), as investigated experimentally by Zhang et al. [77] which showed that the real behavior is a bit different from the conventional understanding. In fact, as normally happens when dealing with TPTL, in order to overcome the pressure drop a certain height difference is required, and if it is smaller than the conventional prediction a saturated gas blockage appears in the liquid line lowering the driving force calculation (Figure 2.10). Furthermore, larger height differences do not lead always to better performance, since there is an intrinsic relationship between liquid head – heat transfer rate.

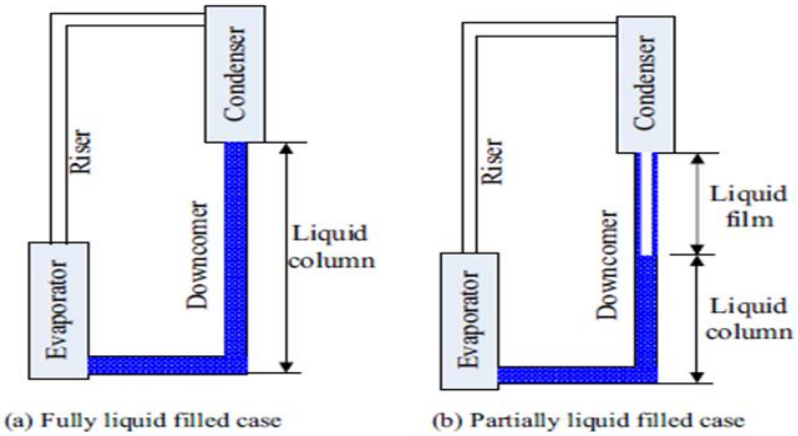

Figure 2.10: Two possible cases for the downcomer [77].

2.3.1 Summary

In this chapter, it was once again underlined the great need for eco-friendly and efficient refrigeration systems around the world. The latest innovation of the R744 refrigeration unit led them to conquer more and more space in the refrigeration field, is a very interesting solution even in warm climates thanks to the advent of ejectors, as well as overfed evaporators and many other improvements. Currently, the third-generation system called R744 IESPC system is the state-of-the-art CO_2 refrigeration unit.

Many authors have proven the IESPC system is one of the most efficient solutions among the HFC-solutions and natural refrigerant-solutions, being environmentally friendly, efficient, more compact and having a great attitude to recover the heat rejected going to satisfy partially or completely the heating demand that nowadays is important in terms of energy consumption.

The evolution of the ejectors has been widely conducted, starting from the born of such technology until today. The last development, the so-called multi-ejector block, represents the state-of-the-art of this technology and it is currently gaining more space in the market since the energy improvements coming from its implementation in the rack, as stated by many types of research in literature.

In the end, an innovative solution to push down the energy consumptions of supermarkets, CTES has been presented even though its application to commercial refrigeration systems is still today a challenge, due to the lack of knowledge. Besides that, the thermosyphon concept, old technology but still not well known, has to be implemented for the working principle.

3 Theory

This chapter introduces the history of CO_2 as a refrigerant and its thermophysical properties. The working principle of all different R744 system layouts are presented, with a particular focus on the multi-ejector supported system. Moreover, a review of the PCM materials, their use in the CTES technology and the heat transfer mechanisms involved have been explained.

3.1 History of CO_2: decline and rebirth as refrigerant

R744 is known as a refrigerant since the discovery of A. Twining which was the first one to propose it in a British Patent in 1850. The lack of a developed industry on synthetic refrigerant allowed natural refrigerants, like carbon dioxide and ammonia, to take a huge space in industrial applications [1]. R744 was commonly used in marine applications, to provide cooling for the cargo, proving to be suited for those applications more than ammonia, is toxic and flammable. Between 1920 – 1930 it has been registered the peak of CO_2 use, reaching 1800 units (ships equipped with CO_2 system).

In the 1990s began the use of CO_2 for air conditioning for comfort cooling, but the problems of leakages and capacity loss being a high-pressure working fluid, encouraged a search for efficient refrigerant especially at high pressure, and around the 1940s, the synthetic refrigerants became available [2]. The discovery of chlorofluorocarbons (CFCs) led in the 1950s to phase out completely R744 from the market, because of the CFC's better performance in cooling and heating, as well as the large propaganda made by the different industries involved in their production [78]. Only ammonia has remained as the preferred refrigerant in large industrial machines.

With the Montreal Protocol in 1987, the research pointed out the adverse effects of the synthetic refrigerants in the atmosphere, identifying their danger thanks to the GWP and ODP. The global warming environmental issues led to prompt new environmental refrigerants into the market and to abandon the ODP refrigerants as CFC, causing the renaissance of the use of the natural refrigerant [2]. At the beginning with particular attention to ODP refrigerants, and later on to the GWP by the Kyoto Protocol in 1997, the synthetic refrigerants (CFCs and HFCs) have been labeled as harmful to the atmosphere. A great contribution to this transition was given by Lorentzen in 1990, emphasizing how the

thermophysical properties of CO_2 can be properly used in the refrigeration systems design [50, 79, 80]. Among all the natural refrigerants, CO_2 is the only non-flammable and non-toxic fluid that can also operate in a vapor compression cycle with temperatures below 0 °C.

The re-introduction of the natural refrigerants in the market has seen the development of a new family of synthetic refrigerants (HFOs), like R1234yf, which is a low-GWP refrigerant [81]. Although these refrigerants are suitable for warm climates, present a very low GWP and insignificant ODP, they are not available in nature and consequently more expensive to produce.

3.2 CO_2 as a refrigerant

CO_2 was proposed as a working fluid in refrigeration application in 1850. The decline and revival of this refrigerant occurred with the advent of the synthetic fluids and with the great contribution by Lorentzen in 1989, respectively. The two main reasons for its revival are the specific thermodynamic properties that play an important role in the design of the system and its components, and being an environmental-friendly refrigerant, neither toxic nor flammable, it has attracted a lot of attention during the phasing out of the synthetic refrigerants. The recent years have been marked by a lot of work addressed to improve as much as possible the COP of the R744 systems, in order to tale a full advantage of the environmentally friendly properties, in particular of the low GWP. An overview of CO_2's properties and comparison with other popular working fluids used in conventional refrigeration systems has been shown afterward.

3.2.1 R744 Properties

The CO_2 phase diagram is represented in Figure 3.1. The critical temperature and pressure are respectively 304.31 K (around 31 degree Celsius) and 73.8 bar, which affects a lot the efficiency of the refrigeration cycle and many other aspects. Above the critical point, the refrigerant is in a supercritical state where there is no distinction between liquid-vapor phase. In this region takes place a process which is called gas cooling, where the refrigerant is not condensing but rejecting heat as long as the pressure is above the critical point.

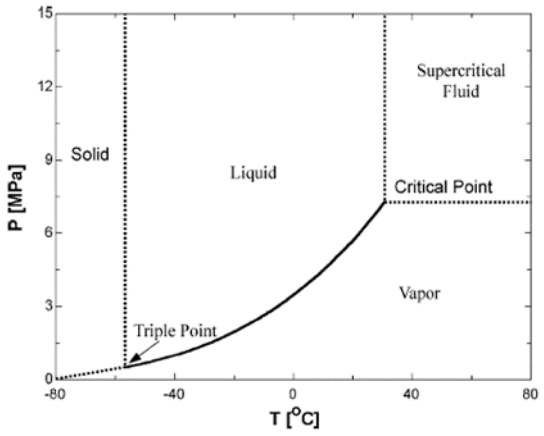

Figure 3.1: Phase diagram of CO_2 [25].

Moreover, the high-side pressure and temperature in the supercritical region are not coupled and can be regulated independently to get the optimum operating condition. Owing to the low critical temperature and high-reduced pressure of CO_2, the low-side conditions will be much closer to the critical point than with conventional refrigerants. The triple point (5.18 bar and -56.57 degree) represents the condition where all the three phases exist and together with the triple point the lower and upper limit of any condensation and evaporation process.

Unlike most refrigerants, R744 thermodynamic properties imply operating both in the subcritical process and transcritical process. It is worth to mention that the heat rejection will take place in most cases at supercritical pressure causing the pressure levels in the system to raise, making the cycle transcritical and very suitable for heat recovery applications, such as DHW, heating space, etc. In Figure 3.2 it is shown the subcritical and transcritical cycle with the main processes occurring.

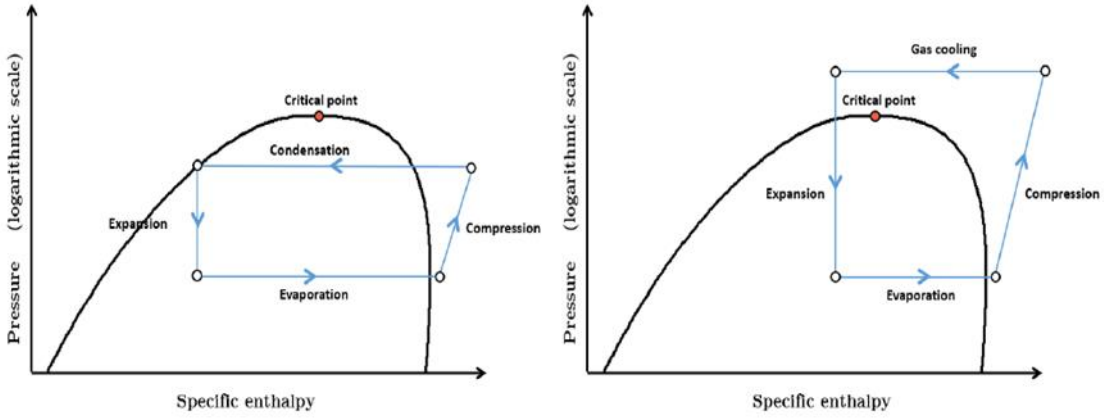

Figure 3.2: Subcritical and transcritical R744 refrigeration cycle, respectively.

As can be seen, the condensing process becomes a gas cooling process during transcritical conditions where a dense gas is progressively cooled down at constant temperature, normally with worst performance than when it's operating in subcritical conditions. Further information will be presented in the following sub-chapter, related to the work of Kim et al. [25], which has been done a review on thermodynamics properties of R744 and compared them to those of other refrigerants normally used in the refrigeration field.

3.2.2 Thermodynamic and transport properties

Figure 3.3 has shown the main properties of some refrigerants which were widely used in the past.

Properties — Ideal Cycle -30°C/+30°C

Fluid	R22	R134a	R404A	R407C	R410A	R290	R717	R744
	HCFC	HFC	HFC (mixture)	HFC (mixture)	HFC (mixture)	propane	ammonia	CO2
Molecular Mass[kg/kmol]	86.47	102.03	97.60	86.20	72.59	44.10	17.03	44.01
Critical Temperature [°C]	96.1	101.1	72.0	86.1	70.2	96.7	132.3	31.1
Critical Pressure [bar]	49.9	40.6	37.3	46.3	47.7	42.5	113.3	73.8
Normal Boiling Point. (glide) [°C]	−40.8	−26.07	−45.8 (0.8)	−40.2 (6.9)	−51.4 (<0.1)	−42.1	−33.3	−78.5 subl
p_{cond} (+30°C) [bar]	11.92	7.70	14.21	12.70	18.90	10.79	11.67	72.05
p_{evap} (−30°C) [bar]	1.64	0.84	2.04	1.54	2.73	1.68	1.19	14.26
Volumetric vaporisation heat [kJ/m³]	1674	972	1999	1655	2677	1595	1414	11230
q_{0v} (−30°C) [kJ/m³]	1143	752	1107	1071	1747	1007	1123	4894
λ_l (−30°C) [W/(mK)]	0.109	0.106	0.086	0.117	0.134	0.122	0.655	0.136
ρ_v (−30°C) [kg/m³]	7.38	4.43	10.55	6.86	10.60	3.87	1.04	37.10
Compression Ratio(-30÷30 °C)	7.27	9.10	6.97	8.25	6.92	6.42	9.81	5.05
ODP	0.05	0	0	0	0	0	0	0
GWP (100 years)	1700	1550	3800	1700	2000	3	<1	1/0

Figure 3.3: Thermodynamic – transport properties of R744 – other common refrigerants used in the past and nowadays.

One of the main advantages coming with the use of R744 is the high volumetric vaporization heat meaning that it is needed a much smaller volume of refrigerant to get the same cooling effect compared to other refrigerants (3-10 times higher than synthetic fluids). This provides a compact system (smaller pipes) that is necessary for many applications where the space is crucial. From the design point of view, the drawback of R744 being a high working pressure fluid implies to carefully design the system as long as the typical pressure in CO_2 systems is 5-10 times higher than in conventional systems requiring thicker pipes and

penalizing, in particular, the compressor's design. In Figure 3.4 it can be seen the much higher CO_2 vapor pressure than conventional refrigerants and the slope of the saturation curves.

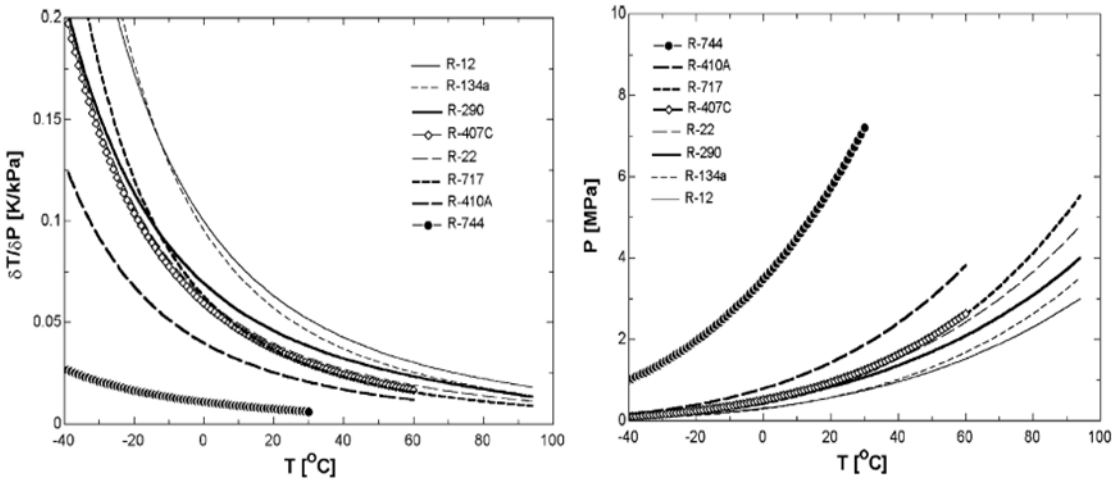

Figure 3.4: Slope of saturation pressure curve dT/dP and vapor pressure for different refrigerants [25].

The slope indicates the saturation temperature drops that occur when there are pressure drops, and it is easily visible how R744 has optimal properties to maximize the heat transfer performance in the cycles. Those pressure and temperature drops must be considered during the design of each heat exchanger in the system, realizing that since for the same pressure drop with CO_2 the temperature drops are very limited, it is acceptable to have higher pressure drop than with conventional fluids in order to increase the velocity and the heat transfer coefficient as consequences. Other properties that positively impact the heat transfer coefficient is a high liquid thermal conductivity.

Furthermore, considering all the previous notes, the best way to maximize and efficiently use the R744 thermodynamic properties is to use higher mass leading to small pipes as a microchannel, which is very suitable for CO_2 applications. A remarkable reduction of the investment costs can be achievable.

3.3 R744 booster refrigeration systems

The first generation of the CO_2 refrigeration unit includes the booster system. As explained in the sub-chapter above, the cooling load can be supplied running the system in two different ways depending at which temperature the heat is rejected: subcritical or transcritical cycle.

The first prototype was developed in the framework of the EU Project “Life” at the Danish Technology Institute in 2006 [6].

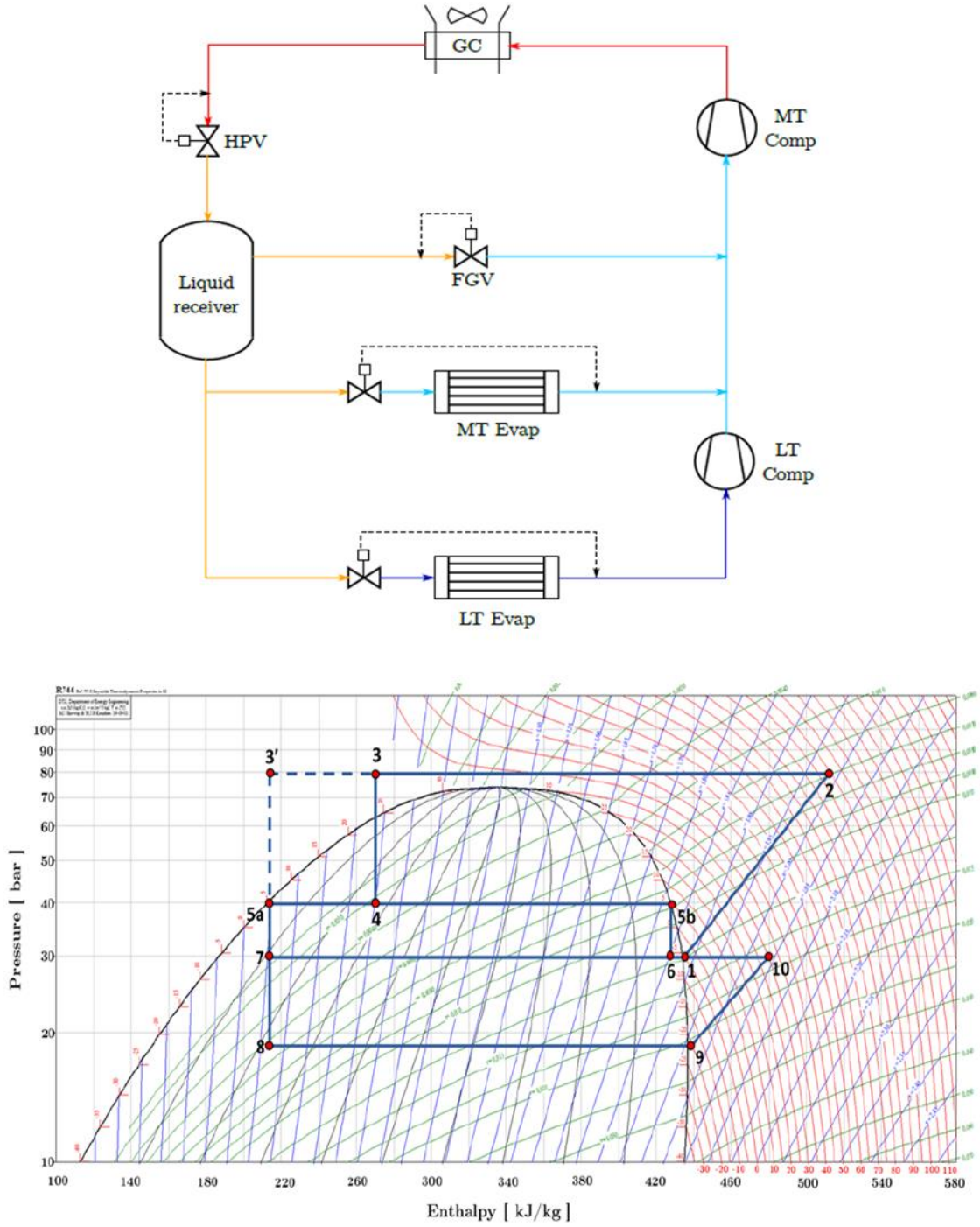

Figure 3.5: Transcritical Booster system and its log(p)-h diagram.

The booster system meets the cooling demand utilizing the following components: high-pressure valve (HPV), the gas cooler (transcritical conditions) or condenser (subcritical

conditions), two-stage compressor cascade LT and MT compressors, and two-stage evaporators (LT and MT). It is illustrated in Figure 3.5.

The booster system is extremely efficient in mild-cold climates and its performance deteriorates fast when the outdoor temperature rises, due to the low critical point of CO_2. The four different colors in Figure 3.5 indicate the different pressure levels in the system, high pressure in red, intermediate pressure in orange, medium pressure in light blue and low pressure in dark. In the p-h diagram, the main operating points are marked. Starting at a high pressure level (2), the superheated vapor goes through the gas cooling process (2→3) (transcritical) or the condensing process (subcritical). After that, the refrigerant is sent to the throttling valve (3 → 4) which represents the main loss in a transcritical cycle pointing out the need to improve as much as possible it's potential compared to conventional refrigeration systems in order to make it competitive even in warm climates. When it comes to the liquid receiver (4), the mixed fluid is separated into two streams (5a and 5b) sending the liquid towards the electronic expansion valves before each evaporating level (5a→7 and 5a→8), while the saturated vapor is throttled to the MT pressure level by using the FGV (5b→6). The role of the FGV is extremely important because it is regulating and maintaining constant the receiver pressure, guaranteeing a safe supply of liquid refrigerant to all evaporators and controllable refrigeration capacity. The refrigerant is then vaporized in the MT (7→1) and LT evaporators (8→9), leaving the evaporators with a certain degree of superheating (usually 5-8 K) ensuring to not have liquid droplets at the inlet of each compressor stage. The superheated vapor at point 9 is then compressed by LT compressor pack to the MT pressure level but because of the high discharge temperature, a desuperheater unit is strongly recommended before the mixing with the vapor coming from the outlet of MT evaporators. In the end, the total mass flow in the system must be compressed from the MT level to the high pressure (1→2), and the cycle restarts.

While the superheating, necessary to ensure proper feeding of the compressors, can have a negligible, negative or positive impact on the COP of the system depending from where the heat is taken (if from the refrigerated space or external ambient), the subcooling (3→3') has always a positive effect on the COP reducing the amount of vapor in the liquid receiver and therefore the throttling losses through the FGV. The degree of subcooling strongly depends on the condensation temperature because if the inlet temperature of HPV drops the pressure difference between the receiver and evaporators become too low, leading the receiver to collapse and proper feeding of the evaporators can no longer be guaranteed. This can be

avoided working with the controller, for instance maintaining a minimum gas cooler outlet temperature, or bypassing some refrigerant by using a three-way valve.

3.3.1 Parallel compression cycle

The second generation of the R744 refrigeration units is the parallel compression cycle. As the external temperature rises the amount of vapor to be throttled by the FGV increases leading to high expansion and heat rejection losses, therefore worst performance than with conventional refrigeration unit with synthetic refrigerant. The R744 refrigeration unit can fit warmer climate employing a parallel (or Intermediate) compressors. The system is presented in Figure 3.6.

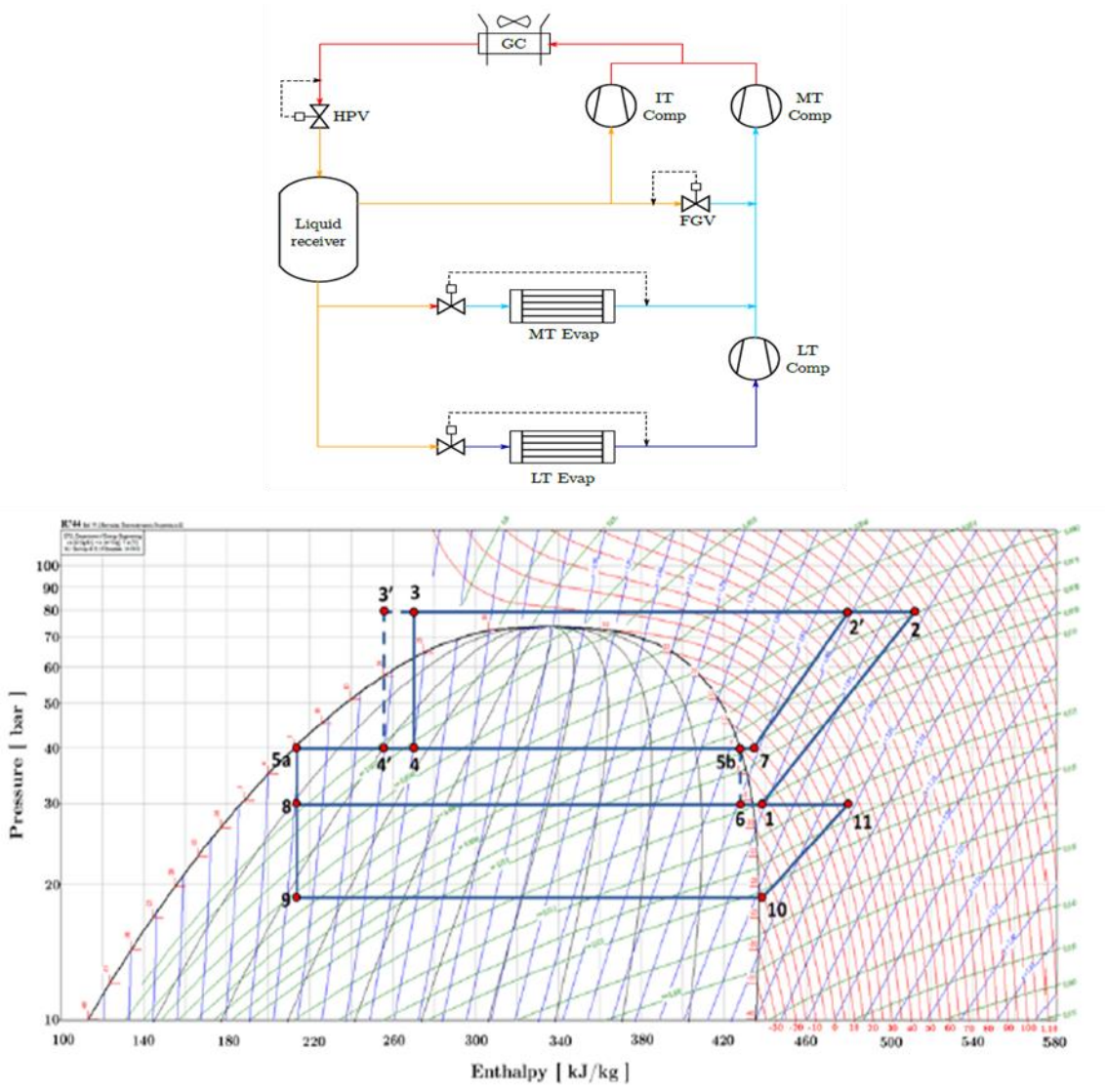

Figure 3.6: Standard booster system with Parallel compression and its log(p)-h diagram (implementation of IHX is shown only in the p-h diagram).

Having an auxiliary compressor reduces the losses due to flashing, and as long as the amount of vapor is sufficiently large it is operative (7→2'), otherwise when the amount of flash gas is too low in order to prevent the very poor performance of those compressors the vapor is throttled by FGV (5b →6), operating as a conventional booster system during winter. Furthermore, an IHX can be employed enhancing the efficiency of the system as aforementioned before since the subcooling has always a positive effect on the cycle (3→3'), and contemporary superheat the suction of the parallel compressors (5b→7) ensuring dry vapor at the suction.

The advent of the parallel compressor concept has made the integration of AC possible and efficient since the AC cooling capacity is provided by the auxiliary compressor, determining the pressure level of the separator.

3.3.2 The multi-ejector system

The latest layout is to replace the high-pressure valve with a multi-ejector block enabling for expansion work recovery showing optimal energy saved in warm climates. This is called the third-generation systems and it is presented in Figure 3.7. The multi-ejector block implemented is normally called MT multi-ejector as it is working with high-pressure lift and low entrainment ratio (see green – red line). Moreover, this layout is equipped with a liquid separator that is connected to the suction lines of two liquid-ejector cartridges, enabling the overfeeding of the evaporators and consequently a better use of the heat transfer area.

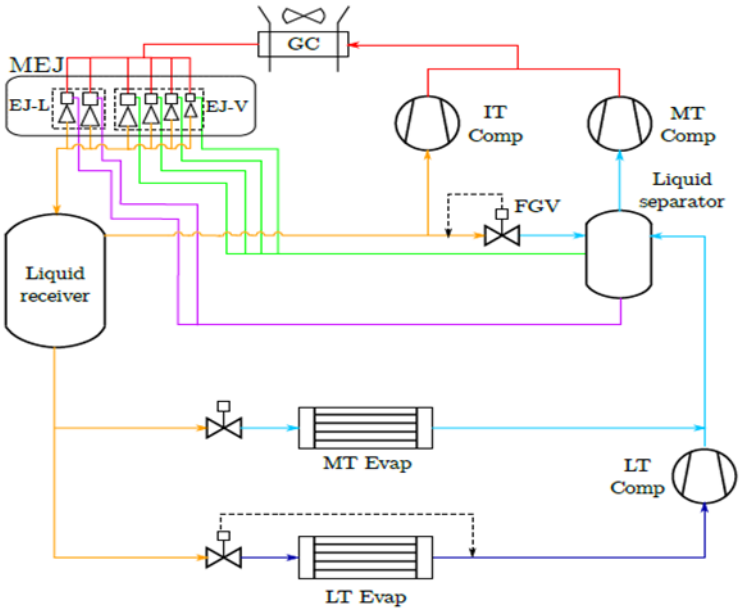

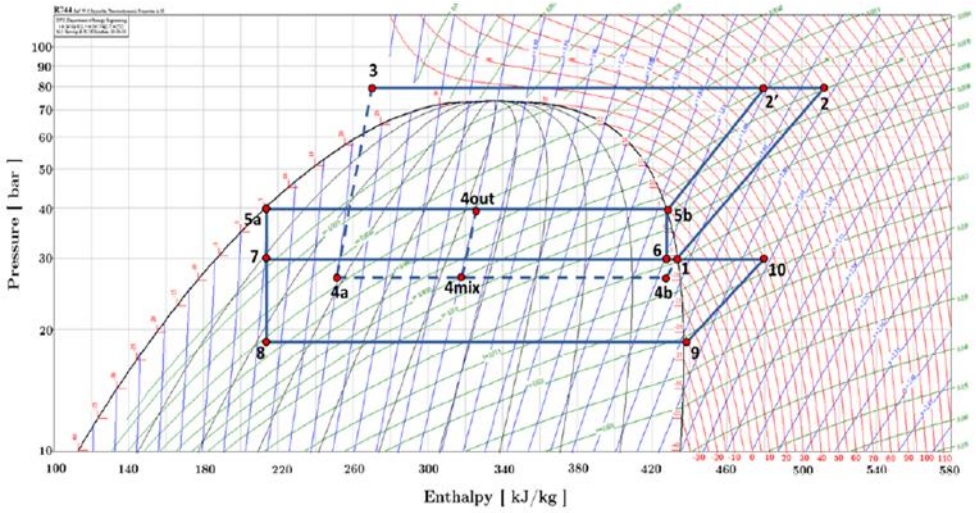

Figure 3.7: Standard booster system equipped with multi-ejector systems and parallel compressor unit with the pertaining cycle in the p-h diagram.

The amount of vapor pre-compressed by the ejectors and discharged into the separator is determined by the available expansion work, extending the operation time of the parallel compressor and lowering their maintenance costs. Substantially part of the MT load is shifted by ejector to the parallel compressor which is working with a lower pressure ratio, hence reducing drastically at very high temperature the power demand.

The high energy stream flow, called motive flow enters in the ejector nozzle (3→4a) contemporary with the suction flow (1→4b), undergoing a throttling process. After mixing (4a&4b → 4mix), the refrigerant is expanded using the energy available by the fluids entering in the nozzles to the receiver pressure (4out), where the two phases separate. For further information about the ejector, the principle sees the sub-chapter.

3.3.3 Multi-ejector system with air conditioning

As stated many times before, the heat rejection losses in R744 refrigeration unit are very large particularly at high ambient temperature but this disadvantage can be turned into a benefit recovering the heat rejected for many purposes (DHW, space heating, etc.) and allowing such systems to become an economically competitive alternative in warm climates.

Pardiñas et al. [9] proposed the two following options to integrate air conditions evaporator in a multi-ejector supported system. These are shown in Figure 3.8.

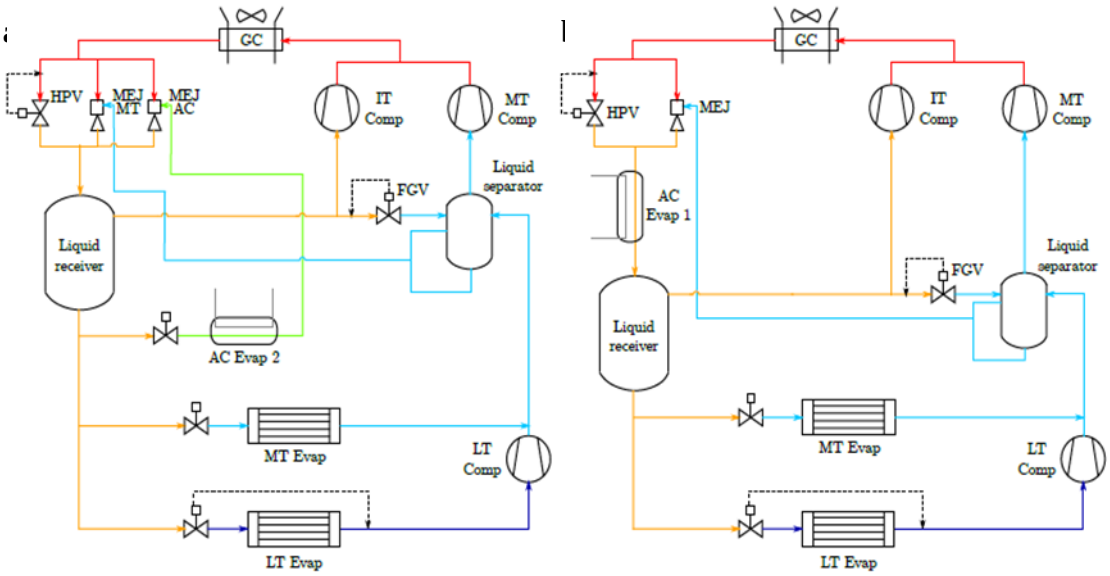

Figure 3.8: R744 booster system equipped with a parallel compressor, multi-ejector block, overfeed MT evaporators and AC production located in two different positions [9].

In the layout b) the AC evaporator is positioned downstream the high-pressure control device, where the HPV is installed in parallel with a multi-ejector block as a safety device. The refrigerant vaporized is sent to the liquid receiver where afterward is sucked by IT compressors. The AC load can be regulated by using a three-way valve installed downstream the high-pressure control device. The system costs depend on the AC load size, which could stand for a considerable part of the total load of the supermarket because a large amount of vapor has to be compressed by IT compressors requiring to have enough capacity at this pressure level. Here it's really interesting the implementation of the pivoting compressors as stated by Hafner et al. [8] and Pardiñas et al. [9].

The innovative solution a) consists of the introduction of an AC evaporator at a pressure level slightly lower than the liquid receiver but at a higher pressure level than the medium pressure located downstream the liquid receiver. The AC evaporator is supported by a second multi-ejector block (MEJ AC). It delivers the refrigerant from the AC evaporating pressure to the receiver pressure, controlling the lift between them. The multi-ejector block covers the AC load with a different combination of cartridges in order to keep constant the pressure lift and suck all the refrigerant.

3.4 Ejector theory

Using an ejector instead of conventional HPV is an approach to improve the energy efficiency of R744 systems. An ejector, Figure 3.9, is a device that uses the energy released during the expansion of a high-pressure stream (motive flow) to pre-compress a low-pressure stream (suction flow).

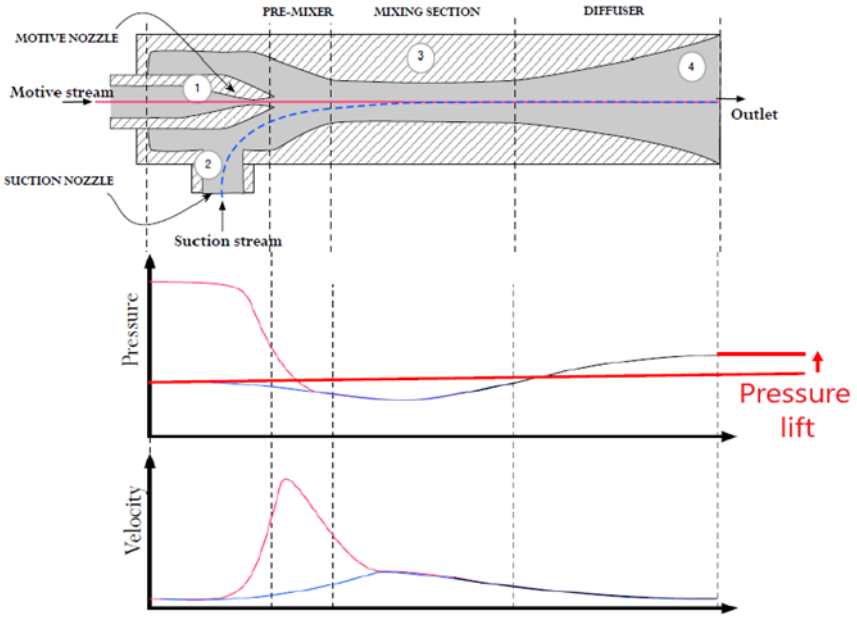

Figure 3.9: Working principle of the ejector [54].

It has no moving parts and consists of four sections: motive and suction chamber, mixing chamber and the diffuser where the refrigerant is delivered to the receiver pressure level. The whole principle is based on the conversion of potential energy to kinetic energy. The high-energy stream (motive flow) enters and when the section decreases the speed is very high, while the low pressure is used to drag vapor from the MT level. The two streams are mixed in the mixing chamber before entering the diffuser section where the cross-section area increases slowing down the velocity and increase the pressure. Here, thanks to the diffuser shape, the conversion from kinetic energy (velocity) to potential energy (pressure) takes place.

According to the load requirements and ambient temperature, a multi-ejector block is more suitable to control the high pressure in the system accurately. Another option that has no gain too much space in carbon dioxide refrigeration applications is the needle-based ejector. In this case, the heat rejection pressure can be regulated either working with the motive nozzle position or with the suction nozzle throat area. The first approach is the standard one used in all the R744 applications. The capacity is matched by using different

combinations of ejectors because the multi-ejector block as mentioned before is a combination of up to six static ejectors in one solid casing. Each cartridge has a different geometry that can be utilized by the logic controller implemented in the system. They are activated by using solenoid shut-off valves at the inlet of the motive nozzle and a check valves at the suction nozzle.

It is worth to explain separately the advantages coming from the implementation of an HP or LP multi-ejector block. HP ejectors are always used in systems with parallel compression, reducing considerably the power consumption, increasing the refrigerating effect as well as permitting overfeeding of the evaporators. As stated before, two liquid cartridges are used for this purpose. HP multi-ejector block is shown in Figure 3.10.

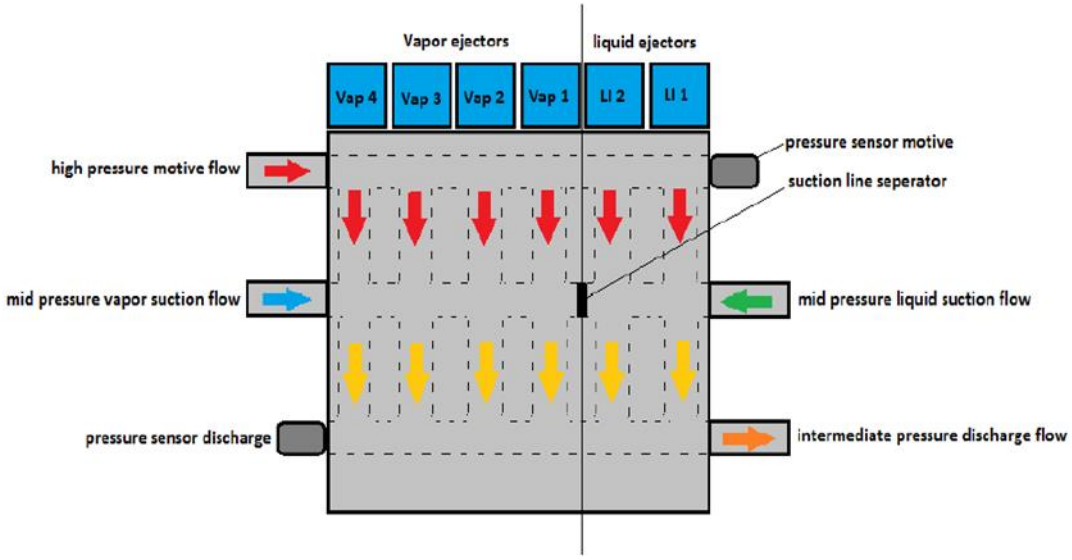

Figure 3.10: Scheme of HP multi-ejector with separated suctions for liquid and vapor.

On the other hand, LP multi-ejector works with a low-pressure lift and high entrainment ratio, pumping the gas from the evaporators back to the receiver. They suit very well systems that are operating in mild climates where little flash gas is formed. However, as mentioned upstream, including both LP and HP multi-ejector blocks are becoming very popular since the trend nowadays is moving towards to compact system able to provide cooling and heating (IESPC systems).

As stated by the research, two phenomena can impact the efficiency of those devices affecting as consequences the overall efficiency of the system, losing partially or completely the work recovery. They are stall condition (critical back pressure) and choking of the entrained flow. The first phenomena is more common in cold climates where the high

pressure is low and no energy is available to be used in the motive flow, it happens every time the ejector is forced to give a lift that is significantly higher than what it was designed for, reducing quickly the suction flow and forcing the entrainment ratio to go to zero. It is not dangerous for the ejector itself, but it will force the ejector operating as a throttling valve only. To prevent this issue the multi-ejector is equipped with individual check valves at each cartridge. As visible in Figure 3.11 a) the ejector efficiency drops from 25% to less than 10%.

Choking flow is the opposite of the stall. This occurs whenever the high pressure is too high, being the ejector capable of making a high lift while at the same time the suction pressure is quite low. The very high mass flow cannot be accommodated in the mixing chamber leading the ejector to chocked conditions. As represented in Figure 3.11 b) if there is too much-entrained flow, the motive flow is not able to provide a high enough lift, deteriorating a lot the efficiency and the cycle performance.

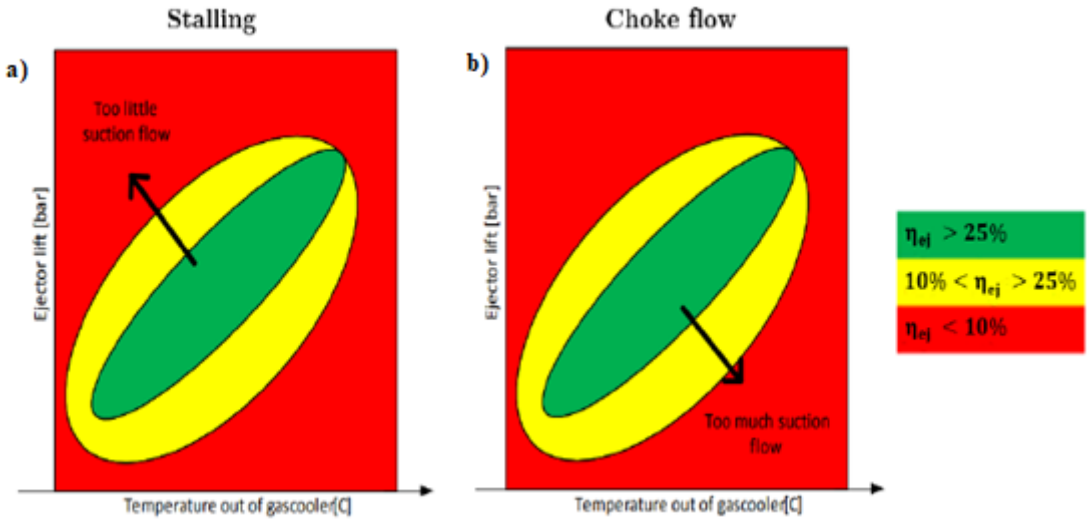

Figure 3.11: Phenomena affecting the ejector performance [53].

3.5 Thermal energy storage and PCMs

In supermarkets, special peaks of cooling load arise in the morning and in the afternoon during the busiest hours of the sale. The refrigeration systems must be designed to cover these peaks, but most of the day they are working at partial load which is not an efficient operation mode. Therefore, thermal energy storage has been found as one of the best options to overcome the challenge of time-shift energy production control. A large part of the refrigeration load can be shifted to the night hours allowing reduction both in the energy demand as well as the installed capacity of the compressor packs, due to a lower ambient

temperature, but also a lower price in electricity at night. This technology has been widely investigated even though it has not been broadly taken into consideration yet because of the unknown aspects involved.

One of the most interesting types of thermal storage applied in supermarkets are phase change materials (PCMs). LHTS consists of a material where the energy needed to change the phase, called latent heat, is used to store thermal energy. The energy of phase change is much larger than that of temperature change alone, resulting in a higher energy density and making as consequences the system more compact. The PCM is usually enclosed into capsules or containers, and because the phase change takes place almost at a constant temperature, the temperature distribution around the PCM will be very stable. Having PCM integrated with the display cabinets and some renewable energy sources could be very smart as long as during periods with high electricity production the excess cold produced by the refrigeration system can be stored in the PCM unit, be utilized later when the electricity production drops (i.e. during the night with photovoltaic systems).

Equation (3.1) defines the thermal energy that can be stored using PCMs. It includes three terms, where two of them represent the sensible energy corresponding to the period of time where the temperature is either raised or decreased, and one term referred to the energy stored throughout the phase change. Therefore, the energy density for LHTS writes:

$$Q = m_s c_{ps}(T_m - T_1) + m_l c_{pl}(T_2 - T_m) + mfL \quad [J] \tag{3.1}$$

where c_{ps} and c_{pl} are respectively the specific heat of the solid and liquid phase, m_l and m_s are, respectively the liquid and solid mass, f is the liquid fraction, L the latent heat and T_m is the melting temperature of the material. As reported in Figure 3.12, it can easily observe that LHTS perform much higher energy density than SHTS [82].

PCMs are the most representative materials of this kind of thermal storage (mainly in the liquid-solid transition). Three different categories can be considered: organic, inorganic, and liquid metals [83]. The organic PCMs are the most popular type of PCM mainly due to their high availability and low cost, and they are characterized by a phase change process that occurs smoothly between a range of temperatures. The inorganic PCMs have usually higher thermal conductivity than organic PCMs (paraffin), which is an important aspect in the choice of the most suitable PCM depending on the application. The metallic PCMs are probably the less commonly found mainly because of their lower latent heat. Nevertheless, some of their

characteristics as the easiness to work with them, chemical stability and wide range of melting points and even higher thermal conductivity make them an interesting option.

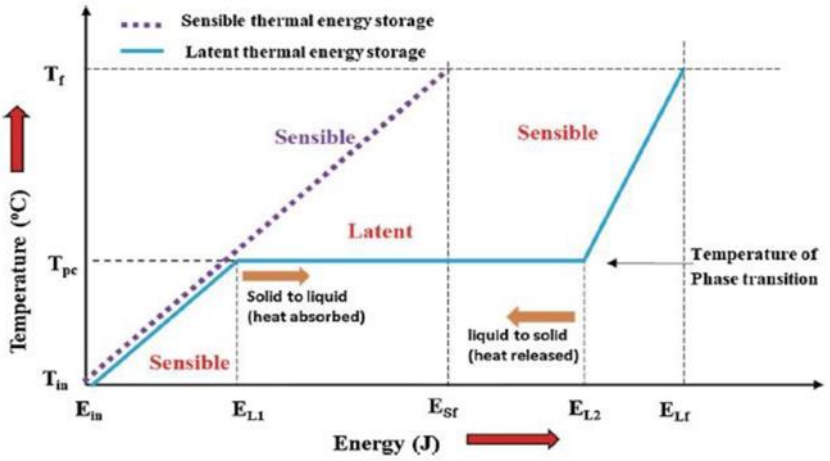

Figure 3.12: Comparison of phase transition profile of a storage medium, between a LHTS and SHTS [82].

3.5.1 Advantages and disadvantages

Some benefits and disadvantages can be summarized as follows:

- No energy consumption since they absorb and release heat without any additional power input
- The high thermal density which means the mass is the system can be easily reduced, as well as the space occupied by the system
- The capacity of maintaining almost a fixed temperature, enhancing the stability of the temperature in the system
- As a disadvantage the compatibility of the PCM with the container has to be taken into account because wrong combinations between PCM-container material can lead to leaks of the PCM or deterioration of the material lowering the heat transfer performance, affecting the freezing/melting of the PCM. That process can occur inside/outside the tube, while the other medium HTF is flowing releasing or absorbing the heat, depending on which phase change process is occurring
- Another one, is the limited life of some kind of PCM, because the charging-discharging process degrades the material, hence losing effectiveness after a given number of cycles.

3.5.2 Cold Thermal Energy Storage

CTES takes usually the form of LHTS leading to energy savings, a more compact system and fewer investment costs. This technology, currently considered as a valuable option to reduce further the consumption in supermarket refrigeration applications, requires two mediums (HTF and the PCM). Commercial cooling is a major contributor to peak power demand, but it represents one of the few areas where the load managements are practical, cost-effective and proven. These units are based on a simple principle of operation that takes place in two different periods of time, which are strongly dependent on the size of the storage. The first process is:

- Charging operation mode: During this period of time, which normally occurs during the night, the display cabinets in the supermarket are connected to the refrigeration systems requiring some power input to raise the vapor refrigerant pressure. In this case, the heat in the cabinet is absorbed both via the air evaporator and the cold storage which is acting as an additional evaporator. Therefore, using water as PCM, a phase change occurs (water to ice). However, this process usually is not considered an issue because it takes place for many hours, turning almost of the water volume to ice which will be used later during the discharging process
- Discharging operation mode: when the charging process was successfully done, the discharge takes place. Now the valves connected to the refrigeration unit must be closed and the CTES is acting as a condenser. The principle is now the two-phase thermosyphon loop, a natural heat transfer device where the working fluid (R744) is circulating along the loop by gravity rather by the pump

3.5.3 Thermosyphon working principle

The heat transfer method that defines the thermosyphon effect is natural convection. It is beginning to be extensively used in the field of air conditioning and heat recovery, as well as for cooling of electronic components (with some difference in terms of power requirement and temperature difference evaporator – condenser).

Natural convection takes place when the density difference is present. In Figure 3.13 is illustrated the systems that consider an evaporator, condenser, downcomer, and riser. The refrigerant vaporized in the evaporator, having a lower density starts to go up (riser) reaching the condenser, where it changes phase to liquid, and due to the high density, the refrigerant

moves towards the evaporator and the cycle restarts again as long as the pressure drops are overcome by the liquid head (downcomer) [77].

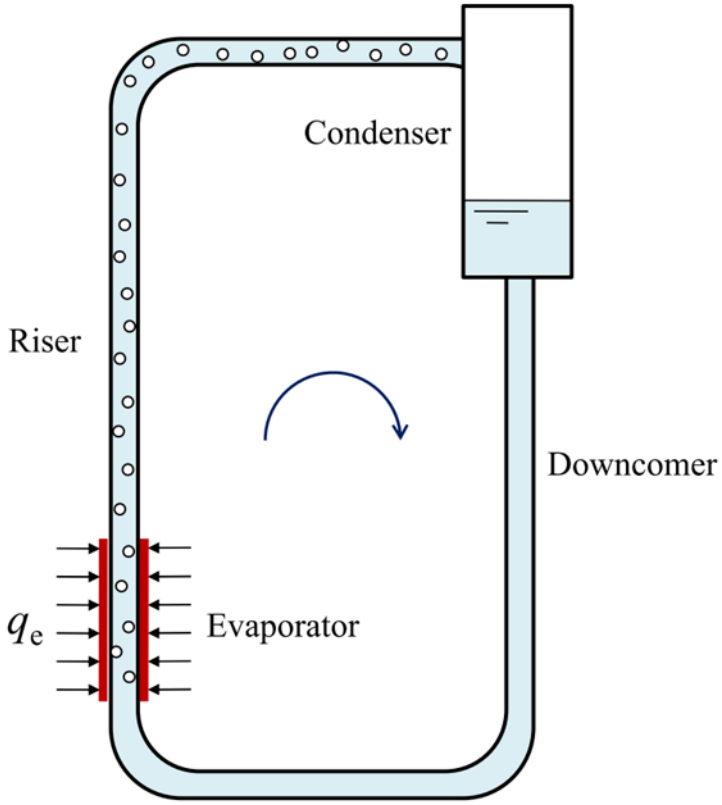

Figure 3.13: Typical structure characteristics of the traditional thermosyphon application [77].

Many differences must be taken into consideration when air conditioning or heat recovery applications are considered. In this case, the system works between two fluid streams rather than fixed heat flux (which is an intrinsic feature of many applications), making the flow of refrigerant more difficult to be predicted. It is remarkable to underline the much smaller temperature difference condenser – evaporator which affects the pressure difference between the two heat exchangers, therefore the driving force. The rise in pressure occurring in the downcomer can be calculated using the following equation (3.2):

$$\Delta P = (\rho_l - \rho_v) g \Delta z \tag{3.2}$$

where ρ_l and ρ_v are liquid and vapor density respectively, g is the gravitational acceleration and Δz is the height difference between evaporator – condenser.

3.5.4 Stefan problem and the enthalpy – porosity method

Historically, the solidification/melting processes, also widely known as Stefan problems, had been challenging to accurately predict due to the moving interface between the solid and liquid phases. Furthermore, in that region, the thermophysical properties change continuously as the latent heat is released or absorbed depending on the conditions of the HTF. During the years many approaches have been carried out with different grades of success. One of them that allows us to track the phase change front indirectly from the solution looking where the energy jumps by an amount equal to the latent heat are the enthalpy-porosity method [84]. It is the easiest, most-popular fixed-domain method, direct and represents a physical way of dealing with this kind of problem.

The success of the enthalpy-porosity method lies in the simple structure of the model and thanks to the fixed grid enthalpy-porosity formulation, where the enthalpy is formulated in the following way (3.3):

$$H = h + \Delta H \tag{3.3}$$

where h = cT is the sum of the sensible heat and ΔH is the latent heat which is expressed as a function of the temperature:

$$H = f(T) = \begin{cases} L & T \geq T_l \\ L \cdot f & T_l > T \geq T_s \\ 0 & T < T_s \end{cases} \tag{3.4}$$

where f is the liquid fraction in order to track the amount of liquid contains in each cell in which it is divided the domain and re-built the liquid zone at every time-step, while T_l and T_s are liquid and solid temperatures respectively. The (3.4) differentiates the three phases developed during the melting process which are the solid phase (ΔH = 0), liquid phase (ΔH = L) and the mushy zone (0 < ΔH < L), that is the transition zone between the liquid and solid phase.

The only drawback is that the accuracy of this method strongly depends on the number of cells, therefore on the spatial discretization decided for a certain domain. A higher number of cells leads to a higher accuracy but also higher computational cost. Moreover, the mushy region is characterized by a small and finite temperature difference in order to reduce the instabilities of the solution for a pure melting material.

An important modification takes place in the momentum equation. A momentum sink terms (called Darcy source term) are added to the momentum equations to bring to zero the velocity in the solid phase, while the velocity in the mushy region is controlled by the mushy zone constant which will affect the melting rate (3.5):

$$S = \frac{(1-f)^2}{(f^3-\varepsilon)} A_{mush}(\vec{v} - \overrightarrow{v_p}) \tag{3.5}$$

where ε is a small number to avoid division by zero, $\vec{v}$ is the velocity and $\overrightarrow{v_p}$ is the pull velocity (not relevant in this project), A_{mush} is the mushy zone constant (usually oscillates between $(10^4 - 10^7)$. Thus, from the equation (3.5), the velocity field on the mushy region will be an increasing function with the liquid fraction (porosity). Whereas the liquid fraction tends to zero the velocity field will be fully developed, while the porosity tends to one, the Darcy term will force the velocity field to zero.

3.5.5 Heat transfer processes occurring in Stefan problems

A summary of the heat transfer processes is done in order to clarify and provide a deeper understanding of the phase change processes. Before explaining the conductive and convective problem, it is worth to introduce a dimensionless number called Stefan number (3.6), that is defined in the following way:

$$Ste = \frac{c_p \Delta T}{L} \tag{3.6}$$

where the numerator is the specific heat and the denominator is the latent heat. It is a useful index to immediately understand if the heat transfer will be dominated by the specific heat (high Stefan number) or latent heat (low Stefan number). PCMs usually have high latent heat, yielding to Stefan number of the order 10^{-1} and below, depending on the type of PCM.

The heat transfer mechanism involved in the phase change process affects a lot the melting rate as well as the shape of the moving front. The first mechanism analyzed is:

- Conduction: it is always present in heat transfer processes and takes place in the presence of physical media. The thermal conductivity is directly linked with the diffusive term of the transport equation (3.7):

$$\frac{\partial Q}{\partial t} = -kS\frac{\partial T}{\partial x} \tag{3.7}$$

where k is the thermal conductivity, that is related to the amount of heat released through section S due to a temperature gradient.

- Natural convection (Rayleigh-Bénard convection): It is the movement of fluid due to a temperature gradient under the effects of gravity. The density is strongly affected by the temperature, and the density difference will produce buoyancy forces that force the fluid to move, enhancing the heat transfer process (Figure 3.14).

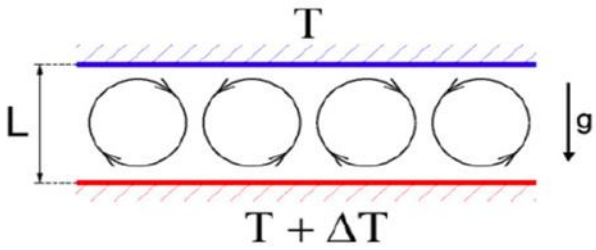

Figure 3.14: Explicative representation of Rayleight-Bénard convection.

An important dimensionless number has to be considered, named Rayleigh number (Ra). It is defined as the ratio between the buoyancy forces to the viscous forces:

$$Ra = \frac{g\beta\Delta T d^3}{v\alpha} \tag{3.8}$$

where d is the thickness of the liquid layer, β is the thermal expansion coefficient, v the dynamic viscosity and α the thermal diffusivity. Thus, from this number, it is easily understood the influence of natural convection in the heat transfer process (at low Rayleigh number conduction is the dominant one, the opposite at high Rayleigh number).

4 Experimental methodology

This section consists of the SuperSmart-Rack supermarket system installed at NTNU/SINTEF laboratory in Trondheim, Norway. The content is based on the research paper of Pardiñas et al. [9] and the facility's handbook. The first section describes the set-up of the facility and the main components in the system, while the second section will describe the case study performed.

4.1 The layout of the test-facility

The SuperSmart-Rack is an IESPC refrigeration system installed at NTNU/SINTEF laboratory. The rack is manufactured by Advansor in collaboration with Danfoss and SINTEF. The system was designed to meet the refrigeration demand for low and medium evaporating temperature, simulating a medium-sized supermarket. Furthermore, heating and air conditioning production can be simulated.

It is a very versatile system allowing a wide range of experiments to be performed, with many possible operating conditions and system configurations. The system is a two-stage transcritical unit which can run with all the generations of booster system analyzed in the previous section.

The test-rig consists basically in three different compressor packs (LT, MT, IT), many evaporators for the low and medium temperature level as well as two evaporators to simulate AC load, high-pressure control devices (HPV, LP and HP multi-ejector block), gas cooler unit, three accumulators (liquid receiver, liquid separator and suction accumulator), some internal heat exchanger.

4.1.1 Refrigerant Loop

A simplified P&ID is presented in Figure 4.1 below. Four different pressure levels are present, and they will be explained starting from the high to the low-pressure level. The high pressure is indicated in red, intermediate pressure in light orange, the medium pressure in light blue, and the low pressure in dark blue. They are also market the AC lines in grey, the glycol loop in green, the cooling water in black, and the auxiliary CO_2 loop in dark orange.

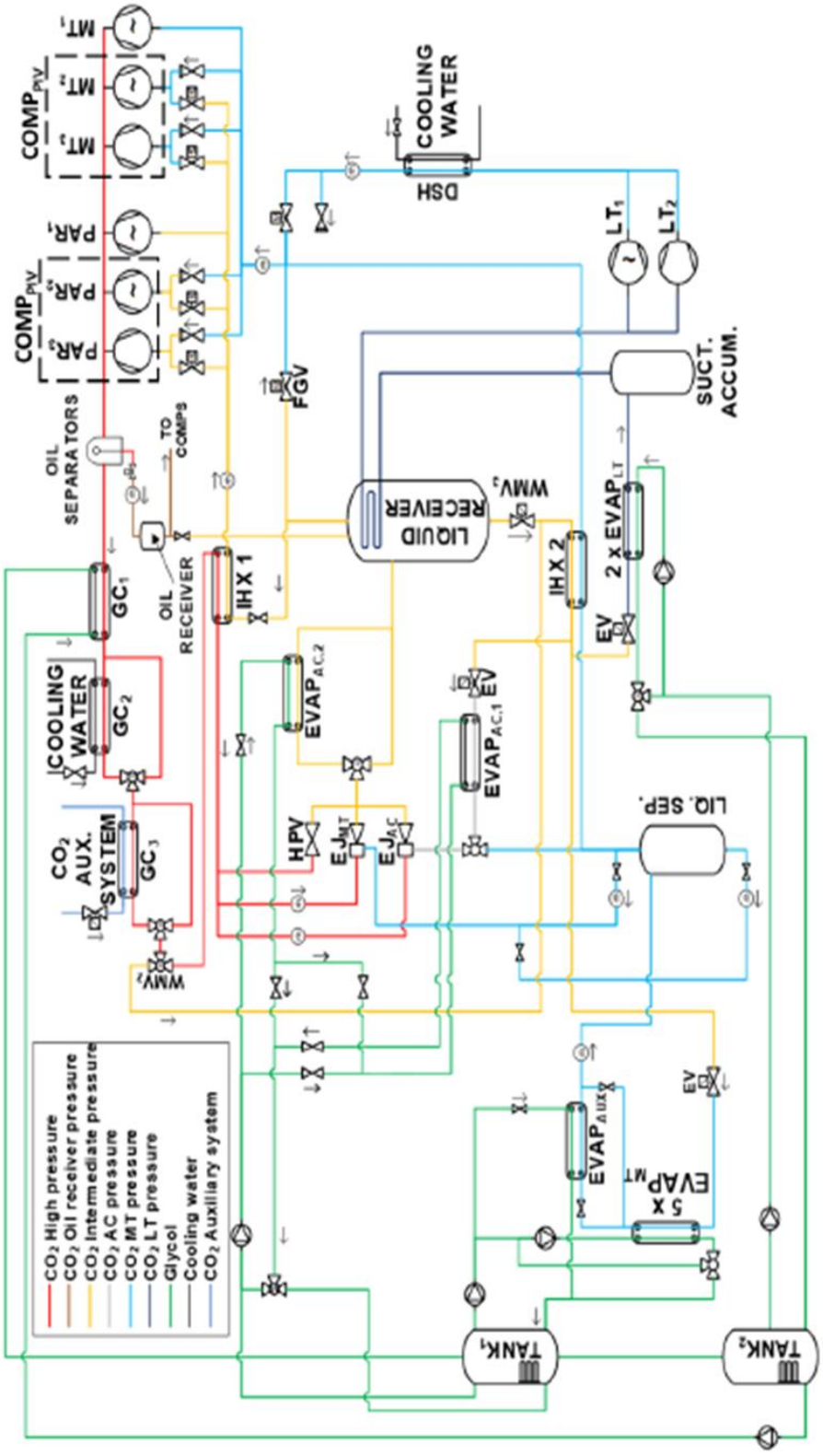

Figure 4.1: Simplified P&ID of the experimental test facility, R744 refrigeration layout and the auxiliary loops [9].

4.1.1.1 High-pressure level: 50 – 130 bar

At the discharge of the compressor, the gas cooler unit consists of three plate heat exchangers (GC_1, GC_2, GC_3) where each of them rejects heat at different temperature levels. A secondary loop is required to absorb the heat, therefore a secondary glycol, water and CO_2 loop is used in GC_1, GC_2, GC_3 respectively. When subcritical conditions need to be tested, the auxiliary CO_2 is very useful since the with water loop the temperature at the gas cooler outlet cannot be too low.

The gas cooler outlet temperature can be adjusted in two ways; therefore, three motorized three-way valves are installed located downstream each gas cooler. First, by bypassing partially or totally, GC_2 and GC_3 and secondly by regulating the mass flow rate and inlet temperature of the secondary fluids. In transcritical conditions, the optimal high pressure must be calculated considering the gas cooler outlet temperature, as stated by many authors [24, 25] because as explained in the previous section the performance of the R744 refrigeration unit strongly depends on the heat rejection pressure. The high-pressure section allows safe operation up to 130 bars.

Between GC_3 and HPV an internal heat exchanger (IHX_1) has the purpose to cool down the refrigerant leading to higher refrigerating effect and contemporary superheat the vapor at the inlet of IT compressors, ensuring gas state and preventing the compressors from damages. As it will state later during the discussion of the results, the IHX affects a lot the amount of refrigerant elaborated by the parallel compressors.

The high-pressure control device is necessary to control the heat rejection pressure, and the SuperSmart-Rack can work under different system set-ups. The HPV and two multi-ejector blocks (EJ_{MT} & EJ_{AC}) installed in parallel are present. The HPV enables the system to operate as a conventional booster with or without the parallel compression, depending on the operating conditions. The EJ_{MT} operates as an HP multi-ejector block, supporting the parallel compressors and unloading the MT compressors, hence working with high-pressure lift and low entrainment ratio. The EJ_{AC} is an LP multi-ejector block with the purpose to suck all the vapor coming out from AC evaporator ($EVAP_{AC,1}$) having a low-pressure lift and high entrainment ratio. The HPV is always working as a safety device even when the multi-ejector block is acting as the main high-pressure control device.

4.1.1.2 Intermediate pressure level: 34 – 50 bar

After the throttling process, the refrigerant enters the liquid receiver. Before the liquid receiver, an additional heat exchanger is specifically employed for satisfying the AC load ($EVAP_{AC,2}$). A motorized three-way valve was installed permitting possible AC production. In booster operation, the receiver pressure level is controlled by the mean of the FGV. In parallel compression arrangement, it is controlled with the parallel compressor as long as the amount of vapor is enough to enable their operation. Therefore, the receiver gas port is connected to the suction port of the IT compressors, while the liquid port is connected to expansion devices of the different evaporators and cabinets, through another internal heat exchanger (IHX_2), which subcools the liquid coming from the receiver superheating the vapor sucked by the MT compressors. Nevertheless, this heat exchanger will work only under certain operating conditions, depending on the pressure level of both sides.

Another heat exchanger (IHX_1) is employed for AC purposes, and it is operating approximately 3 bar lower than receiver pressure. It is equipped with an electronic expansion valve as a metering device to control the refrigerant conditions at the outlet od the evaporator, and when it is operating the LP multi-ejector it should be activated.

4.1.1.3 Medium pressure level: 25 – 33 bar

This pressure level consists of the suction line of MT compressors, MT-evaporators, DSH and the liquid separator. The MT evaporators are constituted of five helical coaxial tube-in-tube heat exchangers assembled in parallel, each of them has its expansion device. When the vaporization occurs, the vapor goes to the liquid separator. This device has two purposes: prevent liquid droplets to be sucked by MT compressors, and supply the liquid (from the bottom)-vapor(from the to) cartridges of HP multi-ejector depending on the level of the tank and so on the test. The tank is equipped with a liquid level indicator that controls the operation of the liquid cartridges and simultaneously prevents liquid droplets to reach the suction line of the compressors.

Furthermore, the MT evaporators could work either in flooded or DX mode. In DX mode the AKV will ensure an injection of liquid such to be fully vaporized, ensuring a superheating of 8 K at the suction line of the compressors. In flooded mode, to overfeed the evaporators the superheating is set to a lower value (around 3 K), leading to a mixture of liquid-vapor that leaves the evaporator, instead as superheated gas.

4.1.1.4Low pressure level: 10 – 15 bar

As well as MT evaporators, LT evaporators are helical coaxial tube-in-tube heat exchangers with individual AKV. The mixture is further sent to the suction accumulator located downstream of the LT-evaporators. It operates as a safety device preventing liquid droplets at the LT suction compressor line, being the vapor superheated inside the liquid receiver before reaching the LT compressors.

The refrigerant elaborated by LT compressors is sent to the plate heat exchanger, called desuperheater (DSH), to cool down the refrigerant seen the high discharge temperature of the LT compressor pack. The heat transfer fluid used is water, simulating what normally happens in refrigeration systems where the heat is released to the air of the machine room. Downstream the DSH, the vapor could either send to the MT suction or IT suction line depending on the position of the valves (V-679 and V-310).

4.1.1.5Oil management: 50 – 130 bars

The oil management system consists mainly of two oil separators, an oil reservoir, solenoid valves that connect each oil separator with the oil reservoir, and oil metering devices that feed the returning oil to particular compressors. Once the refrigerant leaves the compressor packs (IT and MT), is delivered to the oil separator where a coalescing filter is applied to separate the oil from the refrigerant. In the oil separator, an oil sensor level is installed thus every time the oil level passes the threshold the solenoid valve releases the oil to the oil receiver. After that with a similar procedure, the compressors can work stably as long as the oil feeding occurs correctly. It is worth mentioning it exists a differential pressure check valve between the oil-liquid receiver. Its purpose is to keep the pressure of the oil receiver at a value slightly higher than the liquid receiver, guaranteeing a good distribution of the oil to the parallel compressors where it is difficult to ensure proper lubrication.

4.1.2 Secondary loop

The SuperSmart-Rack expects three different secondary loops: glycol, water and CO_2. Each of them is operating as heat rejecters (or heat absorbers in the gas cooler) depending on the need for the test, as well as secondary heat transfer fluids to regulate loads and other parameters.

4.1.2.1Glycol loop

The glycol loop consists of a mixture of propylene glycol – water (70 – 30 % in volume). Its specific heat capacity is 3.9 (kJ/kg K), and the freezing point at atmospheric pressure is approximately -15 °C, meaning that the glycol is able to maintain its properties through the process. A simplified P&ID is illustrated in Figure 4.2. The only thing to take care is when the injection control in the LT evaporators is switched ON because being the LT setpoint set to -30°C the glycol temperature could reach values that bring to the freezing.

The glycol loop comprises two large liquid tanks of 800L each, connected to all the evaporators, first gas cooler unit and cabinets. Each tank is equipped with electric heaters with a total output of 24 kW, helping to regulate the glycol temperature. This becomes important when regulation of high gas cooler temperature is needed, because if at the outlet of the first gas cooler (functioning with the glycol loop) the refrigerant temperature is too low will be impossible to reach the design temperature, hence the glycol has to be warmer in order to raise the refrigerant temperature and simulate the high ambient temperature required in the test.

In the first GC_1 the glycol is heated up for heat recovery purposes, this would provide tap water heating which is normally required in supermarkets. The heat released to the glycol will be stored in the two tanks and afterward provide a thermal load for LT, MT and AC evaporators. In fact, the cooling loads that are normally present in a real supermarket, they have been by the warm glycol.

4.1.2.2Cooling water loop

The water is used as a secondary medium in the GC_2 and DSH for two different purposes. Both of them are equipped with a PID controller which either sets the mass flow entering the heat exchanger and then regulates the outlet temperature or the opposite way. It is crucial to use the water for cooling down the refrigerant when the glycol is not able to absorb all the heat that must be rejected through the first gas cooler unit. As said before, the DSH is crucial to maximize the lifetime of the MT compressor, avoiding huge thermal stress that would be caused by a hot vapor in contact with the wall surface at the suction line.

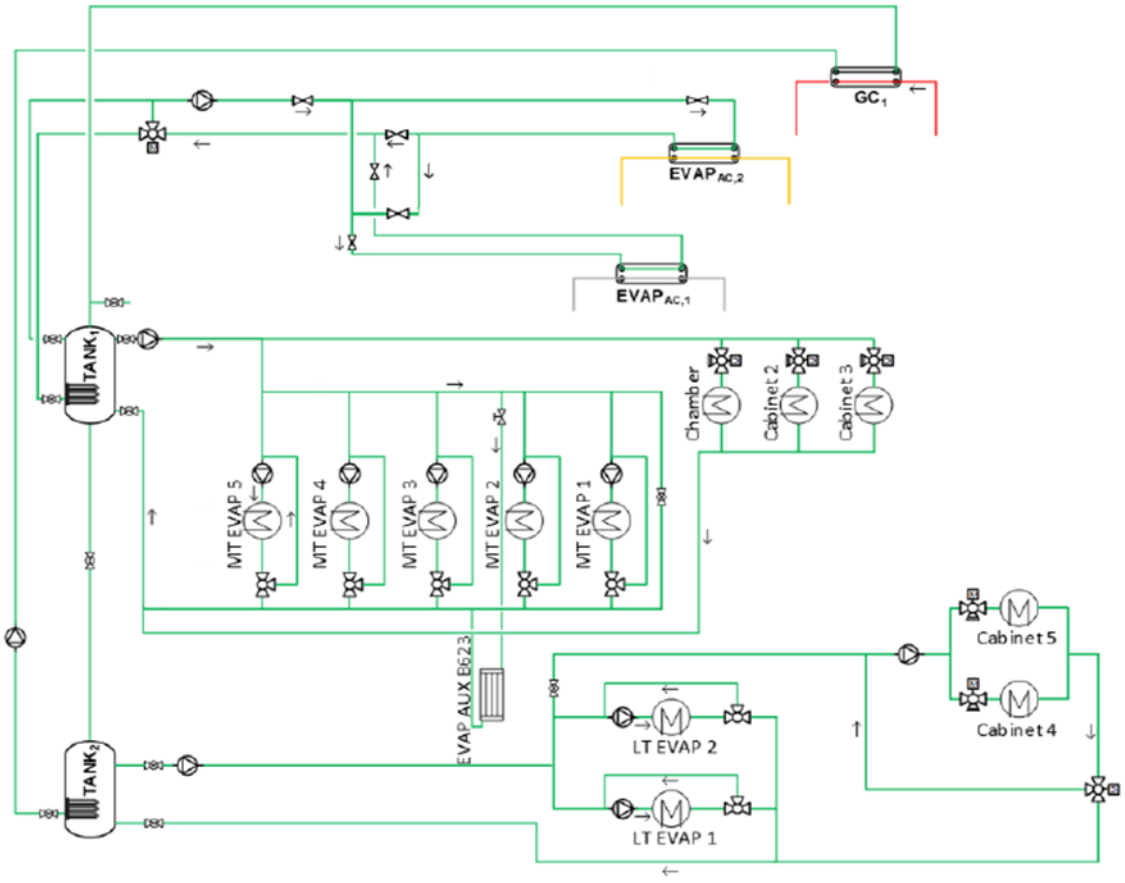

Figure 4.2: Simplified P&ID of the glycol loop at the experimental test facility.

4.1.2.3Auxiliary CO_2 loop

The auxiliary CO_2 loop is very useful when low ambient temperatures need to be tested (0 to -20 °C). This additional loop is located in the basement of the laboratories.

4.1.3 Compressor packs

Being one of the purposes of this thesis the applicability of the pivoting principle, an overview of the compressor packs installed in the test-rig is needed. In total there are 8 compressors, which are all of them semi-hermetic compressors manufactured by Bitzer. The size of each compressor can be seen in Table 4.1. Among them, only three are equipped with VSD (variable speed drive), enabling a better matching of the capacity optimally. The test-rig consists in three compressor packs operating at three different pressure level: two LT compressors operating with a pressure ratio defined by the LT and MT evaporating temperatures, three MT compressors operating between the MT evaporating temperature and the heat rejection pressure, three IT compressors operating between the receiver pressure and the heat rejection pressure. This explanation is referred to as the base arrangement where the

ball valves steered with actuators of the four compressors have been set such as to have the previous configuration (3 MT, 3 IT compressors). In reality, the modifications made in the test-rig allows now to automatically change their position based on the need, being the number of compressors required strongly dependent on the outlet conditions, loads, ejector performance (HP multi-ejector).

When the capacity starts to increase, the controller could either raise the frequency and therefore the rotational speed of the VSD compressor or activate an additional compressor in the pack, while the opposite happens whenever the load decreases. Each compressor pack has its purpose to maintain the pressure level constant to the design point, and whenever the capacity is too high for the size of the compressor pack installed, the corresponding pressure level will increase forcing the pressure ratio to decrease and trying to help the compressors to match the demand.

Table 4.1: Model and capacity of each compressor installed in the SuperSmart-Rack.

Compressor group	**Model**	**Displacement [m^3/h]**	**Name in P&ID**
MT	4 MTC-10K-40S	6.5	E – 111 (VSD)
	4 MTC-10K-40S	6.5	E – 121
	4 JTC-15K-40P	9.2	E – 131
IT	2 KTE – 7K – 40S	4.8	E – 211 (VSD)
	2 KTE – 7K – 40S	4.8	E – 221
	4 JTC – 15K – 40P	9.2	E – 231
LT	2 JME – 3K – 40S	3.5	E – 311 (VSD)
	2 GME – 4K- 40S	5	E - 321

4.1.4 Multi-Ejectors

The test-rig is equipped with two multi-ejector blocks, one working with high-pressure lift while the other one with low-pressure lift, hence able to elaborate a higher or lower suction flow. Since the LP multi-ejector block is not used in the test campaign, only the HP multi-ejector will be analyzed. As already explained, it consists of 6 cartridges, four of them deal with the vapor, the other two with liquid allowing overfeed evaporators. Depending on the load, the capacity controller will switch on/off the cartridges fitting the best capacity and regulating the high pressure. The multi-ejector has binary coupling of various capacities, and close to the suction port, the cartridge with the highest capacity is located. The capacity of each cartridge is illustrated in Table 4.2.

Table 4.2: Capacity of each cartridge used in the HP multi-ejector block.

Ejector Type	**Ejector 1**	**Ejector 2**	**Ejector 3**	**Ejector 4**	**Ejector 5**	**Ejector 6**
MT – Ejector	6 kW	12 kW	25 kW	50 kW	18 kW	9 kW
Capacity	125 kg/h	250 kg/h	500 kg/h	1000 kg/h	400 kg/h	200 kg/h

4.2 Data Acquisition System and Data Analysis

A controlling system by Danfoss, Service Tool, receives all the measurements taken by pressure and temperature sensor to monitor and control the evolution of such quantities over the tests. Other several devices are installed to track the mass flow, liquid, and oil level and to measure power consumption. Some of them are described here below:

Mass flow meter: it measures the mass flow rate of refrigerant, and the type of flow meters are Rheonik RHM which is a Coriolis Effect mass flow meter.

Different Pt100 temperature sensors based on the resistance approach, therefore a platinum element has a resistance value which changes proportionally with the temperature that can be evaluated indirectly.

Pressure transducers, type MBS8250 from Danfoss. They allow to measure the pressure in different points of the refrigerant loop. There are also some differential pressure sensors used to measure the pressure lift in the ejector blocks. This kind of pressure transducer is Deltabar PMD75 manufactured by Endress+Hauser.

The measurement of the power consumption is taken individually for each compressor by using Schneider Electric A9MEM3150.

Moreover, the system is equipped with a pack controller provided by Danfoss, type AK-PC 782A. This controller has the purpose to control and fit as best as possible the compressors and condensers operating conditions, but even other modules could be connected for the following purposes:

- Controlling the liquid receiver pressure, evaporating temperature, gas cooler outlet temperature, heat rejection pressure and pressure of the three different compressor packs
- Ensuring oil flow through the compressors and pressurization of the system
- Regulation of the expansion valve installed in each evaporator, therefore the opening degree which is related to the superheating fixed affecting the mass flow of CO_2 elaborated in each evaporator. It is worth to mention that when the superheating is too high the opening degree increases trying to force more CO_2 flow, while when the superheating is too low less liquid should be sent to the evaporator
- General functions like alarms
- Control of the cartridge combination
- Control the pressure lift in the AC and MT multi-ejector blocks by regulating the mass flow

All the data is stored in Minilog, software provided by Danfoss. It allows to set the manually specific parameter in the system as well as to display them graphically.

The secondary loop is controlled by LabVIEW. LabVIEW is one of the two data acquisition systems employed in the system and it is used to control the components of the secondary loop such as pumps, electric heaters and valves. Furthermore, the load in the refrigeration system can be adjusted setting the loads and the outlet glycol temperatures in each evaporator (not valid for B-622, called $EVAP_{AC,2}$).

Both programs allow to record .csv data files that are combined later and synchronized with a MATLAB script. To obtain the thermodynamic properties, REFPROP, a thermophysical property library has been used. For the glycol loop, the properties have been taken from the ASHRAE Handbook Fundamentals (2009). Each of them has a different sampling time: LabVIEW has been set to 1 s, meanwhile, Minilog's sample rate was set to 5 s. In order to get significant measurements, the time must be at least 5-10 minutes, operating with stable conditions over all the measurements. This is necessary to consider the system operating as steady state when the calculations are performed. This is confirmed by having stable loads, stable gas cooler outlet temperature, high pressure and receiver pressure, AKV's opening degree almost constant. All these parameters can be displayed in Minilog graphically and some of them can be checked continuously in LabVIEW.

4.2.1 Data Calibration

Calibrating correctly the sensors is essential to obtain a successful test campaign. It consists of calculating the relative error from a specific sensor measurement to a reliable reference. The calibration was completely done in the previous project, and all these values are utilized for the uncertainty analysis (even this conducted in the previous project). Some features and accuracy of some sensors can be recorded in the previous project.

4.2.2 Evaporators

The evaluation of the MT and LT loads have been done both in CO_2 side and in the glycol side with the equations (4.1) and (4.2) respectively:

$$\dot{Q}_{evap,CO_2} = \dot{m}_{evap,CO_2} \cdot (h_{out} - h_{in}) \tag{4.1}$$

$$\dot{Q}_{evap,glycol} = \dot{V}_{evap,glycol} \cdot \rho_{glycol} \cdot c_p \cdot (T_{in} - T_{out}) \tag{4.2}$$

Where in equation (4.2) ρ and c_p are the density and specific capacity that is calculated considering the average temperature ($\bar{T}_{glycol}$) of the glycol through the evaporators:

$$\rho = -0.0025 \cdot \bar{T}_{glycol}^2 - 0.3435 \cdot \bar{T}_{glycol} + 1036.2$$

$$c_p = 0.0028 \cdot \bar{T}_{glycol} + 3.7928$$

4.2.3 Compressors

The compressor performance is very important for the evaluation of the system performance and even for further considerations. Thus, they can be represented by the isentropic efficiency, volumetric efficiency and overall efficiency. These indexes indicate if the compressor pack is working with optimal working conditions or not. The isentropic efficiency is defined in equation (4.3):

$$\eta_{is} = \frac{\dot{W}_{is}}{\dot{W}_{shaft}} = \frac{h_{out,is} - h_{in}}{h_{out} - h_{in}} \tag{4.3}$$

Further, the volumetric efficiency is expressed in equation (4.4):

$$\eta_{vol} = \frac{\dot{m}_{CO_2}}{\dot{V}_{disp} \cdot \rho} \tag{4.4}$$

where at the denominator there is the product of the displacement (depending on the frequency at which the compressor is running) and the density at the suction line. The last parameter is the overall efficiency which is obtained for each compressor group:

$$\eta_{comp_i,over} = \dot{m}_{comp,i} \cdot \frac{h_{is} - h_{suc}}{P_{comp,i}} \tag{4.5}$$

with i = LT, MT, IT. The overall efficiency is even defined for all three compressor packs in the following way:

$$\eta_{comp,tot} = \frac{\sum \eta_{comp_i,over} \cdot P_{comp_i}}{P_{tot}} \tag{4.6}$$

These efficiencies are necessary in a complete evaluation of the system performance being an index that might explain why in some cases the power consumption saving is lower rather than to be higher, lowering the performance of the total system and the COP as consequences.

4.2.4 Ejectors

The ejector performance is commonly acknowledged trough the mass entrainment ratio ($Ø_m$), suction pressure ratio (Π_s), pressure lift (p_{lift}), and the ejector efficiency ($\eta_{ejector}$) that is an index of the expansion work recovery efficiency. The entrainment ratio is defined as the

ratio between the mass flow sucked by the ejector ($\dot{m}_{sf}$) and the mass flow of the motive fluid ($\dot{m}_{mf}$), the high energy stream:

$$\Phi_m = \frac{\dot{m}_{sf}}{\dot{m}_{mf}} \tag{4.7}$$

Being in the test campaign only MT multi-ejector block involved, the following specifications are needed. The suction flow can be measured using the mass flow meter FI-I-817, while the motive flow using FI-I-815 (when HPV is not working at all).

The pressure ratio is the ratio of the outlet pressure level to the suction nozzle pressure level:

$$\Pi_s = \frac{p_{outlet}}{p_{suction}} \tag{4.8}$$

while the pressure lift is the difference between them:

$$\Delta p_{lift} = p_{outlet} - p_{suction}$$

that can be directly measured by the differential pressure sensors.

The ejector efficiency [40] can be expressed as the amount of work recovered divided by the maximum potential to recover the expansion work rate by the ejector, assessing the overall ejector performance:

$$\eta_{ej} = \frac{\dot{W}_r}{\dot{W}_{r,max}} = \Phi_m \cdot \frac{h_C - h_D}{h_A - h_B} \tag{4.9}$$

Or

$$\eta_{ej} = \Phi_m \cdot \frac{h\left(P_{diff_{out}}, s_{suc_{in}}\right) - h_{suc\_in}}{h_{mot\_in} - h(P_{diff_{out}}, s_{mot_{in}})} \tag{4.10}$$

The state A, B, C, D are represented in Figure 4.3:

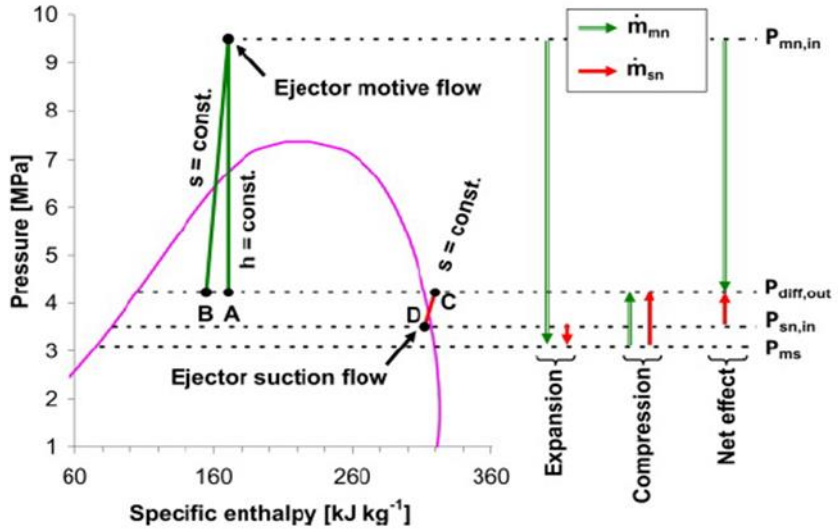

Figure 4.3: Expansion and compression of driving and driven flows inside a two-phase ejector [40].

The ejector efficiency is interpreted as the amount of power to compress the suction flow isentropically from the suction inlet pressure to the outlet ejector pressure (D → C), divided by the theoretical maximum work recovery potential, considered as the isentropic expansion of the motive fluid (A → B). The benefit of using this definition is that it can be applied for an experimental investigation, being avoided the measure of the static pressure in the mixing chamber. To be more precise:

State A = motive flow after isenthalpic throttling on the outlet of the ejector

State B = motive flow after the isentropic expansion (same pressure level of A)

State C = isentropic compression of the suction flow (same pressure level A – B)

State D = suction flow before the isentropic compression (from liquid accumulator after MT evaporators)

4.2.5 System performance

The system performance can be described by three different parameters: Energy Efficiency Ratio (EER), Power Input Ratio (PIR) and Coefficient of Performance (COP). With the power meters the power consumption of each compressor is recorded to define the total power consumption which will be used in the equation to calculate the EER:

$$EER = \frac{\dot{Q}_{MT} + \dot{Q}_{LT} + \dot{Q}_{AC}}{P_{TOT}} \tag{4.11}$$

The COP is expressed by the following equation:

$$COP_i = \frac{\dot{Q}_i}{P_i} \tag{4.12}$$

where *i* is referred to the load/compressor packs. The last parameter, PIR, is the ratio between the actual power consumption to the idea power of Carnot cycle, expressed in equation:

$$PIR = \frac{P_{actual}}{\sum P_{Carnot,i}} \tag{4.13}$$

where *i* has the same meaning as before. The Carnot ideal power consumption is:

$$P_{Carnot} = \Delta\dot{S}_i \cdot (T_{amb} - T_i) = \dot{Q}_{Evap,i} \cdot \frac{T_{amb} - T_i}{T_i} \tag{4.14}$$

with $\Delta\dot{S}_i$ the entropy rate and T_i the temperature of the heat source chosen as arbitrary value for the air at each particular evaporator, in Kelvin. Rather than use the COP, the PIR is taking into account the influence of the ambient conditions leading to a more meaningful comparison when analyzing the performance of systems working under different operating conditions. Lower PIR values mean better system performance as the real cycle performs closest to the ideal Carnot cycle.

4.3 System modifications

4.3.1 Modification of differential pressure valve: Oil Management

There have been some problems in the past with three parallel compressors running at high capacity (when AC load has a considerable weight in the total load) and high ambient temperature that led some of IT compressors to shut down. As it can be seen in Figure 4.4, a differential pressure valve of 3 bar is installed in the line that goes from oil receiver to liquid receiver. The main purpose is to deliver enough oil to the parallel compressors to maintain proper lubrication, and the effectiveness is based on which parameters are set in the system control ServiceTool under the voice “Oil Management”. The first idea was to take out the

differential pressure valve of 3 bar and replace it with another valve of 10 bar. Thus, the oil-receiver can operate at a higher pressure level, being able to deliver a sufficient amount of oil to the parallel compressors.

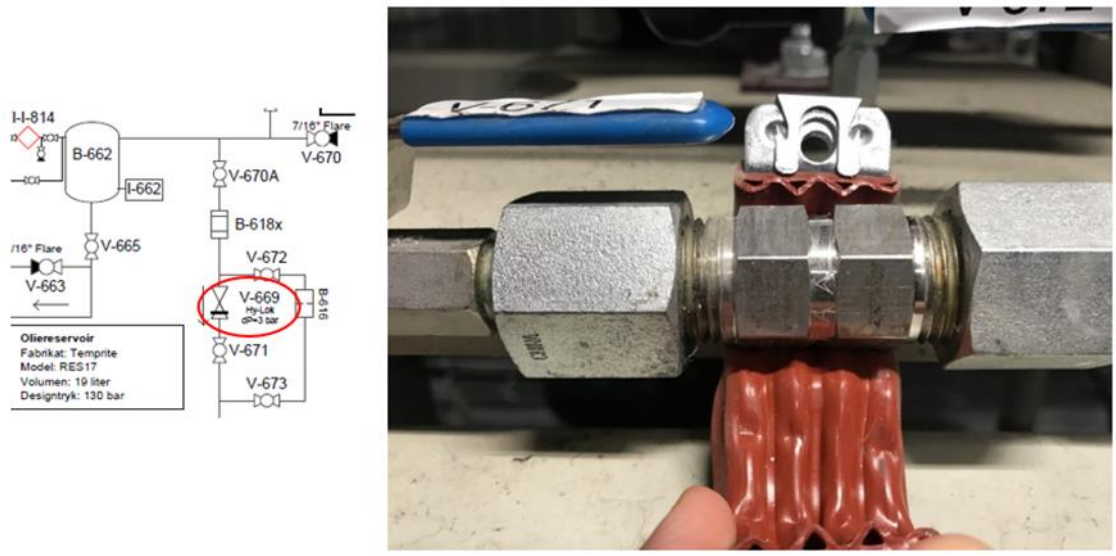

Figure 4.4: Illustration of the differential pressure valve replaced in the system.

Other arrangements have been tested and they will be presented later in detail. It is worth to mention that the differential pressure at which the valve is set depends on how much tight is the valve itself, and its behavior is strongly affected by a pressure range defined by two pressure values, called cut in and cut out pressure. Thus, after testing for the desired pressure, if additional adjusting is required, the valve can be tightened more as illustrated in Figure 4.5.

Figure 4.5: Cracking pressure adjustment.

4.3.2 Implementation of the pivoting automatic control system

One of the two main purposes of the thesis is testing of the pivoting compressors. In order to test them, an automatic control using switches installed in each actuator at the inlet line of each compressor is used. Therefore, the control passed from a manual to electronic

control. The control used in the past is no longer valid since the solenoid valve-check tandem used before has been substituted by two ball valves upstream of each compressor (Figure 4.6).

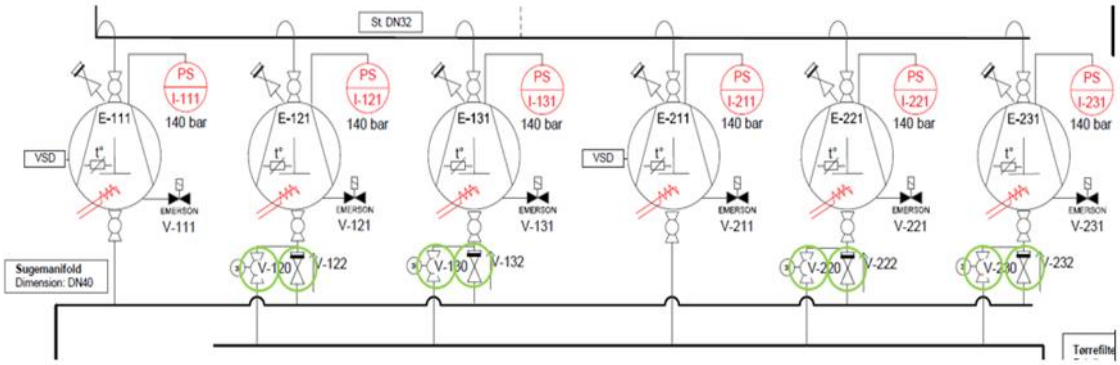

Figure 4.6: Layout of the compressor pack considering MT – IT compressors.

The logic of automatic control is such that only one valve upstream of each compressor can be opened at a time. 8 switches are needed, since E – 111 and E – 211 are always working as MT and IT compressor, respectively. The pivoting principle can be employed even for LT compressors (Figure 4.7), but in that case, the discharge pressure can be changed from MT evaporating pressure to receiver pressure, leading to higher power consumption in the LT compressor pack due to higher pressure ratio.

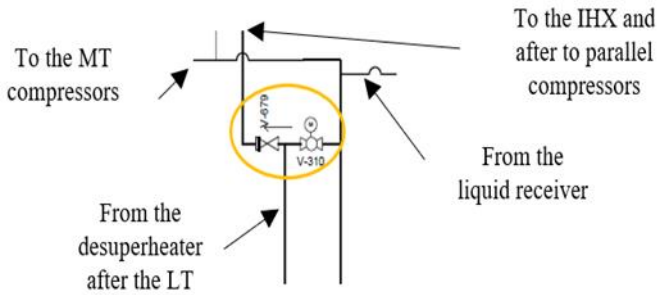

Figure 4.7: LT pivoting principle employed in the test-rig.

In conclusion, 10 switches are needed, all of them bought from Belimo. The commutation time has been tested in the lab, ensuring a no long time before to change the

inlet suction line in each pivoting compressor. The electric system employed is quite simple: with only one signal the commutation from MT to IT occurs, or vice versa depending on the load and operating conditions.

The electric scheme is illustrated in Figure 4.8:

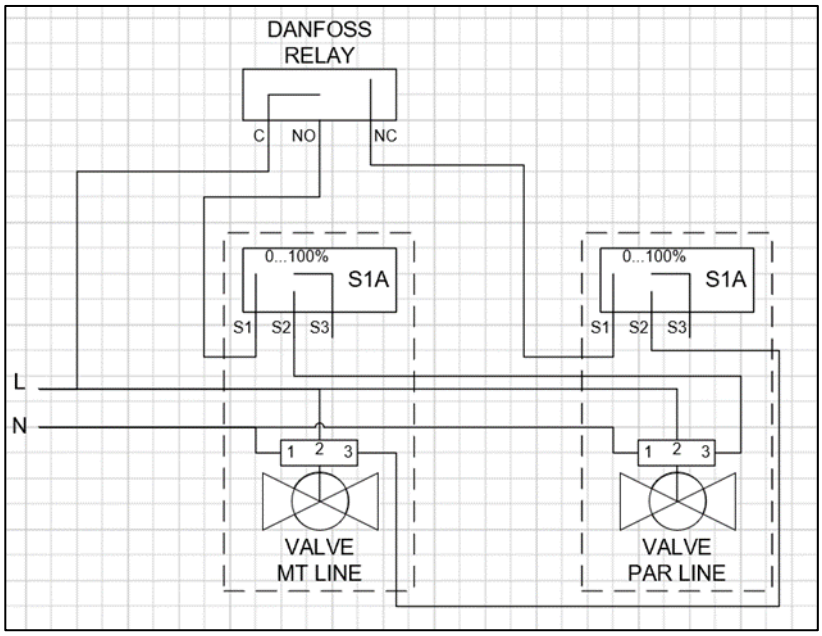

Figure 4.8: Electric scheme employed in the SuperSmart to control the suction line of each pivoting compressor.

The process is dealing in the following way:

- With only one signal, the shut-down of a valve of whichever compressor occurs, and when the valve reaches an opening degree equal to zero, a signal is sent to the other compressor's valve (depending on which valve is been closed firstly)
- The commutation follows the rule for which the valve has first to be close, and afterward, the other valve will open in order to not have two different suctions pressure in contact
- As illustrated in figure upstream, the port S2 of each valve is connected to the port S3 of the other valve, enabling the commutation and the desired logic

5 Oil Management

This chapter presents the challenges coming out of oil management with parallel compressors, at high ambient temperatures with air conditioning needs. The implementation of a differential pressure valve has been investigated, with different configurations looking for the best arrangement to ensure proper oil feeding to the compressors.

5.1 Oil Management

5.1.1 Previous layout

It is worth to mention before starting that the issue related to the parallel compressors was wrongly attributed to a proper oil feeding. In fact, after the test campaign with the pivoting compressors, the problem came out and it has been identified because of the lower current set in the inverter (difference inverter – metal plate in the compressors), hence each time the capacity raises above a certain level due to the limit previously set the compressor shut down. Anyhow, the tests carried out have been useful to find a configuration that leads to more reliable and efficient oil management. The original layout (Figure 5.1) failed to keep enough pressure difference between oil – liquid receiver to drive the oil back to a parallel compressor.

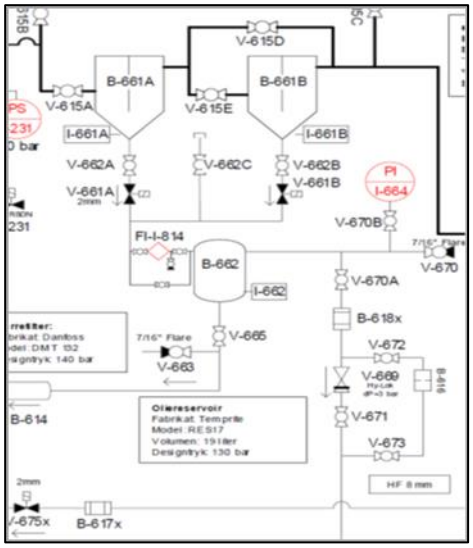

Figure 5.1: Original layout oil circuit.

The purpose of the tests was basically to compare different oil management solutions trying to improve the oil return from oil receiver to compressors, which is important to ensure

proper lubrication and a continued supply of the refrigerating load and air conditioning without any interruption, enhancing if possible the overall system performance.

5.2 Tests conditions and different layout investigated

The conditions for the experiments are presented in Table 5.1: Experimental conditions.

Table 5.1: Experimental conditions.

Parameter	Simulation
Gas cooler outlet temperature	30 & 35 °C
MT evaporating temperature	-8 °C
MT load	20 kW
AC load	45 kW
Receiver pressure	39 bar

The different layouts tested aim at performing an experimental campaign to evaluate the configuration such to ensure proper lubrication of IT compressors, having a look to the "howling cat" which is a noise occurring each time the check valve is activated. It has been specifically required to consider it since the feedback from the customers said it was an issue to be a viable solution long-term.

The different layouts are illustrated in Figure 5.2: Different layouts tested in the SuperSmart-Rack. a) Old arrangement with a check valve of 3 bar pressure difference. b) The check valve of 7.2 bar is operating in series with the orifice of 1 mm. c) The check valve of 7.2 bar is operating in parallel with the orifice. d) The check valve of 7.2 bar is working alone. A summary that describes the different arrangements is the following:

- The first test (a): V671 is open, while V672 and V673 are closed. Only the differential pressure check valve is operating (cut in pressure = 3 bar, cut out pressure = 5 bar)

- The second test (b): V671 is closed, while V672 and V673 are opened. In this case, the new valve installed with higher differential pressure is regulating the oil feeding to the compressors (cut in pressure = 6 bar, cut out pressure = 8 bar)
- The third test (c): The valve with a differential pressure of 7.2 bar is working in parallel with an orifice of 1 mm. Two tests have been carried out with a cut in and cut out pressure equal to 4 and 6 bar respectively. The screw in the check valve used in the third test was adjusted, unscrewing 1.5 turns
- Fourth test (d): Only the check valve has been tested, therefore V671 open while V672 and V673 closed

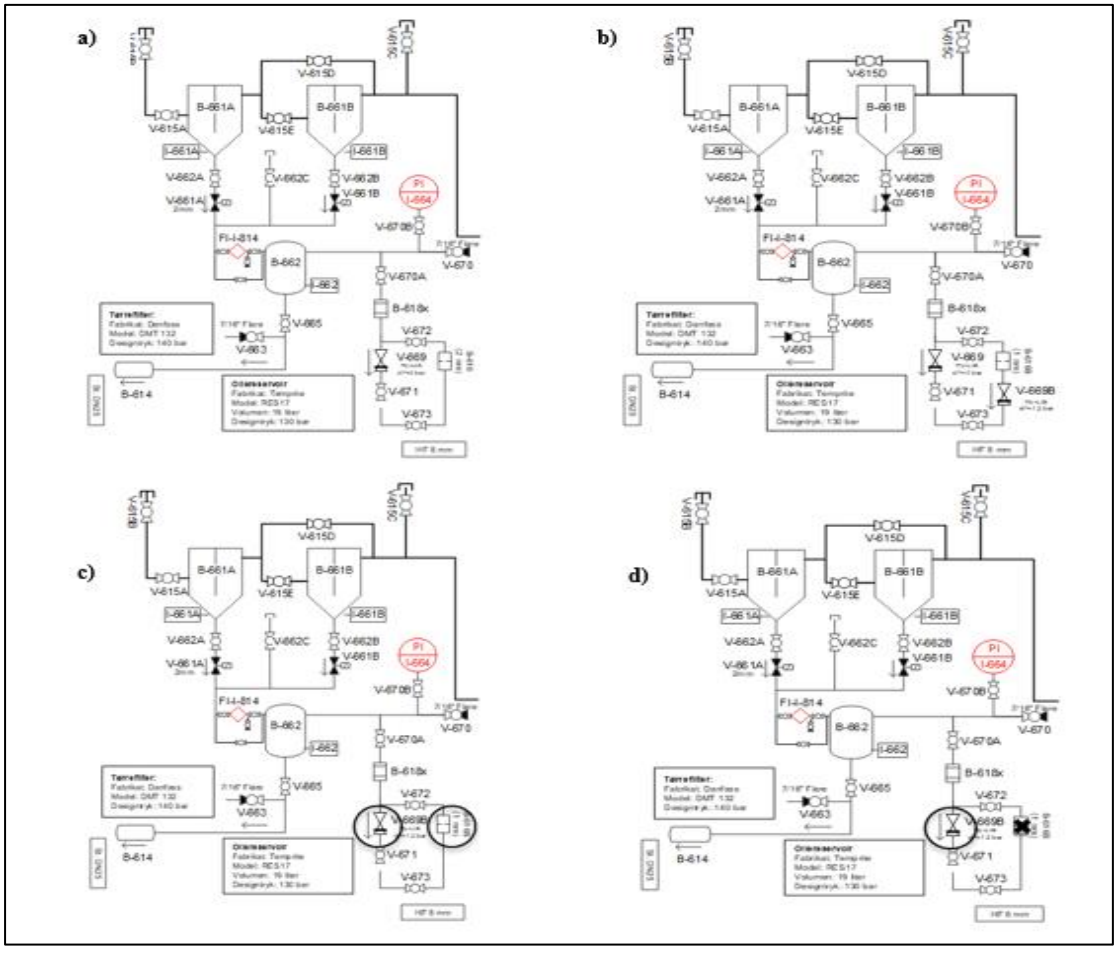

Figure 5.2: Different layouts tested in the SuperSmart-Rack. a) Old arrangement with a check valve of 3 bar pressure difference. b) The check valve of 7.2 bar is operating in series with the orifice of 1 mm. c) The check valve of 7.2 bar is operating in parallel with the orifice. d) The check valve of 7.2 bar is working alone.

For each case the test has already shown in Table 5.1, requires the evaluation at two different gas cooler outlet temperature, nevertheless, it is clear at a higher temperature high

capacity is transferred to the parallel compressors and a consistent and continues oil feeding is necessary.

It is worth specifying which is the meaning of cut in and cut out pressure. The cut-in pressure is the pressure at which the indication of flow occurs every time the pressure decreases to a lower value, forcing the flow from the oil separators to the oil receiver to pressurize it. The cut-out pressure is the upstream pressure at which there is no indication of flow, meaning that each time the pressure in the oil receiver goes above the cut-out pressure, the solenoid valves connection oil separators and oil receiver close.

5.2.1 Experimental results

The experimental data collected from the laboratory have been summarized in the following graphs, focusing on the stable operating conditions reached over all the tests and the oil-CO_2 mass flow detected by the mass flow meter FI-I-814. Each test will be analyzed, concluding that from the performance point of view the last solution with only a check valve of 7.2 bar in operation is the best.

In the first test (a), constant pressurizing of the oil receiver is needed, and the larger mass flow rate peaks when the oil separator switch indicates oil presence. If the cut-out pressure is higher than the pressure difference at which the valve is set (depending on how many turns it has been screwed), the check valve is open relatively often and as consequences, the solenoid valves need to open often to compensate and keep the pressure above the cut-in pressure. The solenoid valves open for two reasons: there is enough oil to be removed from the oil separator or the pressure in the oil receiver is too low compared to the liquid receiver, lower than the cut-in pressure, and it needs to be compensated.

When the pressure in the oil receiver increases due to the higher mass flow rate (oil-CO_2), the check valve opens enabling the flow to stabilize the pressure in the oil receiver.

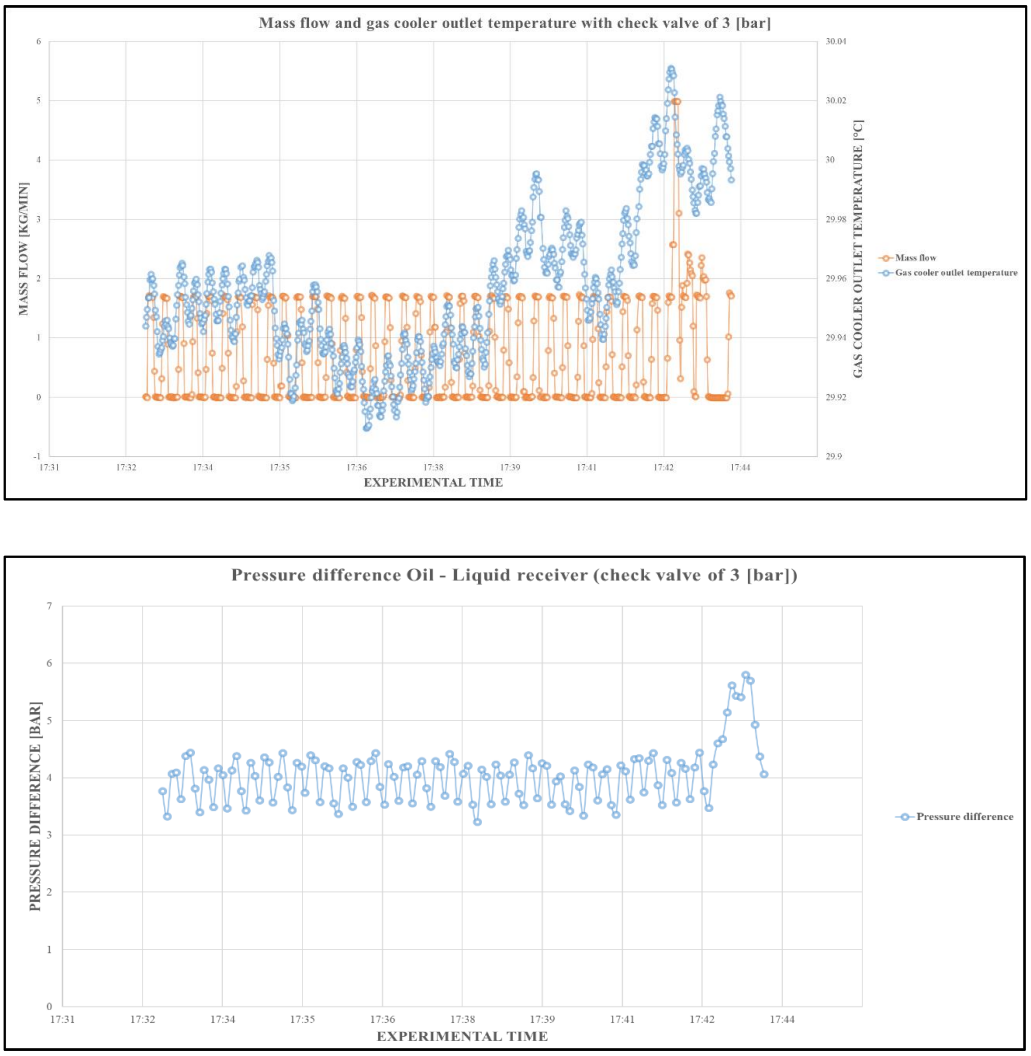

Figure 5.3: Mass flow detected by mass flow meter located between oil – liquid receiver, gas cooler outlet temperature, and pressure difference oil – liquid receiver (First test at 30 °C).

The case at 35 degree shows a more frequent opening of the check valve (Figure 5.4):

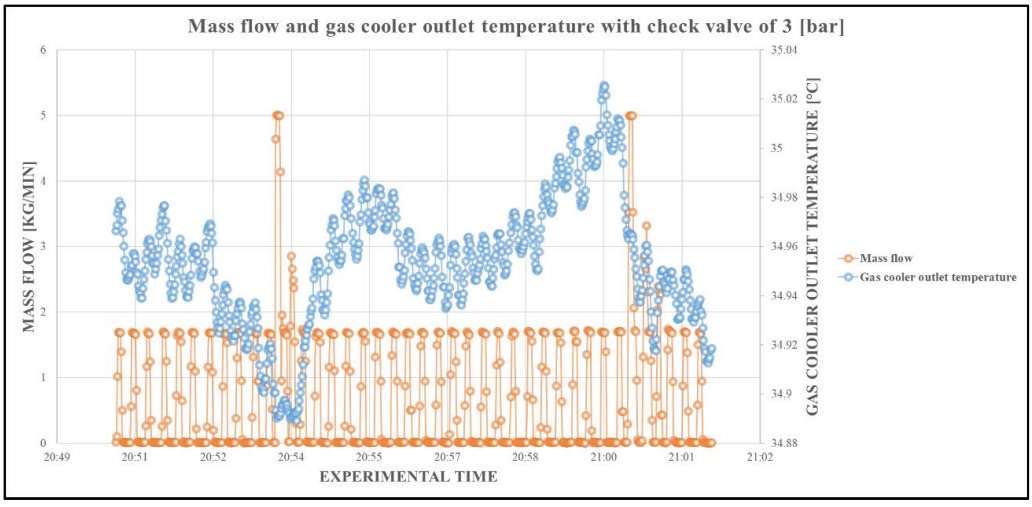

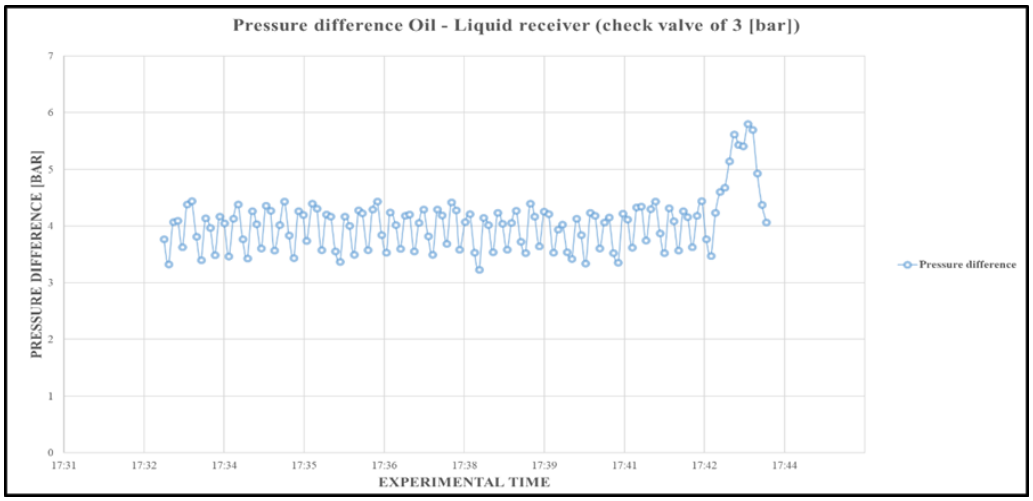

Figure 5.4: Mass flow detected by mass flow meter located between oil – liquid receiver, gas cooler outlet temperature, and pressure difference oil – liquid receiver (First test at 35 °C).

In the second test (b), the check valve with a pressure difference of 7.2 bar is working in series with an orifice of 1 mm, since the usual problem with check valves is that they are never completely tight. Thus, in case of check valve failure, there would be always the pressure difference coming from the orifice but not a continuous bleeding from the oil receiver to the liquid receiver in the case of the appropriate functioning of the check valve, which is not beneficial from the performance point of view. In Figure 5.5 is illustrated how a constant pressurizing is not needed in this case, as well as no opening of solenoid valves from oil separators.

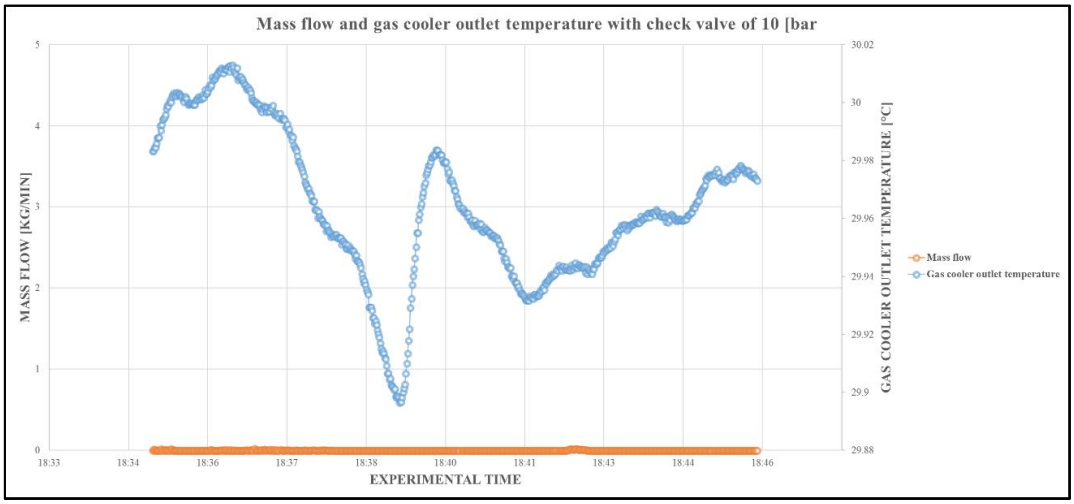

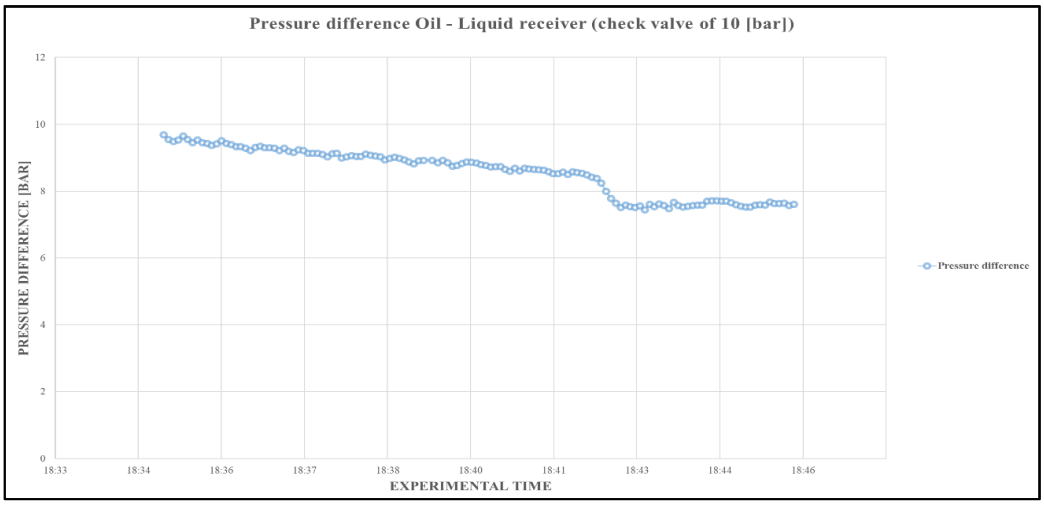

Figure 5.5: Mass flow detected by mass flow meter located between oil – liquid receiver, gas cooler outlet temperature, and pressure difference oil – liquid receiver (Second test at 30 °C).

When the heat rejection pressure increases due to higher gas cooler outlet temperature, the pressure difference, in this case, is pretty constant and the increase of mass flow is because one of the oil separators is probably full of oil and it delivers this oil into the liquid receiver. This can be seen in Figure 5.6 since the oil receiver is depressurized because the check valve vents pressure from the oil receiver to the liquid receiver. The pressure difference is never below cut-in pressure and thus the solenoid valves were never opened to pressurize the oil receiver.

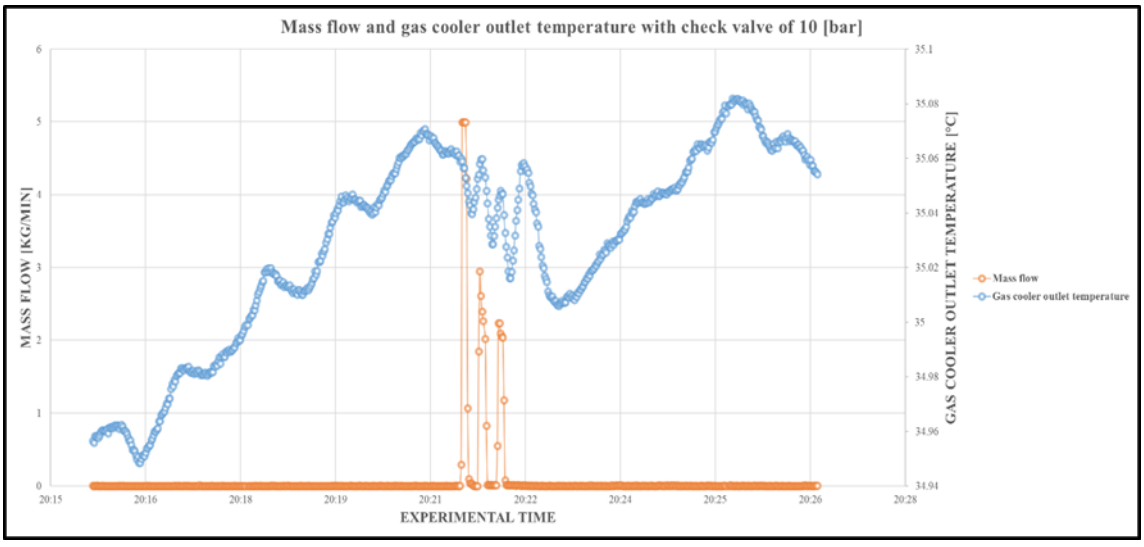

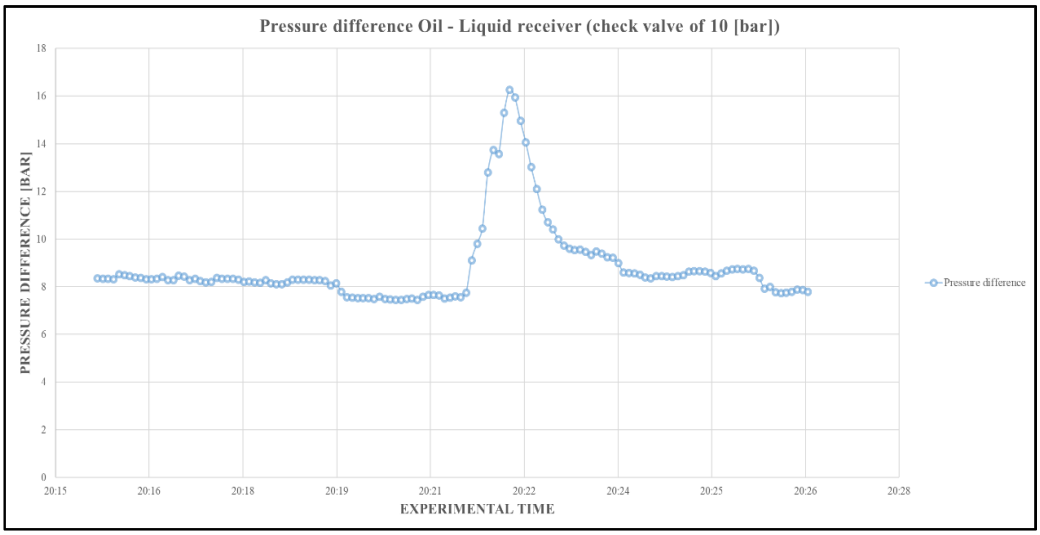

Figure 5.6: Mass flow detected by mass flow meter located between oil – liquid receiver, gas cooler outlet temperature, and pressure difference oil – liquid receiver (Second test at 35 °C).

The third test (c) consists of applying an orifice in parallel with the check valve. In this case, the idea is to use the check valve as a safety device in the event where the orifice nozzle is overburdened by several solenoid valves opening on the oil separators at the same time. Being the orifice on one hand a solution to prevent the noise coming from the check valve when it is in operation, on the other hand leads to the worst performance. This is easily explainable looking the PID in the appendix: a continues flow means the refrigerant is throttled from the high pressure to the oil receiver (through the solenoid valves) and then to the liquid receiver, after that the refrigerant is sucked by the IT compressors and then recompressed consuming additional energy. Figure 5.7 and Figure 5.8 are illustrated the case with cut-in and cut-out pressure equal to 4 and 6 bar, at 30 and 35 °C at the gas cooler outlet respectively.

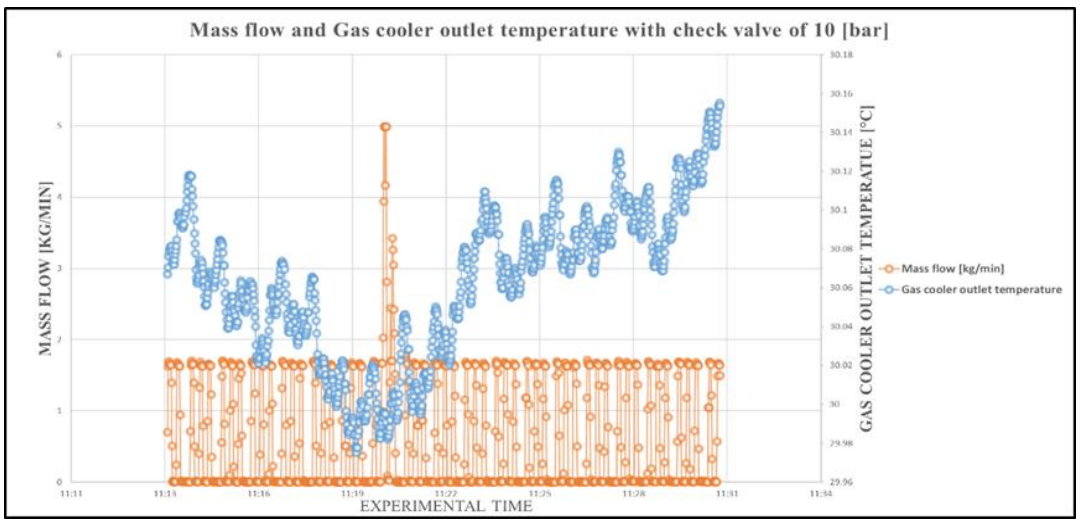

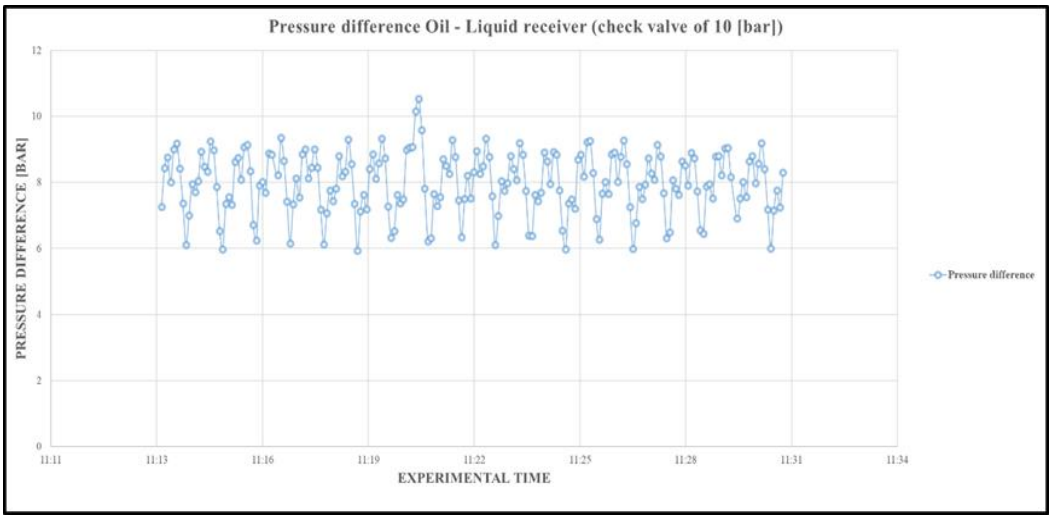

Figure 5.7: Mass flow detected by mass flow meter located between oil – liquid receiver, gas cooler outlet temperature, and pressure difference oil – liquid receiver (Third test at 30 °C).

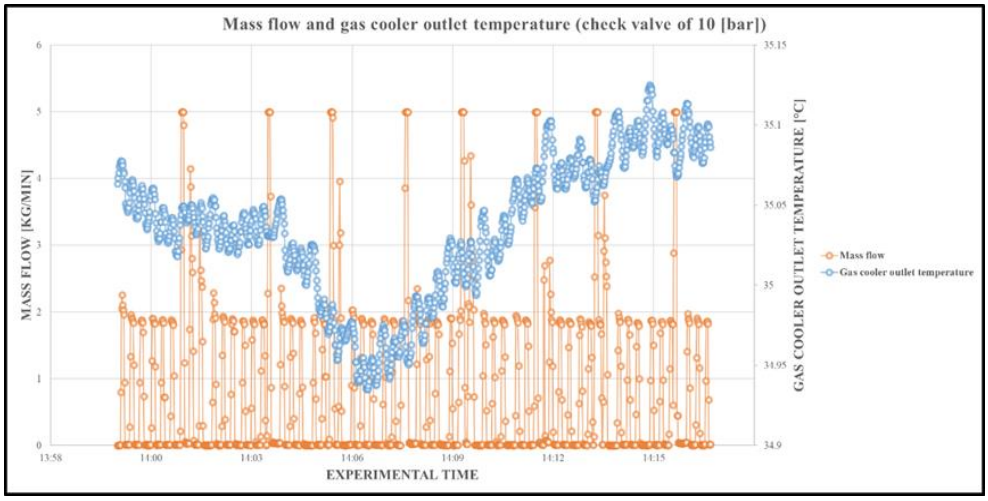

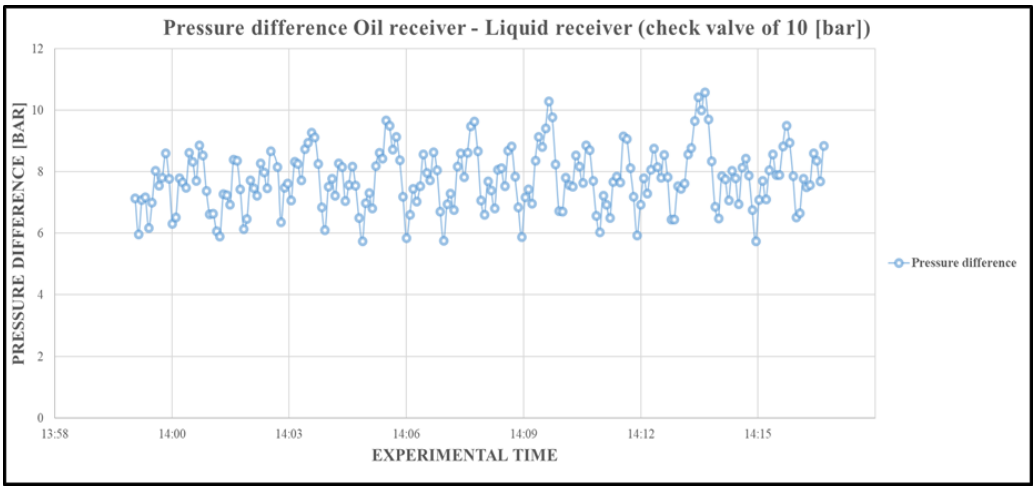

Figure 5.8: Mass flow detected by mass flow meter located between oil – liquid receiver, gas cooler outlet temperature, and pressure difference oil – liquid receiver (Third test at 35 °C).

The last arrangement investigated (d) results to have the best performance. As it is illustrated in Figure 5.9, this solution has a stable pressure difference. The mass flow meter detects some oil coming from the oil separator. When this happens, the pressure difference went above the cut-out pressure set in the check valve This is beneficial from two points of view: first is the less noise caused by the check valve in operation, the second one is the performance. As already explained, less refrigerant is throttled from the oil receiver to the liquid receiver lower the power consumption is due to the re-compression of the refrigerant. At 35 °C, Figure 5.10 is showing more peaks. Whenever the gas cooler exit temperature increases, the capacity required to cover the loads increases too, and more compressors are in operation and the high-pressure stream through the oil separators more oil flows.

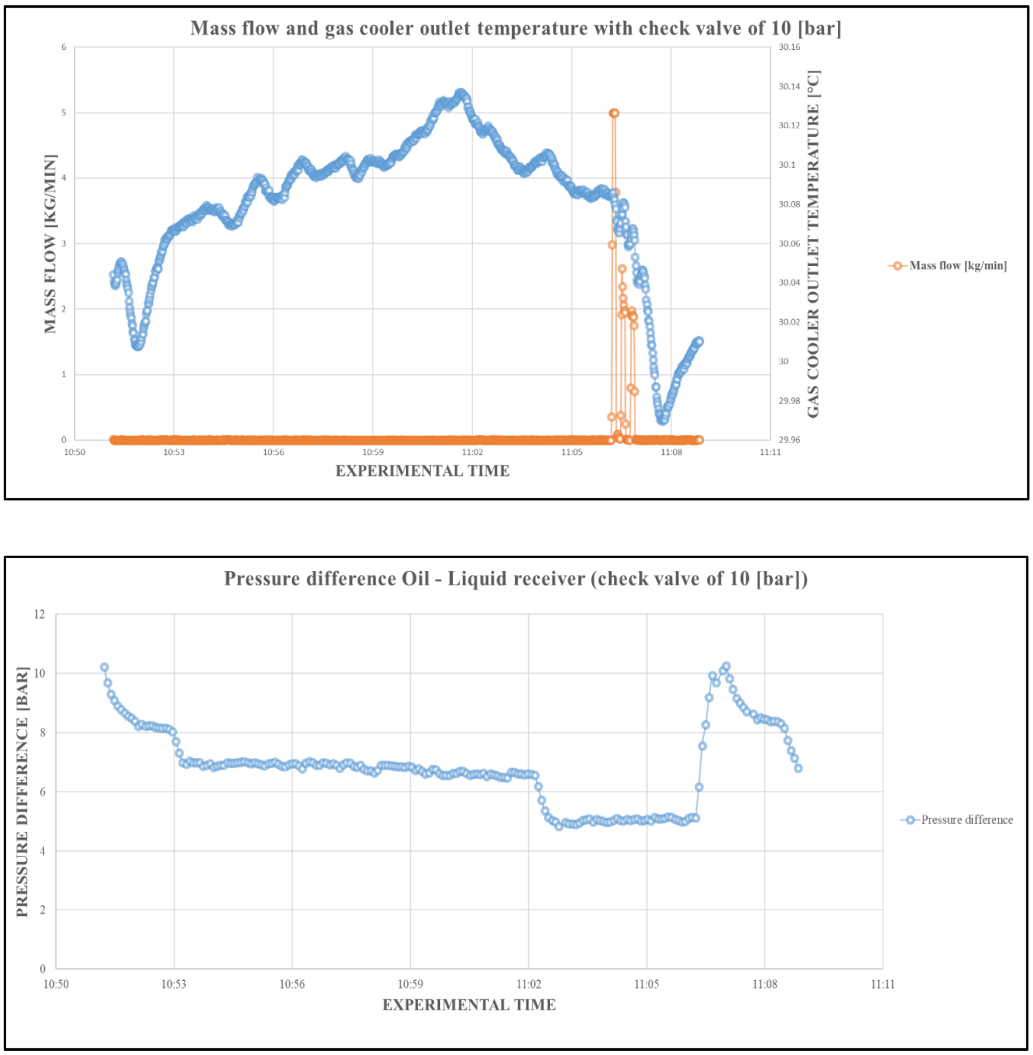

Figure 5.9: mass flow detected by mass flow meter located between oil – liquid receiver, gas cooler outlet temperature, and pressure difference oil – liquid receiver (Fourth test at 30 °C).

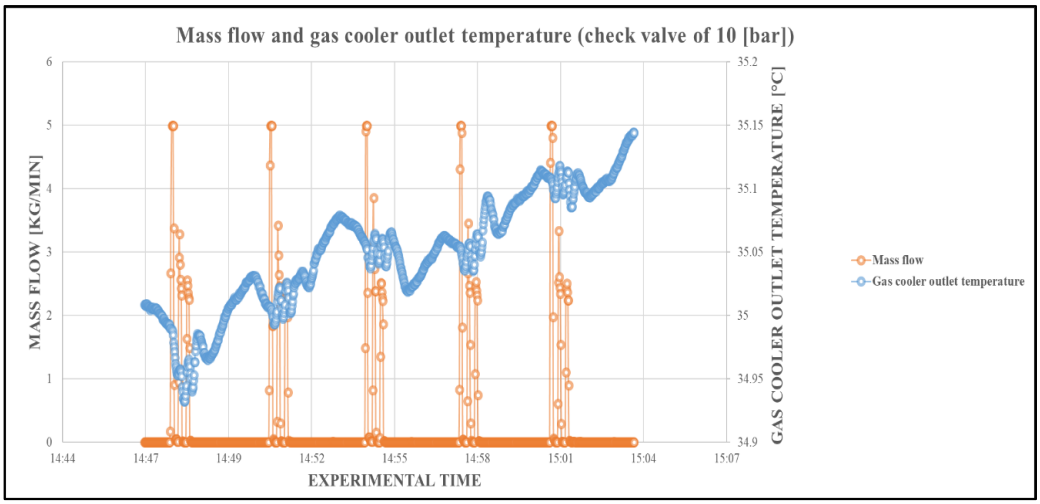

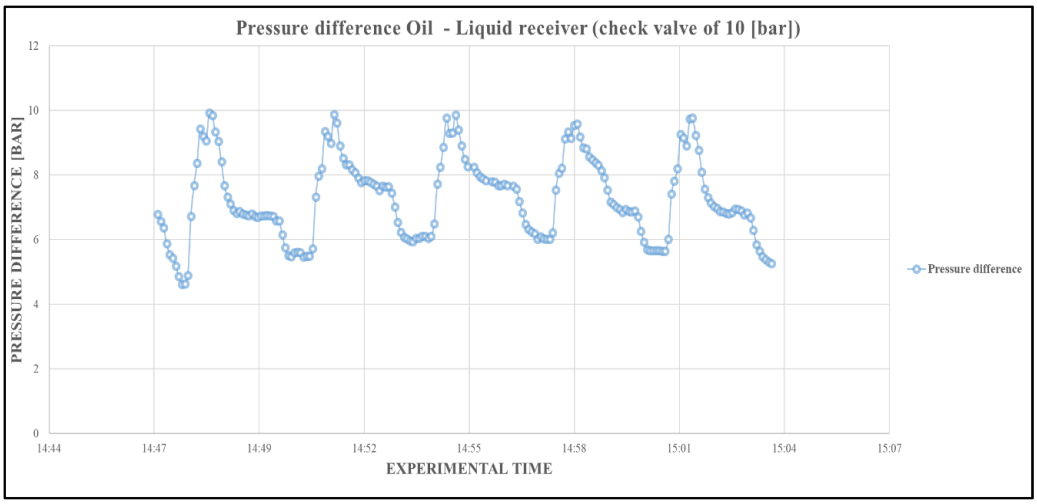

Figure 5.10: mass flow detected by mass flow meter located between oil – liquid receiver, gas cooler outlet temperature, and pressure difference oil – liquid receiver (Fourth test at 35 °C).

5.2.2 Conclusions

In this chapter, oil management is illustrated first presenting the different solutions investigated until to get the best one that ensures better performance and a stable pressure difference between oil – liquid receiver.

6 Pivoting compressors: Simulation and experimental results

In this chapter, the numerical model is presented at first. Later the numerical and experimental results are presented. First, the numerical model presents the combinations to adopt when switching of compressors is applied and not, and after that, the experimental results have been widely analyzed. A comparison for the validation of the numerical work has been carried out with the experimental results, highlighting the principle differences coming out, trying to explain the possible reasons. Furthermore, a numerical analysis at part load has been done considering the real behavior of components as IHX, ejector, etc. tested in the lab to have numerical results closest to what could be got in the test-rig. All case studies will include the analysis of the experimental results considering the uncertainty.

6.1 Pivoting compressors

6.1.1 Numerical model description

In order to set up a numerical model, a simple two-stage compression cycle has been studied at the beginning. The system contains three sets of compressors (LT, MT, IT), high-pressure control devices (HPV and EJMT), throttling valves at the inlet of evaporators, a gas cooler section, an IHX, a desuperheater at the outlet of LT compressor discharge and a liquid receiver (Figure 6.1).

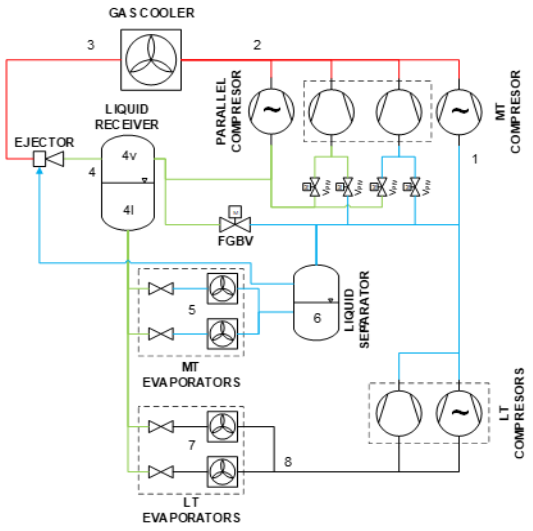

Figure 6.1: Simplified layout of the refrigeration system investigated.

The refrigerant follows the following path:

- In the liquid receiver, the liquid is stored at the bottom, where it is taken and throttled before entering the evaporators (LT and MT). The vapor is sucked by the IT compressors, and before entering it is heated up through the internal heat exchanger.
- The superheated vapor at the outlet of the LT evaporators is compressed and because of the high temperature at the LT compressor discharge is cooled down in the desuperheater. After that, it is mixed with the vapor coming out from MT evaporators, and after compressed by MT compressors to the high-pressure.
- The discharge of the LT compressors can be connected to either the MT compressors suction line or the IT compressors suction line (LT pivoting).
- The pressure in the liquid receiver is maintained constant thanks to the IT compressors, that suck the vapor from it, or by the flash gas bypass valve. State-of-the-art systems have IT compressors dedicated to this purpose. If the pivoting technology is applied, it is possible to switch one or more compressors (pivoting) from the IT to the MT section or vice versa thanks to the automatic control employed in the test-rig.
- After the compression, the refrigerant is condensed (subcritical operation) or -cooled down (transcritical operation) and the high-pressure is controlled by the HPV or EJMT.

6.1.2 Parameters and equations in the case study

Process equations and parameters during calculation are described in the following equations. It is worth to mention that some assumptions have been made to build the model, they will be presented in the next sub-chapter. The description will follow the arrangement of the components in the system:

- Evaporators: for LT and MT evaporators the cooling capacity is shown in (6.1):

$$\dot{Q}_{evap} = \dot{m}_{i,evap} \cdot (h_{i,evap,out} - h_{i,evap,in}) \tag{6.1}$$

where $m_{i,evap}$ is the refrigerant mass flow, $h_{i,evap,out}$ and $h_{i,evap,in}$ are outlet and inlet refrigerant enthalpy of each evaporator.

- Ejector: the entrainment ratio and the ejector efficiency must be implemented using (6.2) and (6.3):

$$\phi_M = \frac{\dot{m}_{sn}}{\dot{m}_{mn}} \tag{6.2}$$

$$\eta_{ejector} = \phi_M \cdot \frac{h_{sn,out} - h_{sn,in}}{h_{mn,out} - h_{mn,in}} \tag{6.3}$$

- To simulate all the operation points, two sets of equations have been defined (energy and mass balance). When the ejector is dealt, a black box is considered simplifying the study since the mixing inside the chamber is quite complicated. The set of equations representing the mass balance is the equation ((6.4) to (6.10)):
- Liquid receiver:

$$\dot{m}_{tot} = \dot{m}_{liq} + \dot{m}_{vap} \tag{6.4}$$

where knowing the vapor quality value is possible to evaluate the total mass flow in the system (motive flow in the case with ejector) and amount of vapor which is a function of the gas cooler outlet temperature, high pressure and subcooling degree. Since the loads and evaporating temperatures are given, the liquid mass flow is already defined. Therefore:

$$\dot{m}_{vap} = \dot{m}_{tot} \cdot x_{receiver} \tag{6.5}$$

$$\dot{m}_{liq} = \dot{m}_{tot} \cdot (1 - x_{receiver}) \tag{6.6}$$

$$\dot{m}_{liq} = \dot{m}_{MT,evap} + \dot{m}_{LT,evap} \tag{6.7}$$

and when the ejector is in operation, the total mass flow considered is the $m_{discharge}$ (outlet of ejector) and the vapor quality to be considered is now a function of the enthalpy of the mass flow discharged by the ejector (at the receiver pressure).

- Inlet MT compressors (LT discharge to MT pressure):

$$\dot{m}_{MT,comp} = \dot{m}_{MT,evap} + \dot{m}_{LT,evap} \quad (6.8)$$

in the case where the high pressure is controlled by HPV. When the ejector is regulating the high pressure and entrain some refrigerant from the outlet of the MT evaporators, the mass and energy balance as well will change at the inlet of MT compressors:

$$\dot{m}_{MT,comp} = \dot{m}_{MT,evap} + \dot{m}_{LT,evap} - \dot{m}_{suction} \quad (6.9)$$

- Ejector:

$$\dot{m}_{mn} + \dot{m}_{sn} = \dot{m}_{discharge} \quad (6.10)$$

Moreover, in this case, the total mass flow entering the mass and energy balance of the liquid receiver is the mass flow discharged by the ejector, considered as already explained before a black box with two streams entering and one exiting.

Regarding the energy balance, the same number of equations are set here:

- Liquid receiver (with HPV):

$$\dot{m}_{tot} \cdot h_{hot,out} = \dot{m}_{liq} \cdot h_{liq} + \dot{m}_{vap} \cdot h_{sat,rec} \quad (6.11)$$

When ejector is regulating the high pressure, the previous equation becomes:

$$\dot{m}_{discharge} \cdot h_{discharge} = \dot{m}_{liq} \cdot h_{liq} + \dot{m}_{vap} \cdot h_{sat,rec} \quad (6.12)$$

- Inlet MT compressors:

$$\dot{m}_{MT,evap} \cdot h_{exit,MT} + \dot{m}_{LT,evap} \cdot h_{disc,desup,LT} = \dot{m}_{MT,comp} \cdot h_{suc,MT} \quad (6.13)$$

The only difference when ejector employed, is the mass flow coming out from the MT evaporator since some refrigerant is sucked by the ejector.

$$(\dot{m}_{MT,evap} - \dot{m}_{sn}) \cdot h_{exit,MT} + \dot{m}_{LT,evap} \cdot h_{disc,desup,LT} = \dot{m}_{MT,comp} \cdot h_{suc,MT} \quad (6.14)$$

- Internal heat exchanger: here, without considering any guess value of effectiveness (which is usually around 0.7), the energy balance has been considered ensuring the

heat released by the total mass flow at gas cooler outlet is the same heat absorbed by the vapor sucked by IT compressors. In the case of HPV:

$$\dot{m}_{tot} \cdot \left(h_{gc,outlet} - h_{hot,out}\right) = \dot{m}_{vap} \cdot (h_{suc,IT} - h_{sat,rec}) \quad (6.15)$$

where $h_{gc,outlet}$, $h_{hot,out}$, $h_{suc,IT}$, $h_{sat,rec}$ are the enthalpy at the gas cooler outlet, at the outlet of the IHX (hot side), at the suction of the parallel compressors (outlet cold side), at the receiver pressure (saturated) respectively. With ejector in operation, the denomination changes a little, but the meaning is the same:

$$\dot{m}_{mn} \cdot \left(h_{gc,outlet} - h_{mn,out}\right) = \dot{m}_{vap} \cdot (h_{suc,IT} - h_{sat,rec}) \quad (6.16)$$

- Ejector:

$$\dot{m}_{mn} \cdot h_{mn,out} + \dot{m}_{sn} \cdot h_{sn,in} = \dot{m}_{discharge} \cdot h_{discharge} \quad (6.17)$$

Here they have not mentioned all the links between the different variables (isenthalpic process, temperature as a function of enthalpy-pressure, etc.). Acquiring all the parameters above, the refrigeration unit can be simplified evaluating at the same time the mass flows that will be displaced by the three different compressor stages. Those values will be used later to find the suitable combination of compressors able to displace that mass flow rate. The polynomial equations (Bitzer) have been used to calculate the mass flow elaborated and the power consumption of each type of compressor, even for the VSD compressors where the change in frequency must be taken into consideration. The following equation is used to calculate the swept volume at any frequency (n):

$$\dot{v}(n) = \dot{v}(50\ Hz) \cdot \frac{n \cdot 30 - 50}{1450} \quad (6.18)$$

At 50 Hz the rotation speed is 1450 rpm, considering asynchronous motor.

6.1.3 Assumptions used in the model

Multiple assumptions have been used for the simulation. They can be summarized as follows:

- Mass flow through the evaporators (LT and MT) are independent of the system having ejector or HPV.
- Steady-state conditions have been considered, all the mass flow coming into the liquid receiver can be split into two mass flows considering the quality.
- MT compressor gets mass flow rate from LT and MT evaporators, IT compressors handle the vapor in the receiver.
- Constant efficiency of the ejector has been considered, and the entrainment ratio will be calculated consequently as soon as the conditions in the motive are known
- The refrigerant sucked by ejector (suction flow) is considered as saturated vapor (see ejector efficiency equation, Figure 4.3).
- The evaporating and receiver pressure are set to constant values.
- The heat rejection pressure is defined using the program "CO_2 simple stage cycle" (https://www.ipu.dk/products/simple-one-stage-co2) for the transcritical cycle, while for the subcritical cycle a subcooling of 3 K is taken (i.e. gas cooler outlet temperature = 15 °C, the condensing temperature is 18 °C and therefore the high-pressure is the saturated pressure at the condensing temperature).

A criterion has been followed in the numerical analysis. Because the suitable compressor combination is chosen making a comparison between the mass flow calculated using the polynomial equation and the mass flow evaluated in the model implemented in EES, sometimes it happens that a certain compressor combination can displace a mass flow which is a bit lower than the design one. Therefore, two approaches have been considered:

- Increasing of evaporating temperature within 0.2 K of the setpoint is allowed, reducing in this way a little the pressure ratio helping the compressor to displace more vapor
- If the difference between mass flow rate from the thermodynamic analysis and the polynomial equations is within 1% of the mass flow rate from the thermodynamic analysis, the compressor combination is considered good enough
- For the parallel compressors, an increment of 0.5 bar maximum is still acceptable to compress all the vapor coming from the liquid receiver.

6.1.4 Objectives of the numerical model

The purpose of the numerical model is to investigate which is the most suitable compressor's combination that allows us to maintain constant the evaporating temperature at two different levels (LT and MT) supplying the refrigerating load. Numerically the study has been conducted concerning different scenario:

- Numerical analysis of the refrigeration unit at different gas cooler outlet temperature, with different devices for controlling the high-pressure
- Mass flows calculated through the model are the reference values to compare them with the mass flows obtainable combining different compressors (using polynomial equations to evaluate mass flow and power consumption)
- The comparison is done considering the test-rig with three MT and three IT compressors, as well as one MT and one IT plus some compressors that are acting as pivoting (switch of the suction line thanks the automatic control installed)
- The analysis is done for a different scenario, being one combination of the pivoting compressor not suitable for a lower temperature
- Investigation on the LT pivoting, seeing if it is possible to get some advantages to discharge the LT mass flow to a higher pressure (receiver pressure), unloading the MT compressors which are working with higher pressure ratio than parallel compressors
- The numerical comparison between parallel compression cycle and booster cycle operating with the FGV.

6.1.5 Input data

Multiple tasks have been investigated in this Master Thesis. The main task was to prove theoretically and experimentally if the switching of compressors allowed reducing the total number of compressors installed. Hence, the initial parameters are listed in Table 6.1:

Table 6.1: Initial parameters used to simulate the refrigeration unit.

Initial Conditions	
MT evaporation temperature	-8 °C
LT evaporation temperature	-30 °C
Superheating (MT and LT)	8 K
Receiver pressure	36 bar
Gas cooler outlet temperature	35 (30, 25, 20, 15, 10) °C
MT Load	60 kW
LT Load	15 kW
Temperature after desuperheater	25 °C
Ejector efficiency	30 % (at 35-30 °C), 20% (at 25 °C)

6.1.6 Experimental work

Based on the cases investigated numerically, several tests have been conducted to validate the numerical results. Since at 35 °C, the capacity required is the highest possible giving information on how many compressors must be installed in the test-rig, it has been considered as the main case. Furthermore, being at lower gas cooler outlet temperature the capacity required on the parallel compressors and the ability to displace mass flow higher both on the IT and MT side lower due to the lower pressure ratio, it might be necessary to have a compressor that has not been installed. This to explain that is important to check case by case in which compressors are needed. The test campaign is shown in Table 6.2, remembering that each test consists of two different compressor arrangements (with and without pivoting):

Table 6.2: Test chosen for the experimental work.

Gas cooler outlet temperature	Parallel compressor configuration	Multi-ejector supported configuration
35	Yes	Yes
30	Yes	Yes
25	Yes	Yes
20	Yes	No

6.2 Theoretical system performance

6.2.1 Calculation results and analysis

The calculation process was conducted through EES. Steady-state calculations are considered in the model. As already explained, higher is the gas cooler outlet temperature higher is the amount of vapor to be sucked by parallel compressors to maintain the receiver pressure constant, increasing the number of compressors dedicated to the parallel section, mostly if AC load would be considered. Vice versa, in colder days with no AC load and with FGV in operation, the capacity installed on the MT side could be too low to meet the MT load, or such as to meet the load with low efficiency due to the frequency at which the VSD compressor is running. In the warmer period, the ejector can deliver some refrigerant to the suction of the parallel compressors allowing a power consumption reduction due to the unloading of MT compressors, or at least no deterioration of the COP at the lowest temperature at which it can be used. Hence, the ejector is regulating the high-pressure at 25, 30, 35 °C, even though HPV can always do the job.

The numerical results, showing which compressors are used and in which section, have been plotted afterward. At each temperature, there will be a comparison between the system equipped with pivoting compressors and without them, with different colors indicating in which section the compressor is employed. In Table 6.3 the denotation used over the analysis is presented:

Table 6.3: Denomination used to represent the results afterward.

Compressor	Denomination	System without Pivoting	System with Pivoting
E – 321	Compressor 1	LT	LT
E – 311 [30-70 Hz]	Compressor 2	LT	LT
E – 111 [30-80 Hz]	Compressor 3	MT	MT
E – 121	Compressor 4	MT	MT/IT
E – 131	Compressor 5	MT	MT/IT
E – 211 [30-80 Hz]	Compressor 6	IT	IT
E – 221	Compressor 7	IT	IT/MT
E – 231	Compressor 8	IT	IT/MT

As can be seen, compressors 4, 5, 7, 8 can be pivoting compressors. During the analysis, the results have shown that different combinations of pivoting can be adopted to supply the design loads but moving towards a pair of pivoting compressors with certain features in terms of displacement might be smarter to cover the partial load with better performance. As it would be expected, the power consumption increases as the heat rejection temperature raise, and the number of compressors needed to cover the load might be higher especially when the multi-ejector block is regulating the high-pressure. This is understandable since when the ambient temperature is very low, all the load is covered by MT compressors, while when the ambient temperature increases a much larger share of the load is transferred to the parallel section requiring the installation of big compressors that will be used only for few hours during the year, increasing the total cost of the system, the unused capacity, maintenance costs and footprint.

According to the analysis above, the following combinations have been found numerically (considering a system with pivoting and not). The energy consumption, as well

as the capacity, required increases drastically when gas cooler outlet temperature and high-pressure are both at a high level. A suitable pair of pivoting compressors is (E – 131 + E – 221) and afterward is illustrated how a compressor or more of them must be added to the compressor pack as the gas cooler outlet temperature raises. Figure 6.2 shows the results at gas cooler outlet temperature equal to 10 °C:

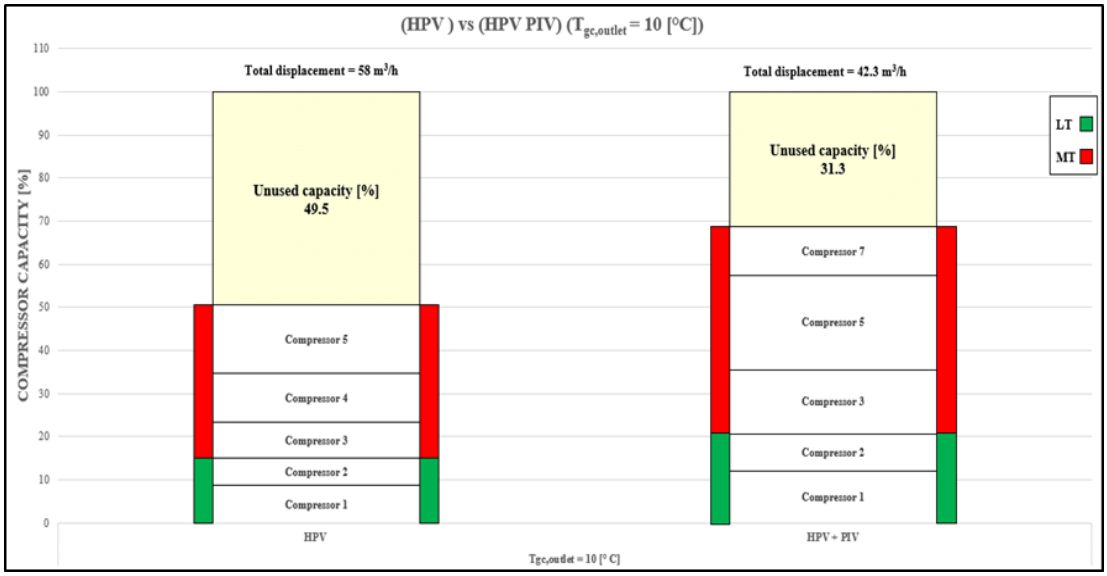

Figure 6.2: Compressors combination (HPV vs HPV + PIV) at gas cooler outlet temperature = 10 °C.

It is worth to mention that the LT compressor pack is working in the same way in both cases since the discharge and the operating conditions do not change. Having E – 221 as pivoting, allows to not use E – 121 getting better performance on the compressor E – 111 (with VSD) since it is running close to the nominal frequency of 50 Hz, which could be considered the frequency at which the efficiency of the compressor is higher. As can be seen, the unused capacity is quite larger in the system without pivoting but this will be easily understood when the case at 35 °C will be presented. Furthermore, being the amount of vapor too low for the minimum capacity of the parallel compressors (taken into consideration even the minimum pressure ratio at which they can work) these compressors are turned off and the flash-gas bypass valve (FGV) regulates the pressure in the liquid receiver, expanding the vapor to the suction of MT compressors.

When the gas cooler outlet temperature reaches 15 °C (Figure 6.3), the FGV is still throttling the vapor from the receiver pressure to the MT evaporating temperature, hence only LT – MT compressors are in operation. Clearly, with a slightly higher pressure ratio and

amount of vapor throttled, the capacity raises but still the same compressors used before are employed, and the controller speeds up the active VSD-compressor. As already said, more and more capacity is necessary when the ambient temperature gets warmer.

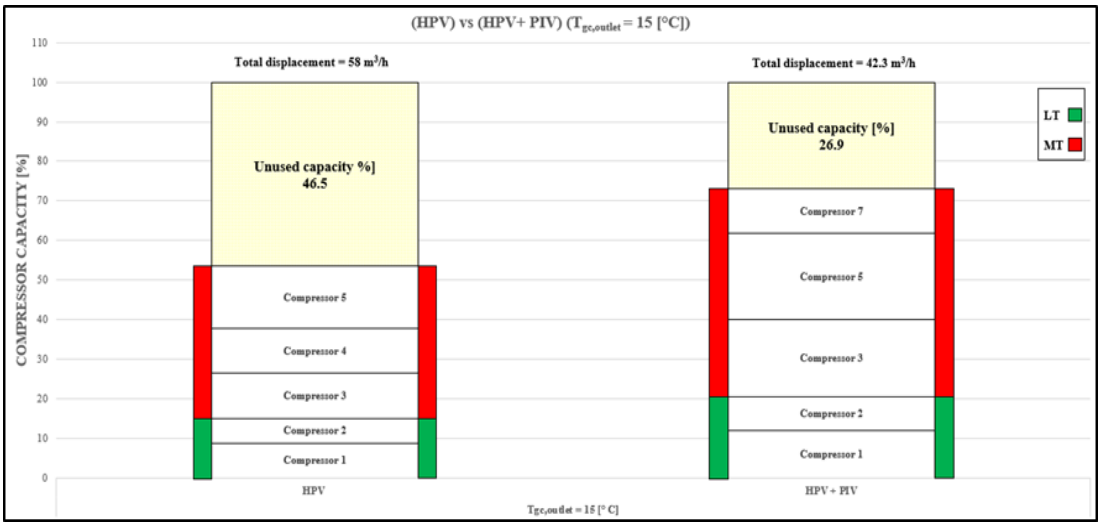

Figure 6.3: Compressors combination (HPV vs HPV + PIV) at gas cooler outlet temperature = 15 °C.

When the gas cooler outlet temperature reaches 20 °C (Figure 6.4), the parallel compressor E - 211 is in operation at low speed. Anyway, since the rotational speed is not at the minimum level, it means that there will be a temperature in the range 15-20 °C where E – 211 is running at the lowest speed (30 Hz) that should be around 17 °C.

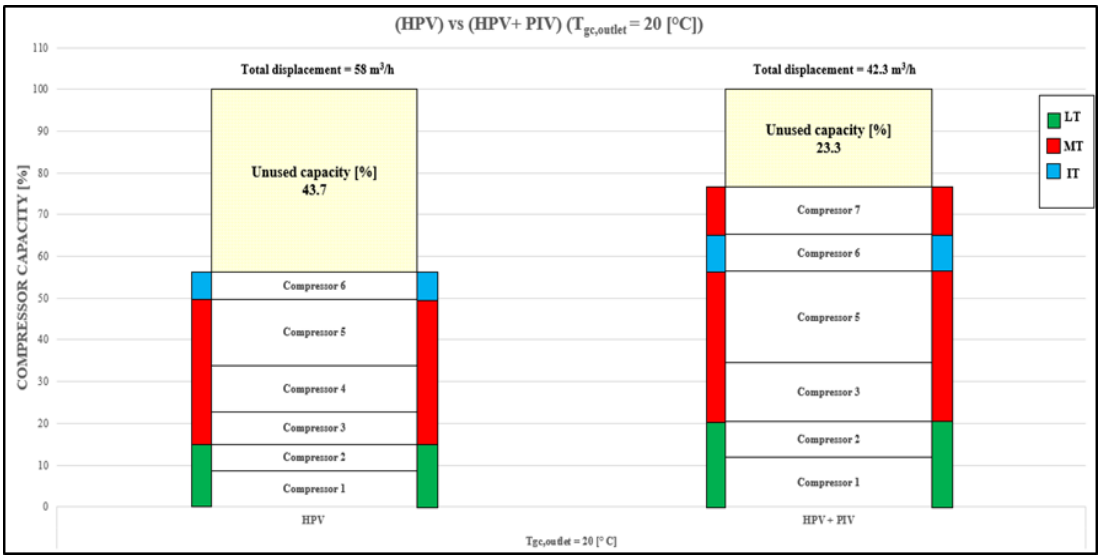

Figure 6.4: Compressors combination (HPV vs HPV + PIV) at gas cooler outlet temperature = 20 °C.

The compressor E – 111 is running at the lowest speed than at lower gas cooler outlet temperatures because of the parallel compressors. The pressure ratio is higher, however, the FGV was throttling such amount of vapor increasing the capacity required on the MT level at 15 °C.

At 25 °C gas cooler outlet (Figure 6.5), the system could regulate the high-pressure with the multi-ejector block. The theoretical analysis has been carried out both with HPV even at high ambient temperatures, and with the HP multi-ejector. It is remarkable to mention that the total displacement is referred to as the total number of compressors installed in the system, which is dependent on the system arrangement. Therefore, the main analysis considers HP multi-ejector as a high-pressure control device. When the only HPV is employed, no difference is noticed since the number of compressors to install is the same, as well as the unused capacity in each case. This is illustrated in Appendix F.

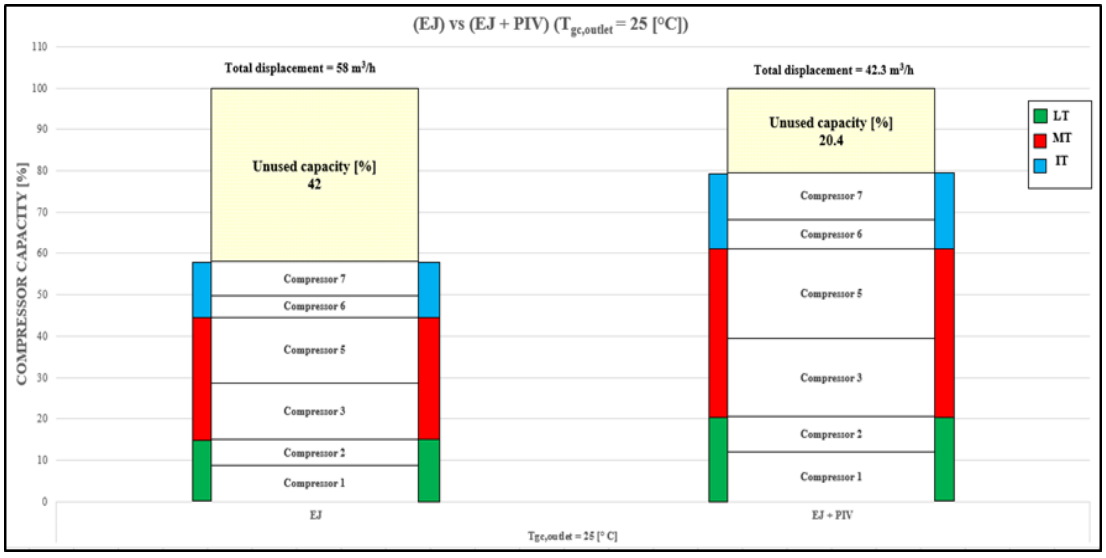

Figure 6.5: Compressors combination (EJ vs EJ + PIV) at gas cooler outlet temperature = 25 °C.

At these operating conditions, the ejector cannot entrain as much refrigerant as in warmer ambient temperatures, and therefore the unloading of the MT compressors is more contained but however, one MT compressor is switched-off (E – 121 without pivoting, E – 221 switched from MT to IT side with pivoting). The same compressors combination has been obtained both with and without the pivoting principle. The difference in height occurs because of the different capacity installed in the system; as already said, the pivoting compressors enables greater flexibility in terms of ability to follow the actual load profile by switching the compressors from one operating condition to the other and as consequences a better use of

the capacity install as expected. Moreover, since the analysis is based on the polynomial equations which have uncertainty as stated by the standard EN12900, it might be that if the compressor equipped with VSD is running almost at full speed and experimentally the mass flow to displace is a bit higher than what it was expected, one more compressor should be switched on to avoid any increment in terms of evaporating temperature or receiver pressure.

When the gas cooler outlet temperature reaches 30 °C (Figure 6.6), an increasing amount of refrigerant is pre-compressed to receiver pressure by the ejector leading to the following scenario:

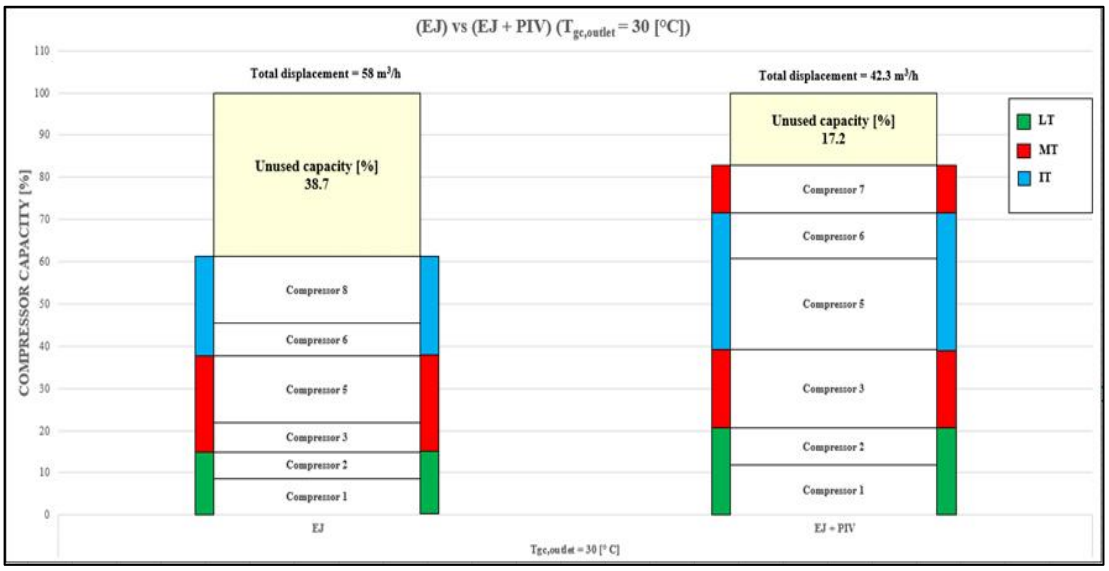

Figure 6.6: Compressors combination (EJ vs EJ + PIV) at gas cooler outlet temperature = 30 °C.

Without the pivoting, a big compressor must be installed in the parallel section to face the increment of refrigerant to compress. This is the main issue: because of this compressor that is going to be used only for few operating hours, the unused capacity increases drastically while when the pivoting compressors are used, the MT load can be supplied increasing the rotational speed of E – 111 and switching E – 131 to parallel compressor to keep under control the receiver pressure, but saving a compressor.

The most important operating condition occurs at 35 °C (Figure 6.7). Here, is the amount of vapor to compress very high, a lot of capacity is needed in the parallel section (depending on ejector performance).

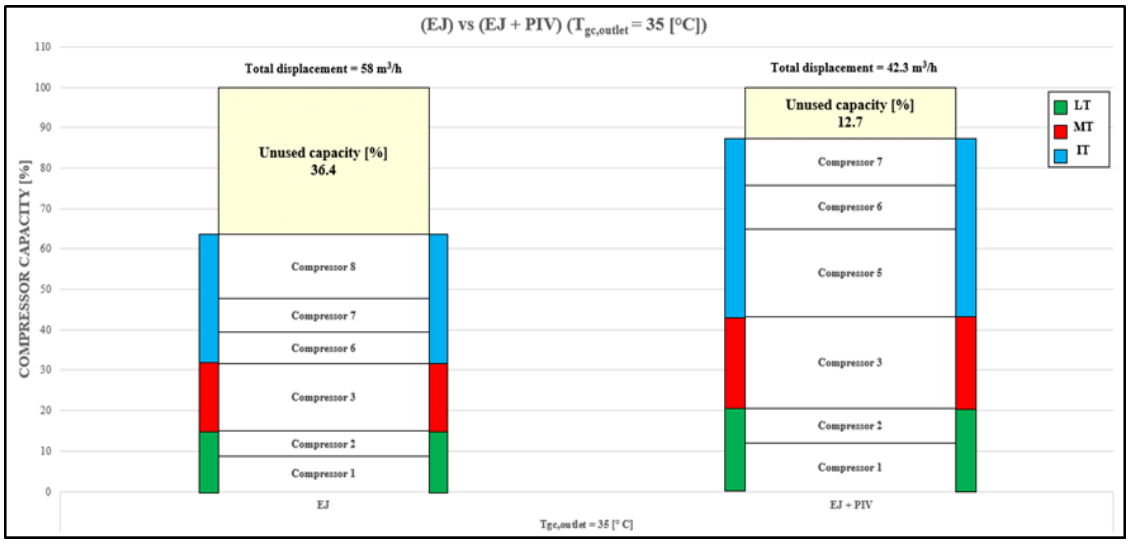

Figure 6.7: Compressors combination (EJ vs EJ + PIV) at gas cooler outlet temperature = 35 °C.

The entrainment ratio is the most important parameter since it is an index of how much the MT compressors are unloaded due to the ejector. Only one MT compressors are theoretically needed because they are heavily unloaded due to the good ejector performance. Because of the pivoting, E – 131 can be used as a parallel compressor together with E – 221, while the LT compressors are operating in the same way since load and working conditions are not changed. A summary of all the cases is in Figure 6.8:

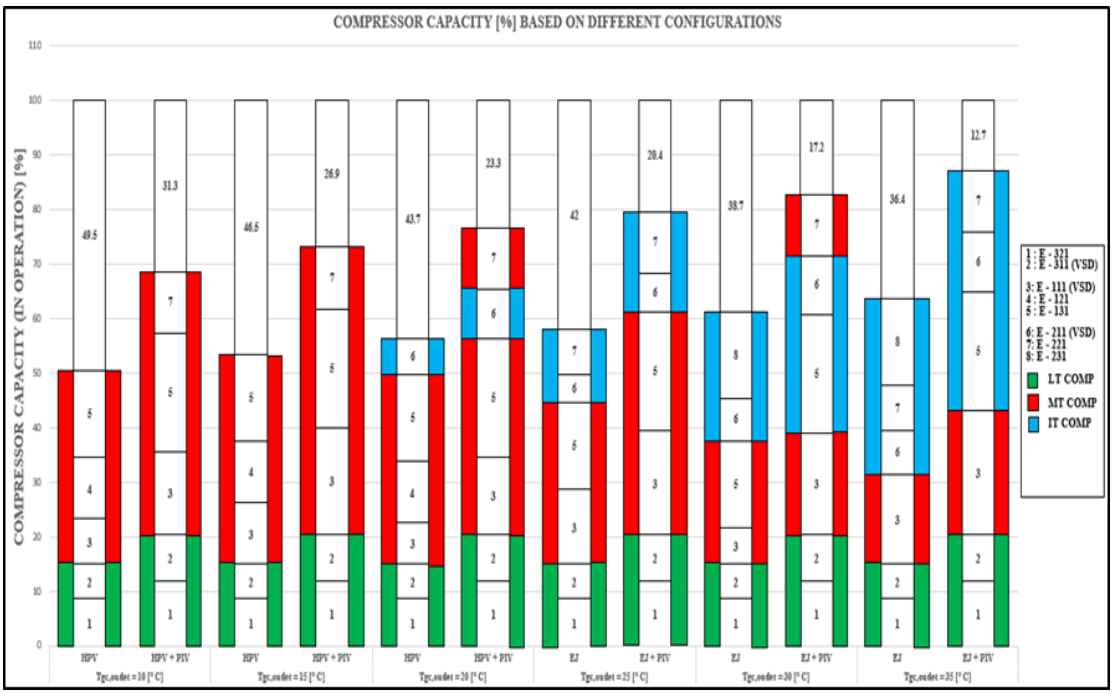

Figure 6.8: Capacity in use under different operating conditions with and without pivoting.

The unused capacity is much larger in the case without pivoting and the reasons for that are already explained. Considering the case where HPV is the high-pressure control device, it does not bring any advantage to have pivoting because of the same number of compressors in the test-rig. This is a consequence of the load split on the MT-IT side differently than what happens with the multi-ejector block, requiring three MT compressors and two IT independently of the use of pivoting or not (the only difference resides on how the compressors could be arranged in the two different compression sections). Therefore, the system with multi-ejector block involves much larger loads to the parallel section and vice versa under changing operating conditions, and when the unit is not flexible as it should be the investment costs increase drastically. It is important to understand that, because of the expense of ejector, the customers have the purpose to save as much energy as possible to repay the investment but because of the poor flexibility of the refrigeration unit the costs rise even more due to the large capacity needed on the IT section in warm ambient condition, and large capacity on the MT section under colder ambient conditions.

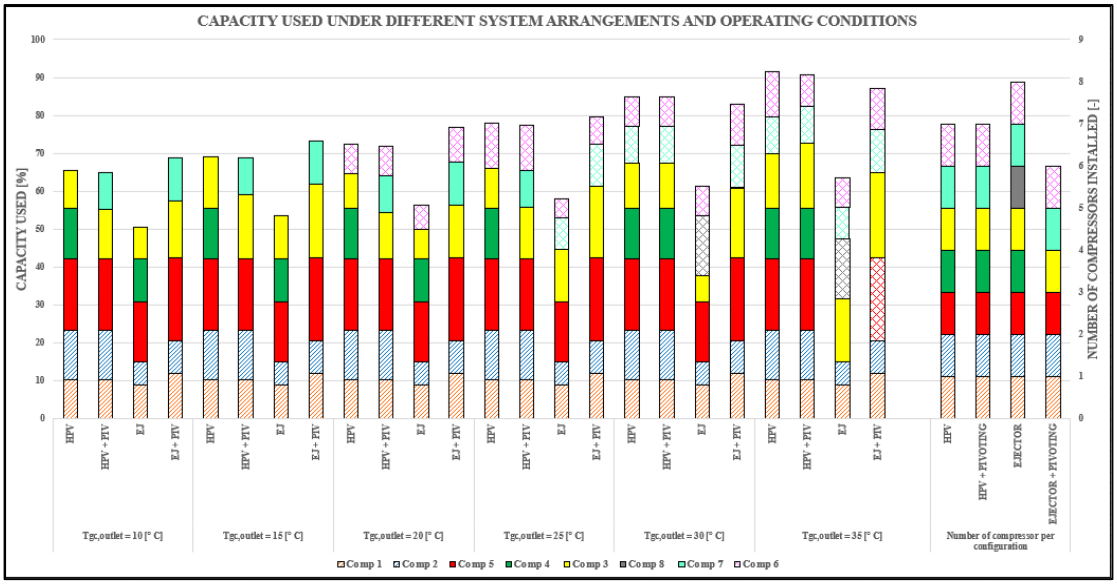

Figure 6.9: Compressor combinations under different operating conditions, and with different high-pressure control devices. The denomination "Ej" has been used even at 20, 15, 10 °C even though HPV is regulating the high pressure. LT compressors indicated with diagonally patterned lines, MT compressors with a solid fill, IT compressors with "diamond-grid lines".

In Figure 6.9 the numerical results have been plotted highlighting on the right side how many compressors are needed to cover the design load under different climatic conditions, with the implementation of the ejector or not. Numerically, the following conclusion can be made:

- The system with HPV does not take any advantage of pivoting, i.e. the same number of compressors must be installed. Furthermore, as it was stated as one of the main points of the analysis, no degradation has been recorded when pivoting compressors are in operation, hence the power consumptions are almost the same with and without "pivoting" (Figure 6.10). A deep analysis will be presented after dealing with the experimental results with a focus on the performance of the compressors. Being the COP defined easily as the ratio between the refrigerating load and the power consumption, a slight difference in the power consumptions leads to small changes in the COP when different solutions are considered
- The multi-ejector system due to the large shift of capacity, without the implementation of the pivoting principle, leads to larger investment costs, reduced effectiveness in the use of the capacity, lower system compactness
- Multi-ejector system equipped with pivoting compressors enables to reduce further the number of compressors installed in the test-rig, saving two compressors and getting all the advantage coming out from the implementation of the ejector technology rather than those coming from HPV use

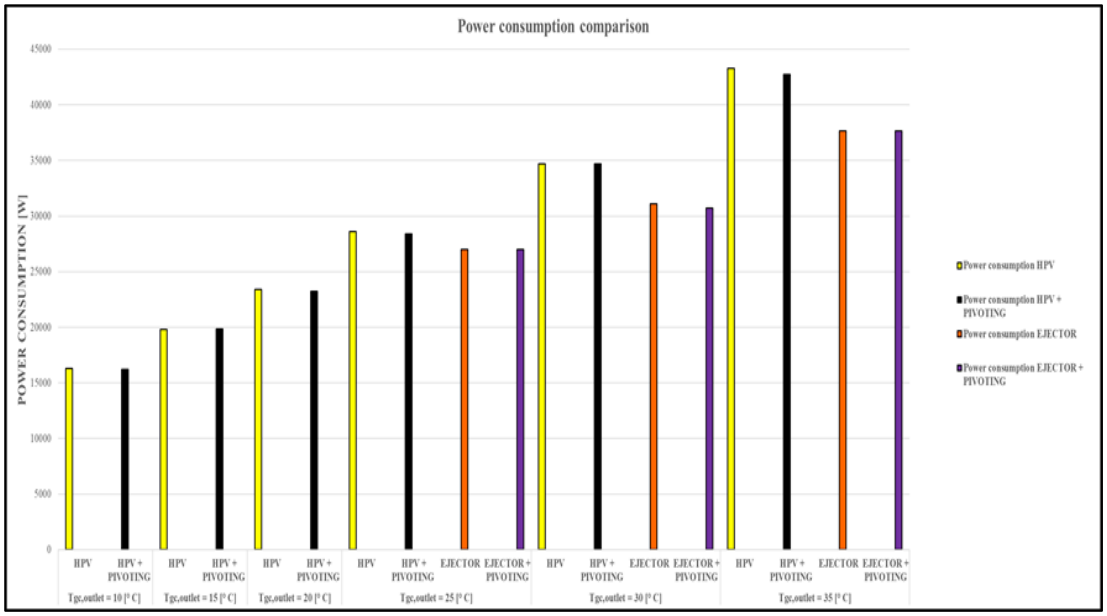

Figure 6.10: Power consumption comparison among the different solutions.

- It is not convenient to implement a multi-ejector block without pivoting. Besides the expense of the ejector itself, a much larger capacity needs to be installed. Of this capacity, only part of it is used leading to waste available space in the test-rig, and

from the economical point of view all the costs related to the maintenance of the system

6.3 Experimental results

As already stated in section 6.1.6, four different cases have been considered. The following guidelines have been taken into consideration over the analysis:

- From the different mass flow meters, obtain the mass flows going through the different compressor section, as well as the refrigerant flows elaborated by the HP multi-ejector block
- To get the pressure levels at the suction and discharge of the compressors, having an idea with which pressure ratio they are working in the case where a higher or lower power consumption needs to be justified
- Gas cooler outlet temperature and high-pressure to see if the experiments have been conducted with stable conditions close as much as possible to the numerical analysis, as well as must be done with the receiver pressure
- The suction temperature of the different compression sections, with attention to the IT suction side. This is strongly related to the IHX performance, which affects the subcooling in the system and the vapor content in the liquid receiver
- Different power consumptions read by the power meters

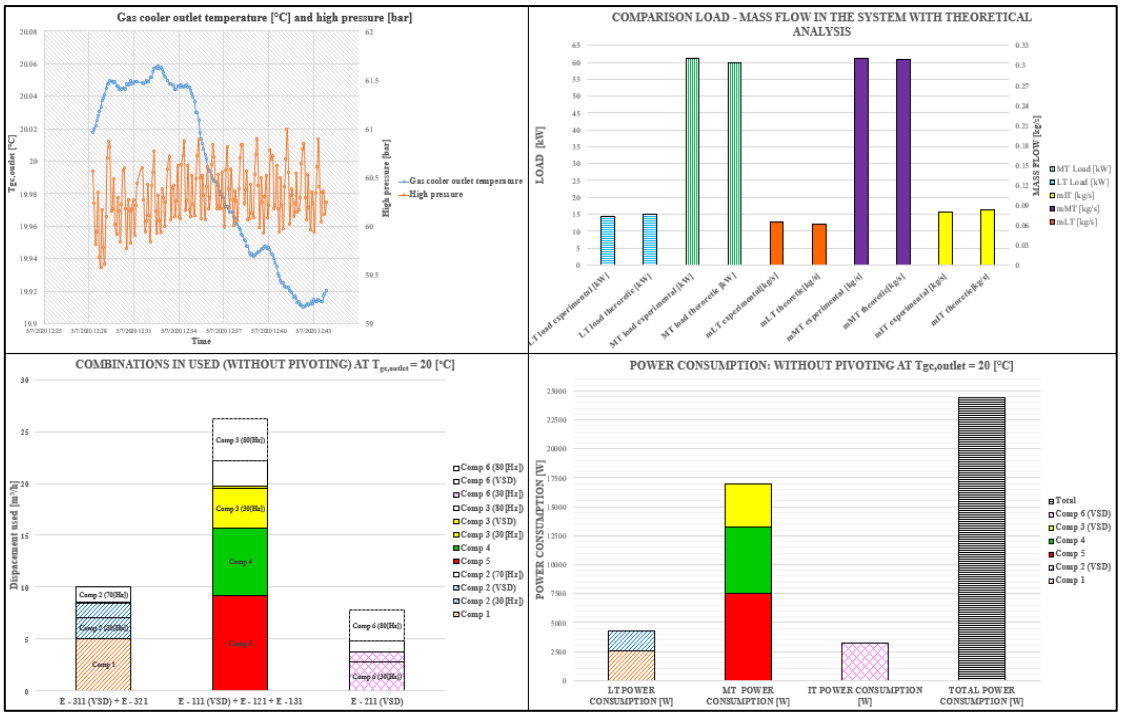

Figure 6.11: Experimental analysis with parallel compression unit (without pivoting) at gas cooler outlet temperature = 20 °C.

The theoretical results have been used to test their validity through experimental tests. As can be seen in Figure 6.11, the loads and mass flows are well predicted, while the high pressure and gas cooler outlet temperature is maintained under control over all the test. It is worth mentioning that the measurement time should be as long as possible to get reliable results. Furthermore, in the third graph on the left corner, the frequency at which the VSD compressors are running can be visualized, getting an idea of how far the compressor is working from the optimal point that can be considered to occur at 50 Hz.

At 25 °C gas cooler outlet, the multi-ejector block could be used. Therefore, four different tests have been done (with HPV, with HP multi-ejector and in both cases with and without pivoting implemented). For simplicity and space, only two graphs indicating which compressor combinations are in operation and the load-mass flows in the system are plotted below (Figure 6.12). The case with HPV (both with and without) has not much to say: the mass flows elaborated are well predicted, but a small difference starts to be visible in IT mass flow because of the different performance of the IHX. This will be discussed later when also the ejector performance will be an argument of discussion.

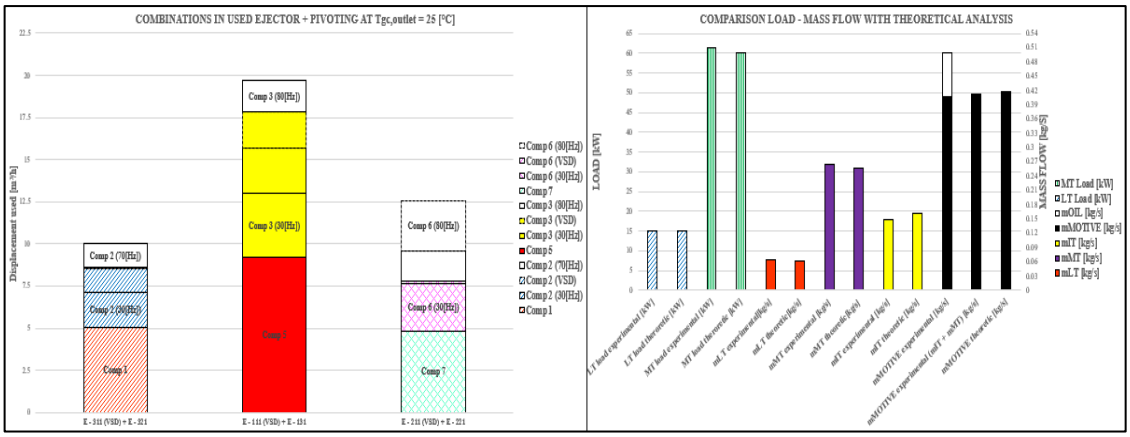

Figure 6.12: Experimental analysis with a multi-ejector compression unit equipped with pivoting compressors at gas cooler outlet temperature = 25 °C.

Now, the cases (EJ + PIV) at 30 (Figure 6.13) and 35 °C (Figure 6.14) are presented. The discussion will take place in the next sub-chapter where the comparison experimental-theoretical results are made. All the other cases, with HPV regulating the high-pressure and with pivoting are shown in Appendix G.

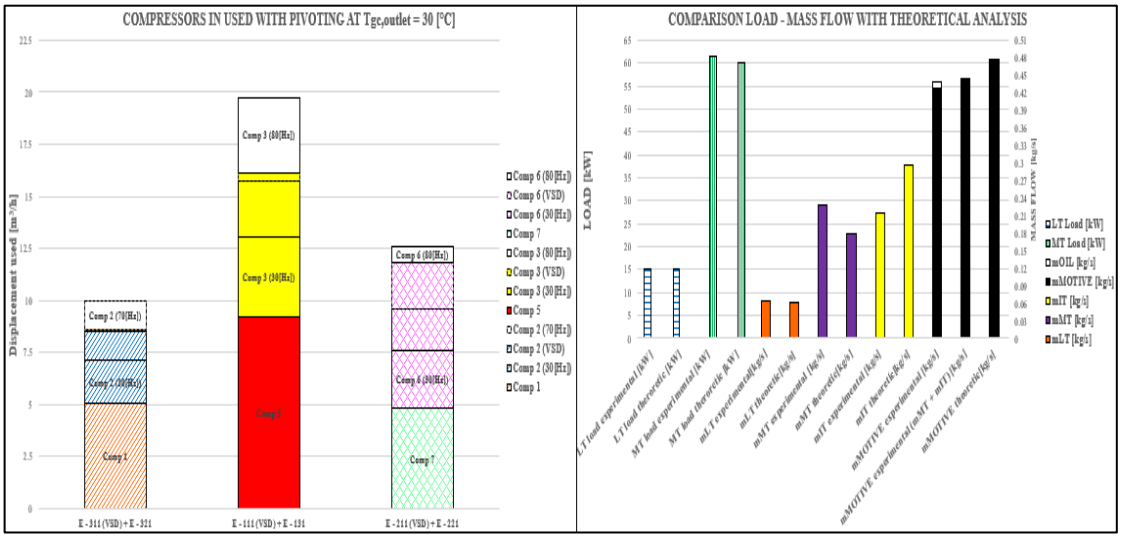

Figure 6.13: Experimental analysis with a multi-ejector compression unit equipped with pivoting compressors at gas cooler outlet temperature = 30 °C.

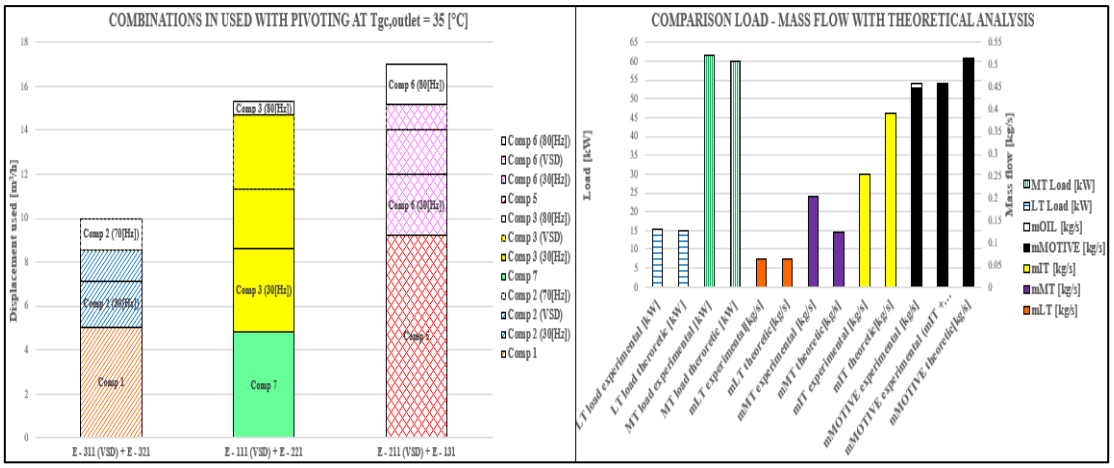

Figure 6.14: Experimental analysis with a multi-ejector compression unit equipped with pivoting compressors at gas cooler outlet temperature = 35 °C.

6.4 Comparison of experimental – theoretical results

From the experimental results, two things can be noticed:

- The IHX has different performance than what was expected, because of its design. The IHX located downstream of the gas cooler is oversized meaning that whatever are the mass flows through it the subcooling will be always larger than what was given in the simulation, affecting the suction temperature of the parallel compressors as well. Being the suction temperature higher, the density decreases and as consequences the ability of the IT compressors to displace a certain mass flow. In the other hand, higher subcooling means moving further on the left side of the p-h diagram, lowering the amount of vapor in the receiver and unloading the IT compressors, therefore in a way the two things are compensated even though at very high gas cooler outlet temperature the difference in terms of mass flow becomes significant
- The main discrepancy in terms of mass flow happens at 30 and 35 °C as gas cooler outlet temperature when the multi-ejector block is regulating the heat rejection pressure. In those cases, the entrainment ratio is lower than the theoretical one leading to a larger amount of refrigerant to be compressed by MT compressors. This could be explained theoretically, referring to Banasiak et al. [42]. As can be seen in Figure 6.15, the ejector efficiency is not so different, but the entrainment ratio is in some cases lower by 30-40%. If the efficiency can be considered almost constant, the entrainment ratio degrades gradually with the increasing mass flow rate expanded,

which happens in warmer conditions. This is related to the intensified flow irreversibility and therefore pressure losses that occur inside the ejector pipes meaning that the ejector is overcoming a higher pressure lift than what is measured. It can be noticed that there is a slight difference between the two experimental results (with and without pivoting), but this shouldn't be wrongly attributed to the pivoting implementation. Being the high-pressure slightly different, the ejector is working with a bit high-pressure lift affecting the efficiency and entrainment ratio

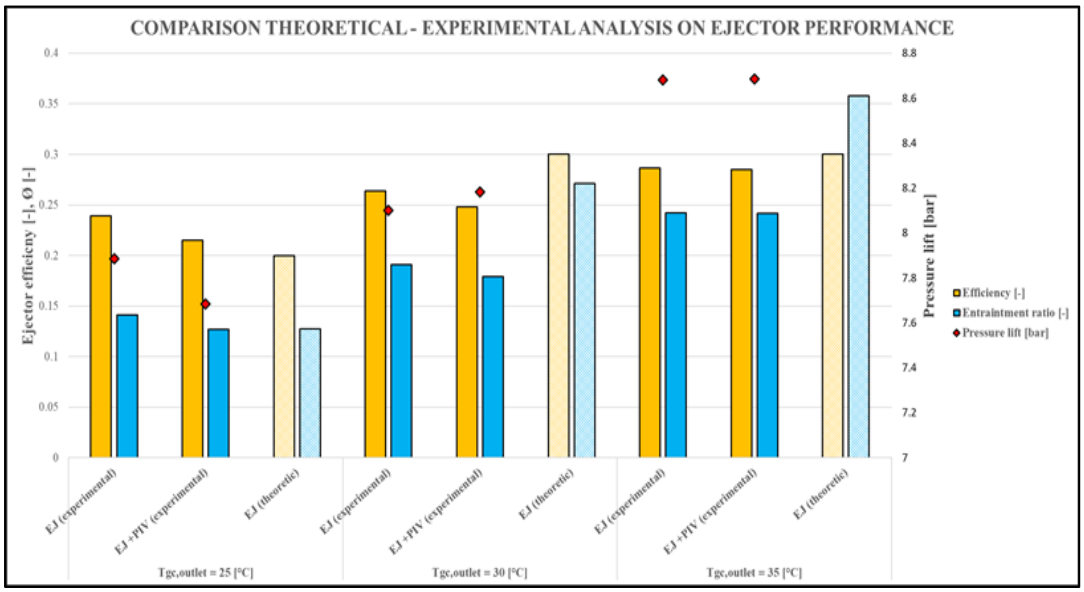

Figure 6.15: Ejector performance (theoretic vs experimental values).

For the reason already explained, the high-pressure profile has been studied since the pressure lift will be slightly difference affecting the ejector performance. In Figure 6.16 and Figure 6.17 the deviation in the high-pressure is defined as following (6.19):

$$Err = p_{HP,setpoint} - p_{HP,actual} \tag{6.19}$$

Therefore, when the deviation is negative the ejector is overcoming a higher pressure lift meaning that the entrainment ratio will be higher, being the high-pressure in the system increased. This concept is different from what has been discussed before when pressure losses inside the multi-ejector block have been considered. Being the deviation negative in the case of a multi-ejector system, more refrigerant is entrained in improving the ejector performance but moving far away from the experimental conditions (Figure 6.15). However, many factors may represent a reason for such differences, i.e. lower subcooling due to the different high-pressure as well as slightly different motive flow.

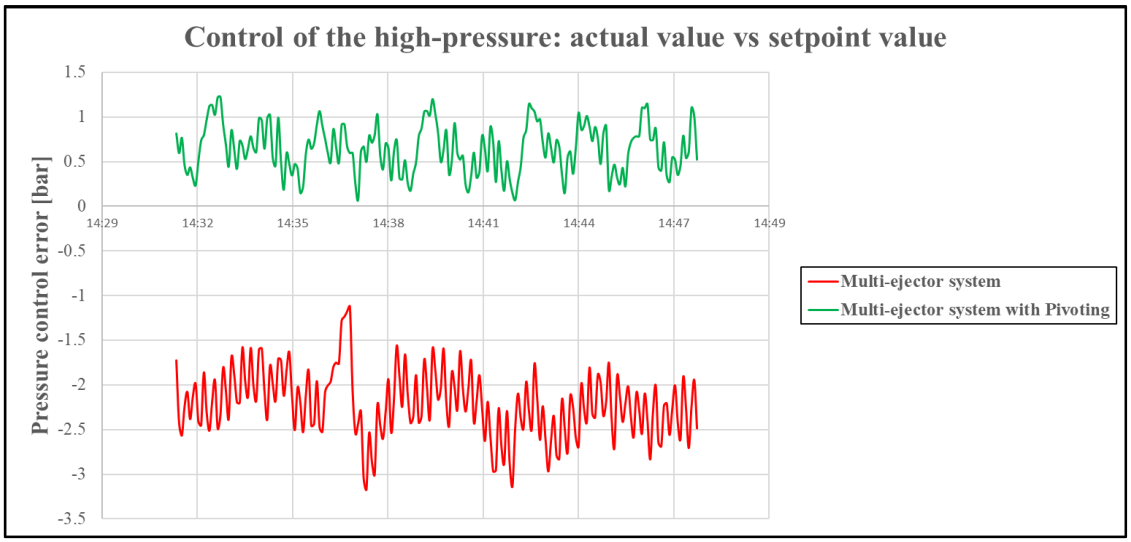

Figure 6.16: Deviation between the actual value and the setpoint value for the discharge pressure, both in a multi-ejector system with and without Pivoting ($T_{gc,outlet}$ = 25 °C).

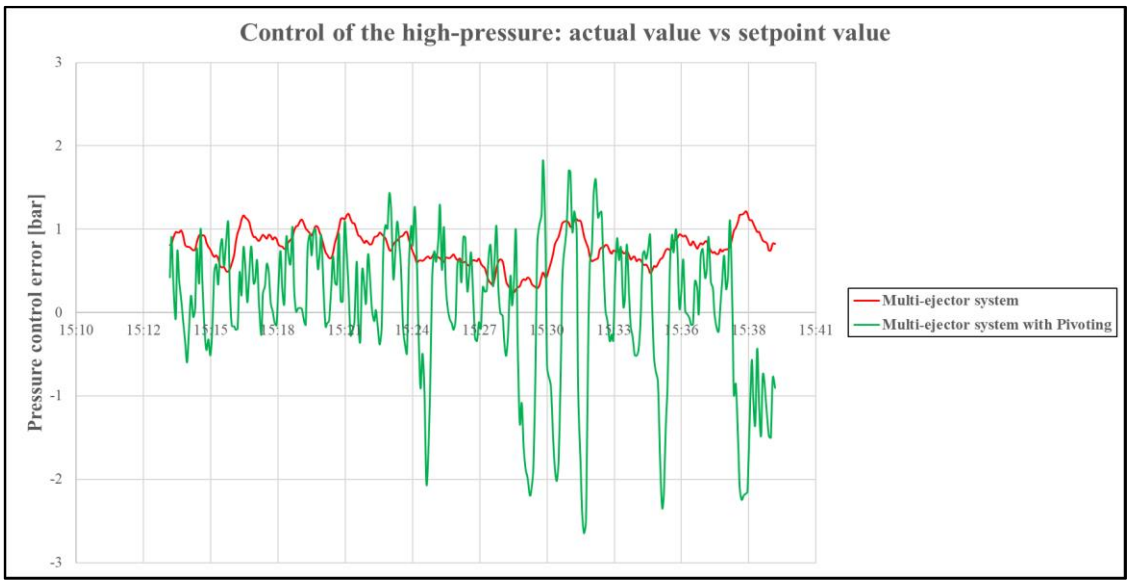

Figure 6.17: Deviation between the actual value and the setpoint value for the discharge pressure, both in a multi-ejector system with and without Pivoting ($T_{gc,outlet}$ = 30 °C).

Concerning only the cases with HPV at 20 °C and HP multi-ejector block for 25, 30, 35 °C, the following comparison can point out if the pivoting compressors are really beneficial for the investment costs and compactness point of view, taking care of the system performance (no degradation in terms of COP). As already said, the prediction in terms of mass flow in the system is accurate when the gas cooler outlet temperature is low and when the high-pressure is regulated by HPV. Therefore, this can be seen in Figure 6.18 where a double comparison is made (experimental (HPV) vs experimental (HPV+PIV) vs theoretic

(HPV+PIV)). The total displacement written at the top of each column is referred to as the system with ejector (with and without pivoting) which is related to the compressors pack active at 35 °C, being the main case investigated.

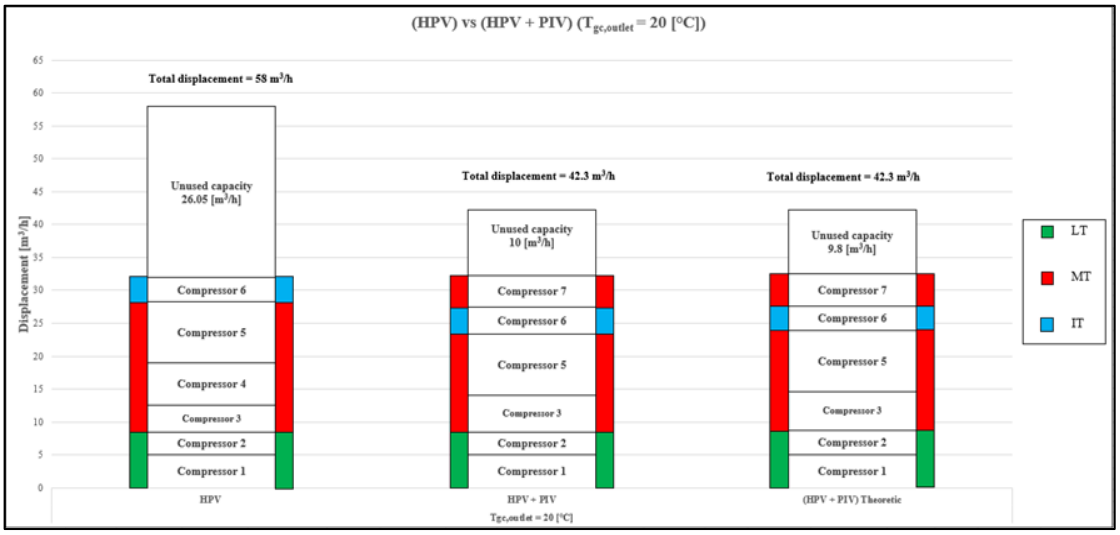

Figure 6.18: Comparison experimental vs theoretical results with $T_{gc,outlet}$= 20 °C, and multi-ejector supported system.

To justify what has been said so far, the case with HPV is plotted. The performances with pivoting are well predicted, leading to a compressor pack composed of three MT compressors and one IT. In this case, the unused capacity is expressed in terms of m^3/h, giving an idea of how much capacity is not utilized for such operating conditions. What is shown in Figure 6.19 is reflected in the following cases:

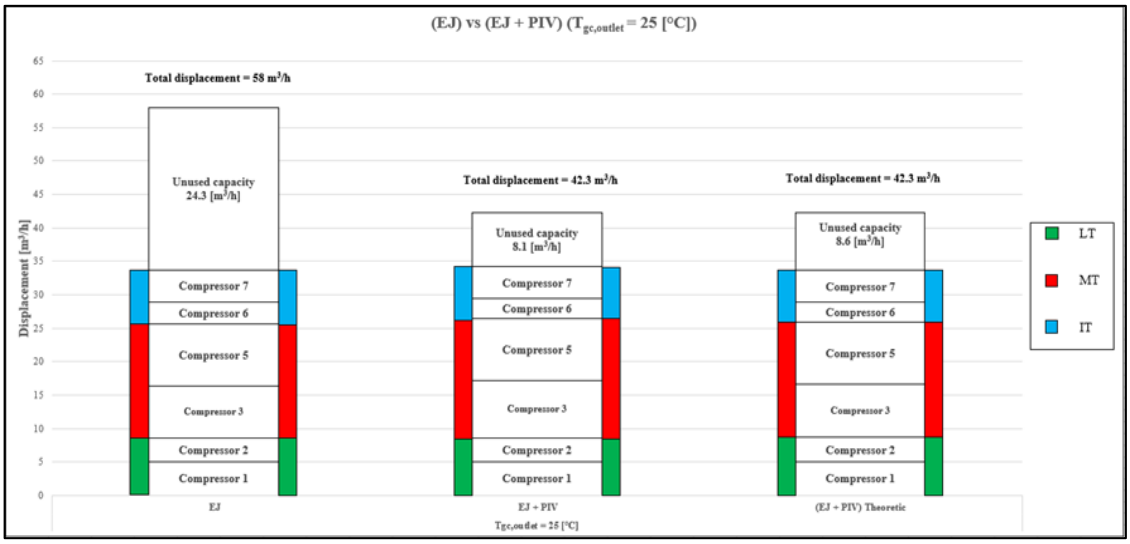

Figure 6.19: Comparison experimental vs theoretical results with $T_{gc,outlet}$ = 25 °C, and multi-ejector supported system.

The combinations adopted with the pivoting is not different, rather the unused capacity once again justifies the need to have pivoting compressors in supermarket applications. Furthermore, this agreement between theoretical-experimental results finds a reason in the ejector performance, which is almost perfectly predicted. Differently, the cases at 30-35 °C show a disagreement (Figure 6.20 and Figure 6.21, respectively). Since the experiments have been carried out first without pivoting, it had been noticed that the ejector is performing worst meaning that when the pivoting principle is applied only a few compressors are available in the compressor pack. Less refrigerant sucked by the ejector means unloading the parallel compressors and force the MT compressors to elaborate more refrigerant which might be a problem if the capacity installed in the MT section is too small. Basically, looking at the experimental results with the multi-ejector supported system without pivoting, the combinations at 30-35 °C in the MT-IT side have been exchanged between them.

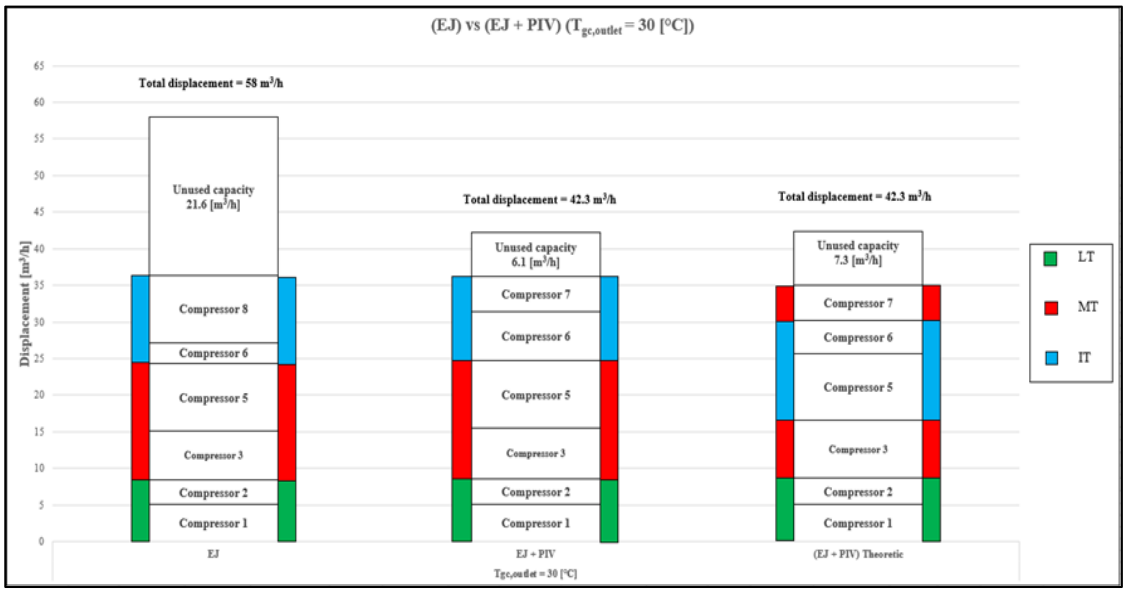

Figure 6.20: Comparison experimental vs theoretical results with $T_{gc,outlet}$ = 30 °C, and multi-ejector supported system.

As plotted upstream, the entrainment ratio theoretically evaluated is larger leading the MT compressor pack to work with the smallest compressor (Compressor 7) and switching the Compressor 5 to parallel compressor. Experimentally, being the entrainment ratio lower the MT compressor packable to match the load should account for the Compressor 5 instead of the Compressor 7. Slightly lower ejector performance leads to a different shifts in capacity between the compressor suction groups and greater overload of the MT compressors. This results in greater total power consumption because of the pressure ratio at which the MT

compressors work, decreasing the energy saving and the COP of the refrigeration unit (mismatch numerical – theoretical results).

Theoretically, the system could operate with up to three parallel compressors when the ejector performs best, having only one MT compressor operating at maximum capacity. Because of the simplicity of the numerical model and overestimation of the ejector performance and underestimation of the IHX performance, a disagreement result. However, it is still possible to supply the design load with only six compressors (installed compressor-capacity would be identical) taking advantage of the pivoting principle. Therefore, the smallest compressor must be placed on the MT side, ending to use almost all the capacity installed.

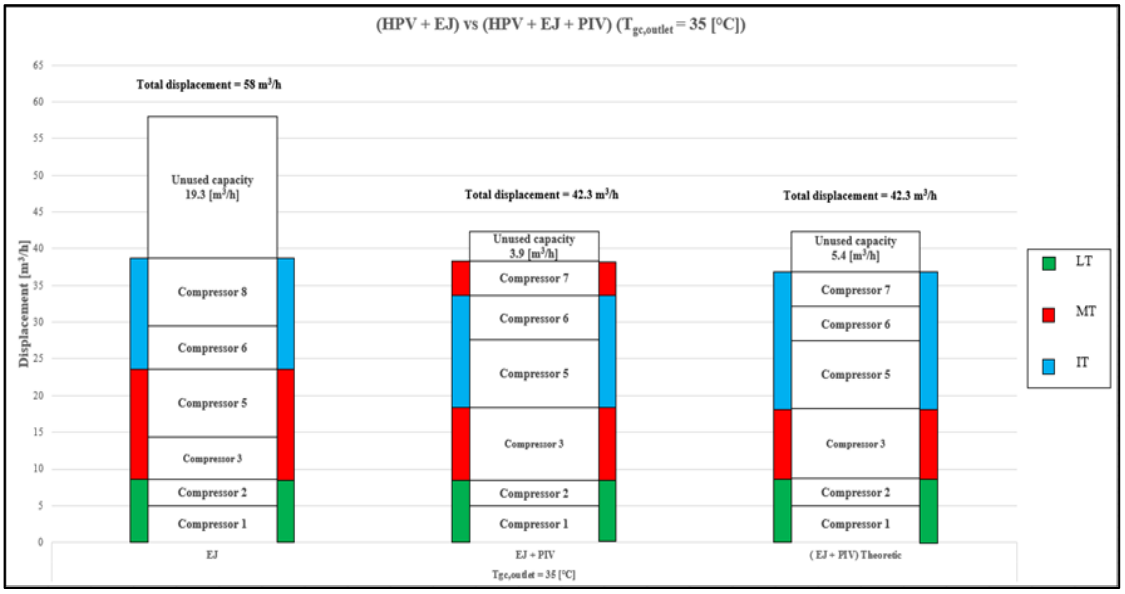

Figure 6.21: Comparison experimental vs theoretical results with $T_{gc,outlet}$ = 35 °C, and multi-ejector supported system.

A simplified cost-analysis can point out the benefit coming with pivoting compressors in an ejector-supported system. In fact, at the same time a power consumption reduction is obtainable due to the unloading of the MT compressors in favor of IT compressors and a reduction of the total number of compressors installed is achievable. Considering to not account the costs for heat exchangers, pipes, etc. that are almost identical independently on the system arrangement, only the costs of compressors and multi-ejector block (which has the same cost of the smallest compressor) were considered. In Figure 6.22 the concept is shown clearly: the highest investment costs come out with a multi-ejector supported system without pivoting compressors. As many times said, and prove now theoretically and

experimentally, the power reduction is not enough to justify economically the implementation of ejector technology. On the other hand, a pivoting solution enables to lower by two the number of compressors, in this specific case that simulates a medium-size supermarket, getting the same costs of the HPV unit and compensating the cost due to the multi-ejector.

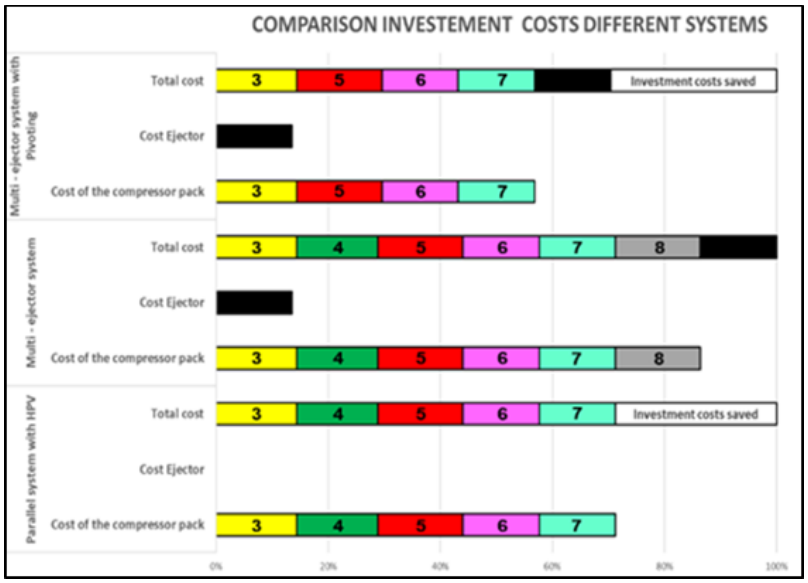

Figure 6.22: Simplified cost analysis of the different configuration of CO_2 compressor rack as function of the high-pressure control device and implementation of the pivoting solution.

6.5 Evaluation of the system performance with Pivoting solution and its potential in R744 integrated systems

Being the LT compressor discharge delivered to the MT pressure level, the pivoting solution does not affect the efficiency of those compressors. Utilizing the ejectors during the experimental investigation significantly reduces the capacity of the MT compressors, mostly at high gas cooler outlet temperatures. The refrigerant vapor entrained by the ejector influences the volumetric and overall compressor efficiency due to the change in capacity and the various frequency. What it could be expected, is a degradation of the volumetric efficiencies of the parallel compressors when a larger amount of refrigerant is split into two or three compressors instead using one or two of them. The case at 35 °C has been analyzed (Appendix L), as well as a comparison of the overall compressor efficiency (both MT and IT) of a parallel compression unit and multi-ejector, supported unit. First of all, the COP must

be evaluated, since it is an index of the power rate required to provide a certain cooling load. A small or no increase in a multi-ejector supported configuration might be related to the worst compressor performance, being the multi-ejector block and the compressor pack interactions very important during the refrigeration unit design. As expected, when the transcritical condition occurs the throttling losses become more and more important leading to a large deterioration in terms of COP, and the improvement coming with the ejector is present at 35-30 °C, but not at 25 °C. A negligible COP difference has been observed between the solution with and without pivoting (Figure 6.23).

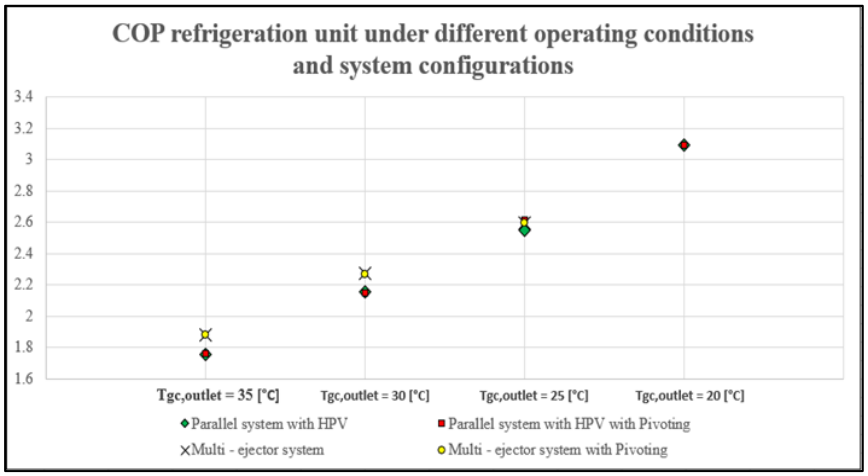

Figure 6.23: System performance for the parallel system and multi-ejector system under different temperature at the gas cooler outlet.

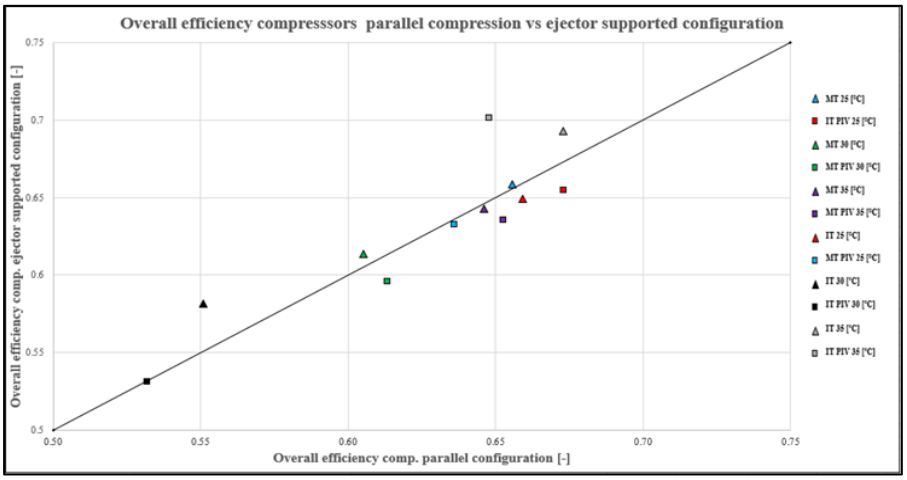

Figure 6.24: Overall efficiency of the MT and IT compressors in case of parallel compression unit vs multi-ejector block under equivalent conditions (the temperature at the outlet of the gas cooler and high pressure).

In Figure 6.24 the solid black line represents the y = x equation, but most of the points are on the left or right side of it. Being on the right side means the parallel compression unit has a better overall efficiency of the compressors than with a multi-ejector supported block. The COP at 25 °C is slightly higher, and the reason could be given to the worst ejector performance at a very low gas cooler outlet temperature. As can be seen, the IT compressors in a multi-ejector supported unit have better efficiency but still, the power reduction is almost negligible. At higher heat-rejection pressure, the IT compressor pack presents better efficiency with ejector and lower efficiency on the MT compressor pack, pointing out one more time the importance to have an efficient compressor pack. It could be considered the worse overall efficiency of the MT compressors a possible reason for the deterioration in terms of power consumption even when the ejector entrains part of the refrigerant from the liquid separator to the liquid receiver.

Although the performance of the system remains almost unchanged when it is pivoting-supported, the flexibility of the rack is finally achievable with the pivoting technology. The adjusted numerical model has been used to illustrate the following scenario in Figure 6.25:

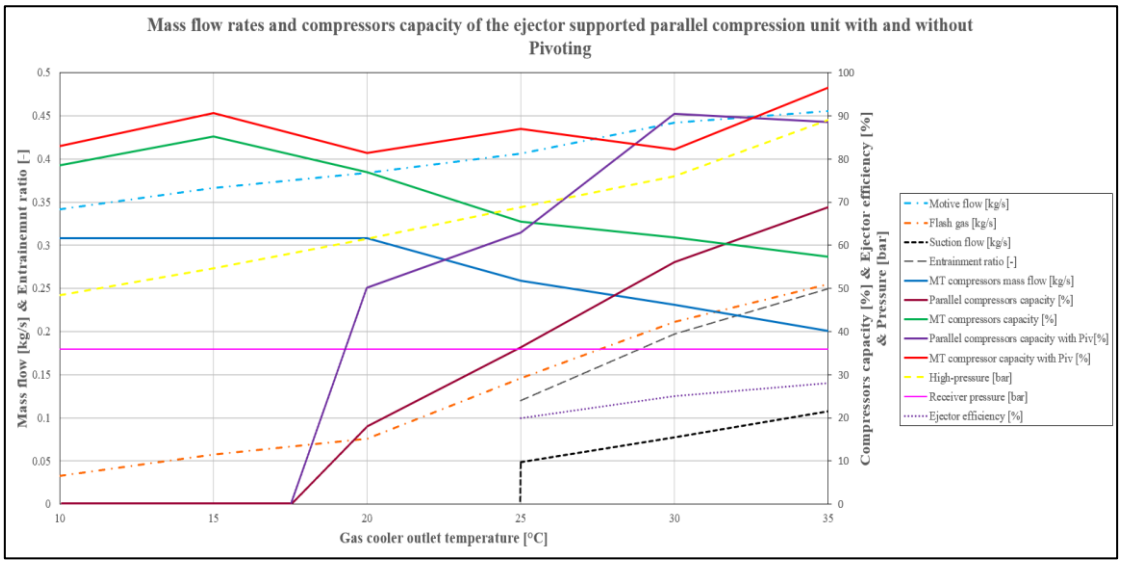

Figure 6.25: Mass flow rates and capacity of MT-IT packs under different operating conditions of the multi-ejector supported system without AC.

At low gas cooler outlet temperature, the parallel compressors are not in operation and the flash gas is throttled by FGV from the receiver pressure to the evaporator pressure level overloading the MT compressors. Around 17 °C, the compressor equipped with VSD is running at the lowest speed as indicated in the graph. As the gas cooler outlet temperature raises, the amount of flash gas (orange line) increases too enabling to use of the multi-ejector

block with a limited advantage at 25 °C because of the reduced available expansion work. The ejector is gradually unloading the MT compressors supporting the parallel compressors more and more towards higher gas cooler exit temperatures. It is interesting to follow the profile of the capacity of the IT-MT compressors. As already seen, the multi-ejector system without pivoting requires three MT and three IT compressors while when the system is pivoting supported the total number of compressors is reduced to four. Being the pivoting compressors a way to increase the flexibility of the rack, the capacity on the MT or IT compressor pack is never fixed over a wide range of operating conditions meaning that it is varying according to the outdoor conditions or cooling load. Thus, it allows better use of the capacity installed as it can be seen in Figure 6.25. As normally happens when ejectors are implemented, the capacity of the parallel compressors increases leading to a shift in capacity from MT to the IT side. When the system is pivoting-supported, considering the same performance of the ejector, the capacity of the parallel compressors (violet line) is still increased but even the MT compressors capacity (red line) is maintained at high-level thanks to the ability to switch the suction lines. Therefore, the potential of such technology is noticeable:

- Total number of compressors can be reduced, making the system more compact
- The investment and maintenances costs are reduced
- Extends the operating time of the compressors, since both the pivoting compressors (Compressor 5 and 7) are in usage at each operating condition
- Better use of the capacity installed, without any degradations in terms of performance.

6.6 MT load fluctuations under different operating conditions

The theoretical analysis, with the model adjusted based on the experimental results (behavior of IHX and ejector), has proven that the combinations of pivoting compressors chosen (Compressor 5 and 7) can cover the partial loads. The LT load was assumed constant as normally happens in a supermarket application, while the MT load has some fluctuations that go from 100 % to 20 % of the design load. This normally happens when the supermarket is closed, and the design MT load no longer is supplied. All the cases can be found in Appendix H, highlighting how far the compressor (with VSD) is working from the optimal

point, considered at 50 Hz. The case with a multi-ejector block is here presented in Figure 6.26.

Even the case with the design load has been modified considering the ejector performance and the subcooling due to the oversized heat exchanger downstream of the gas cooler unit. The pivoting compressor has a positive impact on the flexibility of the system even at partial load, covering with the same number of compressors all the different scenarios. Furthermore, having a big and small compressor as pivoting might be beneficial at partial load since as it occurs at 60% of the design load the capacity in the parallel compressors falls, requiring less and less capacity. It is worth mentioning that if the MT load decreases, less refrigerant is entrained in the multi-ejector block meaning that the entrainment ratio could be even higher due to the lower flow irreversibility inside it. Starting from four compressors in the rack, it ends with only one MT and one IT at a very low partial load.

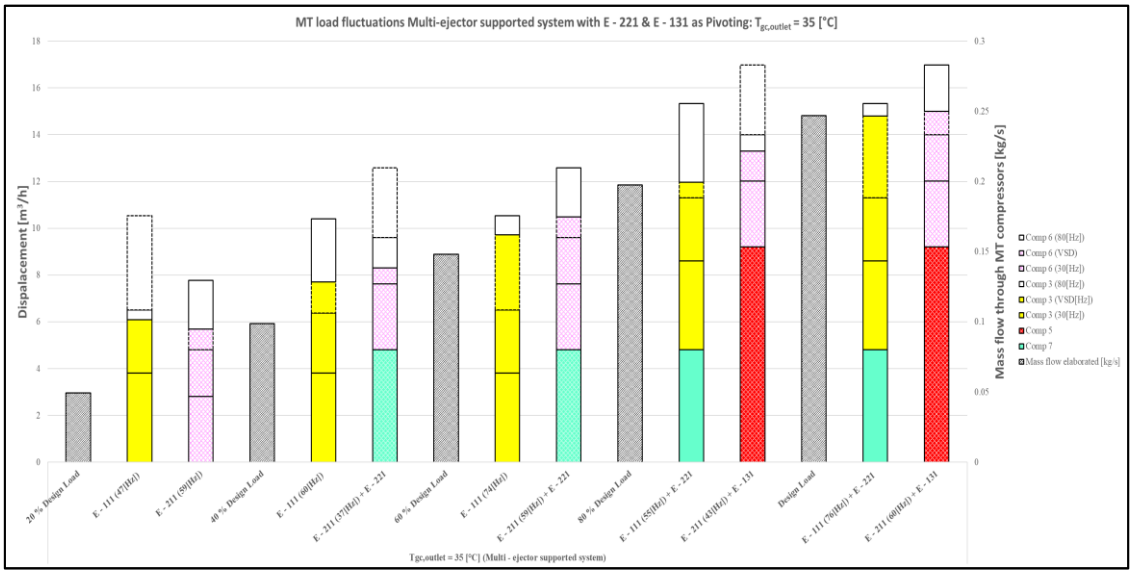

Figure 6.26: Compressor combinations used in a multi-ejector supported system with pivoting solution applied under different MT loads at $T_{gc,outlet}$=35 [°C].

In Figure 6.27 the capacity range covered by the four compressors installed in the system is illustrated.

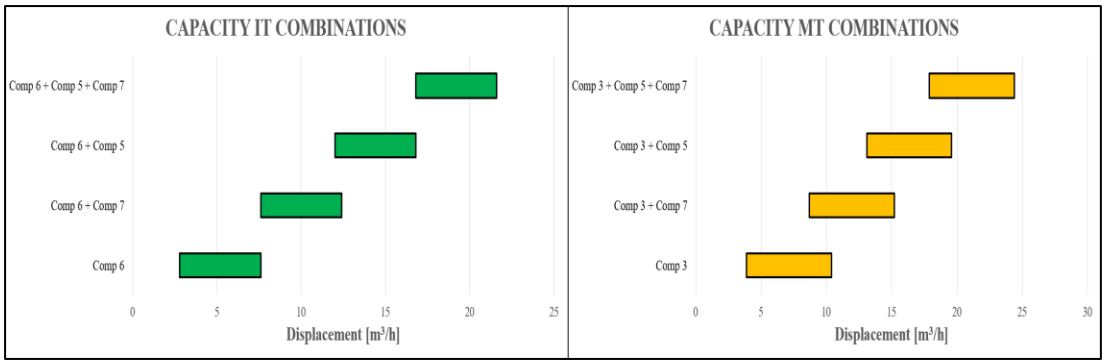

Figure 6.27: Compressor capacity in the IT-MT compressor packs.

It might happen that if the compressor E – 221 is requesting on the MT side, there is a gap in the capacity available for IT. This has to deal with the controller in the system and a possible solution could be the following:

- MT capacity must be fulfilled more accurately, meaning that the combination of compressors must be selected according to the needs
- IT capacity will be too high or too low for the needs since there is a gap in the capacity, meaning that a floating control of the receiver pressure could be implemented. During the night, when the MT load is low and there might be a gap in the capacity required, the receiver pressure can go up when the only E – 211 is on or going down when two compressors are on.

6.7 Pivoting discharge of LT compressors

Another innovative solution to increase the flexibility of the refrigeration system is to connect the LT compressor to the suction line of either MT or IT compressors. The effect to deliver the refrigerant to the suction line of IT compressors has been studied numerically. With the same number of compressors is possible to test the LT pivoting discharge, hence the comparison is made with the same number of compressors but different compressors arrangement. In Appendix, I all the cases, with the distinction based on the system configuration, are illustrated. In Figure 6.28 the total electric power consumption of the compressor rack for all the different scenario is reported:

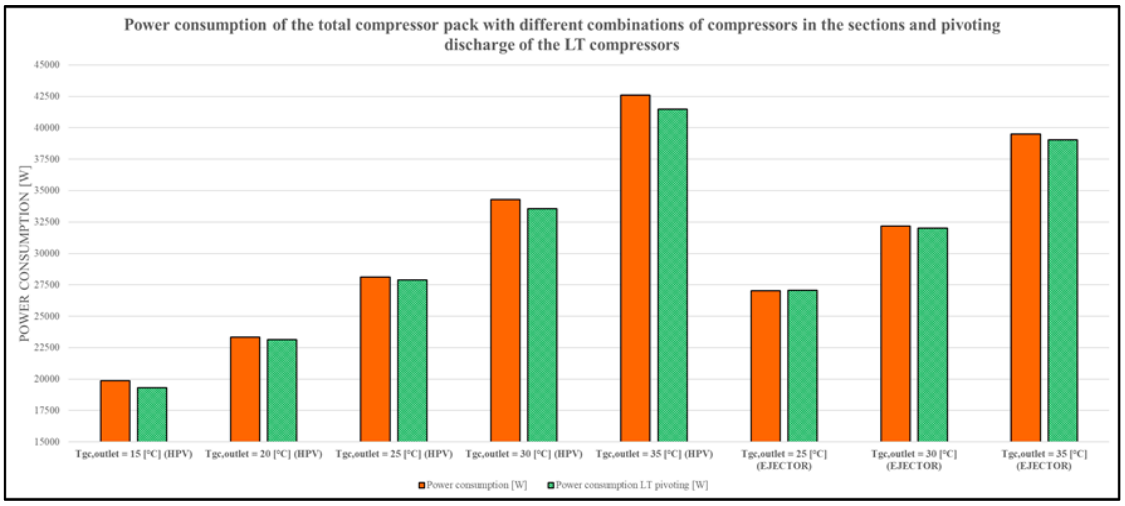

Figure 6.28: Electric power consumption of the compressors in a parallel compression and multi-ejector supported system, under different operating conditions, and pivoting discharge of LT compressors (diagonally patterned lines referred to the discharge of LT compressor.

It can be noticed immediately as at very low gas cooler outlet temperature at which the parallel compressors can work (minimum condensation temperature around 17 °C), the advantage of having the LT discharge delivered to the parallel compressors is translated in a power consumption difference approximately of 550 W. This variation is mainly related to the fact that when the amount of vapor is too low to enable the parallel compressors to work, the FGV throttles the refrigerant causing losses and lowering the system efficiency. In addition, this solution allows the parallel compressors to be employed when not so much vapor needs to be sucked from the liquid receiver.

At 20 °C, the advantage becomes smaller since the IT compressors are already compressing the refrigerant and the pressure ratio with which the MT compressors are working is such as to not bring a considerable energy saving unloading them. When the gas cooler outlet temperature raises and the pressure ratio too, the implementation of the LT pivoting becomes very interesting from the energy saving point of view. This is true for the case with HPV, where at 35 °C the difference reaches approximately 1200 W. When ejector is in operation, the IT compressor pack is already overload with the vapor sucked from the MT evaporators outlet and sending more and more refrigerant becomes advantageous at 30-35 °C, unless the design of the system would be too complicated.

Moreover, the LT pivoting might be a way to completely switch off the MT compressors when the high-pressure is regulated by the HP multi-ejector block. In this scenario, considering the same motive flow, the suction flow could be the total mass flow vaporized in

the MT evaporators, gaining a considerable energy saving. Even at partial load, they might give some advantages, unloading the MT compressors and with a greater share of the total mass flow rate compressed by the parallel compressors, which operate with lower pressure ratio.

6.8 Flash-gas bypass valve vs Parallel compressors

A numerical study has been done considering four different gas cooler outlet temperature the usage of the FGV instead of parallel compressors to evaluate the increment in terms of power consumption. The theoretical power consumption has been calculated with the adjusted model that considers the behavior of the IHX. As can be seen in Figure 6.29 the refrigerating load in a booster cycle can be supplied by different combinations of compressors.

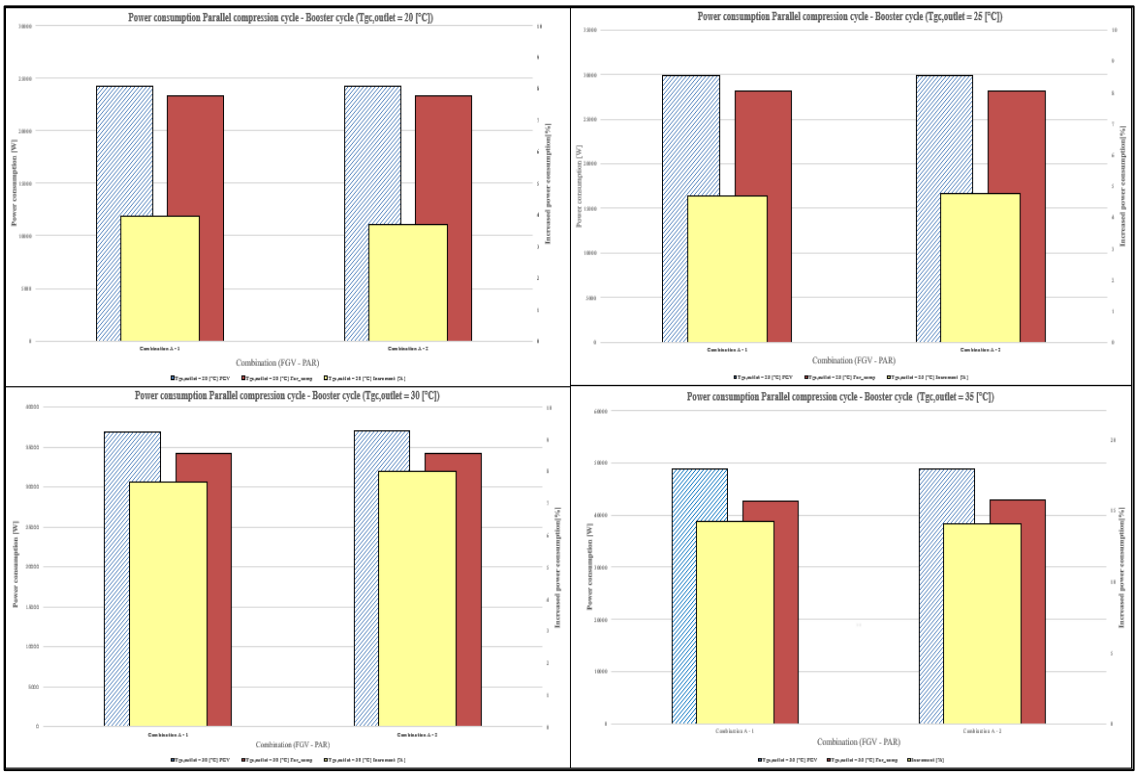

Figure 6.29: Power consumption comparison Booster cycle vs Parallel compression cycle for different gas cooler outlet temperatures.

As widely investigated in the literature, the parallel compression cycle is more efficient than the conventional booster cycle, mostly when the ambient temperature gets warmer. In

fact, with 20 °C at gas cooler outlet, the increment in terms of power consumption is very low (around 3%). Being the FGV on at 15 °C and the parallel compressors on at 20 °C, the explanation is simple. The power reduction will always achieve since some vapor is compressed with a lower pressure ratio (parallel compressors) instead to be first throttled and after compress by MT compressors. There will be a point (around 17 °C as gas cooler outlet temperature) where a balance between the booster and parallel compression unit exists. As expected, warmer temperatures lead to high throttling losses because of the specific properties of R744 as a refrigerant and therefore the increment becomes more and more consistent, reaching almost 15% at 35 °C.

7 CTES and two-phase thermosyphon loop design

This chapter provides the design of the Cold Thermal Energy Storage (CTES) that would ideally be placed on the top of the cabinet in a supermarket, acting as a condenser or evaporator depending on which working regime is on (discharging or charging). The procedure is presented, as well as the results of the two-phase thermosyphon loop.

7.1 Condenser design

The heat exchanger placed on the top of the cabinet is acting as a condenser during the discharging process. Therefore, ice is formed during charging to get heat during the condensation of CO_2 vapors inside the pipes. The medium in which the energy is stored is ice at this stage. The condensation occurs releasing the heat to the ice in the surrounding of the tube pack and between one tube to the other.

The starting value for the air inside the cabinet was set to 4 °C (food conservation temperature). Now, since the ice has a very low heat transfer meaning that the dominant thermal resistance is on its side, a larger heat transfer surface is required because of the very small temperature difference between CO_2-ice. This temperature difference is directly related to the application of the cabinet itself, meaning that it will change depending on which type of food is stored. Considering an isothermal process through the evaporator and a negligible temperature drops in the riser, the temperature at the condenser inlet can be assumed to be the same as in the evaporator. As consequence, the food application will affect the refrigerant temperature and therefore the temperature achievable by the PCM during the charging, where the heat is taken from the water medium.

Furthermore, when ice is considered as a secondary heat transfer medium, a proper mechanical design is necessary to avoid any mechanical stress in the tube and fins, mostly because in this particular design the heat transfer surface must be increased as much as possible due to the low overall heat transfer coefficient. Some other precautions must be considered as free space on the top of the CTES, allowing the ice to expand in volume when the freezing process takes place.

7.1.1 Input data

Firstly, the application must be selected according to the space available on the top of the cabinet (huge heat transfer area needed if the temperature difference is too low). The thermodynamic properties need to be defined, as well as some assumptions for the calculations. The initial parameters are listed in Table 7.1:

Table 7.1: Initial parameters for condenser design.

Initial parameters	
T_{CO_2}	4 [°C]
p_{CO_2}	38.688 [bar]
η_l	9.353∗1e-5 [Pa·s]
η_v	1.5∗1e-5 [Pa·s]
ρ_l	902.557 [kg/m^3]
ρ_v	110.9754 [kg/m^3]
$\Delta H_{melting}$	218.3011 [kJ/kg]
T_{air}	8 [°C]
T_{ice}	0 [°C]

According to the initial parameters, the overall heat transfer coefficient and heat transfer area must be evaluated. The following assumptions have been considered over the design:

- The heat loss in the vapor and liquid lines, the heat absorbed by the evaporator is assumed to be equal to that evacuated by the condenser
- The saturated vapor is assumed at the condenser inlet, considering a complete condensation of the vapor into liquid (x_{inlet} and x_{outlet} equal to 1 and 0 respectively)
- The fouling resistance, even though negligible, has been assumed equal to 0.000176 [(m^2·K)/W] (according to heat exchanger book design et al. [85])

- No saturation temperature drops are considered; therefore, an isothermal process occurs inside the condenser pipes
- A guess value for ice heat transfer coefficient equal to 200 [W/(m^2·K)] is considered, pointing out the main reason for having the dominant thermal resistance on the secondary medium side

The design is an iterative procedure that consists of the following steps:

- The phase change temperature is set according to the application (storage food as vegetables for instance), as well as the quality at the inlet-outlet
- Depending on the space available on the top of the cabinet, a geometry of the box is decided. As consequences, the tube pattern and the arrangement of the tubes must be defined according to the dimension of the box
- The thermophysical properties are calculated at the saturation temperature and relative saturation pressure of the refrigerant
- Once the dimensions of the tubes and fins are defined, the total heat transfer area can be calculated
- Since the load in the condenser is set equal to the load in the evaporator, having the total heat transfer area makes it possible to evaluate the overall heat transfer coefficient
- As stated by Ramesh et al. [86], in a heat exchanging process where one fluid release or absorbs heat under isothermal temperature profile, as well as the secondary fluid, the temperature difference between the two fluids could be considered as the arithmetic temperature difference with a very small error
- Having the heat load, arithmetic temperature difference and overall heat transfer coefficient the new total heat transfer area has been calculated
- Setting at the beginning a ratio between the total and inter heat transfer surface, a new internal surface is calculated according
- Considering as usually happens four tubes per row, the new number of tubes is defined and the iteration restarts until the difference (error) between the two values (old and new iteration) is lower than 0.01

7.1.2 Geometric and heat transfer characteristics of the HEX

As already described upstream, a geometry has initially been set. When the iterative procedure converges, the following features have been calculated (Table 7.2):

Table 7.2: Box geometry and tube arrangements.

Box geometry		
Length [m]	Depth [m]	Height [m]
1.7	0.34	0.662
Tube pack features		
$L_1\ [m]$	$L_2\ [m]$	$L_3\ [m]$
1.5	0.121	0.462
Distance from the box surface		
Up [m]	Down [m]	Left/right
0.12	0.08	0.1

After that, tube geometry and fin geometry are listed in Table 7.3:

Table 7.3: Geometric characteristics of the tube and fin surface area.

Fin geometry and its performance				
D [m]	Fin spacing [m]	Fin thickness [m]	η_{fin}	$\eta_{overall}$
0.0191	0.0254	0.003	0.7746	0.9648
Tube geometry				

d_{in} [m]	d_{out} [m]	Length [m]	N_{tubes}	$N_{tubes,row}$	Material
0.008	0.0095	1.5	48	4	Copper

To have an idea, Figure 7.1 illustrates the position of the CTES and the tube pattern inside it, being an accurate design necessary to ensure proper feeding of the evaporator with liquid.

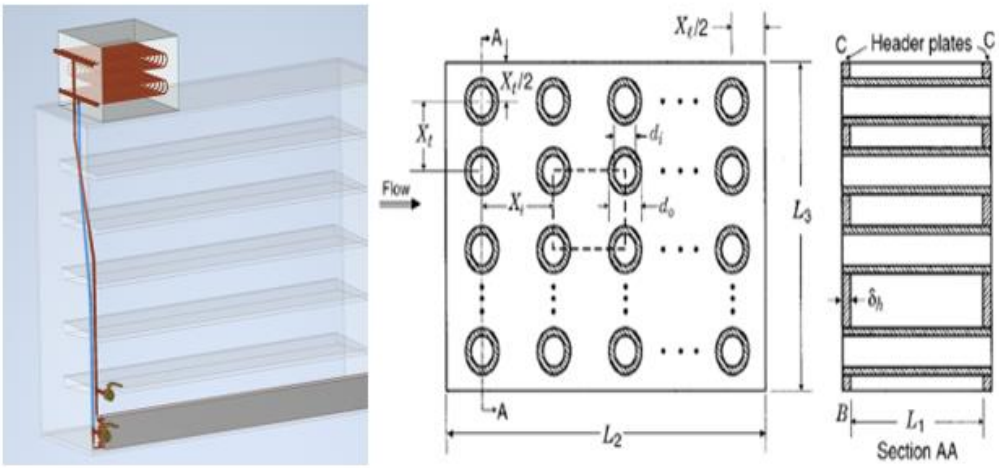

Figure 7.1: CTES location and tube characteristics.

The heat transfer properties are found in Table 7.4:

Table 7.4: Heat transfer characteristics of the heat exchanger.

Heat transfer properties				
HTC_{CO_2} $[\frac{W}{m^2*K}]$	h_{ice} $[\frac{W}{m^2*K}]$	$R_{th,wall}$ $[\frac{m^2*K}{W}]$	$R_{fouling}$ $[\frac{m^2*K}{W}]$	U $[\frac{W}{m^2*K}]$
2396.7	200	2.4211*1e-6	0.000176	150.4

Multiple correlations for the HTC on the refrigerant side have been used to validate the results. As stated in the literature, according to the type of refrigerant and operating conditions, some correlations are more suitable than others giving reasonable results. In Figure 7.2, the heat transfer coefficient is calculated for each value of vapor quality

considering at the end the correlation defined by Shah et al. [87] which considers three different equations form depending on the heat transfer regimes (turbulent, mixed, laminar). Anyhow being the dominant thermal resistance on the ice side, the refrigerant HTC will not affect much the thermal performance of the CTES.

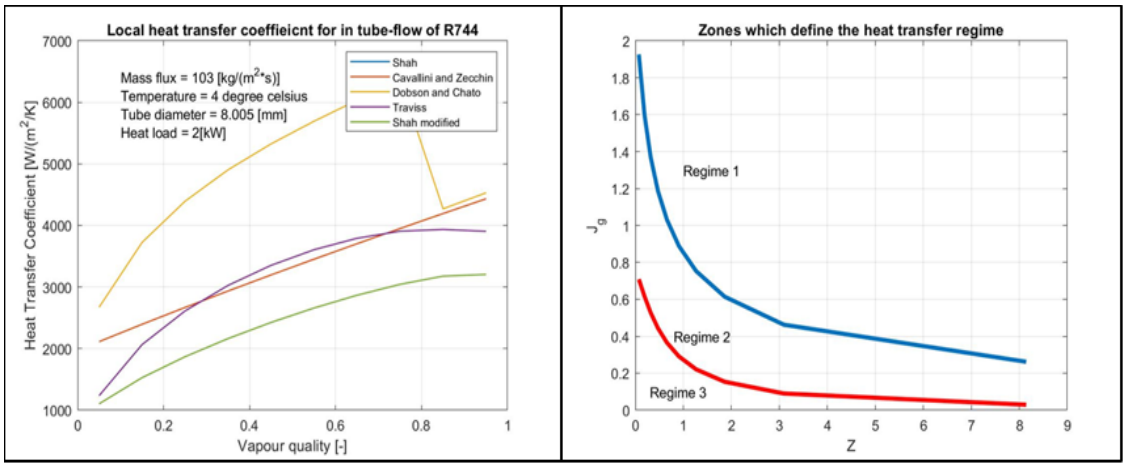

Figure 7.2: Refrigerant HTC and heat transfer regime defined in the Shah correlation.

The parameter called mass flux density must be defined considering the mass flow circulating through the tube pattern. Since the condenser is going to be placed on the top of the cabinet and connected to the inlet-outlet of the evaporator, the mass of refrigerant condensed is defined in the two-phase thermosyphon loop model. Ideally, in a two-phase thermosyphon loop, the condenser should be subcooled to make sure to have liquid head all the time and enabling the flow circulation and the proper conservation of the food in this specific case.

7.2 TPTL Design

The two-phase thermosyphon loop (TPTL) is widely used in air-conditioning systems and for those kinds of systems driven by gravity, the height difference between condenser – evaporator is a key factor in heat transfer performance. Furthermore, it has been proven experimentally for small height differences (less than 2.5 m) that the downcomer could be partially liquid-filled leading to a smaller driving force than what was expected [88].

A gravity-fed evaporator operates on a thermosyphon principle, meaning that if some load is applied to the evaporator a two-phase mixture is present with a differentiation in local

density that takes place according to the refrigerant properties. The pressure drops encountered in the evaporator and riser must be overcome by the hydrostatic pressure achievable in the downcomer. Some studies have taken into consideration a separator instead of a condenser, allowing with a huge expansion liquid formation and continuous flow of refrigerant through the loop. One of these models has been built by Paliwoda et al. [71], initially referred to as ammonia as the refrigerant and then adopted to other refrigerants. His initial layout of the system consists of an air finned cooled evaporator, riser, downcomer and a separator (Figure 7.3).

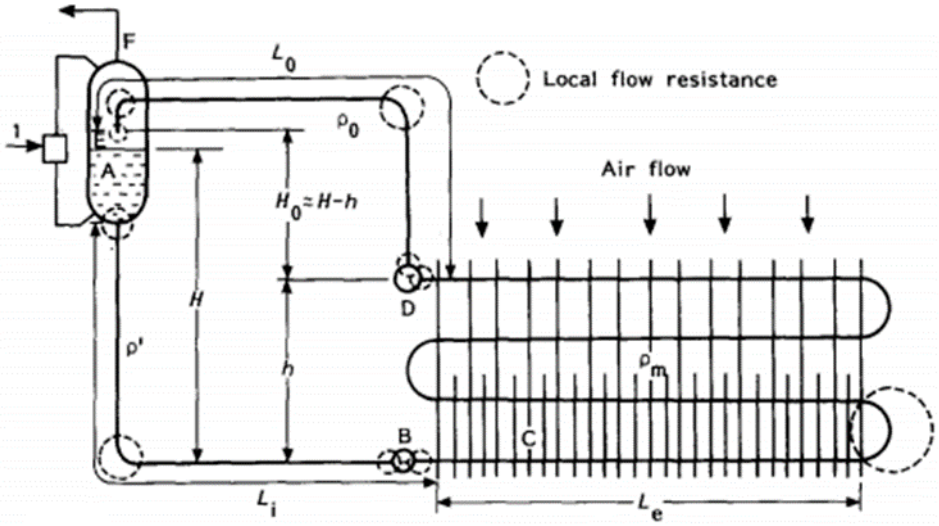

Figure 7.3: System layout of gravity-fed evaporator [71].

7.2.1 Main design parameter and system layout

The net liquid head that results in the circulation of refrigerants is the main goal in a TPTL design. As defined by Paliwoda et al [71], a parameter called recirculation number is the key parameter in the thermosyphon loop design. It is defined as:

$$n = \frac{1}{\dot{x}_0} \tag{7.1}$$

where x_0 is the quality at the outlet of the evaporator. It is the mass ratio of liquid at the inlet and vapor at the outlet of the evaporator. The recirculation number is directly correlated to the flow rate of refrigerant. As consequence, a higher recirculation number means only a small fraction of the liquid mass flow is vaporized inside the evaporator leading to have a

pool boiling evaporator. It will affect not only the refrigerant side heat transfer but also the temperature and pressure drop over the different components. The usage of a flooded evaporator could potentially avoid any interruption of the system due to superheated CO_2 vapor, meaning that its effect on the thermosyphon stability is really important.

As a function of the recirculation number, all the pressure drops in the pipe components (bends) and straight pipes can be calculated. The refrigerant charge is important for the stability of the system itself, however bringing higher pressure drops that must be won by the liquid head. The following equations have been implemented in a code developed in Matlab:

$$H = \frac{[\Delta P_i + \sum \Delta P_i + \Delta P + \sum \Delta P + \Delta P_o + \sum \Delta P_o]}{(\rho' - \rho_o)g} + h(\rho_m - \rho_o)/(\rho' - \rho_o) \qquad (7.2)$$

where H is the height of the liquid column. At the numerator of the first term, there are all the different pressure drops differentiated by component (including straight pipes and pipe components). Depending on the quality value, three regions must be considered: liquid, vapor and two-phase region. Based on them, different correlations are employed to evaluate the pressure drop on such part of the system:

$$\Delta P_i = \frac{0.3164}{2} \cdot \frac{\eta'^{0.25}}{\rho'} \cdot \dot{m}^{1.75} \cdot \frac{L_i}{d_i^{1.25}} = \frac{0.3164}{2} \cdot \frac{\eta'^{0.25}}{\rho'} \cdot \left(\frac{n \cdot \dot{Q}}{r}\right)^{1.75} \cdot \frac{L_i}{d_i^{1.25}} \qquad (7.3)$$

The equation (7.3) is referred to as the single-phase liquid flow, therefore the downcomer. Here, due to the difference in density, there is no chance that the vapor is carried down by the liquid, but it is mandatory to have a continuous liquid supplying to ensure proper operation of the thermosyphon loop. For the evaporator pipes, two-phase flow is presently leading to the following equation that accounts the two-phase multiplier β_m:

$$\Delta P = 0.241 \cdot \beta_m \cdot \frac{\eta''^{0.25}}{\rho''} \cdot \left(\frac{n \cdot \dot{Q}}{r \cdot z}\right)^{1.75} \cdot \frac{L}{d^{4.75}} \qquad (7.4)$$

During the vaporization process, the quality is varying over all the tube patterns turning from a liquid into a liquid-vapor mixture. For the return line an adiabatic two-phase flow is considered assuming a constant quality of the flow:

$$\Delta P_o = 0.241 \cdot \beta_o \cdot \frac{\eta''^{0.25}}{\rho''} \cdot \left(\frac{n \cdot \dot{Q}}{r}\right)^{1.75} \cdot \frac{L_o}{d_o^{4.75}} \qquad (7.5)$$

The two-phase flow factor can easily be determined with the same accuracy given by integration considering pure liquid at the inlet of the evaporator:

$$\beta_m = \Theta + \frac{1}{n}(1-\Theta) = (\Theta + \beta_o)/2 \tag{7.6}$$

where Θ is the ratio between liquid-only and vapor-only pressure drops:

$$\Theta = (\frac{\rho''}{\rho'}) \cdot (\frac{\eta'}{\eta''})^{0.25} \tag{7.7}$$

All these equations can be applied for turbulent liquid-turbulent vapor flow and therefore the Reynolds number must be calculated according to the following condition:

$$Re = \frac{\dot{m} \cdot d}{\eta'} = \frac{4}{\pi} \cdot \frac{n \cdot \dot{Q}}{r \cdot d \cdot z \cdot \eta'} \geq 1187 \tag{7.8}$$

For further information, referring to Paliwoda et al. [73]. Regarding the pressure drops across pipe components containing the two-phase flow of refrigerant mainly through inlet and outlet manifolds, as well as return bends of evaporator and condenser coils, a generalized method proposed by Paliwoda et al. [72] is followed. Differently from his system, a condenser (CTES) is placed in the loop to ensure liquid formation for the driving force. The system is formed by the following components:

- Air finned cooled evaporator: CO_2 is the refrigerant that vaporizes absorbing heat from the air that is sent through the fin surface using fans. The evaporator features have been measured in the lab (diameter of the tubes, length of the coils, number of tubes). Some constraints are present because being the dimension of the cabinet standardized there is no chance to increase the heat transfer area or number of coils in the evaporator, leading to one degree of freedom less
- Riser: pipe component with the purpose to carry the vapor formed in the evaporator to the condenser inlet. Frictional and gravitational pressure drops are considered, having the gravity a negative effect on the circulation of the refrigerant because of the opposite directions of the acting forces
- Condenser: it is a finned tube heat exchanger with ice-water as secondary heat transfer fluid, no motion is present outside the tube. Only the movement due to natural

convection occurs. Moreover, the space available is limited and mechanical support due to its weight must be taken into consideration

- Downcomer: pipe component that connects the outlet of the condenser to the evaporator inlet. Its purpose is to carry the liquid to the evaporator and overcome the total pressure drops using the hydrostatic pressure

7.2.2 Mathematical model and inputs data

A code has been built in Matlab. As already described during the condenser design section, the heat load in the evaporator is the same and the air temperature as well. The input parameters listed in Table 7.1. The sequential method is used:

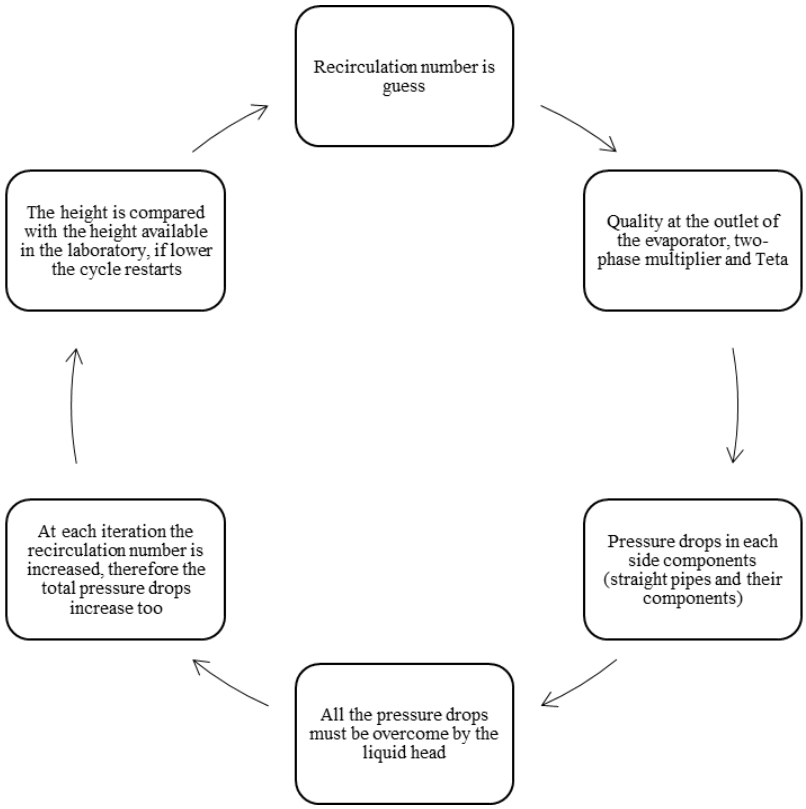

Figure 7.4: System-solving flowchart for TPTL.

Since the cabinet has a standard dimension, the liquid head is set. This means that the liquid head for the driving force is already known but to ensure a refrigerant flow in the loop a specific mass of refrigerant must be charged. Being, as seen before, the recirculation number linked to the vapor quality at the evaporator outlet the amount of refrigerant flowing in the loop is a consequence of the recirculation number. Therefore, at each iteration, the total pressure drop as a function of recirculation number is calculated and the length of the

downcomer too. This length is later compared with the one available in the laboratory and the iteration restarts until these two values of the liquid head are almost equal. The geometrical features of the loop have been chosen as a starting point looking at the evaporator pipe diameter. A certain expansion or contraction of a cross-section occurs at the inlet-outlet of the two heat exchangers because of the different pipe dimensions. As usual happens, the riser has a bigger diameter than the downcomer. In Table 7.5 they are listed:

Table 7.5: Geometrical features of evaporator, liquid, and vapor line.

Downcomer		
Liquid head [m]	d_{liquid} [mm]	L_{liquid} $[m]$
1.88	11.5	2.08
Riser		
Height vapor line [m]	d_{vapor} [mm]	L_{vapor} $[m]$
1.865	20.36	2.15
Evaporator		
L_{coil} $[m]$	$N_{coils}\ in\ parallel$	d_{evap} $[mm]$	$Height_{evap}$ $[m]$
3.4	32	0.8005	0.25

All the diameters are taken according to the Standards for carbon dioxide tubes "Refrigeration system: Pipe sizing".

7.2.3 Simulation results

According to Paliwoda et al. [71], some simplifications have been made maintaining a good accuracy of the results. In this specific procedure, the recirculation number is the key parameter that affects the performance of the TPTL, and therefore all the main parameters used to evaluate all the single pressure drops, such as the two-phase multiplier. In Figure 7.5 the simplified approach to define the two-phase multiplier inside the evaporator and vapor line is illustrated:

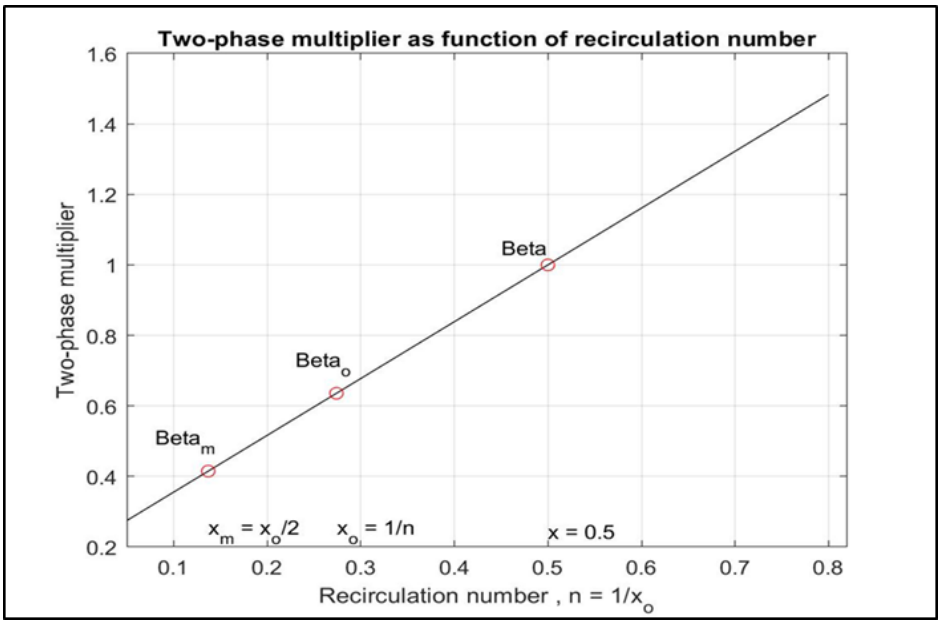

Figure 7.5: Simple and exact method for determining the two-phase multiplier in the evaporator and riser.

The two-phase multiplier in the evaporator is therefore a function of the recirculation number and a parameter Θ that accounts for the thermodynamic properties of the refrigerant, such as dynamic viscosity and density. The following trend has been found:

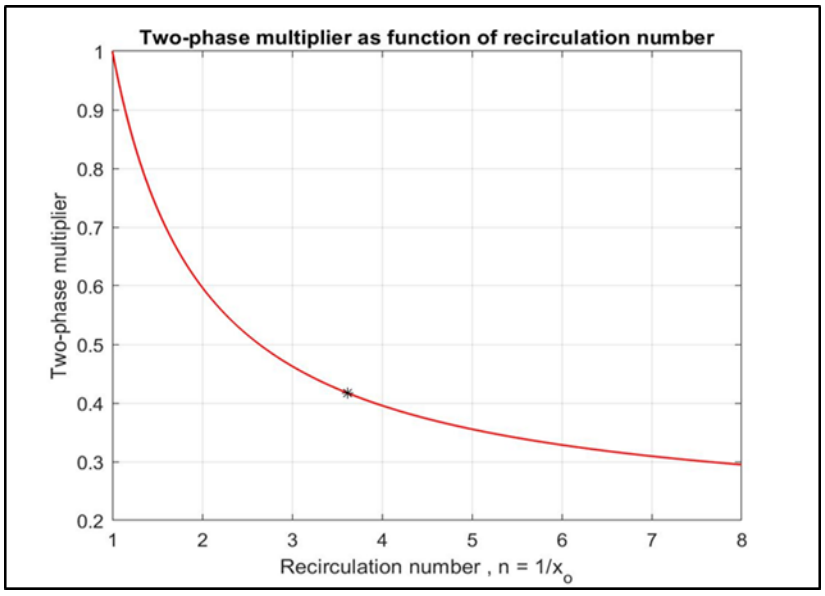

Figure 7.6: Two-phase multiplier as a function of the recirculation number and thermodynamic properties of the refrigerant.

When the recirculation number is set to one, all the liquid going through the evaporator turns into vapor and the pressure drops in the riser increase consequently. Hence, increasing the recirculation number leads to a flooded operating condition in the evaporator and a two-

phase mixture flowing in the riser. The vapor, with a lower density, carries also some liquid to the condenser inlet and when the recirculation number becomes too high only a small fraction of flow is a vapor. On the other hand, more mass of refrigerant needs to be charged in the system.

In Figure 7.7 two important aspects can be noticed: firstly a higher recirculation number leads to larger liquid head to overcome the pressure drops that are increasing with the recirculation number; secondly, more and more liquid is in stagnant conditions in the evaporator as the recirculation number raises and therefore pool boiling occurs in the heat exchanger.

The pressure drops are related to the saturation temperature drops. This will occur during the vaporization of the refrigerant. As stated in the methodology followed in this thesis, an optimum recirculation number is the main parameter affecting the operation economy of the evaporator. The existing relationship between the thermal effectiveness and the temperature drops shows clearly how high efficiency can be reached keeping as low as possible the temperature drops. A parameter "θ" defines the difference between average wall temperature and refrigerant temperature at the outlet of the evaporator.

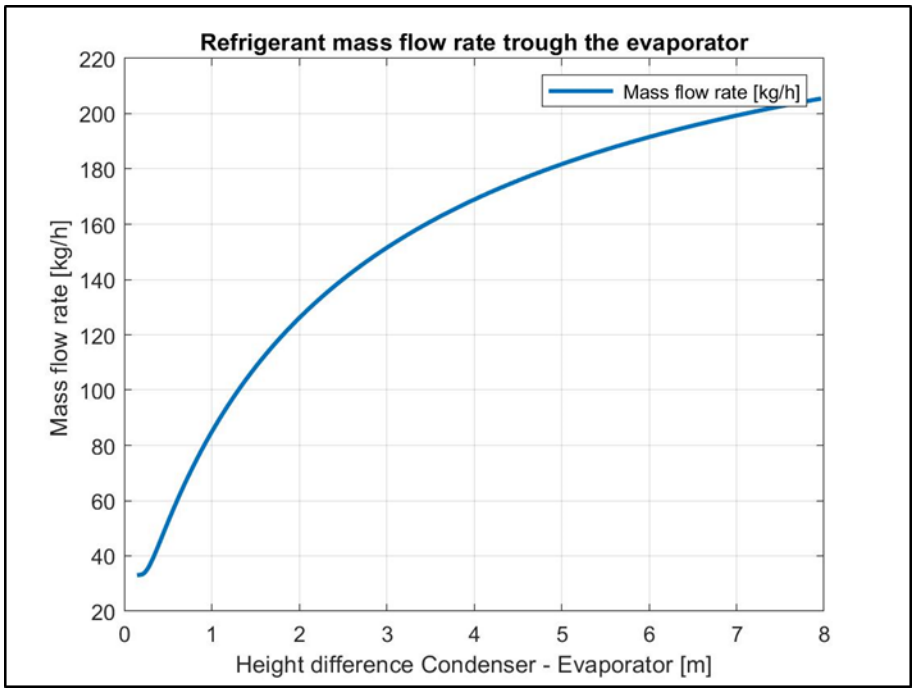

Figure 7.7: Refrigerant mass flow as a function of the liquid head.

According to Paliwoda, an optimum recirculation number that leads to the highest thermal effectiveness of the evaporator exists. This temperature drops can be written as a sum of two terms:

$$\Delta t_{wm} = 870 \cdot \eta' \cdot \lambda' \cdot d \cdot \left(\frac{r}{n \cdot L}\right)^{0.5} \tag{7.9}$$

$$\Delta t_{me} = 0.161 \cdot \frac{T \cdot \eta''^{0.25}}{\rho''^{2} \cdot r^{2.75}} \cdot (\dot{q} \cdot A_o)^{1.75} \cdot (\Theta \cdot n^{1.75} + (1 - \Theta) \cdot n^{0.75}) \cdot \frac{L^{2.75}}{d^{4.75}} \tag{7.10}$$

where the first term and the second term are defined according to Pierre and Granryd, respectively (see Paliwoda et al. [71] for furthers information). As can be seen, the recirculation number is directly proportional to those temperature drops. Whenever the evaporator is short, a high value of recirculation number is recommended to achieve better heat transfer performance.

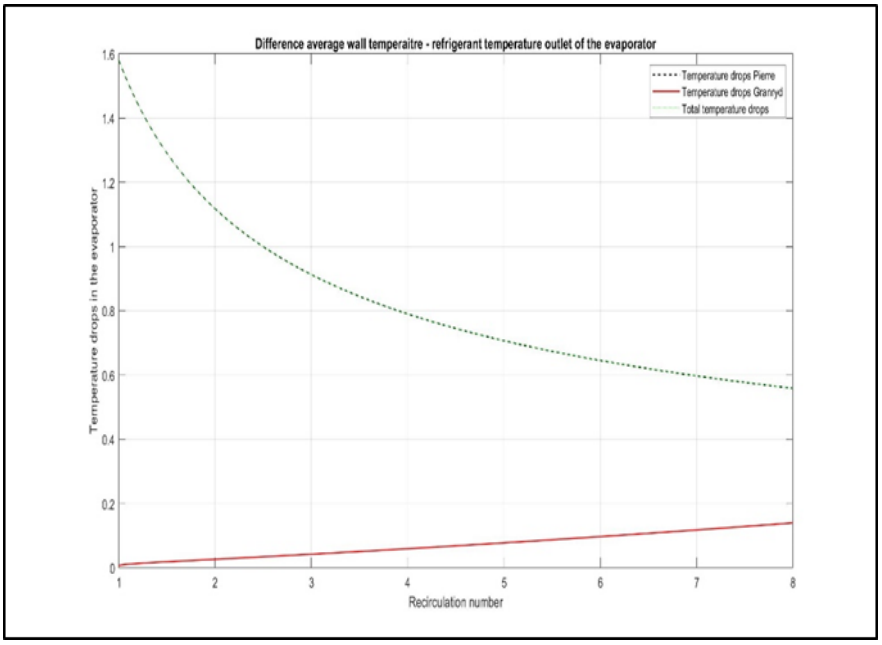

Figure 7.8: Temperature drops in the evaporator affecting the thermal effectiveness.

Because of the fixed dimension of the evaporator in terms of coil length, an optimum recirculation number can't be reached. The shape of the curve should show a decrease and later increase pointing out the minimum value of temperature drops. Therefore, the evaporator is going to work with lower performance. It is strongly suggested to not reach recirculation number lower than one; in these cases, the boiling of the refrigerant stops long

before the evaporator outlet meaning that part of the surface is not used, hence the evaporator is too long or the diameter too small.

Regarding the saturation temperature drops over the vaporization process, the pressure drops along the straight pipes and evaporator bends must be calculated. Using the Clausius-Clapeyron saturated vapor pressure-temperature relationship:

$$\frac{dP}{dT} = \frac{r}{T \cdot (v'' - v')} \tag{7.11}$$

knowing the saturation temperature and thermodynamic properties of the refrigerant, as well as the pressure, drops the saturation temperature drops have been calculated.

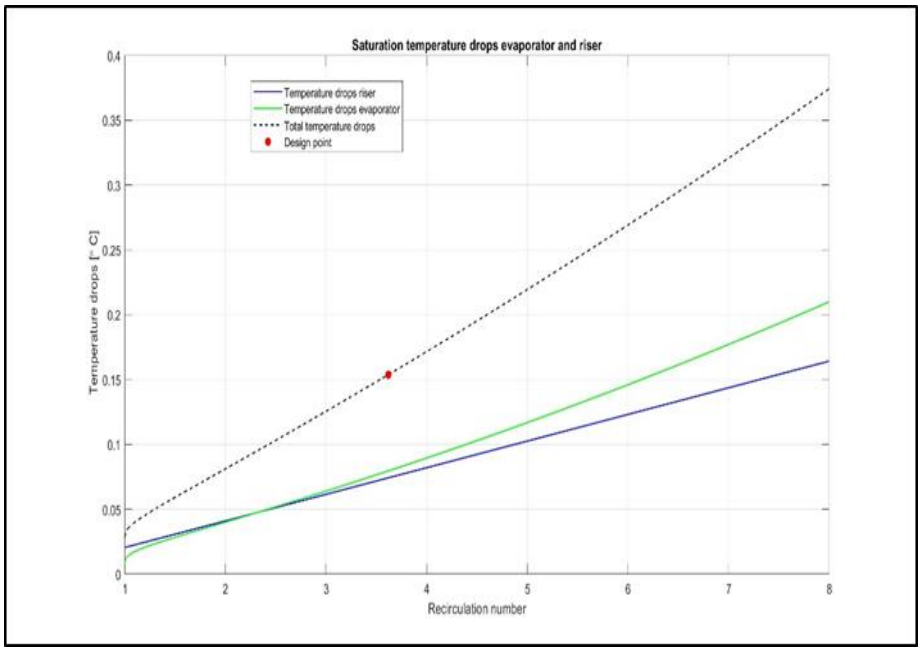

Figure 7.9: Temperature drops in the evaporator and riser.

It should be mentioned that R744 is a high-working pressure fluid as already discussed in chapter 3. Thus, unlike conventional refrigerants, CO_2 has very low-temperature drops given a certain pressure drops. This can be easily seen looking at the slope of the curve. Moreover, to obtain high recirculation numbers a high value of liquid head is needed to overcome the major pressure drops meaning that the recirculation number in the graph above can be seen as the pressure drops in the riser-evaporator, being them a function of "n". Consequently, a high liquid head will adversely influence the boiling temperature.

Figure 7.10 shows the liquid column height in the downcomer. When the total pressure drops value rises, the liquid column height too. In Figure 7.11 the liquid head and the pressure drops are explicitly illustrated as a function of the recirculation number.

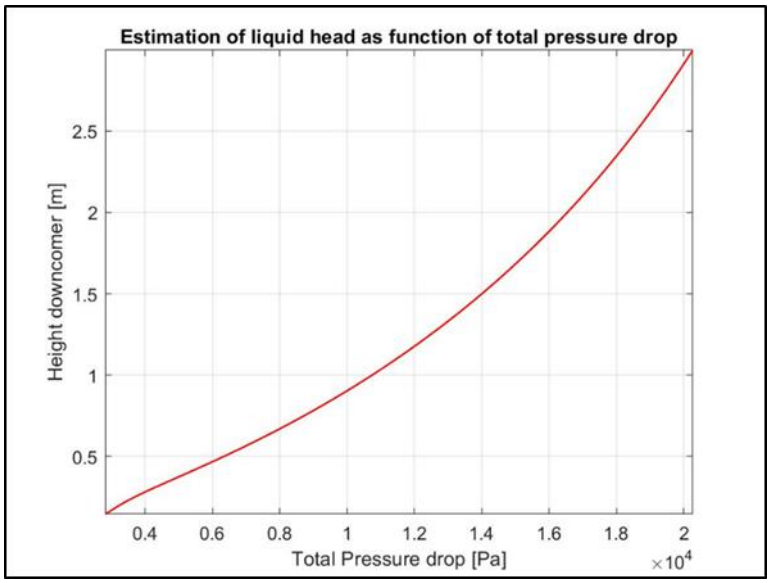

Figure 7.10: Liquid column in downcomer as a function of pressure drops in the system.

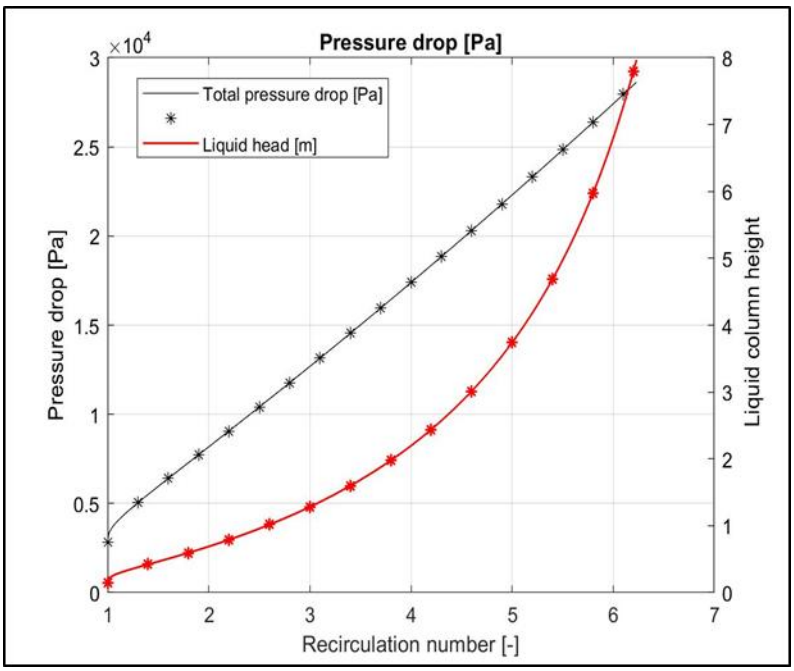

Figure 7.11: TPTL performance as a function of recirculation number.

As stated by many articles [77, 89], the liquid head might be partially filled with liquid with the upper part only surrounded by a hollow liquid film. When this occurs, the height of the liquid head is less than the vertical distance between the condenser outlet – evaporator inlet. Whenever the downcomer is partially liquid filled the driving force is lower and it might be that the hydrostatic pressure is not enough to drive the refrigerant through the evaporator and the riser. In this design, the downcomer has been considered fully liquid filled.

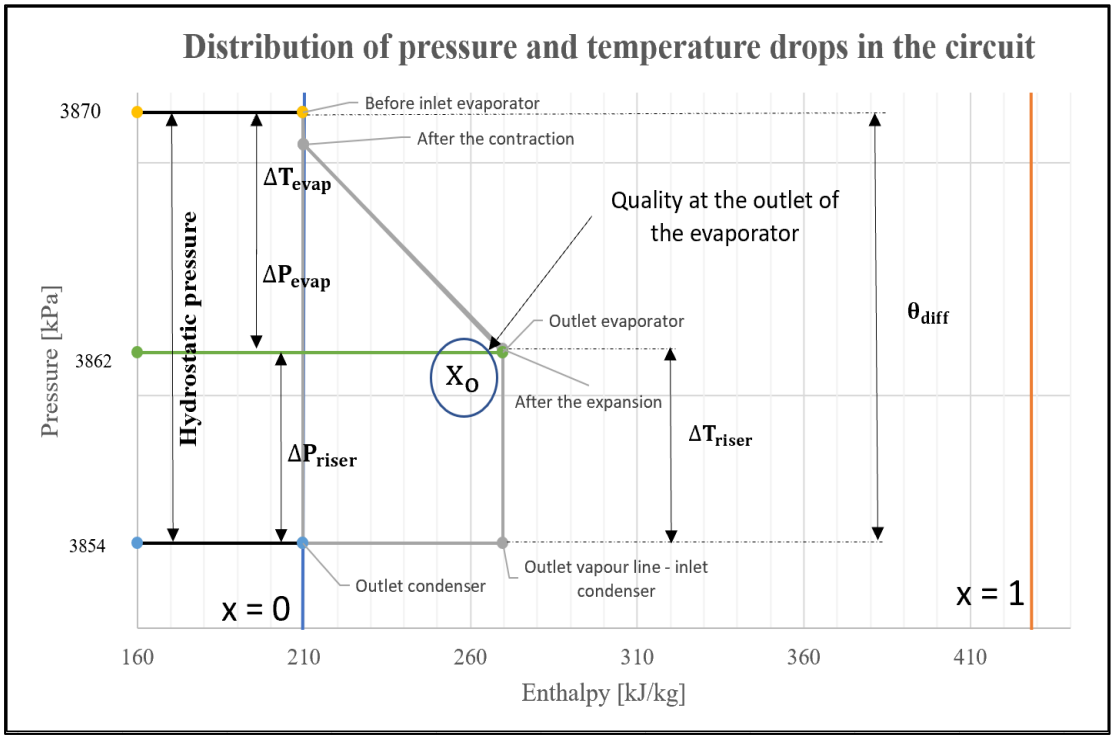

Figure 7.12: Distribution of pressure and temperature drops in the circuit.

In Figure 7.12, the pressure and temperature drops are shown through the different system components. The refrigerant, that might be subcooled depending on the heat transfer performance of the condenser and on the temperature reached by PCM during the charging, flows into the downcomer from the condenser. In the vertical pipe, due to the hydrostatic pressure, the pressure rises sharply (considering the frictional pressure drops as negative contribute). In the evaporator, the pressure decreases gradually because of frictional pressure drop, especially close to the inlet where a contraction occurs and through the bents. A small increment of pressure is obtained at the evaporator outlet when expansion occurs because of the different diameter sizes between riser and evaporator coils. Along the riser, the pressure declines sharply mainly due to the frictional and gravitational pressure drops. As already said, the condenser pressure drops are not accounted here since it was considered as a device to ensure liquid production at the inlet of the downcomer. Normally, it can be considered as a

device that slows down the process but not stops it since the major pressure drops are in the evaporator – riser. The induced pressure drops are much lower than in the evaporator because the liquid phase has a much smaller specific volume than in the gas phase, affecting a lot the fluid velocity and therefore the frictional losses.

It is noteworthy that the temperature drops in the evaporator – riser calculated with the methodology proposed by Paliwoda, have been verified using Refprop. For a certain temperature drop, a pressure drop exists depending on the type of refrigerant. The TPTL design can be summarized in the following table:

Table 7.6: TPTL performance, including temperature and pressure drops. The height of the downcomer is evaluated and compared with the maximum height available in the lab.

TPTL Performance	
Pressure drop evaporator	7935 Pa
Pressure drop riser	7402 Pa
Total pressure drops	15337 Pa
Temperature drop evaporator	0.0796 °C
Temperature drop riser	0.0743 °C
Total temperature drops	0.1539 °C
Height of the downcomer	1.8 m

8 Simulation

During the discharging process, the heat released by the refrigerant melts the ice around the tube pattern. An efficient heat transfer is required to complete the condensation of the refrigerant vapor coming from the evaporator outlet. Although the temperature of ice reached during the charging is quite close to the melting temperature, the heat transfer occurring might be such to melt the ice all around the tubes in a short time. If this happens, the liquid is no longer supplied and the TPTL stops working. Therefore, a numerical simulation has been carried out using Ansys Fluent to quantify the melting rate. As a CFD model of the entire CTES would be too complicated generating high computational costs, the dimensionality of the problem was reduced to a 2D model, assuming a constant temperature on the pipe surface and an adiabatic condition on the ice layer.

8.1 PCM properties

The selected PCM is water which has well-known thermophysical properties. Depending on which type of heat transfer mechanism is involved, convective or conductive, the density should be carefully modeled to simulate the convective case and to consider its non-linear behavior around the critical point (4 °C). A density-temperature relationship that accounts for this behavior was introduced by Gebhart and Mollendorf et al. [90], valid in a temperature range from 0.01 to 10.2 °C. The equation (8.1) has been plotted afterward, as illustrated in Figure 8.1:

$$\rho = \rho_m \cdot (1 - w \cdot |T - T_m|^q) \tag{8.1}$$

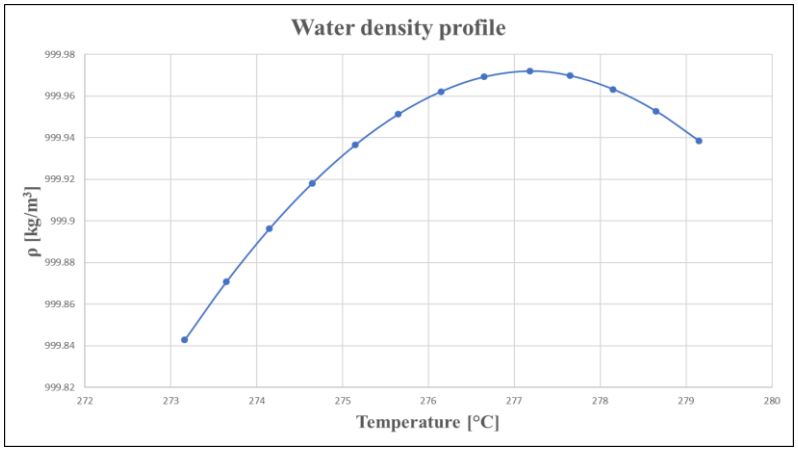

Figure 8.1: Water density profile across the critical point.

where ρ_m is the maximum density of water (999.972 kg/m^3) occurring at T_m = 4.0293 °C, w and q are constants, equal to $9.2793 \cdot 10^{-6}$ and 1.894816 respectively. All the other thermophysical properties are listed in Table 8.1:

Table 8.1: Thermophysical properties of PCM used in the simulation.

Properties	Solid zone (T < -0.49 °C)	Mushy region (ΔT_{mushy} = 0.5 K)	Liquid zone (T > 0.01 °C)
Thermal conductivity [W/(m·K)]	1.918	-	0.579
Specific heat capacity [J/(kg·K)]	2217	-	4180
Density [kg/m^3]	917	-	Equation (8.1)
Viscosity [Pa·s]	-	-	0.001003
Heat of fusion [kJ/kg]	-	333.55	-

Those properties have been inserted in Ansys fluent, after enabling the "Solidification/Melting" model. Using a piecewise-linear relationship it is possible to reproduce the most accurate density functions in the water phase, based on how many points are involved in the relationship. Two points in the solid phase are enough to provide a constant solid density. Regarding the solid phase, subcooled ice is considered for this simulation since the melting process occurs over a temperature range. As illustrated in Table 8.1, a mushy region is introduced. The mushy region is the zone where the phase change occurs over a temperature range rather than at a single point. A temperature range of 0.5 K was set in the simulation.

8.2 Model description and assumptions

A geometrical model of the PCM domain used for the simulation is shown in Figure 8.2. Being a 3-D model too complicated, requiring a high-computational cost, a 2-D model has been investigated mainly focusing on the melting rate between two fins. Substantially, a zone delimited by the two fins and the pipe surface has been considered.

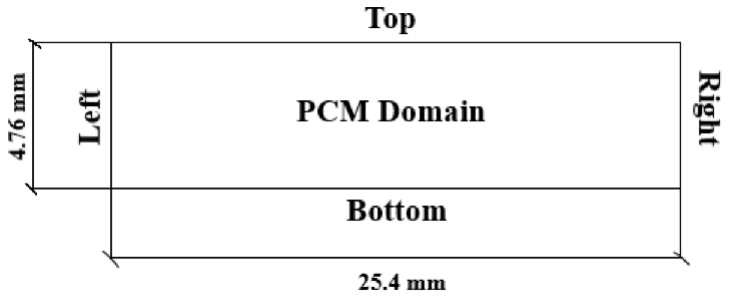

Figure 8.2: Schematic diagram of the domain.

In each side of the domain, a boundary condition is applied. Considering that CO_2 vapor is condensing inside the tubes, a constant wall temperature can be applied with a good approximation (Dirichlet boundary condition). The upper side which represents the "ice wall" is set to heat flux equal to zero to avoid any interaction from other nearby zones.

The following assumptions made during the numerical simulation are:

- Melting process is transient and assumed to be the 2-D phenomenon
- The motion of PCM in the liquid state is incompressible, non-Newtonian
- The density, thermal conductivity, viscosity and specific heat capacity vary as piecewise linear functions. The last three properties differ only between solid and liquid phase, they do not vary with temperature
- No heat generation within the PCM is accounted
- Viscous heating and volume expansion are ignored
- Heat transfer is governed by convection and conduction
- Solidified material is in full contact with the boundary walls
- Negligible contact thermal resistance between copper tube-fins
- Regarding the boundary conditions applied to the fin surfaces, a Dirichlet boundary condition is considered here. At the beginning the fin surface temperature is almost

equal to the ice temperature, however, it will take a short time to get warm when CO_2 vapor is flowing through the tubes because of the high thermal conductivity of the fin's material

8.3 Mesh generation and numerical procedures

The computational domain needs a pre-process called meshing, using Ansys Meshing software. The meshed model is shown in Figure 8.3:

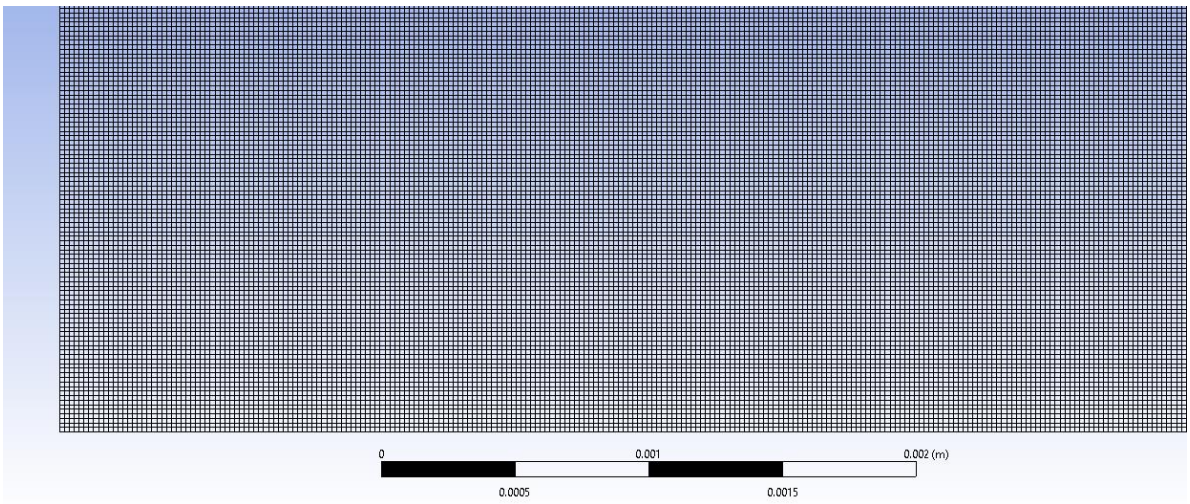

Figure 8.3: Schematic diagram of the meshed PCM domain.

An arrangement that was found sufficiently good for this purpose involves 392000 elements and 393681 nodes. Being the number of elements high, only a small portion of the mesh domain is shown with a square shape the cells.

In order to solve the momentum and energy equations, a suitable solver must be selected according to the different options offered by Ansys Fluent. The simulation was performed using the pressure-based solver. The SIMPLE algorithm was used for pressure-velocity coupling and the PRESTO scheme for the pressure correction equations. For the discretization of the momentum and energy equations, the QUICK scheme was selected. The melting process is discretized using a second-order upwind interpolation scheme. A constant time-step size of 0.1 second was applied to the simulation resulting in a stable convergence. The under-relaxation factors for both liquid fraction and momentum equal to 0.3, 0.5 for both density and body forces, 0.3 for pressure and 1 for energy. Those factors have a great impact on the stability of the simulation. A high or low value will strongly affect the results, leading

to numerical instabilities, slowing down the convergence or they can lead to either poor results or excessive computational times. The convergence criteria for the scaled residuals were defined according to the common approach followed by many authors in literature: 10^{-3} for both continuity and momentum equations, 10^{-6} for the energy equation.

It is worth to remark the importance of the mushy zone constant. The higher the mushy zone constant, the higher the damping of the velocity in the mushy/porous zone. Increasing the mushy zone constant will make the transition from solid to liquid sharper, decreasing the width of the porous zone. Although there is a lack of clarity regarding which value of this parameter should be used for accurate simulations of phase change heat transfer, as stated by Fadl et al. [91] and Selvnes et al. [74], a greater value of such parameter seems to lead to a longer melting time. This is because of the decreased fluid velocity that decreases the convection and the rate of the heat transfer, making the conduction the dominant heat transfer mechanism. Therefore, it is understandable why such parameter delays the melting process whenever its value is high.

8.4 Results and discussion

The results of the simulation were recorded at regular intervals of minutes for a melting cycle of minutes. Those results can be represented using the liquid fraction, static temperature, density and velocity magnitude.

Figure 8.4 represents the variation of the liquid fraction with time, enabling an easy examination of the shape and motion of the melting interface as the time passes. As illustrated in the legend of Figure 8.4, the red color represents the condition where the PCM is completely liquid ($\beta = 1$) while the blue color where the PCM is completely liquid ($\beta = 0$). Wherever the liquid fraction is between 0 and 1, the mushy region is present.

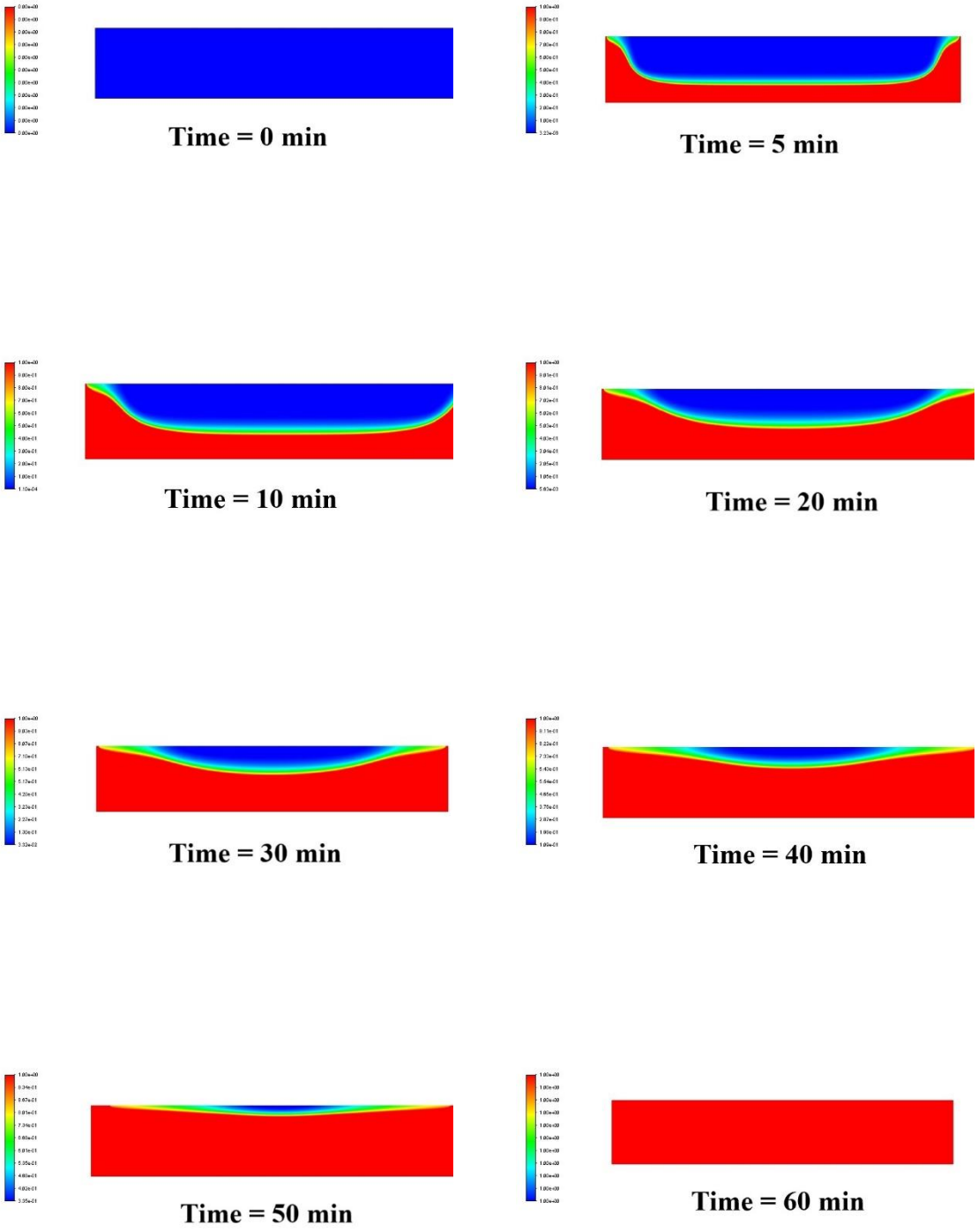

Figure 8.4:Contours of liquid fraction.

It can be seen, at the start, all the domain is occupied by ice. In the first minute a very thin layer of liquid is formed around the hot pipe and fin surfaces. After 5 minutes, this layer is expanded. It can be noticed that the water film falls from the top due to the buoyancy

effects, covering the pipe surface. In fact, as time passes the water layer increase, decreasing the heat transfer and at 10 minutes even the fin surface is covered by the liquid film. It is worth mentioning that, in presence of gravity and due to the density of ice-water phases, being the water phase heavier it is gathering at the bottom of the domain leading to higher thermal resistance and making the conduction the main heat transfer mechanism. It can be observed the shape of the melting interface: in the early stages the convection is the main transfer mechanism, increasing the melting rate (melting interface did not parallel to the hot surface at the bottom). In the last stages, the melting interface becomes more linear indicating the heat transfer is mainly by conduction. After one hour, all the ice domain is melted.

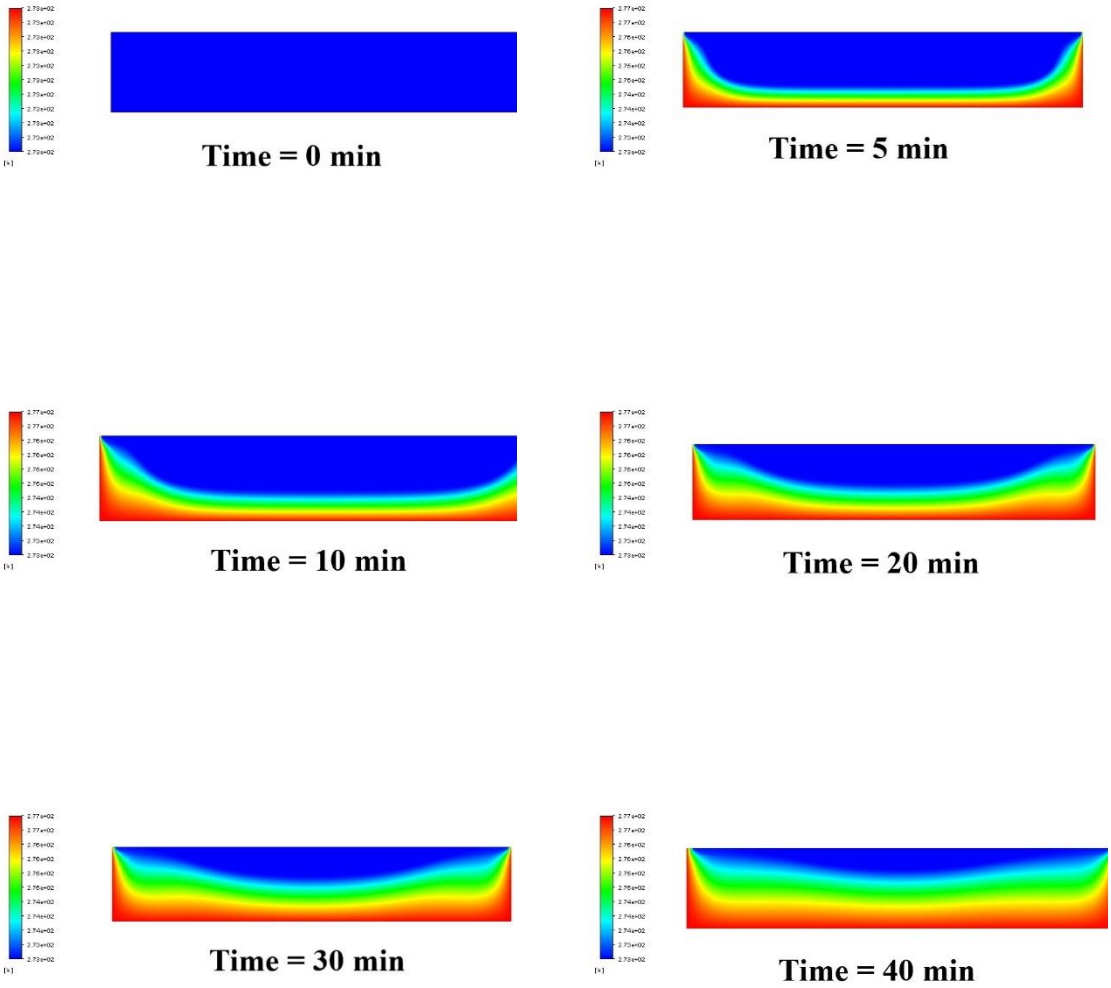

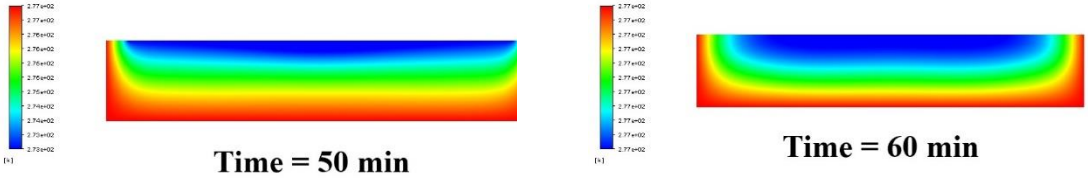

Figure 8.5:Contours of temperature.

Figure 8.5 represents the contours of temperature over the simulation time. Even though, the colors in the last picture could be confusing, the legend shows clearly that all the domain at this particular stage is ice. Furthermore, the shape of the liquid fraction matches the shape of the isothermal lines that act as a boundary between the two phases. As expected, the highest temperature reached is equal to 277.15 K which is the temperature set as a boundary condition on the pipe and fin surfaces. At the end of the melting process all the PCM is in the liquid phase, and being the thermophysical properties such as thermal conductivity, density, and specific heat defined based on a temperature range, constant temperature zones have been developed as it can be seen for Time = 60 minutes.

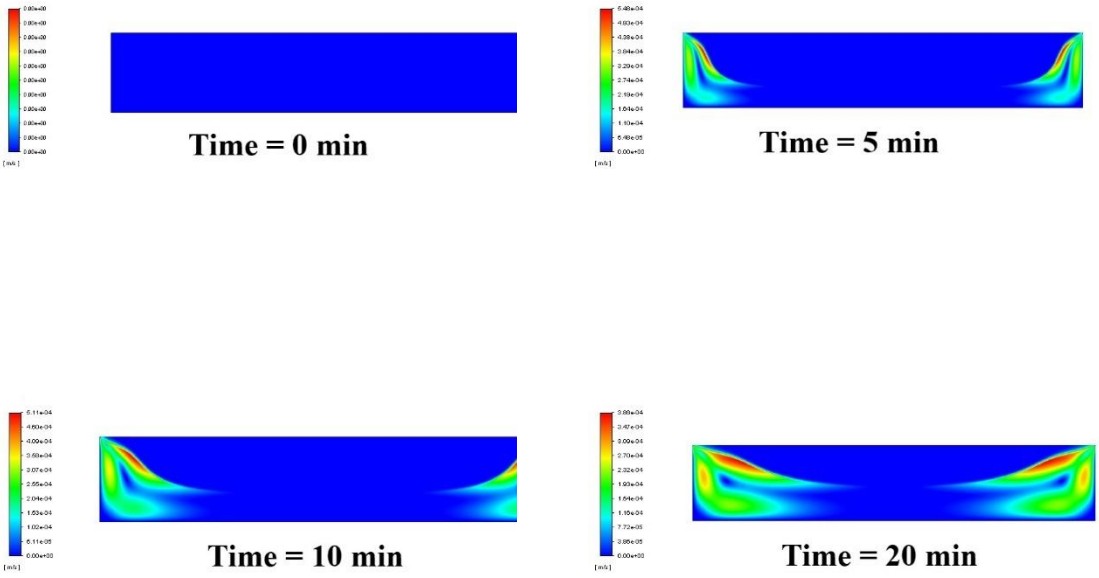

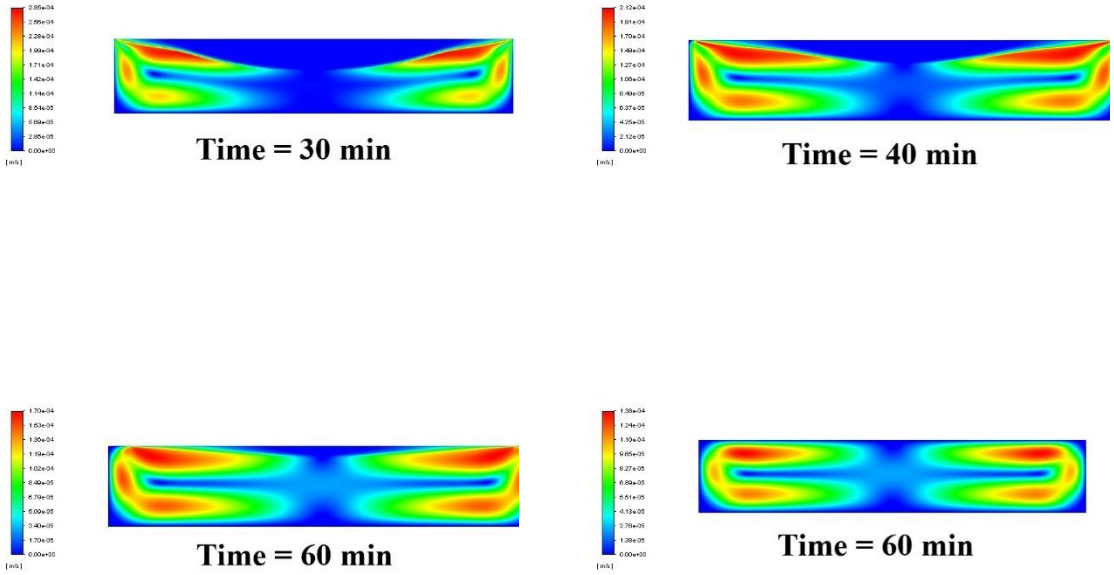

Figure 8.6: Contours of velocity magnitude.

Figure 8.6 helps to better show the effect of natural convection on the melting process. The gradient of temperature (Figure 8.5) between the hot wall and the solid phase translates into different densities in the liquid phase. In the presence of gravity, it activates buoyancy effects generating a convective mechanism. Comparing Figure 8.5 and Figure 8.6 is possible to highlight the relationship between the temperature with the magnitude of the velocity field. The largest velocities are found towards the melting front and the hot surfaces (fin and pipe surface) because there the temperature gradients are higher. The red zone represents the highest magnitude of velocity.

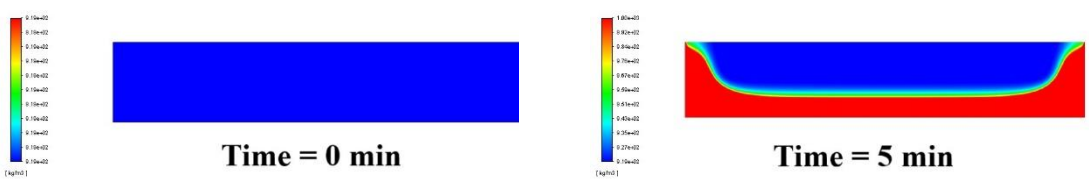

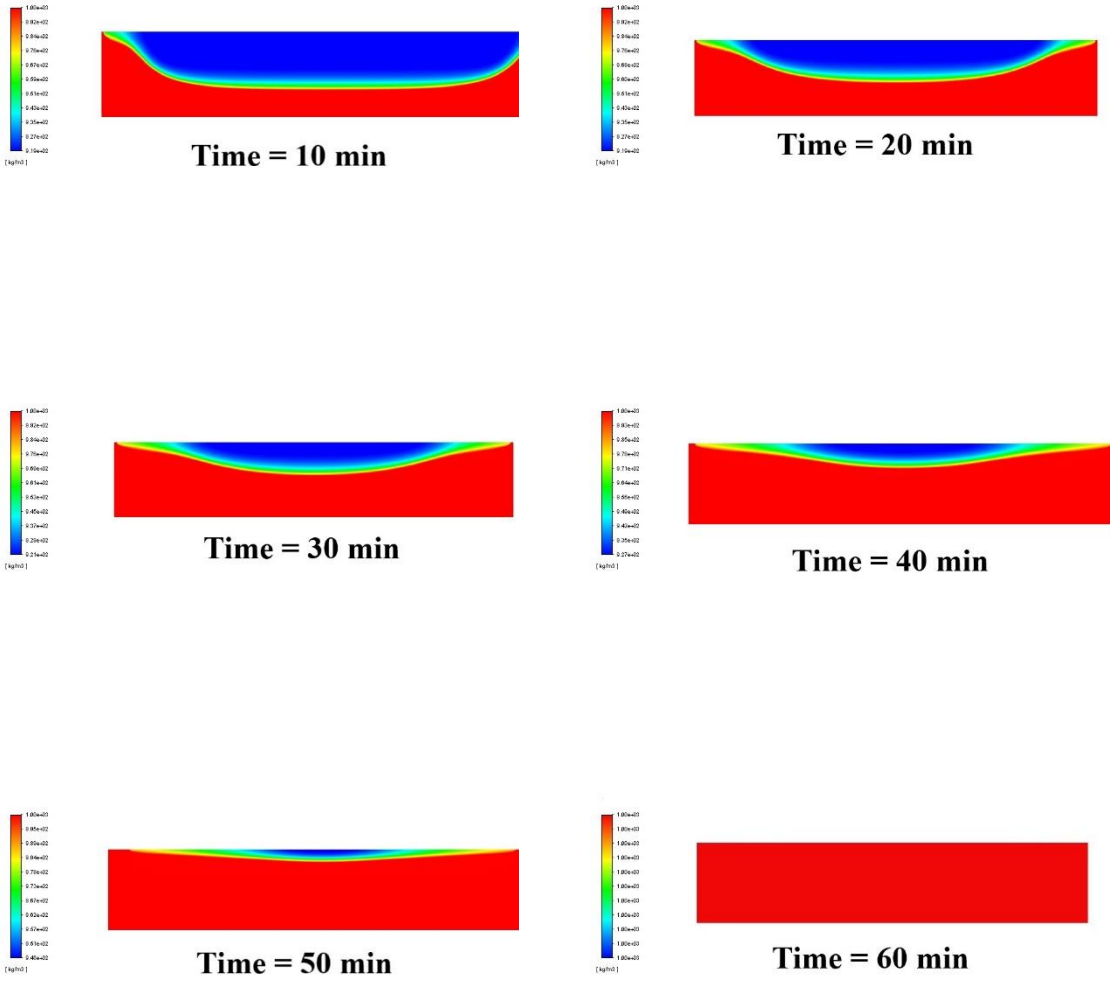

Figure 8.7: Contours of density.

Figure 8.7 represents the contours of density and its variation over time. The density has been defined as a function of the temperature. Thus, as the temperature raises the density of the PCM increases and it is gathering at the bottom while the ice occupies the upper part, forming a zone with low density at the top. Being the maximum temperature achievable equal to 4 °C, the density range will be on the left side of the maximum point illustrated in Figure 8.1. All the values of the ice within the phase-change temperature range are calculated by linear interpolation between the liquid and solid properties.

8.5 Conclusions

Some conclusion can be drawn from the numerical modeling and simulation of the PCM melting process:

- With vertical and horizontal heating walls melting starts from near to those surfaces, and then proceeds mainly through the vertical liquid film parallel to the fin surface. Some heat is still supplied by the pipe surface, but the thermal resistance of the water layer slows down the process.
- From the numerical results, it seems that the melting process is mainly driven by conduction due to the heaviness of the liquid phase which causes the formation of a liquid layer enlarged over time.
- One hour is enough to melt all the ice layer contained between two fins. Being a preliminary design of the condenser, an increase of the space between the fins is a solution to get more ice to melt.
- An increment of the fin spacing results in a higher number of tubes, being their length bonded to the dimensions of the cabinet. Therefore, mechanical support is even more necessary.
- A 3-D model should be used to simulate what is happening around the finned tube pattern. Even though the numerical simulation of the 3-D model has not been investigated, in figure 8.8 is illustrated what could happen during the melting of ice when the hot surface is placed above the ice block. Supposed to not consider the nearby finned tubes, at the bottom of the finned tube due to the relatively large density difference between liquid-solid phase the gravitational forces will promote the movement of the ice upwards, promoting the heat transfer process and reducing the thermal resistance of the water layer in contact with the pipe surface. In the present simulation the ice is fixed in the domain and it does not float upwards.

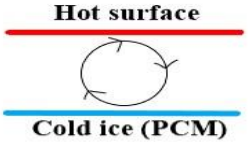

Figure 8.8: Flow pattern between ice and liquid phase at the bottom of the finned tube.

9 Conclusion and future work

This chapter presents the conclusion drawn from the numerical and experimental results of the experimental campaigns. In addition, a proposal for further work has been set.

9.1 Conclusion

In this section, the main results of this Thesis have been classified specifically based on the two different tasks investigated in this study.

9.1.1 Pivoting compressors

The pivoting technology applied to a typical medium-size supermarket, therefore the ability to switch a compressor from one section to another using an automatic control to increase the flexibility of the facility have been deeply investigated both numerically and experimentally. The comparative analysis reveals that no degradation has been recorded when pivoting compressors are used. From experimental data an increment of 7.5% in terms of COP has been found when the system is ejector supported at 35 °C with a negligible difference between a system with and without “pivoting”. The main conclusion of this study is that the implementation of pivoting technology is more beneficial whenever the system is ejector supported. In fact, in very warm climates the ejector technology must be implemented to reduce the throttling losses and maintain as much as possible the R744 system efficiency close to the efficiency of the system using synthetic refrigerant. On the other hand, higher investment costs are required. Considering the capacity in the parallel section raises in warm climates and also some refrigerant flow is pre-compressed to the parallel compressor section line, a lot of capacity needs to be installed. This capacity will be fully used only for few operating conditions leading to high investment costs, low flexibility of the rack and low compactness of the system because of the total number of compressors installed. In the investigated configuration, two compressors could be removed still supplying the refrigerating load under a wide range of operating conditions. Ejector-supported CO_2 compressor racks with pivoting compressors could have the same investment costs of a simple configuration equipped with HPV, keeping at the same time the efficiency improvement due to the unloading of the MT compressors thanks to the ejector. Moreover, not only space can be saved but in a way a push for research on ejector technology to improve their efficiency and justify their investment costs might be attributed to the pivoting. Hence,

one more time the issues coming with the ejector implementation in the test-rig have been proven.

The use of the pivoting system at the discharge of LT compressors has been numerically investigated. It allows the power consumption to be reduced mostly at high ambient temperature. However, the system becomes more complicated due to the connection and valves to install and therefore the investment can be justified only if the kWh saved is high enough. Moreover, the advantage obtained from their implementation is the increment in the number of hours where parallel compressors are in operation.

9.1.2 CTES and TPTL

A numerical approach has been followed for the TPTL design. The flow instabilities and two-phase flow pressure drops make the design a challenge because of the need of hydrostatic pressure, to ensure refrigerant circulation in the loop. Furthermore, an understanding and estimation of the heat interaction between tubes where the storage is changing phase inside the condenser are necessary. As determined by the condenser design, an important role is played by the storage material. Consequently, even though the HTC of the refrigerant is high, the dominant thermal resistant stays in the storage side. Due to the small temperature difference, a huge heat transfer area results leading to change in the cabinet applications (increasing the air temperature). A CTES with finned circular tube has been designed, with a tube path such to ensure the liquid to flow downwards tanks also to gravity. Probably because of the dimension of the condenser a metal structure should be employed to support the cabinet from the weight on the top.

Considering the complete loop, the two pipes that connect evaporator – condenser has been chosen considering the refrigerant phase, liquid in the downcomer and two-phase flow in the riser. A liquid head of 1.8 meters should be enough to force the flow of the refrigerant over the loop winning the frictional and gravitational pressure drops. A recirculation number of 3.6 results in a flooded operation of the evaporator. The main challenge might be the regulation of the refrigerant charge in the system when the valves are closed.

A numerical simulation has been carried out using Ansys Fluent. The results showed that in one hour all the domain is melted, considering Dirichlet boundary conditions on three sides of the domain. Therefore, although the assumptions made in the numerical model are quite strong, i.e. fin surface temperature equal to the pipe surface temperature, an improvement of

the preliminary design must be done considering the two hours in which the TPTL should provide the refrigerating load in the cabinet.

9.2 Assessment of objectives

The main objectives of the thesis presented in the introduction chapter are presented below:

- An extensive literature study of R744 refrigeration systems and ejector technology was performed in Chapter 2. Moreover, an overview of PCM applications and thermosyphon technology has been carried out. In addition to this, in Chapter 3 the basic theory of the CO_2 properties and different R744 system layouts have been included
- A detailed description of the components of the experimental facility is included in Chapter 4, as well as the system modifications made to carry out the experimental campaign
- The experimental campaign regarding oil management and relative results are presented in Chapter 5.
- The theoretical model built to simulate the refrigeration unit in the lab is widely illustrated in the Chapter 6. A Comprehensive test campaign leading to a set of compressor maps with a numerical analysis of the innovative pivoting solution has been performed, highlighting the main difference among them. Furthermore, the LT pivoting discharge have been numerically investigated
- A numerical design has been done for the CTES to place on the top of the cabinet. The TPTL loop has been studied following the principle of compensating the pressure losses using the liquid head
- A numerical model has been investigated, considering a simplified 2-D model that accounts the ice layer surrounded by two fins and the pipe surface
- A scientific paper of the innovative pivoting implementation is presented in the appendix.

9.3 Further work

Some suggestions are given below because of the issues encountered while performing the experimental campaign and the points touched by the analysis:

- Firstly, an innovative software should be designed to face the challenge to change the compressors suction lines without interrupting the operation of the system
- Secondly an experimental campaign should be carried out with the LT pivoting discharge, therefore playing with the valve V-310. With this, the power consumption reduction can be validated with experimental results enabling the IT compressors operation at low ambient temperature and even at partial load
- As seen in the experimental campaign, whenever the motive flow raises the pressure losses inside the chamber increases lowering the entrainment ratio. A way to keep the performance constant even at partial load might be to increase the pressure lift using a floating control of the receiver pressure. This might be used during the night when the MT load falls. It could be tested with a system designed for investigating in the ejector performance first, and later applied to the SuperSmart-Rack
- Another interesting point might be concerning the AC production. At partial load in warmer climates when ejectors are working, if the ejector is sucking all the vapor coming from the MT evaporator the MT evaporating pressure decreases (with the MT compressors off). Two possible ways could be investigated: first one, using the FGV some vapor is sent to the MT evaporating level keeping the suction pressure constant, being the suction of the ejector a function of the motive flow. The second one, instead of leaving the MT pressure to decrease, the receiver pressure could be increased going to increase the pressure lift because of the low amount of vapor to entrain from the MT level. In this way, although the MT compressors are still off, the IT compressors can work with a lower pressure ratio meaning that the power consumption will be reduced at partial load. The main constrain in this last approach might be the supplying of the AC load, which is strongly related to the receiver pressure.
- A pressure and temperature sensors might be installed at the suction of each compressors allowing calculating the opportunity to evaluate the density of the refrigerant, which is not possible today. This would give more accurate results when the performance of the compressors (compressor efficiencies) are investigated

- Regarding the CTES design, a 3-D CFD simulation would also help to verify the rate of melting between tubes and around them, hence it could give a piece of information about the amount of liquid obtained at the condenser outlet
- A numerical simulation using Modelica could give an idea of the pressure losses and hydrostatic pressure in the TPTL. The dynamic simulation could yield valuable knowledge about the refrigerant flow over the loop
- Lastly, an experimental campaign should be carried out to improve the future design of the TPTL focusing on the main discrepancies that will come out after the experiments

Bibliography

1. Pearson, A., *Carbon dioxide—new uses for an old refrigerant.* International Journal of Refrigeration, 2005. **28**(8): p. 1140-1148.
2. Maina, P. and Z. Huan, *A review of carbon dioxide as a refrigerant in refrigeration technology.* South African Journal of Science, 2015. **111**(9/10).
3. Petter Nekså, A.H., Arne M. Bredesen, Trygve M. Eikevik, *CO2 as working fluid - technological development on the road to sustainable refrigeration.* 2016.
4. Hafner, A., S. Försterling, and K. Banasiak, *Multi-ejector concept for R-744 supermarket refrigeration.* International Journal of Refrigeration, 2014. **43**: p. 1-13.
5. Gullo, P., et al., *Multi-Ejector Concept: A Comprehensive Review on its Latest Technological Developments.* Energies, 2019. **12**(3).
6. Gullo, P., A. Hafner, and K. Banasiak, *Transcritical R744 refrigeration systems for supermarket applications: Current status and future perspectives.* International Journal of Refrigeration, 2018. **93**: p. 269-310.
7. Minetto, S., et al., *Experimental analysis of a new method for overfeeding multiple evaporators in refrigeration systems.* International Journal of Refrigeration, 2014. **38**: p. 1-9.
8. Hafner, A., *High efficient integrated CO2 refrigeration systems with ejectors and pivoting compressor arrangements.* 2017.
9. Pardiñas, Á.Á., A. Hafner, and K. Banasiak, *Novel integrated CO2 vapour compression racks for supermarkets. Thermodynamic analysis of possible system configurations and influence of operational conditions.* Applied Thermal Engineering, 2018. **131**: p. 1008-1025.
10. Manescu, R., et al., *A new approach for cold thermal energy storages in supermarket refrigeration systems*. 2017, International Institute of Refrigeration (IIR).
11. Commission, E., *Regulation (EU) No 517-2014 of the European Parliament and of the Council of 16th April 2014 on Fluorinated Greenhouse Gases and Repealing Regulation (EC) No 842/2006.* 2014.
12. IPCC, *Safeguarding the Ozone Layer and the Global Climate system: Special Report of the Intergovernmental Panel on Climate Change.* 2005.
13. EPEE, *Achieving the EU HFC Phase Down: The EPEE "Gapometer" Project.* 2015.
14. programme, E., *Handbook for the Montreal Protocol on Substances that Deplete the Ozone Layer.* 2020.
15. Emerson, *Europe's New F-Gas Phase-Down and Bans Go Into Effect.* 2015.
16. NeksÅ, P., et al., *CO2 as working fluid - technological development on the road to sustainable refrigeration*. 2016, International Institute of Refrigeration (IIR).
17. Shecco, *Guide to natural refrigerants in Japan - State of the industry.* 2016.
18. Sawalha, S., M. Karampour, and J. Rogstam, *Field measurements of supermarket refrigeration systems. Part I: Analysis of CO2 trans-critical refrigeration systems.* Applied Thermal Engineering, 2015. **87**(C): p. 633-647.
19. S., U., *Lawson's action against Global Warming. Proceeding from ATMOsphere Asia 2016.* 2016.
20. Sharma, V., B.A. Fricke, and P. Bansal, *Evaluation of a transcritical CO2 supermarket refrigeration system for the USA market*. 2015, Oak Ridge National Lab.(ORNL), Oak Ridge, TN (United States); Building ….
21. Shilliday, J.A., *Investigation and optimisation of commercial refrigeration cycles using the natural refrigerant CO2*. 2012, Brunel University School of Engineering and Design PhD Theses.

22. Shi, R., et al., *Dynamic modeling of CO2 supermarket refrigeration system.* 2010.
23. Fricke, et al., *Laboratory Evaluation of a commercial CO2 booster refrigeration system.* 2016.
24. Gullo, P. and A. Hafner, *Thermodynamic performance assessment of a CO2 supermarket refrigeration system with auxiliary compression economization by using advanced exergy analysis.* 2017.
25. Kim, M., *Fundamental process and system design issues in CO2 vapor compression systems.* Progress in Energy and Combustion Science, 2004. **30**(2): p. 119-174.
26. Cavallini, A. and C. Zilio, *Carbon dioxide as a natural refrigerant.* International Journal of Low-Carbon Technologies, 2007. **2**(3): p. 225-249.
27. Sawalha, S., *Investigation of heat recovery in CO2 trans-critical solution for supermarket refrigeration.* International Journal of Refrigeration, 2013. **36**(1): p. 145-156.
28. Gullo, P., B. Elmegaard, and G. Cortella, *Energy and environmental performance assessment of R744 booster supermarket refrigeration systems operating in warm climates.* International Journal of Refrigeration, 2016. **64**: p. 61-79.
29. Javerschek, O., J. Craig, and A. Xiao, *CO2 as a refrigerant - Start right away!* 2015, International Institute of Refrigeration (IIR).
30. Hafner, A. and K. Hemmingsen A, *R744 refrigeration technologies for supermarkets in warm climates*. 2015, International Institute of Refrigeration (IIR).
31. Karampour, M. and S. Sawalha. *Theoretical analysis of CO2 trans-critical system with parallel compression for heat recovery and air conditioning in supermarkets*. in *24th IIR Refrigeration Congress of Refrigeration. IIF/IIR, Yokohama, Japan*. 2015.
32. Wiedenmann, E., J. Schoenenberger, and M. Baertsch. *Efficiency analysis and comparison of innovative R744-refrigerating systems in commercial applications*. in *Proceedings of the 11th IIR Gustav Lorentzen Conference on Natural Refrigerants: Natural Refrigerants and Environmental Protection*. 2014.
33. Sarkar, J. and N. Agrawal, *Performance optimization of transcritical CO 2 cycle with parallel compression economization.* International Journal of Thermal Sciences, 2010. **49**(5): p. 838-843.
34. Minetto, S., et al. *Theoretical and experimental analysis of a CO2 refrigerating cycle with two-stage throttling and suction of the flash vapour by an auxiliary compressor*. in *Proceedings of IIR International Conferences–Thermophysical Properties and Transfer Processes of Refrigerants*. 2005.
35. Javerschek, O., M. Reichle, and J. Karbiner. *Optimization of parallel compression systems*. in *12th IIR Gustav Lorentzen Conference on Natural Refrigerants, IIR/IIF, Edinburgh, Scotland*. 2016.
36. Qureshi, B.A. and S.M. Zubair, *Mechanical sub-cooling vapor compression systems: Current status and future directions.* International Journal of Refrigeration, 2013. **36**(8): p. 2097-2110.
37. Kakuda, M., H. Nagata, and F. Ishizono, *Development of a Scroll Expander for the CO2 Refrigeration Cycle.* HVAC&R Research: Topical Issue, 2009. **15**(4): p. 771-783.
38. Banasiak, K. and A. Hafner, *Mathematical modelling of supersonic two-phase R744 flows through converging–diverging nozzles: The effects of phase transition models.* Applied Thermal Engineering, 2013. **51**(1-2): p. 635-643.
39. Banasiak, K., et al., *A CFD-based investigation of the energy performance of two-phase R744 ejectors to recover the expansion work in refrigeration systems: An irreversibility analysis.* International Journal of Refrigeration, 2014. **40**: p. 328-337.

40. Elbel, S. and P. Hrnjak, *Experimental validation of a prototype ejector designed to reduce throttling losses encountered in transcritical R744 system operation.* International Journal of Refrigeration, 2008. **31**(3): p. 411-422.
41. Nakagawa, M., et al., *Experimental investigation on the effect of mixing length on the performance of two-phase ejector for CO2 refrigeration cycle with and without heat exchanger.* International Journal of Refrigeration, 2011. **34**(7): p. 1604-1613.
42. Banasiak, K., et al., *Development and performance mapping of a multi-ejector expansion work recovery pack for R744 vapour compression units.* International Journal of Refrigeration, 2015. **57**: p. 265-276.
43. Girotto, S., *Improved transcritical CO2 refrigeration systems for warm climates*. 2017, International Institute of Refrigeration (IIR).
44. Hafner, A. and K. Banasiak. *Full scale supermarket laboratory R744 ejector supported and AC integrated parallel compression unit*. in *Proceedings of the 12th IIR Gustav Lorentzen Natural Working Fluids Conference, Edinburgh, UK*. 2016.
45. Karampour, M. and S. Sawalha, *Energy efficiency evaluation of integrated CO 2 trans-critical system in supermarkets: A field measurements and modelling analysis.* International Journal of Refrigeration, 2017. **82**: p. 470-486.
46. Gullo, P. and A. Hafner. *Comparative assessment of supermarket refrigeration systems using ultra low-GWP refrigerants—Case study of selected American cities*. in *Proceedings of the 30th International Conference on Efficiency, Cost, Optimisation, Simulation and Environmental Impact of Energy Systems, San Diego, CA, USA*. 2017.
47. Schönenberger, J., et al. *Experience with ejectors implemented in a R744 booster system operating in a supermarket*. in *Proceedings of the 11th IIR Gustav Lorentzen Conference on Natural Refrigerants, Hangzhou, China*. 2014.
48. Ciconkov, R., *Refrigerants: There is still no vision for sustainable solutions.* International Journal of Refrigeration, 2018. **86**: p. 441-448.
49. Elbel, S., *Historical and present developments of ejector refrigeration systems with emphasis on transcritical carbon dioxide air-conditioning applications.* International Journal of Refrigeration, 2011. **34**(7): p. 1545-1561.
50. Lorentzen, G., *Throttling : the internal haemorrhage of the refrigeration proces*. 1984, Carshalton: Institute of Refrigeration.
51. Butrymowicz, D., *Application of two phase ejector as booster compressor in refrigeration system.* 2004.
52. Smolka, J., et al., *Performance comparison of fixed- and controllable-geometry ejectors in a CO2 refrigeration system.* International Journal of Refrigeration, 2016. **65**: p. 172-182.
53. Danfoss, *How to design a transcritical CO2 system with Multi Ejector Solution.* 2018.
54. Smolka, J., et al., *A computational model of a transcritical R744 ejector based on a homogeneous real fluid approach.* Applied Mathematical Modelling, 2013. **37**(3): p. 1208-1224.
55. Palacz, M., et al., *Application range of the HEM approach for CO2 expansion inside two-phase ejectors for supermarket refrigeration systems.* International Journal of Refrigeration, 2015. **59**: p. 251-258.
56. Palacz, M., et al., *HEM and HRM accuracy comparison for the simulation of CO2 expansion in two-phase ejectors for supermarket refrigeration systems.* Applied Thermal Engineering, 2017. **115**: p. 160-169.
57. Palacz, M., et al., *Shape optimisation of a two-phase ejector for CO2 refrigeration systems.* 2016.

58. Haida, M.P., et al., *Experimental analysis of the R744 vapour compression rack equipped with the multi-ejector expansion work recovery module*. 2015, NTNU.
59. Haida, M., et al., *Performance mapping of the R744 ejectors for refrigeration and air conditioning supermarket application: A hybrid reduced-order model.* Energy, 2018. **153**: p. 933-948.
60. Elbel, S. and N. Lawrence, *Review of recent developments in advanced ejector technology.* International Journal of Refrigeration, 2016. **62**: p. 1-18.
61. Hafner, A., A. Hemmingsen, and P. Nekså. *System configuration for supermarkets in warm climates applying R744 refrigeration technologies–Case studies of selected Chinese cities*. in *Proceedings of the 11th IIR Gustav Lorentzen Conference on Natural Refrigerants, Hangzhou, China*. 2014.
62. Kriezi, E., et al. *R744 multi ejector development*. in *Proceedings of the 12th IIR Gustav Lorentzen Natural Working Fluids Conference, Edinburgh, UK*. 2016.
63. Javerschek, O., M. Reichle, and J. Karbiner, *Influence of ejectors on the selection of compressors in carbon dioxide booster systems*. 2017, International Institute of Refrigeration (IIR).
64. Minetto, S., et al. *Recent installations of CO2 supermarket refrigeration system for warm climates: data from field*. in *Proceedings of the 3rd IIR International Conference on Sustainability and Cold Chain, London, UK*. 2014.
65. Pardiñas, Á.Á., *Integrated R744 ejector supported parallel compression racks for supermarkets. Experimental results.* 2018.
66. Cabeza, L., et al., *Introduction to thermal energy storage (TES) systems*, in *Advances in thermal energy storage systems*. 2015, Elsevier. p. 1-28.
67. Fidorra, N., et al. *Analysis of cold thermal energy storage concepts in CO2 refrigeration systems*. in *Gustav Lorentzen Natural Working Fluids Conference, Edinburgh*. 2016.
68. Lu, Y., et al., *Experimental study of heat transfer intensification by using a novel combined shelf in food refrigerated display cabinets (Experimental study of a novel cabinets).* Applied Thermal Engineering, 2010. **30**(2-3): p. 85-91.
69. Alzuwaid, F., et al., *The novel use of phase change materials in a refrigerated display cabinet: An experimental investigation.* Applied Thermal Engineering, 2015. **75**: p. 770-778.
70. Fidorra, N., et al., *Low temperature heat storages in CO2 supermarket refrigeration systems*. 2015, International Institute of Refrigeration (IIR).
71. Paliwoda, A., *Calculation of basic parameters for gravity-fed evaporators for refrigeration and heat pump systems.* International journal of refrigeration, 1992. **15**(1): p. 41-47.
72. Paliwoda, A., *Generalized method of pressure drop calculation across pipe components containing two-phase flow of refrigerants.* International journal of refrigeration, 1992. **15**(2): p. 119-125.
73. Khodabandeh, R., *Pressure drop in riser and evaporator in an advanced two-phase thermosyphon loop.* International Journal of Refrigeration, 2005. **28**(5): p. 725-734.
74. Selvnes, H., et al. *CFD modeling of ice formation and melting in horizontally cooled and heated plates*. in *Eurotherm Seminar# 112-Advances in Thermal Energy Storage*. 2019. Edicions de la Universitat de Lleida Lleida, Spain.
75. Selvnes, H., A. Hafner, and H. Kauko. *Design of a cold thermal energy storage unit for industrial applications using CO2 as refrigerant*. in *25th IIR International Congress of Refrigeration Proceedings*. 2019. IIR.
76. Hartenstine, J.R., et al. *LOOP Thermosyphon design for cooling of large area, high heat flux sources*. in *ASME 2007 InterPACK Conference collocated with the*

ASME/JSME 2007 Thermal Engineering Heat Transfer Summer Conference. 2007. American Society of Mechanical Engineers Digital Collection.
77. Zhang, P., et al., *Experimental investigation on two-phase thermosyphon loop with partially liquid-filled downcomer.* Applied Energy, 2015. **160**: p. 10-17.
78. Lorentzen, G., *Revival of carbon dioxide as a refrigerant*. 1994, Oxford: Butterworth Heinemann.
79. Lorentzen, G., *The use of natural refrigerants : a complete solution to the CFC/HCFC predicament*. 1994, Paris: Issued for International Institute of Refrigeration.
80. Lorentzen, G. and J. Pettersen, *A new, efficient and environmentally benign system for car air-conditioning = Un nouveau système de conditionnement d'air automobile efficace et sans nuisance sur l'environnement*. Un nouveau système de conditionnement d'air automobile efficace et sans nuisance sur l'environnement. 1993, Guildford: IPC Science and Technology Press.
81. Devecioğlu, A.G. and V. Oruç, *Characteristics of some new generation refrigerants with low GWP.* Energy Procedia, 2015. **75**: p. 1452-1457.
82. Reddy, K., V. Mudgal, and T. Mallick, *Review of latent heat thermal energy storage for improved material stability and effective load management.* Journal of Energy Storage, 2018. **15**: p. 205-227.
83. Fleischer, A.S., *Thermal energy storage using phase change materials: fundamentals and applications*. 2015: Springer.
84. Voller, V.R. and C. Prakash, *A fixed grid numerical modelling methodology for convection-diffusion mushy region phase-change problems.* International Journal of Heat and Mass Transfer, 1987. **30**(8): p. 1709-1719.
85. Kakaç, S. and H. Liu, *Heat exchangers : selection, rating, and thermal design*. 2002, Boca Raton, Fla.: CRC Press.
86. Shah, R.K. and D.P. Sekulic, *Fundamentals of Heat Exchanger Design*. 2003: Wiley.
87. Mirza Mohammed Shah PhD, P., *General correlation for heat transfer during condensation in plain tubes: further development and verification.* ASHRAE Transactions, 2013. **119**: p. 3.
88. Zhang, P., et al., *Simulation on the thermal performance of two-phase thermosyphon loop with large height difference.* Applied Thermal Engineering, 2019. **163**: p. 114327.
89. Zhang, P., et al., *Modeling and performance analysis of a two-phase thermosyphon loop with partially/fully liquid-filled downcomer.* International journal of refrigeration, 2015. **58**: p. 172-185.
90. Gebhart, B. and J.C. Mollendorf, *A new density relation for pure and saline water.* Deep Sea Research, 1977. **24**(9): p. 831-848.
91. Fadl, M. and P.C. Eames, *Numerical investigation of the influence of mushy zone parameter Amush on heat transfer characteristics in vertically and horizontally oriented thermal energy storage systems.* Applied Thermal Engineering, 2019. **151**: p. 90-99.

Appendices

List of Appendices

A Scientific Paper – Flexible capacity adjustment with Pivoting compressors in multi-stage CO_2 compressor pack

Attaining a higher flexibility degree in CO_2 compressor racks

Ángel Á. PARDIÑAS[(a)], Luca CONTIERO[(b)], Armin HAFNER[(a),] Krzysztof BANASIAK[(c),] Mads H. NIELSEN[(d),] Lars F.S. LARSEN[(d)]

[(a)] Norwegian University of Science and Technology, Trondheim, 7491, Norway,
angel.a.pardinas@ntnu.no, armin.hafner@ntnu.no
[(b)] Universita Degli Studi di Padova, Padova, 35122, Italy
Luca.contiero@studenti.unipd.it
[(c)] SINTEF Energi AS, Trondheim, 7034, Norway,
krzysztof.banasiak@sintef.no
(d) Danfoss AS, Nordborg, 6430, Denmark,
madsholst@danfoss.com, lars.larsen@danfoss.com

ABSTRACT

CO_2 compressor racks have shown their suitability for commercial and industrial refrigeration systems at any location and climate. Even if some references state that CO_2 units can compete in capital cost with any other alternative solution, often investment costs are still the main barrier for the global expansion of CO_2.

This work explores, numerically and experimentally, the implementation of "pivoting" compressors, i.e. compressors that can operate in the medium temperature (MT) and parallel compressor suction groups, depending on ambient conditions, cooling loads and use of ejector. The objective is to increase the flexibility of CO_2 compressor racks, keeping the efficiency and, potentially, reducing the investment. This study shows that this solution with "pivoting" compressors is beneficial in ejector-supported systems, since the investment cost of the ejectors is compensated by a lower number of installed compressors, as compressor capacities can be applied in more flexible ways.

Keywords: Refrigeration, Carbon Dioxide, Compressors, Switching, Pivoting.

1. INTRODUCTION

CO_2 (R744) is currently the refrigerant choice for commercial refrigeration in many areas of the World, particularly Europe and Japan, and is entering other applications such as industrial refrigeration, small stores or ice rinks (Zolcer Skačanová and Battesti, 2019). Gullo et al. (2018) pointed out that the technological developments implemented nowadays in R744 supermarket-refrigeration systems allow that they outperform HFC-based units under almost any climate conditions. These technological developments comprise, for example, mechanical subcooling, overfed evaporators (with or without liquid ejectors) or vapour ejectors for different purposes such as transferring load to parallel compressor or supporting efficient AC integration. However, they elevate the level of complexity and investment cost, hindering their implementation and any positive impact they would have.

Vapour ejectors to transfer the load from the medium-temperature (MT) compressors to the parallel compressor suction group contribute to reducing the energy consumption of the refrigeration system. However, application of ejectors entails a significant initial cost that could also come with the requirement of additional parallel-compressor capacity only used when the ambient temperature (gas cooler outlet temperature) is high. The present work explores the implementation of "pivoting"

compressors, i.e. compressors that can alternate between the MT- and parallel-compressor sections depending on the operating conditions. This reduces the installed compressor capacity in ejector-supported CO_2 refrigeration systems without any negative impact on the capacity delivered. Such technology was already discussed in Pardiñas et al. (2018a) to increase the flexibility of compressors packs and to optimize energy efficiency by choosing the right configuration of active compressors per section, but that study disregarded the potential to reduce the number of compressors installed and investment cost. The present article describes the solution proposed and compares it with the state-of-the-art system. A numerical model was used to evaluate this "pivoting" compressor solution, and the study was complemented with experimental data. The results are discussed in this paper looking into compressor-capacity installed (and unused) in an existing installation, energy efficiency and a simplified cost analysis.

2. CO_2 COMPRESSOR RACK WITH PIVOTING COMPRESSORS

Figure 1 shows a CO_2 compressor rack for supermarket refrigeration at two temperature levels, medium-temperature (MT) and low-temperature (LT), with parallel compression and vapour ejectors. The main modification that is suggested in this study is the implementation of a set of two valves upstream of compressors, which become the "pivoting" compressors. In the configuration represented in Figure 1, there would one dedicated MT compressor, one parallel compressor, while the other two compressors are "pivoting" compressors.

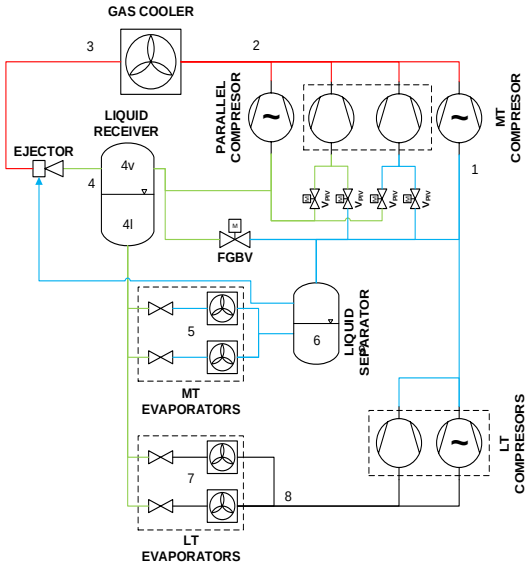

Figure 1. CO_2 compressor rack with "pivoting" compressors.

"Pivoting" compressors can alternate between the MT and parallel compressor suction groups depending on the capacity requirements by activating the corresponding valve. The aim is that the compressor-capacity (number of compressors) installed in the rack can be reduced without any effect on the delivered cooling or efficiency, using compressors during longer periods of the year exactly for the purpose that they are needed at each time. This is particularly important in ejector-supported systems, as a larger parallel-compressor capacity is needed when the vapour ejector is able to unload the MT compressors. On the other hand, parallel compressors would be idle during the cold part of the year, when mostly MT compressors are needed, i.e. compressor capacity ends up unused and occupying valuable space. The implementation of "pivoting" compressors involves that they could be used as parallel compressors when the ejectors are entraining a relatively large mass flow rate from the MT section to the parallel-compressor suction group; else these compressors are connected to the MT suction group.

3. METHODOLOGIES

3.1 EXPERIMENTAL SETUP

SuperSmart-Rack is the experimental setup available at Varmeteknisk laboratory at NTNU (Trondheim, Norway) that was utilized to analyze the benefit of implementing the "pivoting" compressor concept to CO_2 compressor racks. A detailed description can be found in Pardiñas et al. (2018b) and cannot be included here for space reasons. The setup consists of a versatile CO_2 refrigeration system, which allows testing very different system configurations (booster, ejector supported, air conditioning integration, etc.), and several auxiliary circuits to emulate the demands and operating conditions in a supermarket.

The unit comprises eight semi-hermetic reciprocating compressors manufactured by Bitzer, with the characteristics shown in **Table 1** and arranged as in Figure 1: two LT compressors, one MT compressor, one parallel (or IT) compressor, and four "pivoting" compressors (default operating mode indicated also in the table). The ejector installed is a Multi Ejector HP 1875 LE 400 CTM 6 from Danfoss (https://assets.danfoss.com/documents/DOC300732394440/DOC300732394440.pdf), and the system has a high-pressure valve (HPV) in parallel to allow direct comparison between ejector-supported and HPV configurations. Up to seven helical coaxial tube-in-tube heat exchangers can be operated as evaporators, using a glycol solution as heat source. Five of them are MT evaporators and can provide more than 60 kW load, and the other two are LT evaporators and provide between 15 kW and 20 kW. AC evaporators and ejectors are not considered in the present study. Up to three brazed plate heat exchangers can be used as gas coolers, using three different loops at different temperature as heat sinks.

3.2 SIMULATION MODEL

Prior to any experimental campaign, the research question of this article was investigated numerically to minimize the number of tests needed by pre-selecting potential combinations of compressors. The simplified and steady-state numerical model emulated SuperSmart-Rack experimental setup and was programed in EES (Engineering Equation Solver http://www.fchartsoftware.com/ees/). Compressors from **Table 1** were modelled using the polynomials available in the software of the manufacturer (https://www.bitzer.de/websoftware/), and accounting for the effect of density (if actual superheating different to reference conditions) and of frequency with VSD compressors. Concerning the ejector, fixed efficiency was used, defined as in the work by Elbel and Hrnjak (2008), e.g. equal to 30% @35 °C gas cooler outlet temperature. The remaining components were modelled neglecting heat losses and pressure drops.

Table 1. Characteristics of the compressors in SuperSmart-Rack. VSD stands for variable speed drive.

Compressor No. (Model)	Operating mode (default mode)	Displacement [m^3/h] @ 50 Hz	VSD? (frequency range)
1 (2GME-4K)	LT	5	No
2 (2JME-3K)	LT	3.5	Yes (30 – 70 Hz)
3 (4MTC-10K-40S)	MT	6.5	Yes (30 – 80 Hz)
4 (4MTC-10K-40S)	Pivoting (MT)	6.5	No
5 (4JTC-15K-40P)	Pivoting (MT)	9.2	No
6 (2KTE-7K-40S)	IT	4.8	Yes (30 – 80 Hz)
7 (2KTE-7K-40S)	Pivoting (IT)	4.8	No
8 (4JTC-15K-40P)	Pivoting (IT)	9.2	No

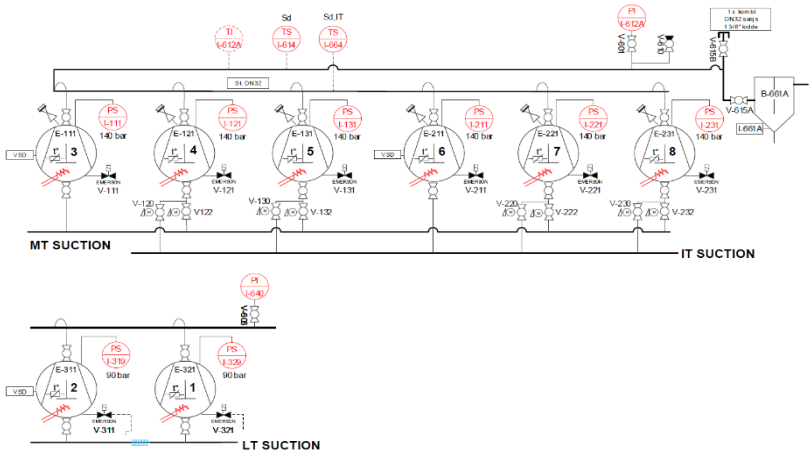

Figure 2. Compressor arrangement in the experimental setup SuperSmart-Rack, made by Advansor. The largest numbers in the centre of the compressor symbol correspond to the reference number in Table 1.

3.3 CONDITIONS AND CONFIGURATIONS INVESTIGATED

CO_2 compressor racks are sized at the design conditions, considering the maximum loads and harsh (high) ambient temperature. It is in these conditions that the compressor-capacity is defined and that the potential to reduce the number of compressors installed should be evaluated when implementing "pivoting" compressors. In our case, the design conditions listed below were those considered for the actual sizing of the SuperSmart-Rack facility, which aimed at the typical refrigeration loads for medium-sized supermarkets in Norway.

- Gas cooler outlet temperature 35 °C, with high pressure setpoint 89 bar(a). Simulations and tests were also performed at gas cooler outlet temperatures ranging from 10 °C to 35 °C to evaluate if the selected compressor rack would meet the refrigeration loads also at these conditions, but these results are not shown in this paper due to space constraints.
- Receiver pressure 36 bar(a).
- MT load 60 kW, at evaporation temperature -8 °C (approximate pressure 28 bar(a)).
- LT load 15 kW, at evaporation temperature -30 °C (approximate pressure14.3 bar(a)). Both LT compressors (see **Table 1**) are always in operation to meet the specified load, and thus this will not be discussed further in the RESULTS section.
- Regulation of evaporators' expansion valves, at MT and LT levels, to achieve 8 K superheating degree. This setting differs from the flooded operation recommended with CO_2 evaporators, but is still common practice in an important part of the compressor racks installed worldwide.

Concerning the configurations investigated, the booster system with parallel compression and HPV was taken as base, and the ejector-supported booster system with parallel compression as alternative. In both cases, the effect of "pivoting" compression was investigated.

4. RESULTS

4.1 Parallel compression system with HPV

Figure 3 shows the effect that "pivoting" compressors would have on a booster system with parallel compression and HPV, by representing how compressors need to be distributed in the different groups if the system has "pivoting" compressors (right) or not (left), and which would be the unused capacity in each case at the design conditions. Compressor numbering corresponds to that defined in section 0 (**Table 1**). It should be specified here that the configuration without the "pivoting" feature has compressors 4, 5, 7 and 8 arranged as shown in **Table 1** under "default mode" (in parenthesis).

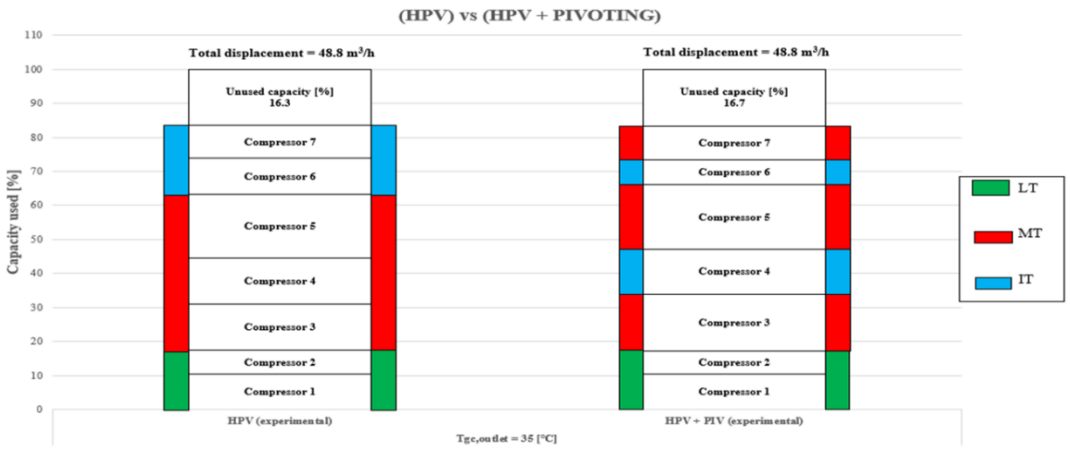

Figure 3. Effect of implementing "pivoting" compressors on the compressor-capacity used by a booster system with parallel compression and HPV (without ejector) at design conditions as defined in section 0.

As can be seen in **Figure 3**, implementing "pivoting" compressors has negligible effects on this configuration of CO_2 compressor rack. Three MT compressors and two parallel (IT) compressors are needed at this point, independently of the use of "pivoting" or not, and the only difference resides on how the compressors could be arranged between the MT- and parallel-compressor groups. The unused capacity at the design point would be in the range of 16% and 17%, adding up the remaining capacity of the VSD compressors (2, 3 and 5). Under any other conditions, it would be enough with these compressors to meet the load requirements, and thus compressor 8 would be unnecessary under this configuration. It must be also pointed out that "pivoting" has a negligible effect on the performance of the compressor rack. For this comparison, COP was defined in a very simple way as the ratio of the total refrigeration load produced by the system, summing up refrigeration at LT and MT levels, to the total power consumption of the compressors in the rack. The COP values retrieved from the experimental campaign were equal to 1.75 and 1.76 without and with "pivoting" compressors, respectively.

4.2 Ejector-supported parallel compression system

The same exercise was performed in **Figure 4** with the ejector-supported CO_2 compressor rack. The traditional configuration without "pivoting" compressors (left) has much higher unused capacity at the design point than the corresponding unit without ejector, being these values equal to 33.2% and 16.3%, respectively (or 19.2 m^3/h and 7.8 m^3/h, respectively). The origin of all this unused capacity in the ejector-supported configuration without "pivoting" could be unclear looking only at the active compressors at the design point. The explanation is that, due to the good performance of the ejector at 35 °C gas cooler outlet temperature, MT compressors are heavily unloaded in favour of parallel (IT) compressors. The two parallel compressors from the system without ejector, compressors 6 and 7, are insufficient to meet the capacity requirements at those conditions, and a larger parallel compressor is in operation (compressor 8). However, as soon as the unit is operating below full load or with heat rejection at lower temperatures, the combination of compressors 6 and 8 becomes too high, and compressor 7 would be needed to close the capacity gap between compressor 6 only (at highest frequency) and compressors 6 (at lowest frequency) and 8. An analogous effect is observed with the MT compressors, and thus compressor 4 needs to be installed even if it is not in operation at the design point. In conclusion, the ejector implementation involves higher shifts of the capacity from the MT to the parallel section and vice versa under changing operating conditions, than a system with HPV.

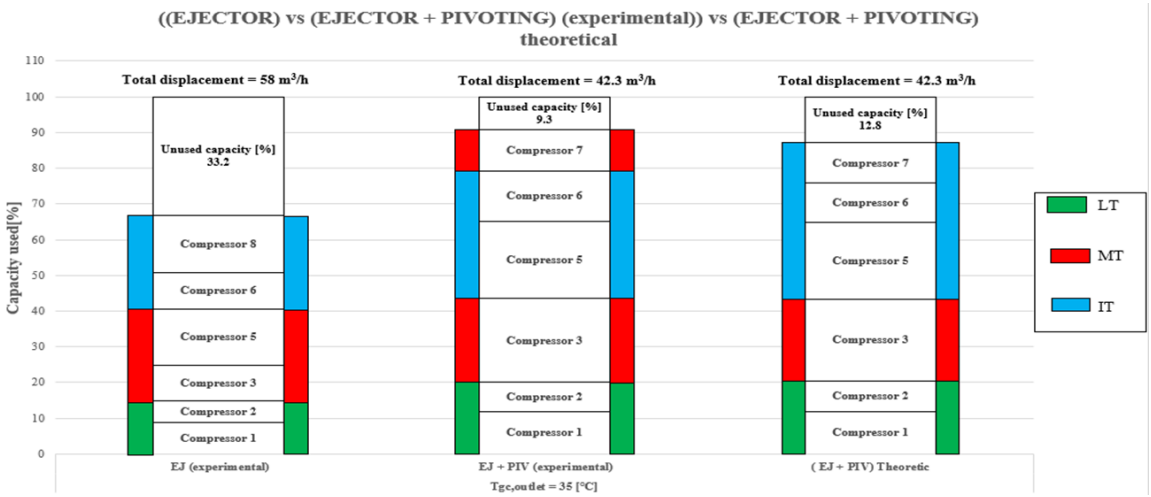

Figure 4. Effect of implementing "pivoting" compressors on the compressor-capacity used by an ejector-supported booster system with parallel compression at design conditions as defined in section 0.

Figure 4 indicates also how the implementation of "pivoting" compressors affects the ejector-supported CO_2 compressor rack, reducing importantly the unused and installed compressor-capacity compared to the case without "pivoting" compressors. The reason is that the large shifts of capacity

between the compressor suction groups (MT and parallel) caused by the introduction of ejector can be covered with fewer compressors, if these units are flexibly operated where they are needed. As indicated in **Table 1** and **Figure 2**, compressor 3 and 6 are dedicated to fixed suction groups (MT and parallel compressor, respectively) and are always in operation since they are coupled to the VSD. Two additional "pivoting" compressors (5 and 7) would be enough to cover these changes in the capacity requested at the different temperature levels avoiding capacity gaps. Thus, the system could operate with up to three parallel compressors when the ejector performs best and unloads significantly the MT section, and up to three MT compressors when heat rejection is performed at lower ambient temperatures and the ejector performs basically as a high-pressure control valve.

The reason why there are two "pivoting" cases in **Figure 4** at the same design conditions is that one comes from the experimental campaign (middle column) and the other from the numerical analysis (right column). According to the simulations, only one MT compressor operating at maximum capacity would suffice due to the ejector support, leading to three parallel (IT) compressors. However, the experimental campaign showed that the share should be two MT compressors and two IT compressors instead. Here lies the main disagreement between the experimental and numerical results, which otherwise was very positive given the relative simplicity of the numerical model. The reason behind this mismatch is that the numerical model underestimates the performance of the internal heat exchanger located downstream of the gas cooler and used to superheat the suction stream to the parallel compressors. Thus, the temperature of the ejector motive flow was lower in the tests, leading to slightly lower ejector performance and entrainment ratio. In any case, the installed compressor-capacity would be identical, and the difference in unused capacity low (approximately 1.5 m^3/h).

The COPs of the CO_2 compressor racks with and without ejector at the design point, calculated with the experimental data, were 1.88 and 1.75, respectively (around 7.5% higher with the ejector-supported unit). A negligible COP difference was observed between the ejector-supported system with and without "pivoting".

4.3 Cost analysis

A simplified cost analysis was done to compare the different configurations with and without "pivoting" compressors. Only the costs of the compressors and, eventually, Multi Ejector were considered. It was assumed that compressor cost is almost independent of the compressor capacity (in the range used in SuperSmart-Rack) and that the Multi Ejector costs approximately the same as a compressor. Other components in the compressor rack were not accounted for in this analysis since they are almost identical independently of the configuration. The cost of the set of valves to turn a compressor into "pivoting" was also neglected. It can be clearly seen in Figure 5 that the highest investment cost would come from the ejector-supported unit without "pivoting" solution. This could hinder the implementation of ejector technology, even when it leads to a reduction in the power demand. On the other hand, at equal cooling capacities, the use of "pivoting" compressors with ejector reduces significantly the number of installed compressors and compensates the increase of cost due to the Multi Ejector, having a comparable investment to the HPV unit.

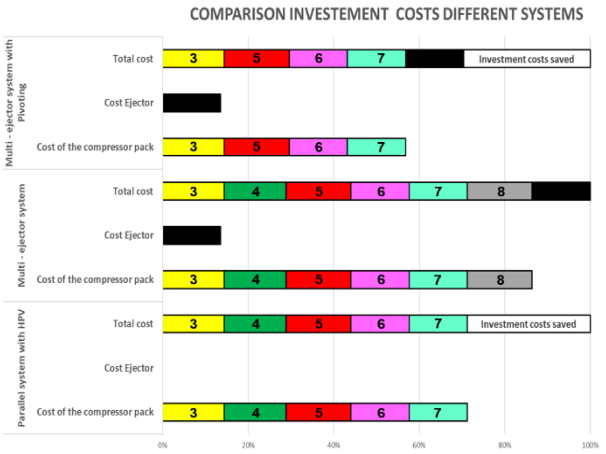

Figure 5. Simplified cost analysis of the different configuration of CO_2 compressor rack.

5. CONCLUSIONS

This paper investigated if the implementation in a CO_2 compressor rack of "pivoting" compressors, i.e. compressors that can operate as MT or parallel compressors depending on ambient

conditions, cooling loads and ejector performance, has a positive impact on the flexibility of the system and could reduce the installed compressor-capacity and thus the investment cost. The main conclusion from this study is that "pivoting" is mostly beneficial if the system is ejector-supported, since it is possible to keep the efficiency improvement due to the vapour ejector that unloads the MT compressors in favour of the parallel compressors, and reduce at the same time the total number of compressors installed. In the investigated configuration, a typical case for a medium size supermarket, two compressors could be removed. All in all, ejector-supported CO_2 compressor racks with "pivoting" compressors could be at the same level of investment cost as relatively simpler configurations. Test of layouts with integrated AC load as well as development of a dedicated control system (hardware & software) will be the next steps of the joint development within the teams.

ACKNOWLEDGEMENTS

The authors gratefully acknowledge the support received from the Research Council of Norway and user partners through HighEFF - Centre for an Energy Efficient and Competitive Industry for the Future, an 8-year Research Centre under the FME-scheme (Centre for Environment-friendly Energy Research, 257632/E20).

REFERENCES

Elbel, S., Hrnjak, P., 2008. Experimental validation of a prototype ejector designed to reduce throttling losses encountered in transcritical R744 system operation. Int. J. Refrigeration 31, 411-422.

Gullo, P., Hafner, A., Banasiak, K. 2018. Transcritical R744 refrigeration systems for supermarkets applications: Current status and future perspectives. Int. J. Refrigeration 93, 269-310.

Pardiñas, Á.Á., Hafner, A., Banasiak, K., 2018a. Novel integrated CO_2 vapour compression racks for supermarkets. Thermodynamic analysis of possible system configurations and influence of operational conditions. Appl. Therm. Eng. 131, 1008-1025.

Pardiñas, Á.Á., Hafner, A., Banasiak, K., 2018b. Integrated R744 ejector supported parallel compression racks for supermarkets. Experimental results. Proceedings of the 13th IIR Gustav Lorentzen Conference, Valencia, 2018.

Zolcer Skačanová, K., Battesti M., 2019. Global market and policy trends for CO_2 in refrigeration. Int. J. Refrigeration 107, 98-104.

B P&ID of refrigerant loop (CO_2) and oil circuit

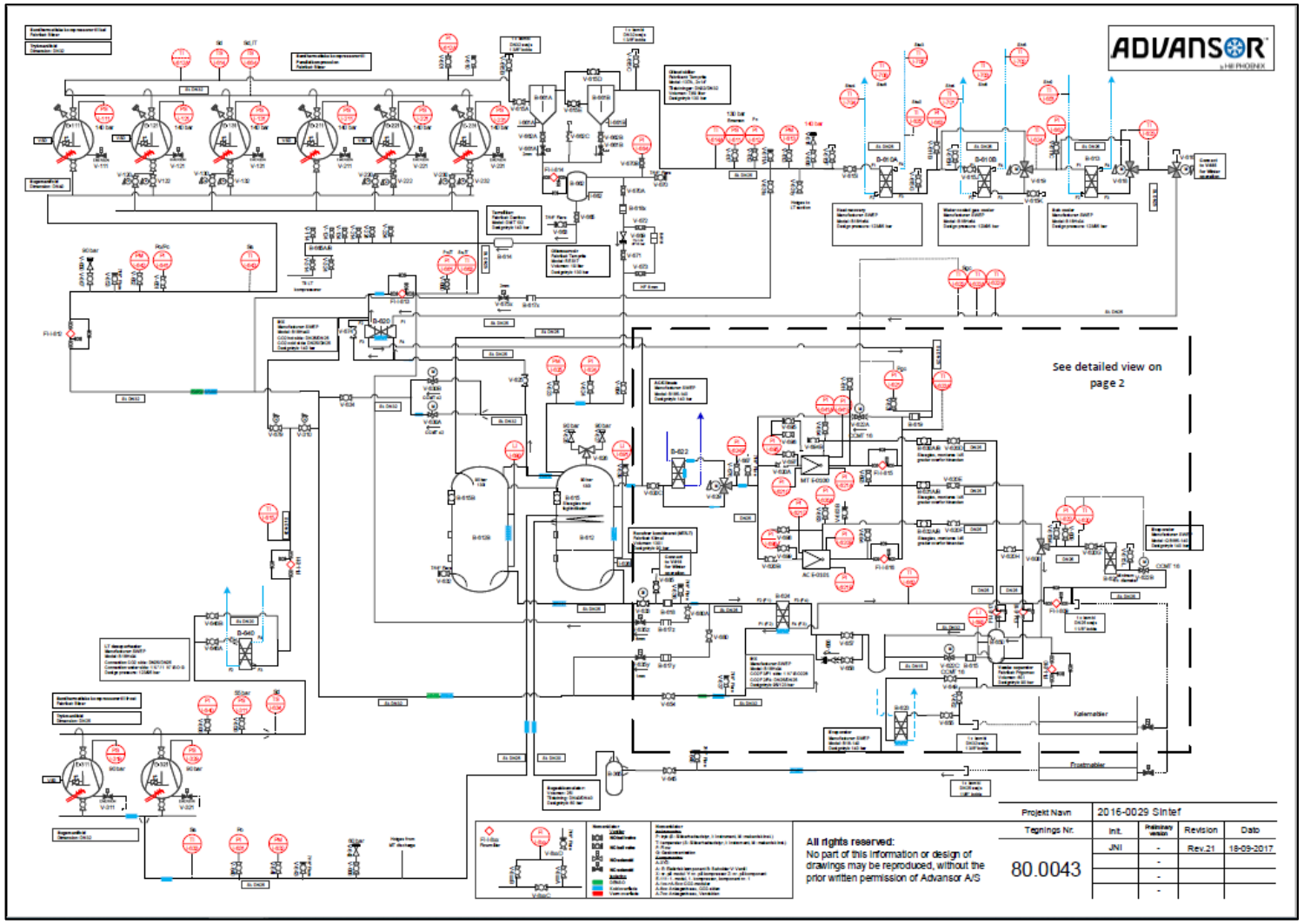

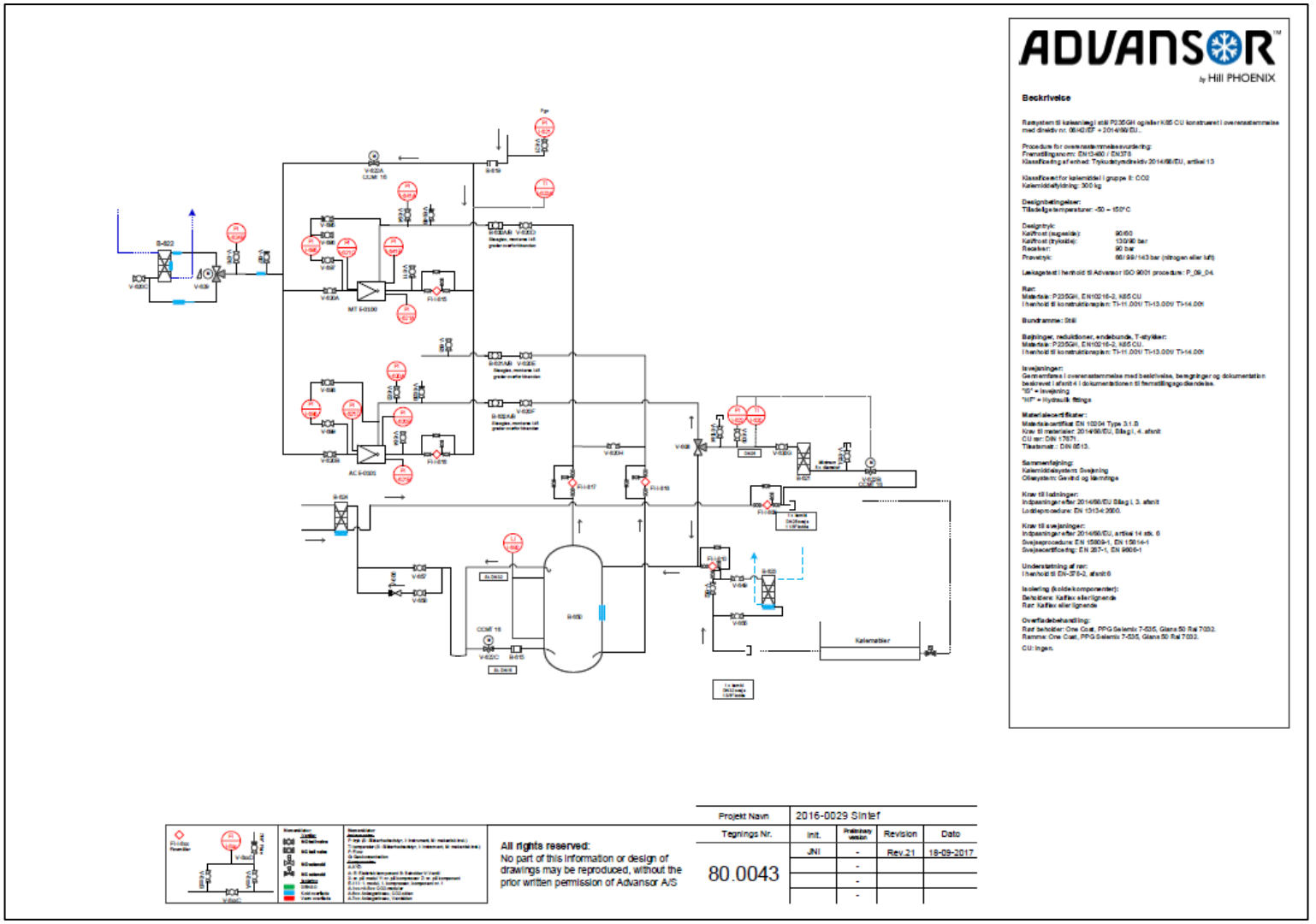
ADVANSOR
by Hill PHOENIX
Beskrivelse
Kalemateer
All rights reserved:
No part of this information or design of drawings may be reproduced, without the prior written permission of Advansor A/S
Projekt Navn
2016-0029 Sintef
Tegnings Nr.
80.0043
Init.
Preliminary version
Revision
Dato
JNI
-
Rev.21
18-09-2017

C P&ID of evaporators and cabinet

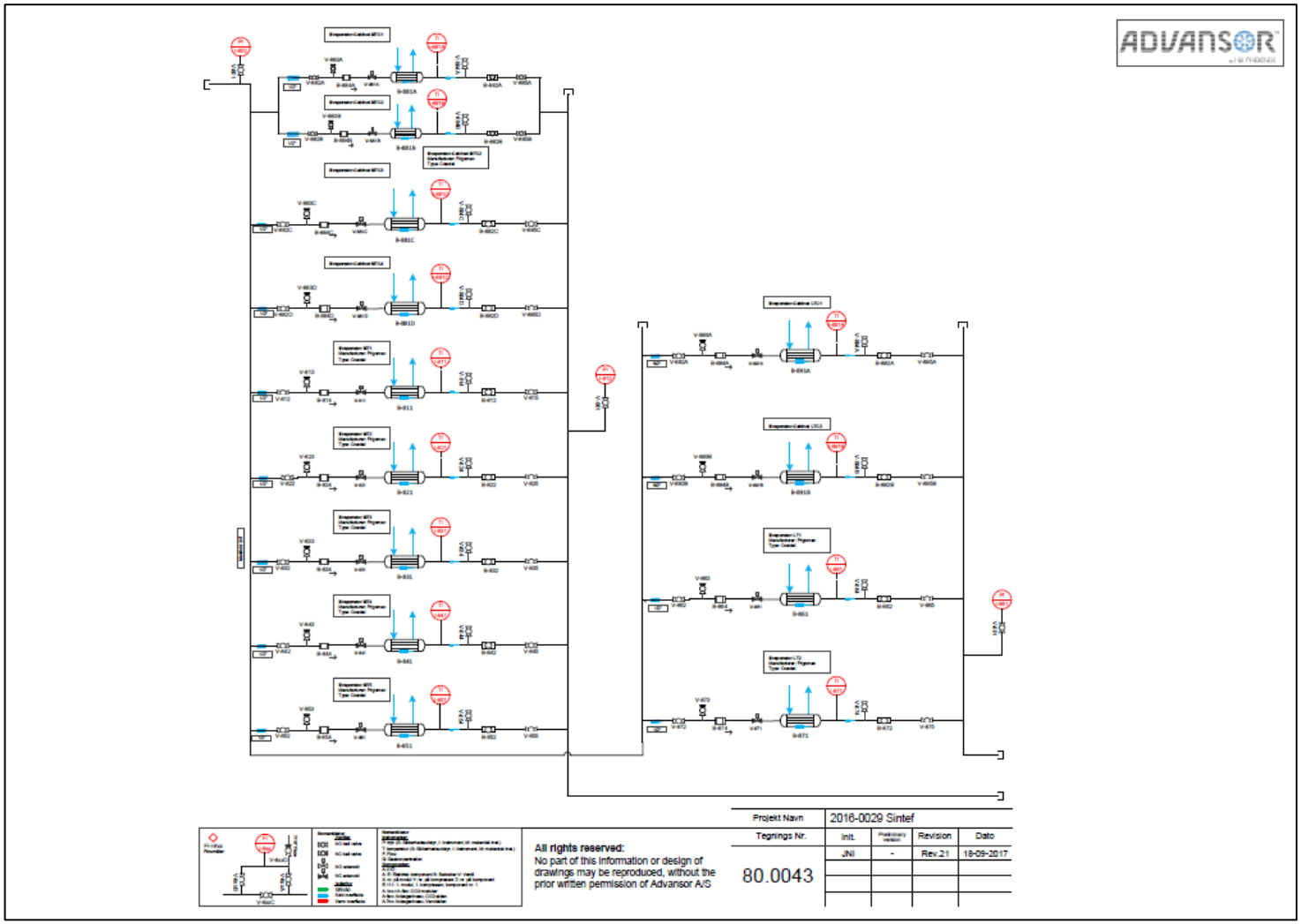

D P&ID of secondary loops

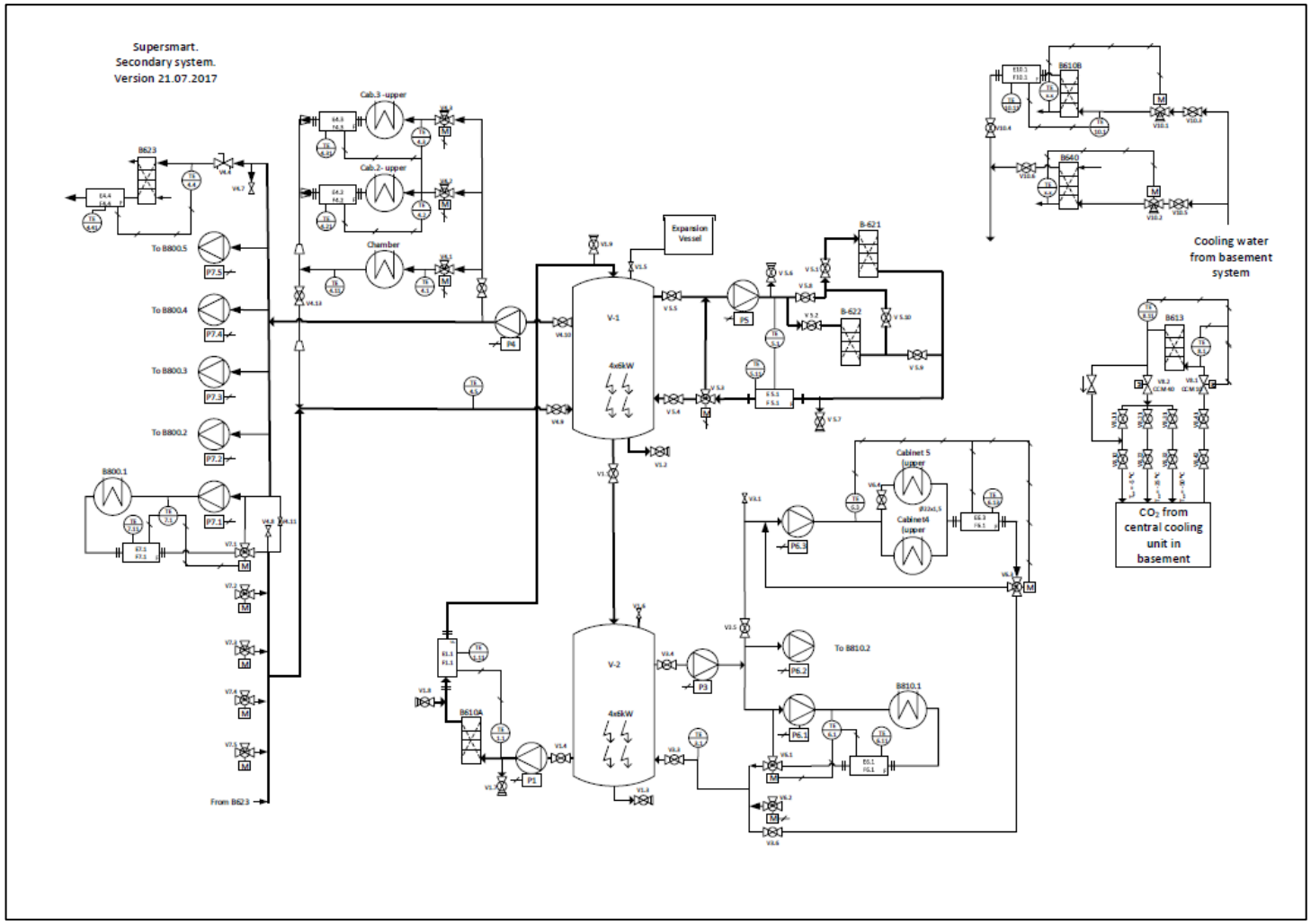

E Charging of the SS-R

From the experimental campaign there was a reason to believe that a leakage was present in the system requiring to charge it two times. Being the amount of CO_2 charged around 50 kg, and because of the leakage that led the liquid level in the receiver down to the first glass, the leakage had to be very close to the liquid receiver. More small leakages were identified in the connection between oil receiver – liquid receiver, and oil separator – oil receiver. In figure 1 a), the biggest leakage was identified to be close to the mass flow meter E – 814, while in figure 1 b) another small leakage was found in the cap of the valve V – 663.

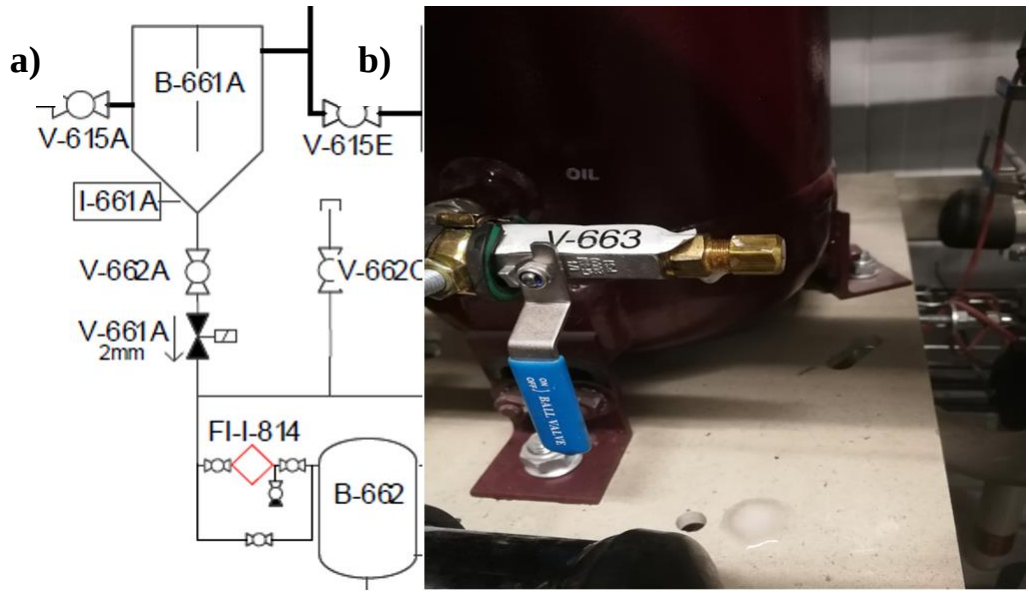

Fig I:Leakages placed in the SS-R.

In order to charge the system, it needs to be running because of the low pressure of the CO_2 tank from which the refrigerant is taken. Furthermore, the setpoint of LT compressors must be lower (around -43 °C) but without any LT evaporator running. This enables the operator to record how much refrigerant is charged reading the mass flow meter E – 811. The MT load must be set to keep MT compressors running all the time.

The valve V-643 is connected to the tube pipe that goes to the CO_2 tank. To ensure a proper feeding of the liquid receiver, the refrigerant should pass the second glass in the tank without reaching the third one. Moreover, the charging flow will be even lower during the time probably due to the lower pressure in the refrigerant tank located outside the laboratory.

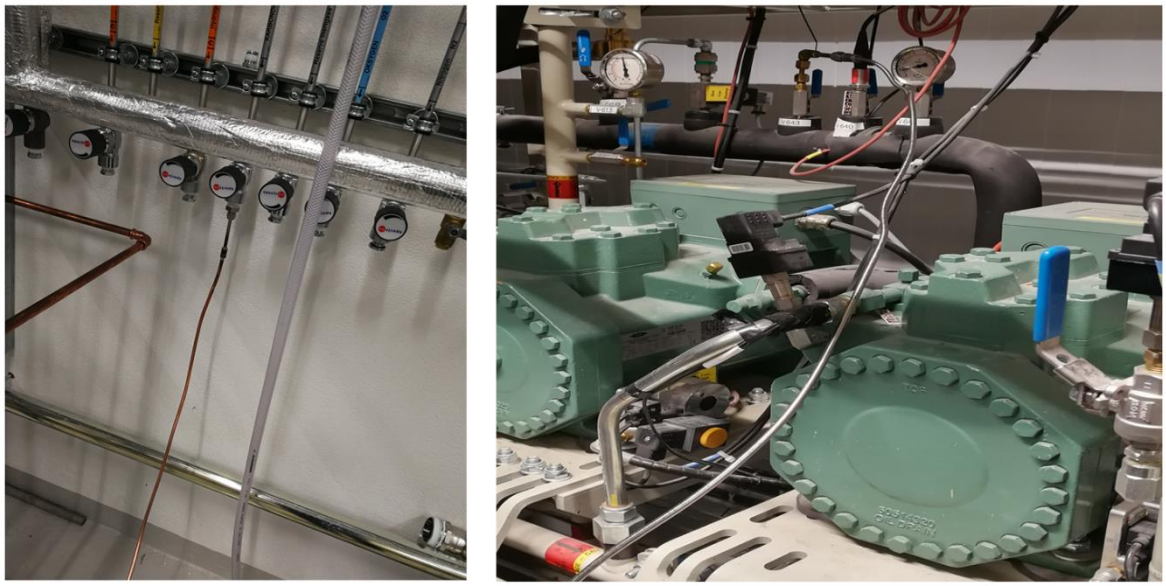

Fig II: Pipe connection for the charging.

F Theoretical results with Pivoting arrangement (25-30-35 °C)

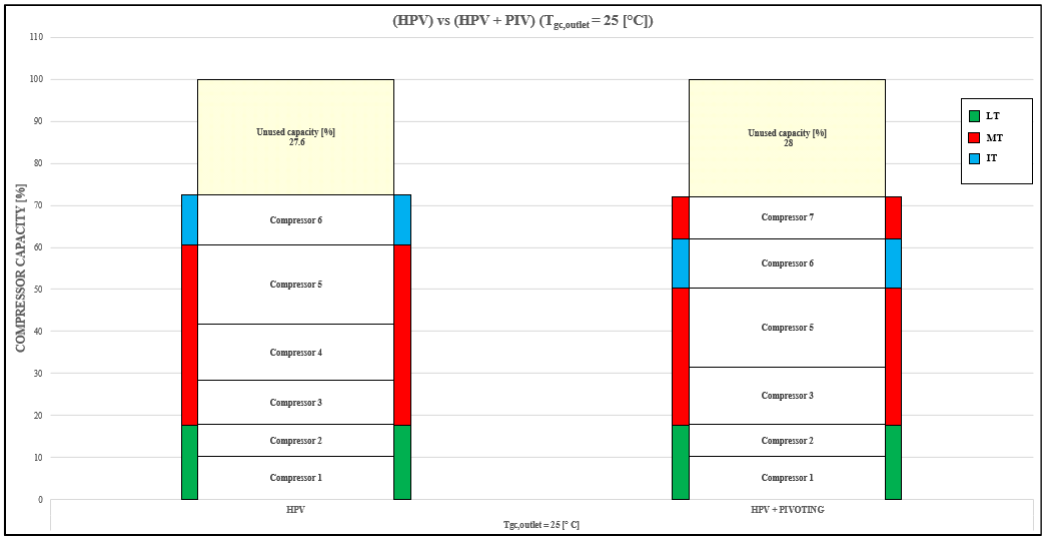

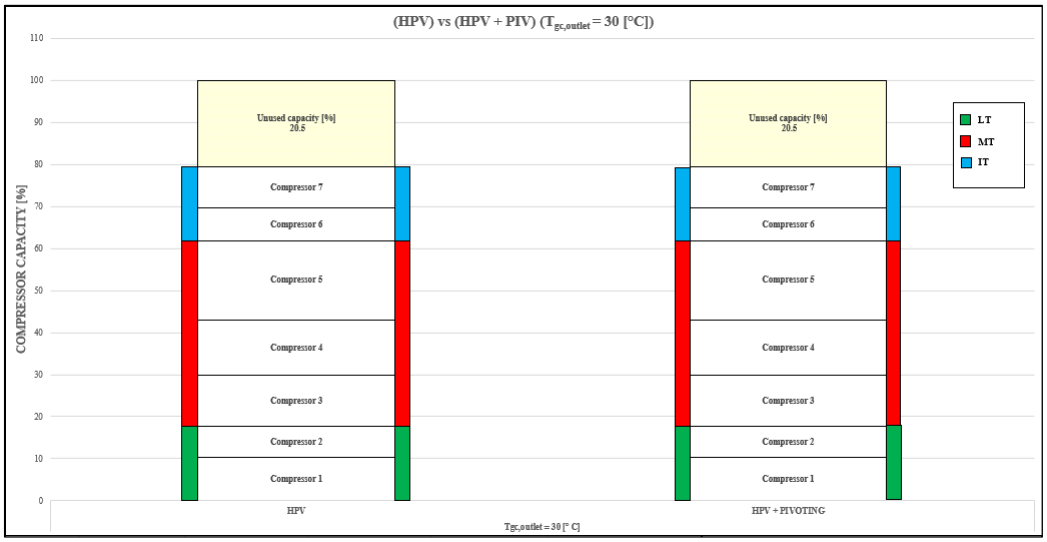

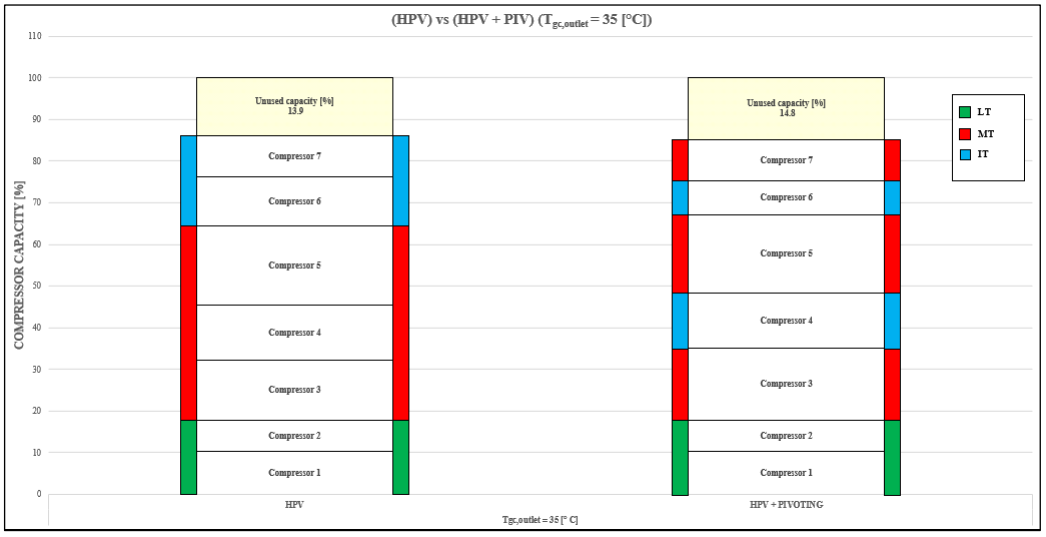

G Experimental results with Pivoting arrangement (25-30-35 °C)

I) $T_{gc,outlet}$ = 25 °C, p_{HP} = 68.98 bar

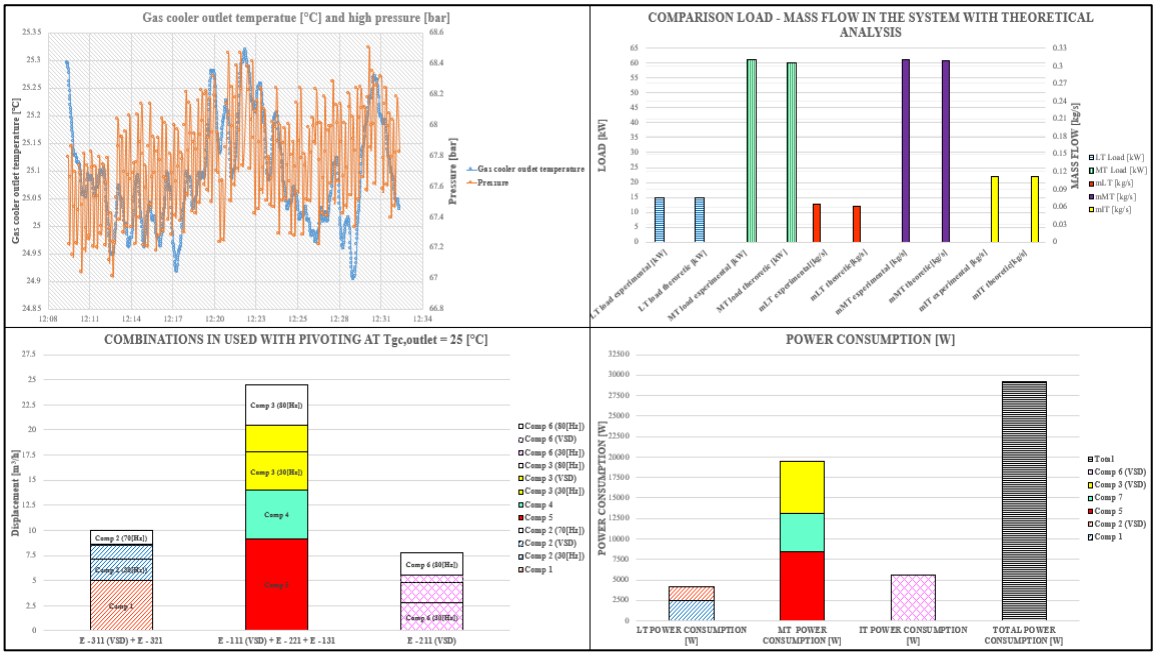

II) $T_{gc,outlet}$ = 30 °C, p_{HP} = 76 bar

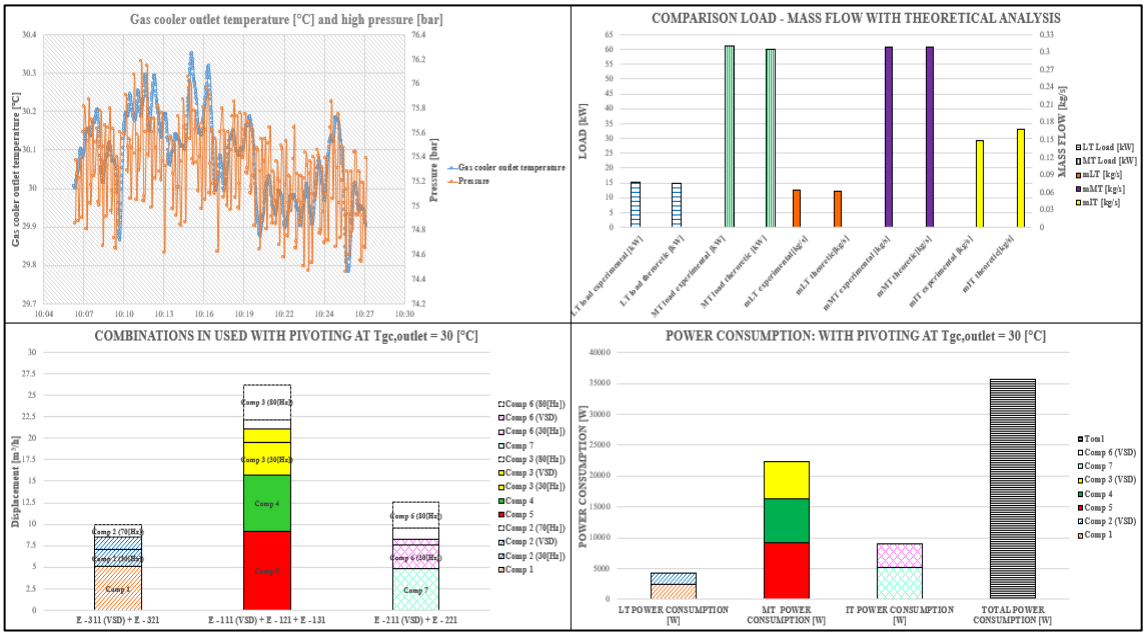

III) $T_{gc,outlet}$ = 35 °C, p_{HP} = 89 bar

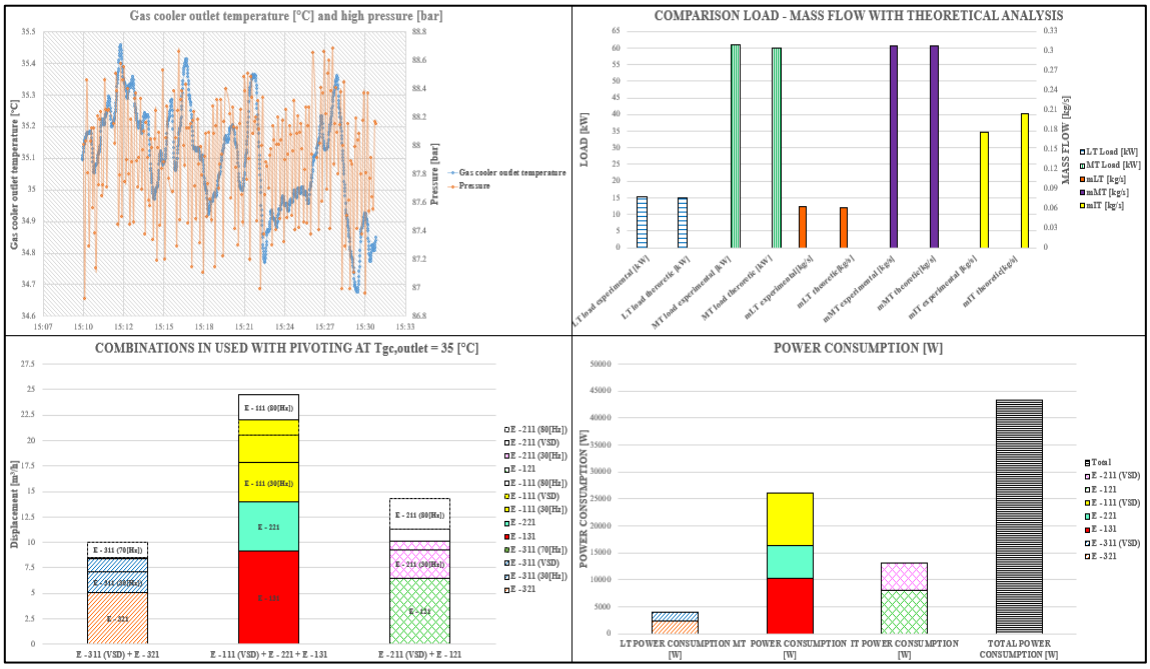

H MT load fluctuations (15-20-25-30 °C)

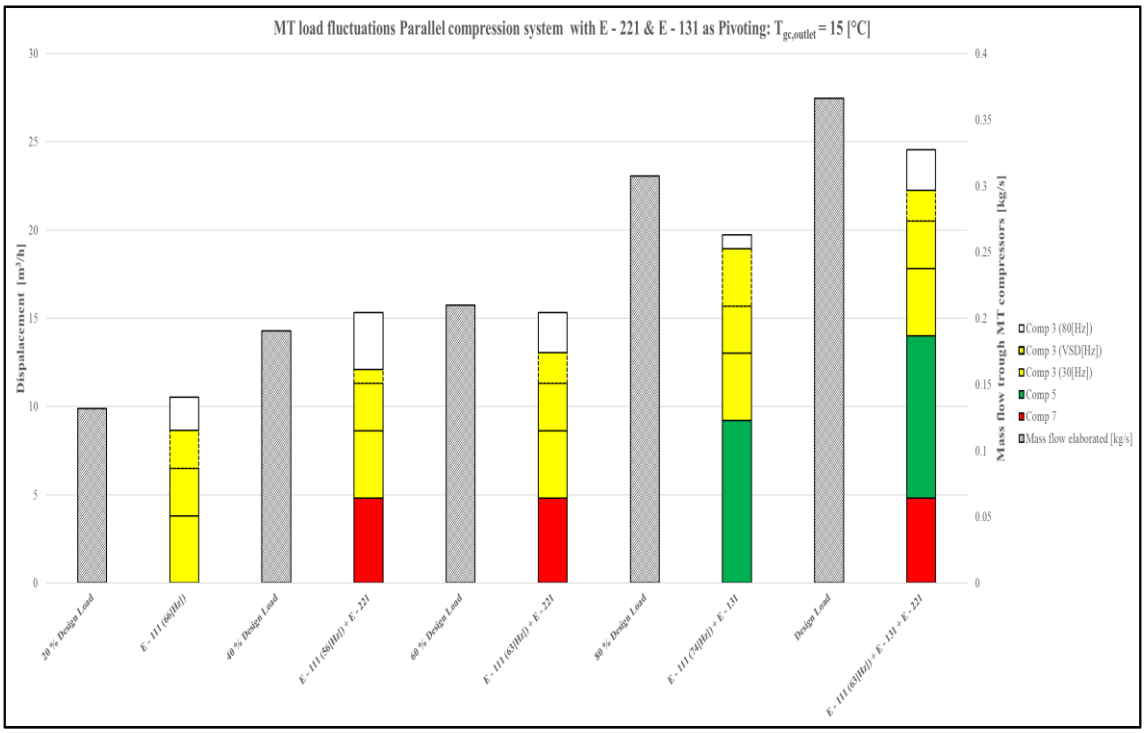

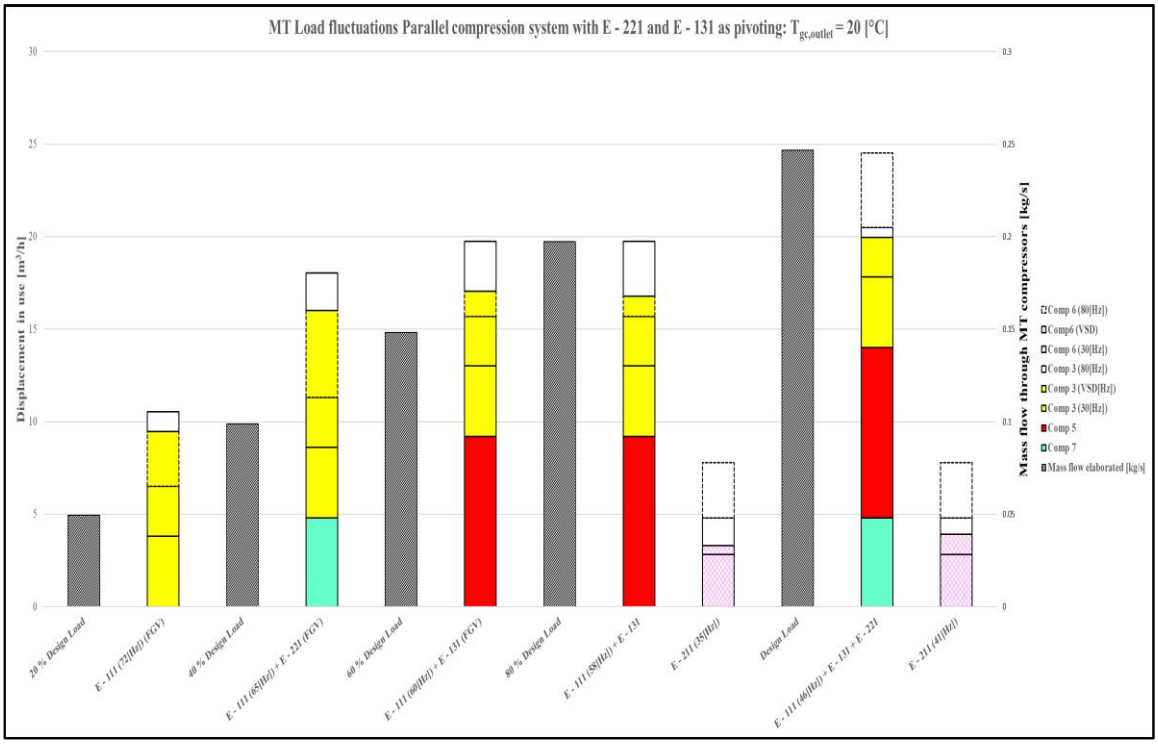

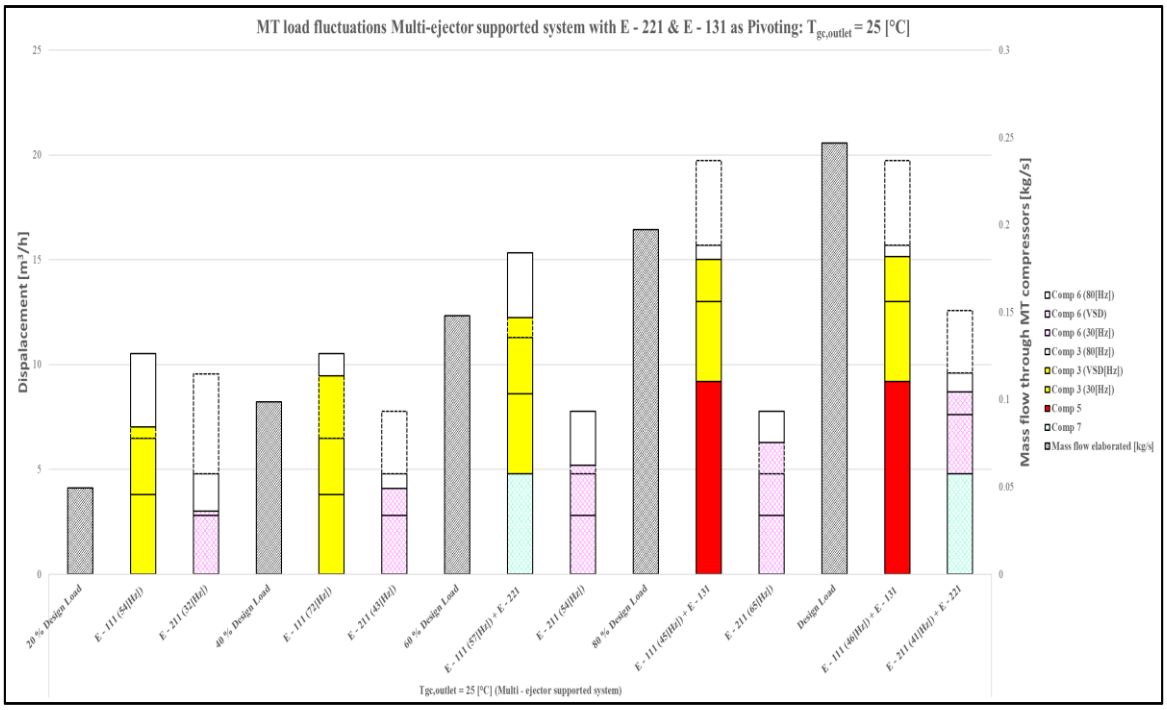
MT load fluctuations Multi-ejector supported system with E - 221 & E - 131 as Pivoting: $T_{gc,outlet}$ = 25 [°C]
Dispalacement [m³/h]
Mass flow through MT compressors [kg/s]
Comp 6 (80[Hz])
Comp 6 (VSD)
Comp 6 (30[Hz])
Comp 3 (80[Hz])
Comp 3 (VSD[Hz])
Comp 3 (30[Hz])
Comp 5
Comp 7
Mass flow elaborated [kg/s]
20 % Design Load
E - 111 (54[Hz])
E - 211 (32[Hz])
40 % Design Load
E - 111 (72[Hz])
E - 211 (45[Hz])
60 % Design Load
E - 111 (57[Hz]) + E - 221
E - 211 (54[Hz])
80 % Design Load
E - 111 (45[Hz]) + E - 131
E - 211 (65[Hz])
Design Load
E - 111 (46[Hz]) + E - 131
E - 211 (41[Hz]) + E - 221
Tgc,outlet = 25 [°C] (Multi - ejector supported system)

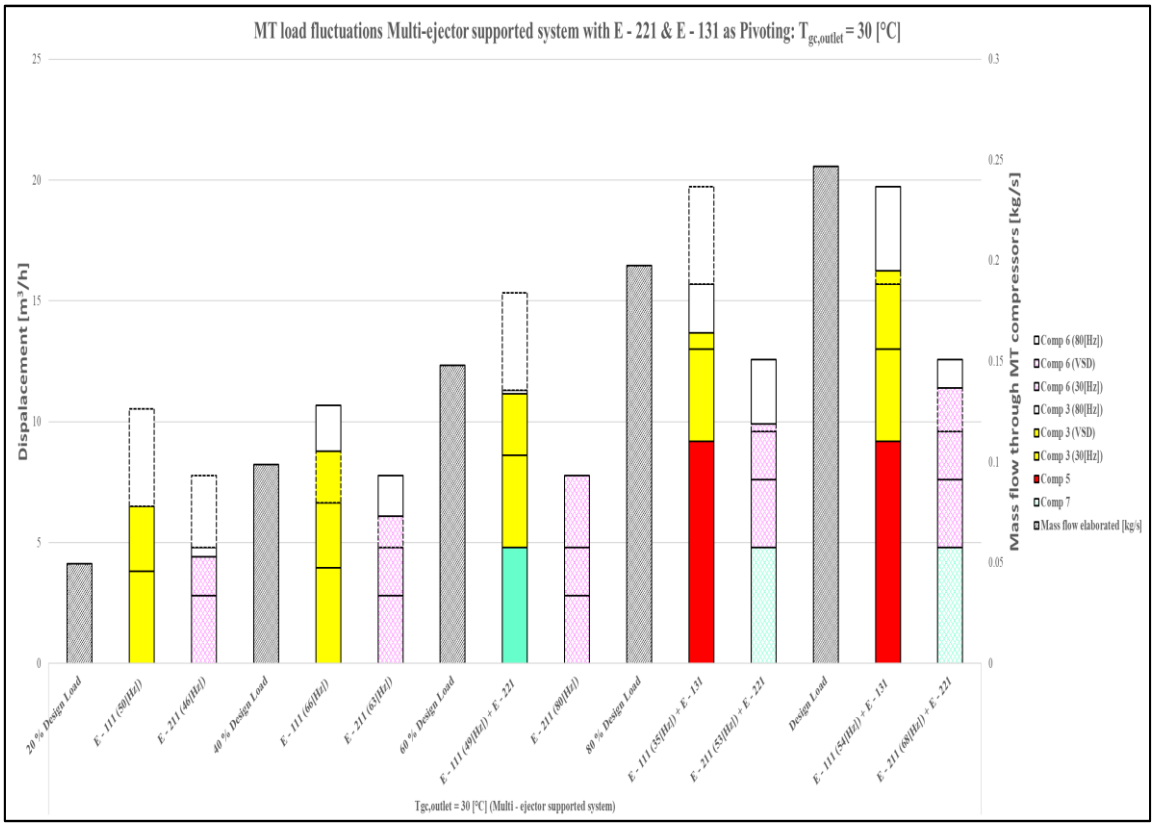
MT load fluctuations Multi-ejector supported system with E - 221 & E - 131 as Pivoting: $T_{gc,outlet}$ = 30 [°C]
Dispalacement [m³/h]
Mass flow through MT compressors [kg/s]
Comp 6 (80[Hz])
Comp 6 (VSD)
Comp 6 (30[Hz])
Comp 3 (80[Hz])
Comp 3 (VSD)
Comp 3 (30[Hz])
Comp 5
Comp 7
Mass flow elaborated [kg/s]
20 % Design Load
E - 111 (50[Hz])
E - 211 (46[Hz])
40 % Design Load
E - 111 (60[Hz])
E - 211 (63[Hz])
60 % Design Load
E - 111 (49[Hz]) + E - 221
E - 211 (80[Hz])
80 % Design Load
E - 111 (55[Hz]) + E - 131
E - 211 (53[Hz]) + E - 221
Design Load
E - 111 (54[Hz]) + E - 131
E - 211 (68[Hz]) + E - 221
Tgc,outlet = 30 [°C] (Multi - ejector supported system)

I LT Pivoting: Compressors in use and Power consumption

a) LT Pivoting discharge in a parallel compression unit

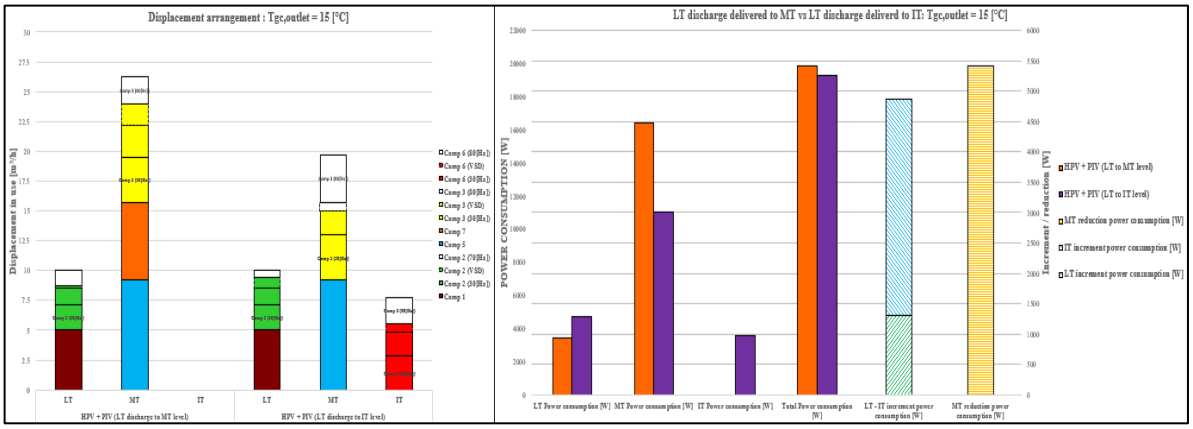

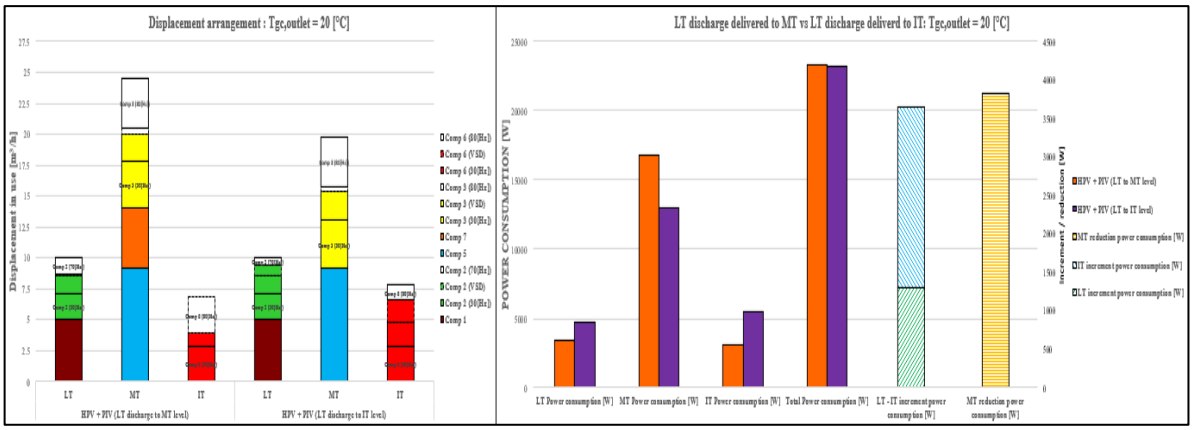

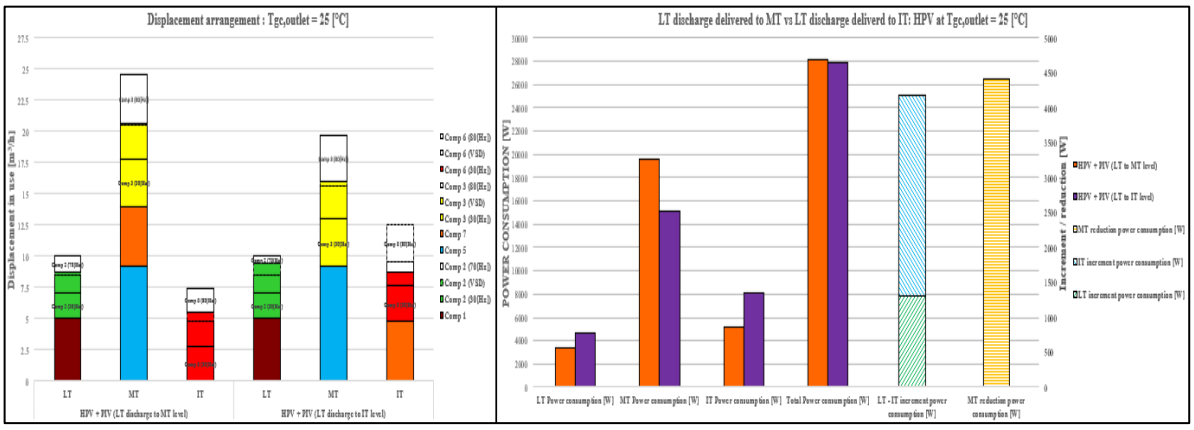

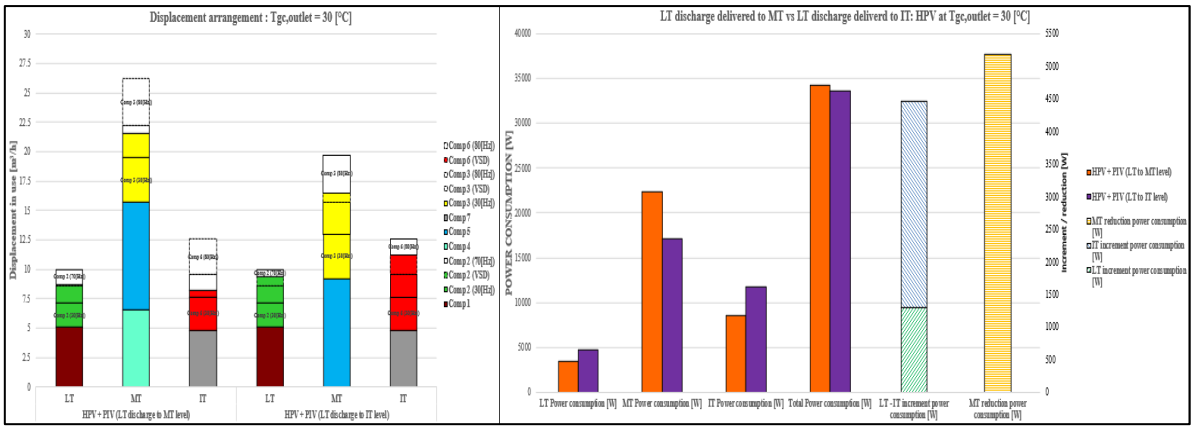

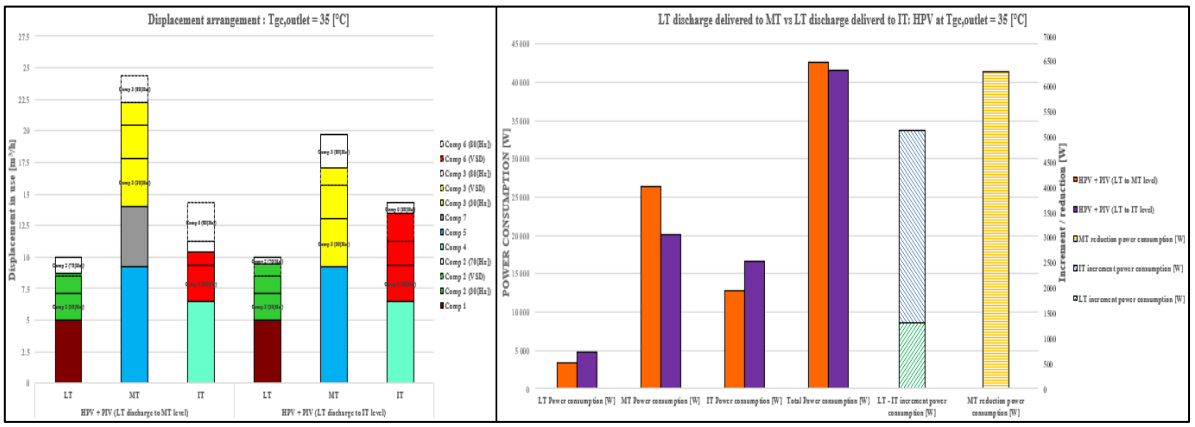

b) LT Pivoting discharge in a multi-ejector supported system

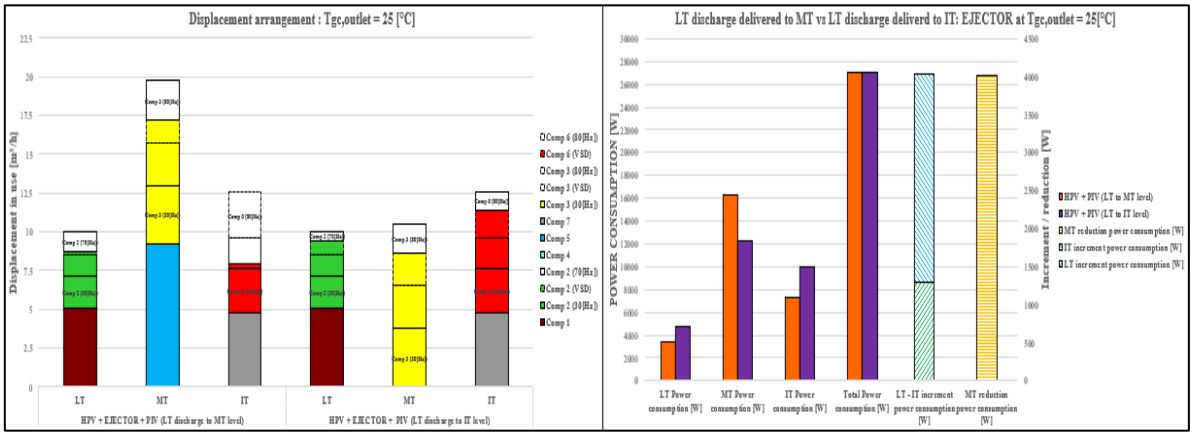

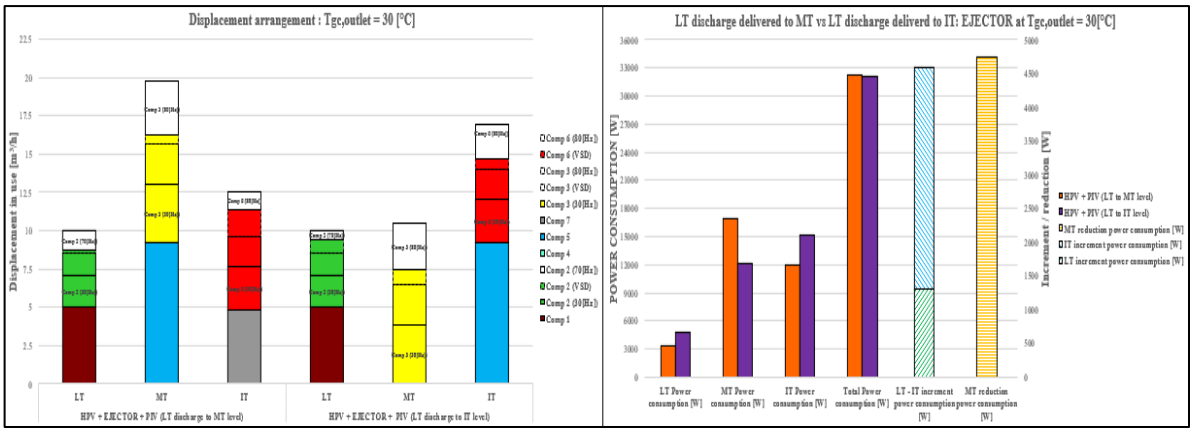
Displacement arrangement : Tgc,outlet = 30 [°C]
Displacement in use [m³/h]
LT
MT
IT
HPV + EJECTOR + PIV (LT discharge to MT level)
HPV + EJECTOR + PIV (LT discharge to IT level)
Comp 6 (60Hz)
Comp 6 (VSD)
Comp 3 (60Hz)
Comp 3 (VSD)
Comp 3 (30Hz)
Comp 7
Comp 5
Comp 4
Comp 2 (70Hz)
Comp 2 (VSD)
Comp 2 (30Hz)
Comp 1
LT discharge delivered to MT vs LT discharge deliverd to IT: EJECTOR at Tgc,outlet = 30[°C]
POWER CONSUMPTION [W]
Increment / reduction [W]
LT Power consumption [W]
MT Power consumption [W]
IT Power consumption [W]
Total Power consumption [W]
LT - IT increment power consumption [W]
MT reduction power consumption [W]
HPV + PIV (LT to MT level)
HPV + PIV (LT to IT level)
MT reduction power consumption [W]
IT increment power consumption [W]
LT increment power consumption [W]

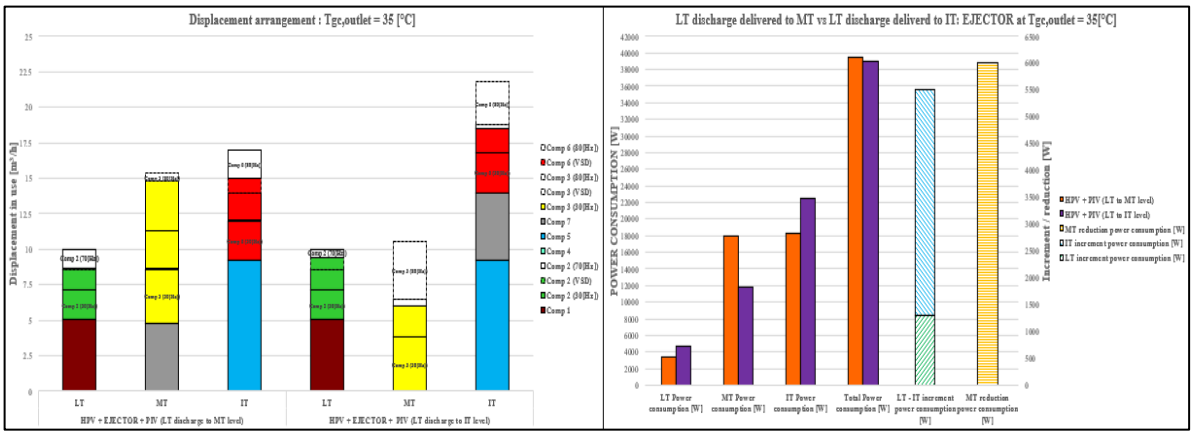
Displacement arrangement : Tgc,outlet = 35 [°C]
Displacement in use [m³/h]
LT
MT
IT
HPV + EJECTOR + PIV (LT discharge to MT level)
HPV + EJECTOR + PIV (LT discharge to IT level)
Comp 6 (60Hz)
Comp 6 (VSD)
Comp 3 (60Hz)
Comp 3 (VSD)
Comp 3 (30Hz)
Comp 7
Comp 5
Comp 4
Comp 2 (70Hz)
Comp 2 (VSD)
Comp 2 (30Hz)
Comp 1
LT discharge delivered to MT vs LT discharge deliverd to IT: EJECTOR at Tgc,outlet = 35[°C]
POWER CONSUMPTION [W]
Increment / reduction [W]
LT Power consumption [W]
MT Power consumption [W]
IT Power consumption [W]
Total Power consumption [W]
LT - IT increment power consumption [W]
MT reduction power consumption [W]
HPV + PIV (LT to MT level)
HPV + PIV (LT to IT level)
MT reduction power consumption [W]
IT increment power consumption [W]
LT increment power consumption [W]

L Compressor packs efficiencies ($T_{gc,outlet}$ = 35 °C)